



TECHNICAL UNIVERSITY OF CRETE

School of Chemical and Environmental Engineering

Biochemical Engineering and Environmental Biotechnology Laboratory

Application of Nano-Bubbles in Drinking Water Disinfection and the Operation of Bioreactors

Seridou Petroula

Chemical Engineer, MSc



**Operational Programme
Human Resources Development,
Education and Lifelong Learning**

Co-financed by Greece and the European Union



June 2023

APPLICATION OF NANO-BUBBLES IN DRINKING WATER DISINFECTION AND THE OPERATION OF BIOREACTORS

ΕΦΑΡΜΟΓΗ ΝΑΝΟΦΥΣΑΛΙΔΩΝ ΣΤΗΝ ΑΠΟΛΥΜΑΝΣΗ ΠΟΣΙΜΟΥ ΝΕΡΟΥ ΚΑΙ ΣΤΗ ΛΕΙΤΟΥΡΓΙΑ ΒΙΟ-ΑΝΤΙΔΡΑΣΤΗΡΩΝ

“This report is submitted as partial fulfillment of the requirements in order to achieve the Ph.D. degree in School of Chemical and Environmental Engineering at the Technical University of Crete”

“This research is co-financed by Greece and the European Union (European Social Fund- ESF) through the Operational Programme «Human Resources Development, Education and Lifelong Learning» in the context of the project “Strengthening Human Resources Research Potential via Doctorate Research” (MIS-5000432), implemented by the State Scholarships Foundation (IKY).”

Copyright © 2023 Seridou Petroula

School of Chemical and Environmental Engineering

Technical University of Crete

Examination committee

Nicolas Kalogerakis – Supervisor

Professor Emeritus
School of Chemical and Environmental Engineering
Technical University of Crete, Chania, Greece

Danae Venieri – Advisory Committee

Associate Professor
School of Chemical and Environmental Engineering
Technical University of Crete, Chania, Greece

Ioannis V. Yentekakis – Advisory Committee

Professor
School of Chemical and Environmental Engineering
Technical University of Crete, Chania, Greece

Nikolaos Nikolaidis

Professor
School of Chemical and Environmental Engineering
Technical University of Crete, Chania, Greece

Konstantinos Komnitsas

Professor
School of Mineral Resources Engineering
Technical University of Crete, Chania, Greece

Anestis Vlysidis

Assistant Professor
School of Chemical Engineering
National Technical University of Athens, Athens, Greece

Dionissios Mantzavinos

Professor
Department of Chemical Engineering
University of Patras, Patras, Greece

Acknowledgments

This work was carried out in the Biochemical Engineering and Environmental Biotechnology (BEEB) Laboratory under the supervision of Professor Nicolas Kalogerakis. Firstly, I would like to express my sincere gratitude to my supervisor Professor Emeritus Nicolas Kalogerakis, who trusted me and offered me this Ph.D. opportunity. I truly appreciate the continuous support of my Ph.D. study and related research, his contagious and motivational enthusiasm and immense knowledge. His guidance helped me in all the time of research and writing of this thesis. Besides my supervisor, I would like to thank the rest of my Ph.D. thesis committee; Associate Professor Danae Venieri and Professor Ioannis V. Yentekakis for their continuous collaboration and their insightful comments and advice. I would also like to thank the other members of the examination committee, Professor Nikolaos Nikolaidis, Professor Konstantinos Komnitsas, Assistant Professor Anestis Vlysidis and Professor Dionissios Mantzavinos for their willingness to evaluate this thesis.

I gratefully acknowledge the help provided by the technical assistant of the lab Ariadni Pantidou, Postdoc researchers Evdokia Syranidou, Eleftheria Antoniou and Evina Gontikaki and my fellow labmates Georgia Charalampous, Katerina Karkanorachaki and Efsevia Fragkou. Thank you not only for the scientific discussions that stimulated my research but also for all the fun we have had in the lab. Moreover, I want to express my gratitude to Stella Voutsadaki, Lilly Saru and Ioannis Moukazis for their help and their collaboration. During my research, I had the honour to work with some great BSc students (Konstantinos, Eleftheria, Mary and Sofia). Thank you for all these good moments.

I would like to thank my family; my parents Anastasios and Morfi and my sisters Katerina and Anna. Even though they are miles away, they supported me continuously throughout my stay in Chania. Without their encouragement this work would never have been possible. And finally, last but by no means least, I would like to thank Andreas for his precious support and understanding but mainly for tolerating me during the pursuit of my Ph.D. research, even though he still doesn't know exactly the topic of my Ph.D. thesis!

Abstract

A major threat to human health is considered the bacterial contamination and the subsequent infections and there is dire need to prevent the waterborne diseases to ensure water safety. Moreover, the occurrence and the fate of trace organic compounds in wastewater have attracted the attention and the concern of the scientific community since conventional wastewater treatment plants (WWTPs) have not been designed for their elimination leading to their discharge to natural water bodies and the effects of chronic exposure to low levels of these compounds are unknown. Within the context of upgrading the water and wastewater treatment processes, the development of new treatment technologies is addressed, with a view to provide high quality water at the least possible cost to the consumers.

Nanobubbles (NBs) technology is an emerging solution, which is considered that has brought revolution in the field of water treatment and contaminants remediation. NBs are tiny spherical bubbles with a diameter less than 1 μm and exhibit notable characteristics in comparison to the macrobubbles (MaBs). First and foremost, the long residence time thanks to their stability is highlighted as a vital property, since it has been found that NBs remain stable in aqueous solution for a long period of time, due to their negligible buoyancy. Moreover, NBs improve the mass transfer effect and the oxidation ability, on account of the fact that the contact area of gas and water is increased. In addition, the gas solubility and chemical reactions at the gas-liquid boundary are remarkably enhanced.

In terms of water disinfection processes, ozonation is widely used since ozone is a strong oxidant and highly efficient to inactivate pathogenic organisms for the prevention of waterborne diseases spread to users and the environment. However, the performance of this method is limited by the fact that ozone is unstable and short lived as the decay rate in water is high. By combining the higher gaseous ozone half-life time (3 days versus 20 min at 20 °C) and the noteworthy properties of NBs technology, the use of ozone nanobubbles (OzNBs) is proposed for water and ballast water disinfection. The main objective of this

study is to compare the effect of ozone nanobubbles on the inactivation of the pathogenic microorganisms and the residual activity compared to the conventional ozonation in tap water and ballast water. In this study, four harmful types of bacteria commonly used as primary indicators of contamination in fresh water quality were selected (*Escherichia coli*, *Bacillus cereus*, *Staphylococcus aureus*, *Enterococcus faecalis*). Based on the experimental results, applying OzNBs technology had a considerable effect on inactivation and the ozone decay rate was greatly decreased, hence it can be concluded that it is a promising technology for drinking water treatment. As regards the ballast water disinfection, the survival rate of *Escherichia coli* (*E. coli*), which was used as indicator microorganism, along with the ozone consumption at different salinities (1.5, 4, 8 and 15 PSU) and bacterial concentrations (10^7 , 10^6 , and 10^5 CFU/mL) with and without supplementation of OzNBs were investigated. The results indicated a statistical difference in the residual concentration of total residual oxidants (TRO) with the presence of OzNBs at salinity level 1.5 PSU and at 4 PSU only at the lowest bacterial content. At a low salinity and high bacterial concentration, the concentration of TRO was 6-fold higher in the presence of OzNBs. The salinity of water has a strong impact on the residual concentration of ozone. When salinity is increased, ozone reacts more rapidly with the bromide and chloride ions. The use of OzNBs exhibited a greater disinfection performance and higher residual activity.

In this thesis, another application of NBs technology that was investigated was the implementation of air nanobubbles (ANBs) in constructed wetlands (CWs) as it has been found that artificial aeration enhances the removal rate of conventional pollutants (COD, nitrogen and phosphorus) as well as organic compounds. The oxygen supply was conducted via nanobubble injection by a nanotube porous diffuser and in-situ electrochemical production. A higher removal rate was observed when ANBs were supplemented in wetland bed through the nanotube diffuser in phenol and toluene removal and in combination of both compared to the control. In addition, the oxygen content remained at a high level (above 7 mg/L) in all experimental cycles. Moreover, primary-treated wastewater collected from Wastewater Treatment Plant (WWTP) in Platanias (Chania) was used as substrate in wetlands along with the concentration of phenol and toluene at 100 ppm. Also in this case, the CW supplemented with ANBs by nanotube diffuser exhibited better performance in phenol and toluene removal, while the addition of

wastewater enhanced the efficiency of integrated-electrolysis CW. All the wastewater quality parameters were measured, exhibiting great removal efficiencies in all CWs, however no significant difference was reported among the treatments.

Finally, another field in which NBs were applied was bioremediation. In particular, the impact of irrigation with water supplemented with oxygen nanobubbles (ONBs) was also examined. In this study, soil from a shooting range was collected and spiked with an initial antimonite (Sb(III)) concentration of 50 mg/kg and a pot experiment was conducted to investigate whether *Nerium oleander* assisted by organic acids (OAs) and ONBs could accumulate Sb in the root and further translocate it to the aboveground tissue. The translocation of Sb for every treatment was very low, confirming that *N. oleander* plant cannot transfer Sb from the root to the shoots. A higher amount of Sb was accumulated in the plants that were irrigated with the ONBs. As regards the bioaccumulation of the elements Fe, Mg and Mn from soil to plant tissues, Fe and Mn were not mobilized, whereas Mg was extracted as the bioconcentration factor (BCF) was evaluated above one and significant higher with the presence of ONBs. The BCF of Mn and Mg were significantly greater when ONBs were used for irrigation, while the opposite trend was observed regarding the translocation factor. Nanobubbles can enhance the stabilization of these elements in roots and not the translocation to the upper part of the plants. Moreover, the mobilization of antimony (Sb) from soil by non-bioaugmented and bioaugmented processes coupled with nanobubble technology was investigated. ONBs enhanced the mobilization of Sb in the non-bioaugmented experiments. The bioaugmentation had a significant effect in Sb release to the aqueous phase since the percentage of Sb remaining in the soil was found to be lower in the bioaugmented experiment implying the mobilization of about 75% of the original Sb in the soil. Nanobubbles were found to have no significant effect on Sb release from the soils, since the same percentage of Sb was also found in the bioaugmented treatment with NBs water.

In conclusion, the overall outcome of this study based on the experimental evidence is the significant contribution of NBs technology to various environmental fields including disinfection, wastewater treatment, and phytoremediation. In this regard, the application of NBs technology is paving the way to novel integrated and highly efficient water and soil treatment systems.

“This page intentionally left blank”

Περίληψη

Η βακτηριακή μόλυνση του νερού αποτελεί σοβαρή απειλή για τη δημόσια υγεία και είναι επιτακτική ανάγκη να αποφευχθεί, διασφαλίζοντας την ποιότητα του νερού ώστε να μην υπάρξει μετάδοση ασθενειών μέσω του νερού. Επίσης, η παρουσία των οργανικών ρύπων κρίνεται ως θέμα μείζονος σημασίας από την διεθνή επιστημονική κοινότητα, καθώς οι συμβατικές εγκαταστάσεις λυμάτων δεν έχουν σχεδιαστεί με την προοπτική της απομάκρυνσης των ενώσεων αυτών, με αποτέλεσμα να γίνεται μερική ή ολική απόρριψή τους στους τελικούς αποδέκτες. Στο πλαίσιο αναβάθμισης των μεθόδων επεξεργασίας του νερού και των λυμάτων, η ανάπτυξη νέων τεχνολογιών που έχουν ως σκοπό να προσφέρουν υψηλής ποιότητας νερό στο χαμηλότερο δυνατό κόστος είναι στο επίκεντρο.

Σε αυτό το πλαίσιο εντάσσεται η τεχνολογία των νανοφουσαλίδων (Nanobubbles, NBs), η οποία είναι μια τεχνολογία αιχμής που έχει τραβήξει το επιστημονικό ενδιαφέρον τα τελευταία χρόνια λόγω των πιθανών εφαρμογών τους σε πολλούς τομείς της επιστήμης και τεχνολογίας. Η σημασία τους είναι ευρέως γνωστή για τον ρόλο που διαδραματίζουν σε σχέση με το μέγεθος του και την σταθερότητα τους. Πιο συγκεκριμένα, πρόκειται για μικροσκοπικές σφαιρικές φουσαλίδες κάτω από 1 μm με μοναδικές φυσικές και μηχανικές ιδιότητες και σημαντικά πλεονεκτήματα έναντι των μακροφουσαλίδων. Μία από τις πιο αξιοσημείωτες ιδιότητες τους είναι η μεγάλη διάρκεια ζωής λόγω της σχεδόν αμελητέας άνωσης/πλευστότητας. Επιπρόσθετα, λόγω των μοναδικών τους ιδιοτήτων, οι νανοφουσαλίδες οδηγούν σε υψηλούς ρυθμούς μεταφοράς μάζας καθώς η εσωτερική πίεση της φουσαλίδας είναι αντιστρόφως ανάλογη με το μέγεθος της. Επομένως, οι νανοφουσαλίδες έχουν μεγάλη ειδική επιφάνεια που εντείνει τον ρυθμό μεταφοράς μάζας λόγω της μεγαλύτερης επιφάνειας επαφής μεταξύ της αέριας και της υγρής φάσης. Επιπλέον, η μεγάλη ειδική επιφάνεια τους συμβάλλει στην προώθηση χημικών αντιδράσεων, φυσικής προσρόφησης, και μεταφοράς μάζας στη διεπιφάνεια αερίου-υγρού.

Ο οζονισμός είναι μια μέθοδος απολύμανσης που χρησιμοποιείται ευρέως, καθώς είναι γνωστό ότι το όζον είναι ένα από τα ισχυρά οξειδωτικά και είναι αποτελεσματικό

εναντίον των βακτηρίων και των ιών. Ωστόσο είναι μια ασταθής ένωση και η αποτελεσματικότητα της μεθόδου περιορίζεται από το γρήγορο ρυθμό μείωσης της οξειδωτικής ικανότητας του διαλυμένου όζοντος. Ο χρόνος ημιζωής του όζοντος στην αέρια φάση είναι πολύ μεγαλύτερος (3 μέρες έναντι 20 min στους 20 °C) και επομένως η σύζευξη του όζοντος με την τεχνολογία των νανοφουσαλιδών δύναται να ενισχύσει την απολυμαντική δράση (και υπολειπόμενη δραστηριότητα). Η παρούσα διδακτορική διατριβή έχει ως στόχο την μελέτη των εφαρμογών των νανοφουσαλιδών με ιδιαίτερη αναφορά στην επεξεργασία πόσιμου νερού για καλύτερη απόδοση στην εξουδετέρωση παθογόνων βακτηρίων. Επιπλέον, διερευνήθηκε η υπολειπόμενη δράση των νανοφουσαλιδών όζοντος. Ο κύριος στόχος της μελέτης είναι η σύγκριση της τεχνολογίας των νανοφουσαλιδών όζοντος σε σύγκριση με τον συμβατικό οζονισμό ως προς την απολύμανση καθώς και την απολυμαντική δράση του όζοντος. Τέσσερα είδη βακτηρίων (*Escherichia coli*, *Bacillus cereus*, *Staphylococcus aureus*, *Enterococcus faecalis*) μελετήθηκαν, τα οποία είναι σημαντικά για την ποιότητα του νερού. Με βάση τα αποτελέσματα, η εφαρμογή της τεχνολογίας των νανοφουσαλιδών όζοντος παρουσίασε σημαντική επίδραση στην αδρανοποίηση των βακτηρίων και στον ρυθμό διάσπασης του όζοντος, καθιστώντας την μια πολλά υποσχόμενη τεχνολογία για την επεξεργασία του πόσιμου νερού. Επιπλέον όσον αφορά την επεξεργασία του θαλάσσιου έρματος, μελετήθηκε η απόδοση της απολύμανσης της αρχικής συγκέντρωσης του βακτηρίου *Escherichia coli* (*E. coli*) (10^7 , 10^6 , and 10^5 CFU/mL) και της υπολειπόμενης συγκέντρωσης του όζοντος σε διάφορες αλατότητες (1.5, 4, 8 and 15 PSU) με την χρήση των νανοφουσαλιδών όζοντος σε σύγκριση με τον συμβατικό οζονισμό. Τα αποτελέσματα έδειξαν στατιστική διαφορά στην υπολειπόμενη συγκέντρωση οξειδωτικών που έχουν δημιουργηθεί από την αντίδραση του θαλασσινού νερού με το όζον με την χρήση των νανοφουσαλιδών όζοντος στην χαμηλότερη αλατότητα, 1.5 PSU για όλες τις βακτηριακές συγκεντρώσεις καθώς και στα 4 PSU αλατότητα μόνο στην χαμηλότερη συγκέντρωση. Στην χαμηλότερη αλατότητα, η υπολειπόμενη συγκέντρωση των οξειδωτικών με την εφαρμογή των νανοφουσαλιδών όζοντος είναι 6 φορές μεγαλύτερη σε σύγκριση με τον συμβατικό οζονισμό. Η αλατότητα παρουσιάζει ισχυρή επιρροή στην υπολειπόμενη δραστηριότητα του όζοντος, καθώς όσο αυξάνεται η αλατότητα, αυξάνονται τα ιόντα χλωρίου και βρωμίου με τα οποία το όζον αντιδρά ταχέως. Η χρήση

νανοφουσαλίδων όζοντος φαίνεται να αποδίδει καλύτερα καθώς επιτυγχάνεται μεγαλύτερη απόδοση απολύμανσης και μεγαλύτερη υπολειπόμενη συγκέντρωση.

Μια επιπλέον εφαρμογή των νανοφουσαλίδων που μελετήθηκε στην συγκεκριμένη διδακτορική διατριβή είναι η εφαρμογή των νανοφουσαλίδων αέρα σε τεχνητούς υγροβιότοπους, καθώς μελέτες έχουν δείξει ότι η παροχή αερισμού στους τεχνητούς υγροβιότοπους οδηγεί σε καλύτερη απόδοση απομάκρυνσης οργανικών ρύπων. Η παροχή αερισμού επετεύχθη μέσω των νανοφουσαλίδων, οι οποίες παρήχθησαν μέσω ενός νανοσωλήνα-διαχυτήρα και μέσω της ηλεκτρόλυσης. Στον τεχνητό υγροβιότοπο με τον διαχυτήρα των νανοφουσαλίδων εντοπίστηκε η καλύτερη απομάκρυνση της φαινόλης και του τολουολίου καθώς και στον συνδυασμό των δύο ρύπων σε σύγκριση με τον υγροβιότοπο ελέγχου. Επιπλέον, η συγκέντρωση του οξυγόνου σε αυτό το σύστημα διατηρήθηκε σε υψηλά επίπεδα (πάνω από 7 mg/L) σε όλους τους πειραματικούς κύκλους. Στη συνέχεια, πρωτοβάθμια-επεξεργασμένο αστικό λύμα προερχόμενο από τον βιολογικό καθαρισμό της περιοχής του Πλατανιά (Χανιά) χρησιμοποιήθηκε ως υπόστρωμα μαζί με τους οργανικούς ρύπους φαινόλης και τολουολίου αρχικής συγκέντρωσης 100 ppm. Και σε αυτή την περίπτωση, αυτός ο υγροβιότοπος επέδειξε την καλύτερη απομάκρυνση των οργανικών ρύπων, φαινόλη και τολουόλιο, καθώς η προσθήκη του αστικού λύματος ενίσχυσε την απόδοση του υγροβιότοπου, ο οποίος λειτουργεί με την ηλεκτρόλυση. Μετρήθηκαν όλες οι παράμετροι ποιότητας των λυμάτων, παρουσιάζοντας μεγάλη αποτελεσματικότητα απομάκρυνσης σε όλα τα συστήματα, ωστόσο δεν αναφέρθηκε σημαντική διαφορά μεταξύ των τεχνητών υγροβιότοπων.

Τέλος, ένας άλλος τομέας στον οποίο εφαρμόστηκαν οι νανοφουσαλίδες είναι η βιολογική αποκατάσταση. Ειδικότερα, στην φυτοαποκατάσταση εξετάστηκε η επίδραση της άρδευσης με νερό με νανοφουσαλίδες οξυγόνου (ONBs). Σε αυτή τη μελέτη, χώμα από ένα πεδίο βολής συλλέχθηκε και εμπλουτίστηκε με αντιμονίτη (Sb(III)) αρχικής συγκέντρωσης 50 mg/kg και διεξήχθη ένα πείραμα για να διερευνηθεί εάν η πικροδάφνη (*Nerium oleander*) σε συνδυασμό με οργανικά οξέα (OAs) και ONBs μπορεί να συσσωρεύσει το αντιμόνιο Sb στη ρίζα και να το μεταφέρει περαιτέρω στον υπέργειο ιστό. Η μετατόπιση του Sb για κάθε επεξεργασία ήταν πολύ χαμηλή, επιβεβαιώνοντας ότι το φυτό *N. oleander* δεν μπορεί να μεταφέρει το Sb από τη ρίζα στους βλαστούς. Μεγαλύτερη ποσότητα Sb συσσωρεύτηκε στα φυτά που ποτίστηκαν με τα ONBs. Όσον αφορά στην

βιοσυσσώρευση των στοιχείων Fe, Mg και Mn από το έδαφος στους φυτικούς ιστούς, το Fe και το Mn δεν κινητοποιήθηκαν, ενώ το Mg εκχυλίστηκε καθώς ο παράγοντας βιοσυγκέντρωσης αξιολογήθηκε πάνω από ένα και σημαντικά υψηλότερος με την παρουσία ONBs. Ο παράγοντας βιοσυσσώρευσης του Mn και του Mg ήταν σημαντικά μεγαλύτερος όταν τα ONBs χρησιμοποιήθηκαν, ενώ η αντίθετη τάση παρατηρήθηκε όσον αφορά τον παράγοντα μετατόπισης. Οι νανοφουσαλίδες μπορούν να ενισχύσουν τη σταθεροποίηση αυτών των μετάλλων στις ρίζες ενώ δεν συμβάλουν στην μετατόπιση τους στο υπέργειο τμήμα του φυτού. Επιπλέον, διερευνήθηκε η κινητοποίηση του αντιμονίου (Sb) από το έδαφος με βιοενισχυμένες ή όχι διαδικασίες σε συνδυασμό με την τεχνολογία νανοφουσαλιδών. Τα ONBs ενίσχυσαν την κινητοποίηση του Sb στα μη-βιοενισχυμένα πειράματα. Η βιοενίσχυση είχε σημαντική επίδραση στην απελευθέρωση Sb στην υδατική φάση αφού το ποσοστό του Sb που παραμένει στο έδαφος βρέθηκε να είναι χαμηλότερο στο βιοενισχυμένο πείραμα υποδηλώνοντας την κινητοποίηση περίπου 75% του αρχικού Sb στο έδαφος. Οι νανοφουσαλίδες βρέθηκε να μην έχουν σημαντική επίδραση στην απελευθέρωση Sb από τα εδάφη, καθώς το ίδιο ποσοστό Sb βρέθηκε επίσης στη βιοενισχυμένη επεξεργασία με νερό NBs.

Εν κατακλείδι, το βασικό συμπέρασμα που προκύπτει από την συγκεκριμένη έρευνα είναι η σημαντική συμβολή της τεχνολογίας των νανοφουσαλιδών καθώς βρέθηκε να είναι αποτελεσματική σε διάφορους περιβαλλοντικούς τομείς, όπως η απολύμανση, η διαχείριση λυμάτων και η φυτοεξυγίανση. Επομένως, η εφαρμογή των νανοφουσαλιδών είναι μια πολλά υποσχόμενη μέθοδος και συνίσταται για συστήματα επεξεργασίας νερού και εδάφους.

Table of Contents

Abstract.....	I
Περίληψη.....	V
List of Tables	XIV
List of Figures.....	XV
List of Images	XVIII
Abbreviations	XIX
Reader’s guide	XX
Chapter 1. Introduction and Objectives	1
1.1. Introduction	1
1.2. Objectives of the doctoral thesis	5
1.2.1. Drinking Water and Ballast Water Disinfection by Ozone Nanobubbles (OzNBs)	5
1.2.2. Enhanced aeration in constructed wetland by Air Nanobubbles (ANBs)	5
1.2.3. Antimony removal from soil assisted by Oxygen Nanobubbles (ONBs)	6
Chapter 2. Theoretical Background	7
2.1. Micro- and nanobubbles.....	7
2.1.1. Fundamental Properties	7
2.1.2. Generation Methods.....	11
2.1.3. Monitoring Methods.....	12
Light Scattering Technique.....	12
Nanoparticle Tracking Analysis (NTA)	12
Dynamic Light Scattering (DLS).....	13
Zeta Potential.....	13
Chapter 3. Ozone Nanobubbles in disinfection.....	15
3.1. Ozone micro- and nanobubbles.....	15
3.1.1. Ozone	17
3.1.1.1. Health risks of ozone	18
3.1.1.2. Ozone disinfection mechanism	18
3.1.1.3. Ozone interaction with microorganisms	20
3.1.2. Properties of ozone micro- and nanobubbles	21
Temperature	21

pH	21
Salt concentration	22
Hydroxyl radicals.....	22
3.1.3. Ozone dissolution with micro- and nanobubbles	22
3.1.4. Ozone decomposition rate.....	24
3.1.5. Application of ozone–based Macro- and Nanobubble Technology in Disinfection	28
3.1.5.1. Antimicrobial and disinfection process	28
3.1.5.2. Disinfection of wastewater treatment plant effluents	29
3.1.5.3. Aquaculture	30
Effect of ozone nanobubbles on fish health	32
3.1.5.4. Agriculture	33
3.1.6. Drinking water disinfection.....	35
3.1.7. Ballast water treatment	36
3.2. Materials and Methods.....	39
3.2.1. Ozonation experiments.....	39
3.2.2 Microorganisms, growth condition and cell viability test.....	42
3.2.3. Measurement of dissolved ozone- Indigo Colorimetric Method.....	42
3.2.5. Dynamic Light Scattering (DLS) method	45
3.3. Results.....	46
3.3.1. The size distribution of Ozone Nanobubbles (OzNBs) over time.....	46
3.3.2. Drinking water disinfection.....	47
3.3.2.1. Ozone decay	47
3.3.2.2. Inactivation of bacteria.....	49
<i>Escherichia coli</i>	49
<i>Staphylococcus aureus</i>	52
<i>Bacillus cereus</i>	53
<i>Enterococcus faecalis</i>	54
3.3.3. Seawater disinfection.....	56
3.3.3.1. The effect of ozone concentration and salinity on ozone reaction	56
3.3.3.2 Comparison of effect on ozone reaction with and without the presence of OzNBs	59
3.3.3.3 Comparison of disinfection capacity of ozone with and without OzNBs at different salinities.....	60
3.3.3.4 Reduction of chloride (Cl ⁻) and bromide (Br ⁻) at salinity 15 PSU	65

3.3.4. BPA degradation.....	66
3.4. Conclusions	68
Chapter 4. Air Nanobubbles in constructed wetlands	71
4.1. Hydrocarbon removal performance of CWs supplied by oxygen.....	71
4.1.1. Constructed wetlands (CWs).....	71
4.1.2. Artificial aeration	72
4.1.3 Electrochemical technology.....	72
4.1.4. Hydrocarbons removal in CWs.....	73
4.1.4.1 Phenol.....	73
4.1.4.2. Toluene	73
4.2 Materials and Methods.....	74
4.2.1 Experimental set-up.....	74
4.2.1.1. Vegetation	75
4.2.2 Experimental cycles	76
4.2.2.1. Physicochemical parameters	76
4.2.2.2. Wastewater quality parameters	77
4.2.2.3 Cell concentration and microbial analysis	77
4.2.2.4. Organic compounds analysis	78
4.3. Results.....	78
4.3.1 Cycle 1.....	78
4.3.2. Cycle 2.....	80
4.3.3. Cycle 3.....	82
4.3.4. Cycle 4.....	84
4.3.5. Cycle 5.....	86
4.3.6. Cycle 6.....	88
4.3.7. Cycle 7.....	90
4.3.8. Cycle 8.....	92
4.3.9. Microbial Analysis	95
4.3.9.1 Diversity and composition of bacterial community based on the contaminant and the matrix	96
4.4 Conclusions	102
Chapter 5. Oxygen Nanobubbles in bioremediation	105

5.1 Sb phytoremediation by <i>N. oleander</i> assisted by biostimulation and oxygen nanobubbles	105
5.1.1. Introduction	105
5.1.2. Materials and Methods.....	109
5.1.2.1. Pot experiment	109
5.1.2.2. Soil Characterization	110
5.1.2.3. Soil amendments.....	111
Organic Acids	111
Oxygen Nanobubbles (ONBs) production.....	111
5.1.2.4. Chlorophyll measurements	111
5.1.2.5. Measurement of antioxidant enzymes activity	112
5.1.2.6. Water content and biomass measurement.....	112
5.1.2.7. Heavy metal analysis	113
5.1.2.8. Bioaccumulation factor (BC) and translocation factor (TF)	113
5.1.3. Results.....	114
5.1.3.1. Protein content.....	114
5.1.3.2. Loss of biomass and water content	115
5.1.4. Conclusions	121
5.2. Mobilization of Sb from soil by non-bioaugmented and bioaugmented processes coupled with nanobubble technology.	122
5.2.1. Introduction	122
5.2.2. Materials and Methods.....	123
5.2.2.1. First experimental phase	123
5.2.2.1.2. Isolation of microbial communities resistant to Sb.	124
5.2.2.2. Second experimental phase	125
5.2.2.3. Heavy metals concentration.....	126
5.2.2.3. Physicochemical parameters	126
5.2.3. Results.....	126
5.2.3.1. First experimental phase	126
5.2.3.2. Second experimental phase	136
5.2.4. Conclusions	139
Chapter 6. Conclusions & Future Perspectives	141
Bibliography	143

Appendices	165
Appendix A. The reaction of indigo trisulfonate with the bromine inhibited by the addition of malonic acid	165
Appendix B. Comparison Indigotrisulfonate (ITS) Method to Ozone Test Kit (Hach).....	166
Appendix C. Control bacterial concentration at different salinities without ozone addition .	167
About the Author.....	168

List of Tables

Table 1. Physico-Chemical Properties of Ozone	18
Table 2. Ozone Reactions	19
Table 3. Comparison of ozone dissolution between ozone macrobubbles (OzMaBs) and ozone micro- and nanobubbles (OzMNBs)	26
Table 4. Applications of ozone micro- and nanobubbles (OzMNBs) in Aquaculture	31
Table 5. Acceptable limit of indicator microbes according to the D2 standard (176).	37
Table 6. Reaction of bromide and chloride with ozone (185).	38
Table 7. Fresh water and Seawater Content Description: Physicochemical Parameters	39
Table 8. Effect of time on OzNBs median diameter.	47
Table 9. Ozone half-life time at ozone concentration 1.16, 0.82 and 0.56 ppm with and without the presence of NBs.	51
Table 10. Ozone half-life time at ozone concentration 1.11 and 0.74 ppm with and without the presence of NBs.	51
Table 11. Ozone half-life time at ozone concentration 1.20 ppm and bacterial concentration of <i>S. aureus</i> 10 ⁷ , 10 ⁶ , 10 ⁵ and 10 ⁴ CFU/mL with and without the presence of NBs.	53
Table 12. Ozone half-life time at ozone concentration 1.0 ppm and bacterial concentration of <i>B. cereus</i> 10 ⁶ , 10 ⁵ , 10 ⁴ and 10 ³ CFU/mL with and without the presence of NBs.	54
Table 13. Ozone half-life time at ozone concentration 1.0 ppm and bacterial concentration of <i>E. faecalis</i> 10 ⁷ , 10 ⁶ , 10 ⁵ and 10 ⁴ CFU/mL with and without the presence of NBs.	55
Table 14. TRO half-life time in different salinities	57
Table 15. ORP values in different salinities at ozone concentration 2.5 ppm	59
Table 16. Experimental design of CWs.	76
Table 17. Selected cycles for microbial analysis.	77
Table 18. Experimental Design.	109
Table 19. Measurement of pH before and after the experiment for all treatments.	110
Table 20. Physical and chemical characteristics of the soil used in this study.	110
Table 21. Sb bioconcentration factor (BCF) and translocation factor (TF) for treatments without and with ONBs (star indicates the level of significance: **** for p < 0.0001).	119
Table 22. Fe, Mg and Mn bioconcentration factor (BCF) and translocation factor (TF) for treatments irrigated with and without ONBs * for p < 0.05, **for p < 0.01, **** for p < 0.0001).	121
Table 23. Contaminants concentrations in soils from Swiss shooting range.	124
Table 24. Percent of Mn, Fe and Sb remaining in soil A at the end of non-bioaugmented experiment.	133
Table 25. Percent of Mn, Fe and Sb remaining in soil A at the end of bioaugmented experiment.	133
Table 26. Percent of Sb remaining in soil A at the end of bioaugmented experiment.	137
Table A. 1. Comparison of DPD method with Indigo method with and without malonic acid for residual concentration of oxidants (mg/ L) after 25 min.	165

List of Figures

Figure 1. (a) Annual number of publications for nanobubbles, (b) Annual number of publications for microbubbles.	9
Figure 2. Effect of time on air NBs diameter distribution and zeta potential.....	46
Figure 3. Effect of time on OzNBs diameter distribution.	47
Figure 4. Ozone decay rate with and without the presence of OzNBs in pH a) 5, and b) 7.5 at 13.5°C.	48
Figure 5. Ozone decay rate with and without the presence of OzNBs at 27.5°C.	49
Figure 6. Inactivation of <i>E. coli</i> at bacterial concentration 10^7 CFU/mL and ozone concentration a) 1.16, b) 0.82 and c) 0.56 ppm with and without the presence of NBs.....	50
Figure 7. Inactivation of <i>E. coli</i> at bacterial concentration 10^6 CFU/mL and ozone concentration a) 1.11 and b) 0.74 with and without the presence of NBs.....	51
Figure 8. Inactivation of <i>S. aureus</i> at ozone concentration 1.20 ppm a) 10^7 , b) 10^6 , c) 10^5 and b) 10^4 CFU/mL with and without the presence of NBs.	52
Figure 9. Inactivation of <i>B. cereus</i> at ozone concentration 1.0 ppm a) 10^6 , b) 10^5 , c) 10^4 and b) 10^3 CFU/mL with and without the presence of NBs.....	54
Figure 10. Inactivation of <i>E. faecalis</i> at ozone concentration 1.0 ppm a) 10^7 , b) 10^6 , c) 10^5 and b) 10^4 CFU/mL with and without the presence of NBs.....	55
Figure 11. Effect of salinity on TRO remaining expressed as a percentage of different initial ozone concentrations (0.86 ppm, 1.6 ppm and 2.6 ppm).....	57
Figure 12. Effect of ozone dose on TRO remaining expressed as a percentage of different initial ozone concentrations resulting from transferred ozone doses of 0.86, 1.6 and 2.6 ppm at different salinities (0, 1.5, 4, 8 and 15 PSU).....	58
Figure 13. TRO remaining in different salinities (1.5, 4, 8 and 15 PSU) with and without the presence of OzNBs.....	59
Figure 14. TRO remaining and bacterial concentration after disinfection experiment with and without the presence of ONBs in salinity 1.5 PSU and at bacterial concentration a) 10^7 , b) 10^6 and c) 10^5 CFU/mL (NBD=No bacteria detected).	61
Figure 15. TRO remaining and bacterial concentration after disinfection experiment with and without the presence of OzNBs in salinity 4 PSU and at bacterial concentration a) 10^7 , b) 10^6 and c) 10^5 CFU/mL (NBD=No bacteria detected).	62
Figure 16. TRO remaining and bacterial concentration after disinfection experiment with and without the presence of OzNBs in saline water (8 PSU) and at an initial bacterial concentration a) 10^7 , b) 10^6 and c) 10^5 CFU/mL (NBD implies No Bacteria Detected).....	63
Figure 17. Total residual oxidants (TRO) remaining and bacterial concentrations after disinfection experiments with and without the presence of OzNBs in salinity 15 PSU and at bacterial concentrations: a) 10^7 , b) 10^6 and c) 10^5 CFU/mL (NBD, No Bacteria Detected).	64
Figure 18. Reduction of Chloride (Cl^-) and Bromide (Br^-) at salinity 15 PSU after 10 min of exposure to dissolved ozone with and without OzNBs and for three different initial microbial concentrations.....	66
Figure 19. Degradation of BPA by dissolved ozone with and without OzNBs at initial BPA concentration 0.85 ± 0.04 ppm.	67

Figure 20. Degradation of BPA by dissolved ozone with and without OzNBs at initial BPA concentration 2.1 ± 0.06 ppm. 67

Figure 21. Degradation of BPA by dissolved ozone with and without OzNBs at initial BPA concentration 5.7 ± 0.04 ppm. 68

Figure 22. Phenol removal efficiency (%) versus time (Cycle 1: initial conc.=50 ppm & HRT=12 h). 79

Figure 23. Oxidation- reduction potential (mV) and b) dissolved oxygen (mg/L), c) pH and d) temperature (T °C) in wetlands throughout Cycle 1. 80

Figure 24. Phenol removal efficiency (%) versus time (Cycle 2: initial conc.=50 ppm & HRT=24 h). 81

Figure 25. Oxidation- reduction potential (mV) and b) dissolved oxygen (mg/L), c) pH and d) temperature (T °C) in wetlands throughout the Cycle 2. 82

Figure 26. Phenol removal efficiency (%) versus time (Cycle 3: initial conc.=100 ppm & HRT=24 h). 83

Figure 27. a) Oxidation- reduction potential (mV) and b) dissolved oxygen (mg/L), c) pH and d) temperature (T °C) in wetlands throughout the Cycle 3. 84

Figure 28. Phenol removal efficiency (%) versus time (Cycle 4: initial conc.=200 ppm & HRT=24 h). 85

Figure 29. Oxidation- reduction potential (mV) and b) dissolved oxygen (mg/L), c) pH and d) temperature (T °C) in wetlands throughout the Cycle 4. 86

Figure 30. Toluene removal efficiency (%) versus time (Cycle 5: initial conc.=50 ppm & HRT=24 h). 87

Figure 31. Oxidation- reduction potential (mV) and b) dissolved oxygen (mg/L), c) pH and d) temperature (T °C) in wetlands throughout the Cycle 5. 88

Figure 32. Toluene removal efficiency (%) versus time (Cycle 6: initial conc.=100 ppm & HRT=24 h). 89

Figure 33. Oxidation- reduction potential (mV) and b) dissolved oxygen (mg/L), c) pH and d) temperature (T °C) in wetlands throughout the Cycle 6. 90

Figure 34. a) phenol and b) toluene removal efficiency (%) versus time (Cycle 7: initial conc.=100 ppm & HRT=24 h). 91

Figure 35. Oxidation- reduction potential (mV) and b) dissolved oxygen (mg/L), c) pH and d) temperature (T °C) in wetlands throughout the Cycle 7. 92

Figure 36. a) phenol and b) toluene removal efficiency (%) versus time in wastewater matrix (Cycle 8: initial conc.=100 ppm & HRT=24 h) 93

Figure 37. Oxidation- reduction potential (mV) and b) dissolved oxygen (mg/L), c) pH and d) temperature (T °C) in wetlands throughout the Cycle 7. 94

Figure 38. Wastewater quality parameters in wetlands. 95

Figure 39. Cells concentrations in the three CWs in every cycle. 96

Figure 40. Bacterial community at phylum level in WW. 97

Figure 41. Bacterial community at phylum level in CWs. 98

Figure 42. Bacterial community at class level in WW. 99

Figure 43. Bacterial community at class level in CWs. 100

Figure 44. Bacterial community at genus level in WW. 101

Figure 45. Bacterial community at genus level in CWs. 102

Figure 46. Protein content (mg protein/g FW) in (a) root and (b) leaves for all treatments; control (TR.0), irrigated with tap water (TR.1) and with ONBs (TR.2) (star indicates the level of significance: * for $p < 0.05$).....	115
Figure 47. Loss of weight and water content at the end of the experiment for all treatments; control (TR.0), irrigated with tap water (TR.1) and with ONBs (TR.2) (star indicates the level of significance: * for $p < 0.05$).....	116
Figure 48. GPOD activity in a) leaves b) roots and c) CAT activity in roots per g protein for all treatments; control (TR.0), irrigated with tap water (TR.1) and with ONBs (TR.2) (star indicates the level of significance: *** for $p < 0.001$).....	117
Figure 49. Chlorophyll (a, b, total) content in plant tissues (leaves) for all treatments; control (TR.0), irrigated with tap water (TR.1) and with ONBs (TR.2) at the end of the experiment.	118
Figure 50. Sb accumulation in roots and leaves for for all treatments; control (TR.0), irrigated with tap water (TR.1) and with ONBs (TR.2) (star indicates the level of significance: * for $p < 0.05$).....	119
Figure 51. Accumulation of (a) Fe, (b) Mg, (c) Mn and (d) Sb in roots and leaves for treatments irrigated without and with ONBs (Star indicates the level of significance: * for $p < 0.05$, ** for $p < 0.01$).....	120
Figure 52. Dissolved oxygen concentration in flasks of non-bioaugmented and bioaugmented treatments with ONBs for the three soils (A, B & C).	127
Figure 53. Initial and final concentration of Mn, Fe and Sb in soil A (mg/kg soil) [TW=tap water; NB=tap water with ONBs; A=non-bioaugmented; B=bioaugmented].	128
Figure 54. Initial and final concentration of Mn, Fe and Sb in soil C (mg/kg soil) [TW=tap water; NB=tap water with ONBs; A=non-bioaugmented; B=bioaugmented].	129
Figure 55. Initial and final concentration of Mn, Fe and Sb in soil C (mg/kg soil) [TW=tap water; NB=tap water with ONBs; A=non-bioaugmented; B=bioaugmented].	130
Figure 56. Dissolved oxygen concentration (mg/L) in soils A, B, C [TW=tap water; NB=tap water with ONBs; A=non-bioaugmented; B=bioaugmented].....	131
Figure 57. pH in soils A, B, C [TW=tap water; NB=tap water with ONBs; A=non-bioaugmented; B=bioaugmented].	131
Figure 58. Oxidation- reduction potential (mV) in soils A, B, C [TW=tap water; NB=tap water with ONBs; A=non-bioaugmented; B=bioaugmented].....	132
Figure 59. Bacterial concentration in soils A, B, C throughout the experiments [TW=tap water; NB=tap water with ONBs].	134
Figure 60. The microbial composition (12 most abundant phyla) of the initial community (B2), and the communities in soil and water from soil A and B (A). the heatmap of the 15 most abundant genera of the initial community (B2), and the communities in soil and water from soil A and B (B).	135
Figure 61. The diversity index Shannon within the treatments.	136
Figure 62. Final mass of Mn, Fe and Sb in aqueous phase (mg) in bioaugmented experiments with soil A coupled with ONBs technology.....	137
Figure 63. ORP (mV), pH, DO (mg/L) during the experiment.....	138
Figure 64. Bacterial concentration in bioreactor.....	139

Figure A. 1. Comparison of DPD method with Indigo method for residual concentration of oxidants (mg/ L)..... 165

Figure B. 1. Comparison of the ozone concentrations with Indigo-trisulfonate Method and the Ozone Test Kit (Hach)..... 166

Figure C. 1. Control bacterial concentration at different salinities without ozone addition at initial bacterial concentration a) 10^7 CFU/mL, b). 10^6 CFU/mL and c) 10^5 CFU/mL. 167

List of Images

Image 1. Range of bubbles sizes and corresponding major properties. 8

Image 2. Experimental set-up for generation of fresh water with dissolved ozone and with the presence of ozone nanobubbles for treatment of tap water and seawater..... 40

Image 3. Indigo decolorization with regards to ozone concentration..... 43

Image 4. Three constructed wetlands; left) control- CW1, middle) air nanobubble-integrated- CW2, and right) electrolysis-integrated- CW3..... 75

Image 5. Experimental set up of the first experimental phase. 124

Image 6. Experimental set-up of the second experimental phase..... 125

Abbreviations

ANBs	Air Nanobubbles
AOPs	Advanced Oxidation Processes
BCF	Bioaccumulation factor
BPA	Bisphenol A
BTEX	Benzene, Toluene, Ethylbenzene and Xylene
CAT	Catalase
CFU	Colony forming unit
CWs	Constructed Wetlands
DLS	Dynamic Light Scattering
DO	Dissolved oxygen
DOC	Dissolved organic carbon
EOCs	Emerging Organic Contaminants
GPOD	Guaiacol-peroxidase
HRT	Hydraulic residence time
HSF	Horizontal subsurface flow
EDCs	Endocrine-disrupting chemicals
MaBs	Millibubbles or macrobubbles
MBs	Microbubbles
MNBs	Micro-nanobubbles
NB	Tap water with ONBs
NBs	Nanobubbles
NTA	Nanoparticle Tracking Analysis
OAs	Organic acids
ONBs	Oxygen Nanobubbles
OOM	Ozone Oxidation Method
ORP	Oxidation-reduction potential
OTR	Oxygen Transfer Rate
OzMaBs	Ozone Macrobubbles
OzMBs	Ozone Microbubbles
OzMNBs	Ozone Micro-nanobubbles
OzNBs	Ozone Nanobubbles
RI	Refractive index
PSU	Practical salinity units
Sb	Antimony
Sb (III)	Antimonite
Sb (IV)	Antimonate
TF	Translocation factor
TOD	Transferred ozone dose
TRO	Total residual oxidants
TW	Tap water
WW	Wastewater
WWTPs	Wastewater Treatment Plants

Reader's guide

Chapter 1 presents a brief introduction in the proposed application of nanobubbles technology in various environmental sectors and describes the main objectives of this dissertation thesis.

Chapter 2 begins by laying out the theoretical background concerning the nanobubbles. This part covers the methods of the generation and the applications that are used for.

Chapter 3 is concerned with the implementation of ozone nanobubbles technology in drinking water and ballast water disinfection. The experimental design, the results and the main conclusions are analytically presented.

Chapter 4 focuses on the application of air nanobubbles in constructed wetlands. The methodology used for this study is described. The remaining part presents the results and the conclusions that can be drawn.

Chapter 5 analyzes the performance of oxygen nanobubbles in phytoremediation and bioreactor operation. All the experimental processes are extensively described. Finally, the results and the conclusions that arise from this study are provided.

Chapter 6 discusses in detail the main conclusions derived from the experimental results of the aforementioned experimental processes. A discussion of the contribution of the findings to future research is also included.

Chapter 1.

Introduction and Objectives

1.1. Introduction

Nowadays, the mass production of wastewater, due to extensive urbanization and industrialization, is of major concern since it poses a remarkable threat to existing water resources and it is accounted for the water scarcity that is now among the most serious problems faced by many countries (1). Consequently, wastewater reclamation and reuse are extremely important to meet the demands arising from the inadequate water supply. Wastewater treatment focuses on decreasing the concentration of specific pollutants to safe levels for effluent reuse and discharge on the environment. Treatment methods including a combination of biological and physical processes are employed for wastewater treatment, depending primarily on operational costs, as well as the source and the quality of wastewater and the intended reuse of the effluent (2). Conventional wastewater treatment is not sufficient to meet the required standards for the wastewater effluent disposal, since it cannot reduce the levels of heavy metals, toxic compounds and the emerging organic contaminants (EOCs) due to the persistent occurrence of these contaminants in the aquatic environment (3). As it is well known, the treated effluent from the Wastewater Treatment Plants (WWTPs) is the major pathway of the micro-pollutants (e.g pharmaceuticals, personal care products, estrogens, etc.) discharge in water bodies, considering the conventional WWTPs have not been designed for their elimination, attracting increasing concern from the international scientific community (4,5). Within the context of upgrading the wastewater treatment process, the development of new technologies is addressed, with

a view to providing high quality water at the least possible cost to the consumers. Therefore, new technologies have emerged to enhance the removal efficiency for a sustainable and effective treatment. For instance, in the wastewater treatment systems, the oxidation reactions are augmented by increased dissolved oxygen levels (6). Hence, methods that can enhance the dissolution efficiency of oxygen and increase its aqueous concentration are of great importance. Oxygen delivered as nanobubbles (NBs) with radii less than 1 μm may enhance the mass transfer efficiency as they can persist and even stay for weeks in the aqueous phase in contrast to conventional bubbles. In this regard, the application of NBs technology is paving the way to novel integrated and highly efficient treatment system.

NBs are tiny spherical bubbles with a diameter less than 1 μm and exhibit notable properties in comparison to macrobubbles (MaBs). First and foremost, the long residence time thanks to their stability is highlighted as a vital property (7–9). It has been found that NBs remain stable in aqueous solution for a long period of time, due to their negligible buoyancy, when compared to use of MaBs, which take a short period of time to reach the liquid surface, where they burst out (10,11). Considering their unique characteristics, NBs improve the mass transfer effect and the oxidation ability, on account of the fact that the contact area of gas and water is increased (12). Moreover, the gas solubility and chemical reactions at the gas-liquid boundary are remarkably enhanced (8,11). A few experimental tests on NBs in water found that there is a great potential to promote the growth of lives of plants, fishes and mice (11). In addition, as stated in findings in biology, the application of NBs is thought to promote the germination of barley seeds (13). Preliminary work in this field shows that this technology has attracted attention and is considered a great breakthrough with many applications in wastewater treatment.

In terms of water treatment processes, the Ozone Oxidation Method (OOM) is widely used in Europe. Ozonation is included in Advanced Oxidation Processes (AOPs) and is applied in order to inactivate pathogenic organisms for the prevention of waterborne diseases spread to users and the environment. Ozone has a considerable oxidizing capacity, and it can be rapidly decomposed in water partly in more reactive and less selective free radical form (OH^\cdot). Both HO_2 and the OH^\cdot radicals are highly reactive and play a fundamental role in disinfection process since the bacteria are destroyed due to the

protoplasmic oxidation leading to cell wall disintegration (cell lysis) (14). It is well-documented that ozonation is far more effective against bacteria and viruses than the process of chlorination. However, the effectiveness of this method is limited by the fact that ozone is unstable and short-lived as the decay rate in water is high, resulting in an approximate half-life time (as a function of temperature) over a time frame ranging from one to thirty minutes (15). It is worth-mentioning that the half-life time of ozone in gas phase is much higher than in aqueous phase. In more detail, at 20°C the gaseous ozone will be degraded in 3 days, in contrast the degradation of dissolved ozone in water will take place within only 20 minutes. Due to its low utilization efficiency, more attention must be paid on how the ozone can be used in a more efficient way. By exploiting the higher gaseous ozone half-life time (3 days versus 20 min at 20°C) and the noteworthy properties of NBs technology, the Ozone Nanobubbles technology (OzNBs) is proposed, which is expected to improve the disinfecting effect and even more the residual activity in a feasible way. Apart from water treatment, research on their disinfection capacity in ballast water treatment remains limited. There are some investigations about the generation of nanobubbles under different salt concentrations, however, there is no literature about the disinfection capacity of OzNBs in real seawater (12). The sodium chloride present in seawater reacts quickly with ozone generating a mixture of oxidants which kill microbial pathogens. In addition, it is important to examine the inactivation efficiency when OzNBs are used in the presence of bromide in order to estimate the concentration of by-products derived from the reaction between the ozone and the bromide and compare with that created in a typical ozonation (16).

As stated previously, the wastewater treatment is insufficient to handle the input of pollutants in the environment. Hydrocarbon contamination is considered a serious concern for the environment and is becoming prevalent across the globe due to their extensive use. Among the various hydrocarbons, phenolic compounds derived from industrial, agricultural and domestic activities exist into water bodies (17). Constructed Wetlands (CWs) have been verified to be a low-cost and environmentally sustainable technology frequently used to treat different types of wastewater, including municipal, urban, agricultural, industrial etc. (18) CWs have been used to treat hydrocarbons contaminated waters since they offer numerous advantages (19). Specifically, the removal of phenols and

polyaromatic hydrocarbons were selected as targeted pollutants because of the dire need to address their remediation since they are highly accumulative in water and non-biodegradable (20). CWs display an efficient performance of PAH removal; over 99% of PAHs were removed with *Phragmites australis* and other kinds of wetland plants from subsurface flow CW (21). The performance of the CWs can be influenced by various operational and environmental factors, such as hydraulic loading rate (HLR), hydraulic retention time (HRT), pH, temperature, dissolved oxygen (DO) (22). The latter is among the most fundamental factors that plays a key role in pollutants removal in CWs, since it can have a strong impact on microbial activities and subsequently on efficiency of pollutants removal. Supplying additional sources of aeration can enhance both the oxidations and nitrification processes (23). The addition of artificial aeration can provide air bubbles to the saturated water column of the wetland and can lead on oxygen intensification. Hence, oxygen is transferred from the gaseous to dissolved phase, increasing the oxygen transfer rate (OTR) into the treated water, therefore aerated wetlands offer an enhanced treatment capacity (24). Hence, the oxygen delivery via nanobubbles can further enhance the transfer rate owing to their high stagnation time. A comprehensive study is performed in order to investigate the hydrocarbons removal by constructed wetlands assisted by air nanobubbles (ANBs).

Soil contamination by heavy metals and metalloids is a worldwide problem due to their accumulation, since they are non-biodegradable. Therefore, they can cause damage associated to adverse effects on the environment, animals and humans (25). Sb is recognized as a priority pollutant, that can cause acute environmental issues since it is released into soils and aquatic environments by natural processes and mainly by human activities such as mining, coal combustion and shooting of weapons (26). Apart from the environmental risk, Sb is considered hazardous to human health as it is a suspected carcinogen due to its toxicity (27). Specifically, trivalent compounds of antimony have been found to be more toxic (10 times) than the pentavalent ones. In soil, Sb is mostly encountered in the forms of Sb(III) and Sb(V) and the latter shows higher water solubility (28). Sb has been recorded to exceed the value of 5000 mg/kg when background concentration in the natural environment is only 0.2 mg/kg and the maximum permissible concentration according to the World Health Organization is set at 36 mg/kg (29). The

remediation of metal polluted soils has attracted attention and ranges from physical and chemical methods to biological methods. An economical and environmentally friendly remediation technique is the biological approach; bioremediation. The use of microorganisms in metals' removal from contaminated environment is generally considered promising, since several microorganisms exhibit degradation capacity (30). Moreover, the present research study investigates bioremediation potential of microbial culture isolated from heavy metal-contaminated site using oxygen nanobubbles (ONBs) on Sb removal from soil.

1.2. Objectives of the doctoral thesis

1.2.1. Drinking Water and Ballast Water Disinfection by Ozone Nanobubbles (OzNBs)

One of the main objectives of this dissertation thesis was to develop and implement an innovative and cost-effective technology for drinking water disinfection, using ozone nanobubbles as an alternative to chlorination, which is prone to form harmful byproducts. The research was focused on the inactivation of bacteria commonly used as primary indicators of contamination in fresh water quality. The correlation between the disinfection efficiency and the ozone dose was examined. Furthermore, the aim of this study was to investigate the disinfection capacity in ballast water treatment compared to a conventional ozonation system, in order to reassure the good quality of discharged ballast water. The main objective of this research is to evaluate whether the use of OzNBs has any significant impact on microorganism inactivation and residual activity of ozone in different salinities.

1.2.2. Enhanced aeration in constructed wetland by Air Nanobubbles (ANBs)

This thesis was a preliminary attempt to evaluate the treatment efficiency of the designed CWs tested for the treatment of target pollutants (phenol, toluene) with and without the addition of domestic wastewater from WWTP located in Platania (Chania, Greece) assisted by the supplementation of additional source of aeration. The main objective of this study were to gain an insight of hydrocarbon degradation and to identify

the microbial communities that may participate in this process exhibiting degradation capability.

1.2.3. Antimony removal from soil assisted by Oxygen Nanobubbles (ONBs)

The goal of this study was to evaluate the effectiveness of ONBs technology for remediation of Sb from contaminated soils. The phytoremediation potential of *Nerium oleander* for antimony-contaminated soils was examined. The ability of *N. oleander* to uptake, translocate and tolerate Sb using nanobubbles technology was investigated. Furthermore, the Sb remediation potential of microbial communities and isolates collected from contaminated soils with gradient Sb concentration was investigated. Enrichment cultures were performed and the ability of the communities to remove and oxidize Sb(III) was assessed. Sb resistant bacteria inoculum was added in a bioreactor containing Sb-contaminated soil to examine the mobilization of Sb in the aqueous phase by biotic processes coupled with nanobubble technology.

Chapter 2.

Theoretical Background

2.1. Micro- and nanobubbles

Micro- and nanobubbles (MNBs) are microscopic gas bodies sized at micro (<100 μm) and nanoscale (<1 μm), that have a long lifetime in aqueous solutions and large specific surface area due to their small size. MNBs technology is novel and vitally important owing to the ability to generate highly reactive free radicals (7). In general, microbubbles (MBs) and nanobubbles (NBs) are microscopic gaseous bodies sized with diameters from tens of nanometres to several tens of micrometres. Since the majority of commercially available generators produce gas-carrying bubbles with a diameter within micro- and nano-range, a significant amount of research has been conducted on the use of MNBs technology (31–34). Properties of MNBs and generation techniques are briefly discussed besides the monitoring methods for their characterization in terms of size and number.

2.1.1. Fundamental Properties

According to Temesgen *et al.*, there is no clear definition in terms of diameter size of MNBs. A proposed categorization is that MBs and NBs are in size scale at 10–100 μm and less than a micron, respectively even though in many studies MBs are classified less than 50 μm and NBs less than 200 nm. In this study, based on the majority of existing studies, MBs are defined less than 100 μm and NBs less than 1 μm (35). As seen in Image 1, bubbles have different properties based on their size. In particular, large bubbles, known as millibubbles or macrobubbles (MaBs) rise rapidly and directly to the liquid surface, where they burst out (36). Compared to ordinary large bubbles, microbubbles have several interesting features such as longevity in aqueous solutions

due to low rising velocity, large gas-liquid interfacial area (37) and the most important the generation of hydroxyl radicals by their collapse providing an oxidation ability, which makes the dissolution easier (38).

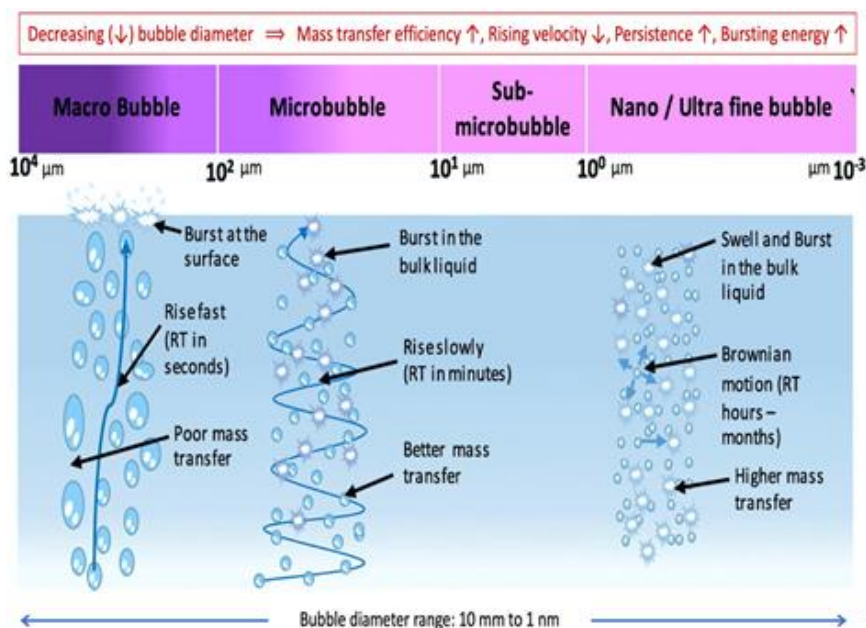


Image 1. Range of bubbles sizes and corresponding major properties.
«Schematic diagram adapted from Temesgen *et al.* (35)»

So far, a number of researchers have recognized the significance of these properties and they have employed MBs technology in various applications (39–44). In particular, the striking property of MBs, high surface area per unit volume has been used for degradation of organic pollutants and water disinfection (7). Nevertheless, they have been found to be unstable for a long period of time (~min), rising slowly to the liquid surface (35). Smaller bubbles than MBs, classified as nanobubbles display noteworthy stability resulting in high stagnation times (11,45). NBs can remain stable in aqueous solution for a long period of time (weeks), due to their negligible buoyancy and excellent stability against coalescence (8,10). Considering their unique characteristics, they improve the mass transfer and oxidation ability, simply because the gas/liquid contact area is increased (12). Moreover, the gas solubility and chemical reactions at the gas-liquid interface are remarkably enhanced (8,11).

The degree of nanobubbles stability is associated with the absolute value of zeta potential, which is presented in detail in the “Monitoring Methods” section. More recent evidence (46) highlights that the generation of smaller and more stable nanobubbles is

achieved in solutions of high pH, low temperature and low salt concentrations. Another study by Hewage *et al.* demonstrated the stability of nanobubbles for one week in solutions of different electrolytes at a low concentration (0.001 M), confirming that the neutral and high pH values under low valency cation adsorption leads to negative charged bubbles (47). The highest negative charge of bulk nanobubbles and therefore their stability was also reported in alkaline solutions by Michailidi *et al.* In the case of oxygen and air nanobubbles, the magnitude of negative zeta potential increases as pH increases (48). Thus far, a number of studies have reported that they have widely applied NBs in water treatment, aquaculture, agricultural cultivation, health preservation, mineral flotation (49) and in removing organic pollutants in wastewater treatment (50,51). It is crucial to note that in relevant scientific literature, there is remarkable growth in microbubbles and nanobubbles-related citations and publications over the last 20 years as presented in Figure 1 (52).

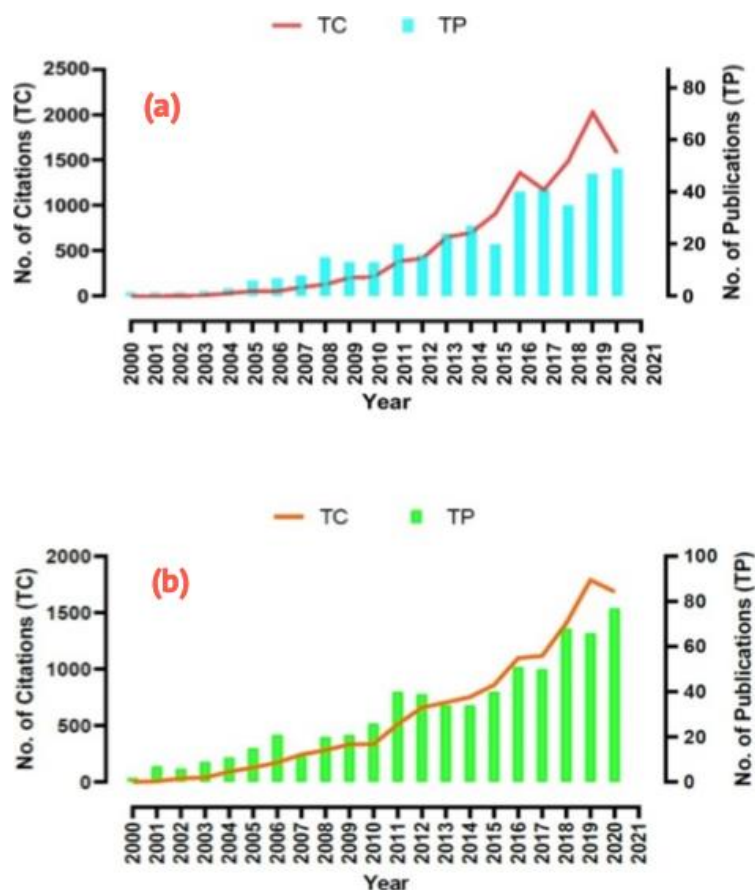


Figure 1. (a) Annual number of publications for nanobubbles, (b) Annual number of publications for microbubbles.

«Figure adapted from Movahed and Sarmah (52) »

However, there is still considerable controversy surrounding the existence and the stability of bulk NBs. In order to ascertain that the stable detected nonentities are gas-filled domains and not impurities or nanodroplets, many analytical experimental techniques have been employed (53–58).

Even though, there is considerable discussion in the literature on whether NBs can exist or are thermodynamically stable, it has been demonstrated that the Young-Laplace equation is valid even at nanoscale (59). More precisely, the pressure inside the gas cavities is defined in relation to the diameter of bubbles in accordance to the thermodynamic calculation based on Young –Laplace:

$$P_{in} = P_{out} + \frac{2 \cdot \gamma}{r}$$

where, P_{in} is the internal pressure inside a gaseous bubble (N/m^2), P_{out} is the pressure of bulk liquid (N/m^2), γ is the surface tension (mN/m) and r is the radius of bubbles (nm). It is estimated that a radius of NBs equal to 100 nm can result in an internal pressure $1.5 \times 10^6 N/m^2$ when the surface tension is 72 mN/m and the atmospheric pressure in the surrounding water is $10^5 N/m^2$ (9) .

Hence, the inner pressure of the bubble increases when the size decreases which is expected to lead to a rapid dissolution and disappearance within seconds. Prior study describes the lifetime (t_b) of a bubble according to the following equation:

$$t_b = \frac{Kd_o^2}{12RTD}$$

where, K is the Henry's law constant (J/mol), d_o is the bubble diameter at $t=0$ (nm), R is the gas constant $J/(K \cdot mol)$, T is the temperature (K) and D is the diffusion constant (m^2/s). For instance, a nanobubble with a diameter 100 nm should exist for only 10 μs (53,60). Surprisingly, this is not the case with nanosized gas cavities which can stay in aqueous solutions for prolonged periods of time (up to 12 months) compared to larger bubbles (11).

In order to explain the longevity of nanobubbles, Ohgaki *et al.* proposed that the surfaces of nanobubbles contain strong hydrogen bonds at the gas-liquid interface similar to those found in ice and dehydrated gas. This ameliorates the stability of NBs as it decreases the gas diffusion in liquid, which contributes to kinetic balance against high internal pressure (45). Another possible explanation for the stability of NBs is that

it may be dependent on the selective adsorption of anions at the interface that could result in electrostatic repulsive forces, leading to balance the compressive force from surface tension. Hence, a non-contact between gas molecules inside the NBs and the bulk liquid is created due to balance of these forces from the surface tension (61).

2.1.2. Generation Methods

In the case of bulk nanobubbles, as mentioned in a recent review by Zhou *et al.*, two main pathways can lead to their formation and generation. The first one is the emergence of the new gas phase from the liquid phase through nucleation and the second through the collapse of microbubbles (49). The formation, the growth and the collapse of microbubbles in solution can be defined as cavitation and there are four types based on the mode of generation (7,46,61,62) :

- Hydrodynamic cavitation describes the pressure variation in a moving fluid due to the change in the geometry of the system leading to the occurrence of vaporization and generation of bubbles. In order to enhance the generation of nanobubbles, hydrodynamic cavitation by mechanical agitation, by axial flow shearing and through depressurized flow constriction have been proposed (63).
- Acoustic cavitation can be created by applying ultrasonic waves to liquids leading to local pressure variations and subsequently to the formation of bubbles.
- Optical cavitation includes short-pulsed lasers focused into low absorption coefficient solutions.
- Particle cavitation produces nanobubbles by electric discharge or elementary particles in water through passing high intensity light photons in liquids.

Moreover, electrolysis (64), applying nanopore membranes (65), sonochemistry using ultrasound (66) and water-solvent mixing (57) have been used to form ultra-fine bubbles.

The generation of nanobubbles is influenced by several factors such as pressure, temperature, type and concentration of dissolved gas and electrolyte solution (61). As

of today, there are many commercially available nanobubble generators, mostly for laboratory or small pilot applications (9).

2.1.3. Monitoring Methods

Several methods have been reported in the literature for the measurement of the size distribution of MNBs (49,67–69). The size detection of bubbles has become a crucial issue in classification of ultrafine bubbles due to the fact that it is complex to distinguish the gas bubbles from other colloidal dispersions such as oil nanodroplets or nanoparticles. Undoubtedly, there is a need for the development of techniques with higher level of sensitivity and spatial resolution. Until now, most researchers have utilized mostly Dynamic Light Scattering (DLS) and Nanoparticle Tracking Analysis (NTA), both based on scattering and diffraction of laser on the micro- and nanobubbles (70).

Light Scattering Technique

The light scattering method is a simple and easy monitoring method based on Tyndall effect (48,71). More precisely, as a light beam passes through a colloid, the light scatters and reflects light, making the beam visible (72). Hence, as the nanobubbles do not rise quickly they can be illuminated by a laser beam and can be viewed with bare eyes while in a clean solution no laser beam can be detected (73). It is an ideal method for simple detection in clear water.

Nanoparticle Tracking Analysis (NTA)

Nanoparticle tracking analysis offers direct and real-time visualisation of nanoparticles in liquids and size determination within the size range ~10 to 1000 nm (74). This technique captures the movement of each scattering object with dark field microscopy and their sizes are derived from the analysis of the particles trajectories. It should be highlighted that this technique can also provide adequate information about the particle concentration (75), which is fundamental for the estimation of the micro/nanobubbles generator performance. The main advantage of this technique is that it can record individual particles providing higher resolution and visual information, and thus some kinetic processes can be observed, such as aggregation phenomena (76). However, the main drawback is the analysis of particles with low refractive indices (RI)

compared to the background, as it becomes somewhat challenging due to low light scattering intensity (75).

Dynamic Light Scattering (DLS)

Dynamic Light Scattering is among the most widely used methods to measure the size distribution of micro- and nanobubbles, typically ranging from 0.5 nm to 6 μm . A laser beam illuminates the sample and the fluctuations of the scattered light are detected by a photon detector at a scattering angle θ . The particles follow the Brownian motion, with the larger giving greater scattering but slower fluctuations. Analysis of the intensity fluctuations can provide the particle size distribution (9). The results obtained by light scattering alone may be misleading as a result of the high sensitivity to nano-sized contaminants. Therefore, it is recommended the combination of this technique with acoustic-based flow cytometry in order to ascertain the existence of nanobubbles instead of particles (77). A study conducted by Gnyawali *et al.* demonstrated that the acoustic flow cytometer can be used in order to detect individual NBs using high-frequency ultrasound and photoacoustic waves since the amplitude of the detected ultrasound backscatter signal is dependent on the NBs size (78).

Zeta Potential

Another method of gas bubbles detection that is often used is the measurement of the zeta potential value. Nanobubbles have strong electron affinity and that is identified by a high magnitude of zeta potential ranging from 10 to 50 mV in absolute values. The measurement of zeta potential shows high negative values in most studies verifying that NBs in solution are normally negatively charged (46,79,80). This can be illustrated by the preferential adsorption of hydroxide ions (OH^-) at the gas-liquid interface (81), which results in electrostatic repulsive forces leading to balance the compressive force from surface tension. Thus, aggregation and coalescence of NBs are prevented (82). Other methods employed for monitoring of nanobubbles are Resonant Mass Measurement (RMM) (83), Electron Microscopy (84) and Electrical Sensing Zone method (85).

“This page intentionally left blank”

Chapter 3.

Ozone Nanobubbles in disinfection

Part of this chapter is based on the following publications:

Seridou P., Kalogerakis N. Disinfection applications of ozone micro- And nanobubbles. *Environ Sci Nano*. 2021;8(12):3493–510.

Seridou P., Kotzia E., Katris K. and Kalogerakis N. Ballast water treatment by ozone nanobubbles. *J Chem Technol Biotechnol*. 2023; <https://doi.org/10.1002/jctb.7385>

3.1. Ozone micro- and nanobubbles

Nowadays, the mass production of wastewater derived from increasing population and industrialization is of major concern since it poses a remarkable threat to existing water resources. Consequently, reclamation and reuse of wastewater are extremely important to meet the human needs arising from inadequate water supplies. However, the core problem of reclaimed water is that it may contain different types of resistant pathogens and persistent organic compounds (86). The microbiological quality plays a crucial role for any potential reuse options, and hence, the presence and persistence of antibiotic-resistant bacteria (ARB) and antibiotic resistance genes (ARG) after tertiary treatment is considered an issue of great importance regarding public health (87–91). In order to prevent the dispersal of ARB, several treatment strategies have been tested and their inactivation efficiency was evaluated (92–94), however, most of these studies have not been conducted in real drinking water and/or wastewater revealing a considerable risk arising from the reduced disinfection ability compared to non-resistant bacteria (95). Emerging organic contaminants (EOCs) consist of a large and relatively new group of compounds covering complex synthetic or naturally occurring molecules or even any microorganism, not commonly monitored in the

environment (96). These chemical compounds are classified as endocrine disrupting chemicals (EDCs), pharmaceutically active compounds (PhACs) and personal care products (PCPs), which even in low concentrations (from ng/L to µg/L) may have detrimental ecological and human health effects (97–99). Moreover, in the last couple of decades, it is well documented that the effluent of WWTPs is the major pathway to aquatic environment (3,100–103), since they are poorly removed by the conventional activated sludge treatment (5). The emergence of new contaminants in effluent wastewater streams has led to the development of advanced technologies in order to achieve an efficient degradation of these emerging contaminants (104–106).

Conclusively, bacterial contamination and subsequent infections are recognized as a major threat to human health and there is dire need to prevent the waterborne diseases to ensure water safety. Moreover, attention must be paid on the occurrence and fate of trace organic compounds that have become an emerging concern, since conventional wastewater treatment plants (WWTPs) have not been designed for their elimination leading to their discharge to natural water bodies. Within the context of upgrading the water and wastewater treatment processes, the development of new disinfection technologies is addressed, with a view to provide high quality water at the least possible cost to the consumers

Recently, scientific interest has been focused on ozone micro- and nanobubbles (OzMNBs) used in disinfection processes since research findings support the idea that ozone micro and nanosized bubbles can significantly improve the disinfection capacity and the residual activity of ozone. Specifically, air MNBs are used to improve gas-liquid contacting and achieve increased effectiveness and enhanced mass transfer compared to conventional aeration including the use of ozone/air mixtures for more efficient ozonation (56,57). By utilizing the higher gaseous ozone half-life time (3 days versus 20 min at 20 °C) and the remarkable properties of ultra-fine bubbles, the ozone delivery by MNBs has been found to improve the disinfection capacity and the residual concentration. In this regard, the application of OzMNBs technology is paving the way to novel integrated and highly efficient disinfection systems.

The attribute of micro and nanobubbles to ozonation has stimulated widespread interest, and hence, a growing body of literature has investigated the effect of combined micro- and nanobubbles technology and ozonation in many fields of engineering and wastewater treatment (58–61). Despite the considerable progress in academic studies

related to MNBs, there are limited comprehensive reviews that focus on the ozonation technology applied to disinfection. The aim of this chapter is to investigate the feasibility of ozone-based disinfection processes by exploiting the strong oxidizing ability of ozone and the noteworthy longevity of MNBs in aqueous solutions.

3.1.1. Ozone

Ozonation is recognized as a favourable treatment method since ozone is an extremely powerful oxidant and is used to inactivate pathogenic microorganisms for the prevention of waterborne diseases spread to users and the environment (14). Furthermore, ozone in aqueous solution auto-decomposes quickly and is converted to oxygen resulting in no harmful residues. However, this is also the main limitation of this method as ozone dissolved in water is unstable and short-lived and hence, the residual action in a drinking water network is very limited. Ozone has been applied for primary disinfection in drinking water treatment since the beginning of the 20th century and its use is becoming gradually more common. It is an unstable trioxygen molecule and therefore it must be generated onsite. As it is a very strong oxidant among other commonly used disinfectants (free chlorine, chlorine dioxide and UV light), it provides an excellent inactivation capacity against waterborne pathogens including bacteria, viruses, protozoa and endospores (107). Disinfection parameters such as ozone concentration and contact time are very important for the design of disinfection systems and depend strongly on the operating temperature. Moreover, the rate of inactivation of microorganisms by ozone depends on the type of organism and can vary by about four orders of magnitude. Moreover, other factors that influence the disinfection efficiency are the dissolved organic carbon (DOC), pH and bromide concentration.

Table 1. Physico-Chemical Properties of Ozone

Property	Value
Molecular Weight	48
Density	2.144
Melting Point, °C	-251
Boiling Point, °C	-112
Specific gravity	1.658 higher than air 1.71 gcm ⁻³ at -183°C
Oxidation Potential, V	2.07 (Hydroxyl radical 2.80)
Henry Constant at 20 °C	100 atmM ⁻¹

3.1.1.1. Health risks of ozone

In waters containing significant concentrations of bromide, the required ozone exposures for a certain degree of inactivation may lead to high levels of bromate, which is a carcinogen for humans (108). Thus, in many applications bromate formation may be the limiting factor, and measures have to be taken to comply with the drinking water standard (109). According to a study conducted by Rice *et al.*, in order to meet the requirements for an efficient microbial disinfection in drinking water treatment, the usual ozone dosage is 1.5 to 2 mg/L, while for viral inactivation, a residual ozone concentration of 0.4 mg/L should be detected at least 4 min after the initial ozone dosage (110). Ingestion of drinking water treated by ozone poses no danger since ozone is short-lived and all the concentration present in water will decline to zero when reaching the consumer through the distribution system. However, there is a significant risk though the direct exposure to ozone; inhalation since it is very corrosive. Exposure to ozone at levels below 1 ppm for 10 min is asymptomatic. More severe exposures (1.5 to 2 ppm of ozone for 2 h) produce acute symptoms, such as dryness of mouth and throat, chest pains, coughing etc. (110).

3.1.1.2. Ozone disinfection mechanism

Ozone can react with microbes and contaminants in two different ways, directly and indirectly. Direct reactions involve ozone molecules and are very specific. On the other hand, the indirect reaction involves free hydroxyl radicals (OH•) produced by the ozone decomposition in water and are more reactive ($E_o = 2.80$ V) and less selective

than ozone ($E_0 = 2.07$ V). The pH of water is a vital factor in ozone decomposition, because of the fact that hydroxyl ions can initiate the reactions that take place. The direct ozonation dominates when $\text{pH} < 4$, while the indirect pathway prevails above pH 10. In waters with $\text{pH} = 7$, both direct and indirect ozone reactions can be important and they should be taken into account in the process of treatment design (111). The mechanism and kinetics of the basic reactions regarding the ozone decomposition was under investigation by many researchers (112). The interpretation of the processes is based on the following reactions in alkaline medium proposed by Tomiyasu *et al.* (113). In acidic medium, the sequence of reactions taking place are also listed in Table 2 (114).

Table 2. Ozone Reactions

No	Reactions	Rate constant
In alkaline medium		
1	$\text{O}_3 + \text{OH}^- \rightarrow \text{O}_2 + \text{HO}_2^-$	$k_1 = 40 \text{ M}^{-1} \text{ s}^{-1}$
2	$\text{O}_3 + \text{HO}_2^- \rightarrow \text{O}_3^{\bullet-} + \text{HO}_2$	$k_2 = 2.2 \times 10^6 \text{ M}^{-1} \text{ s}^{-1}$
3	$\text{HO}_2 + \text{OH}^- \leftrightarrow \text{O}_2^- + \text{H}_2\text{O}$	$\text{pK} = 4.8$
4	$\text{O}_2^{\bullet-} + \text{O}_3 \rightarrow \text{O}_3^{\bullet-} + \text{O}_2$	$k_4 = 1.6 \times 10^9 \text{ M}^{-1} \text{ s}^{-1}$
5	$\text{O}_3^{\bullet-} + \text{H}_2\text{O} \leftrightarrow \text{HO}^\bullet + \text{O}_2 + \text{OH}^-$	$k_5 = 20\text{-}30 \text{ s}^{-1}$
6	$\text{O}_3^{\bullet-} + \text{HO}^\bullet \rightarrow \text{O}_2^- + \text{HO}_2$	$k_6 = 6 \times 10^9 \text{ M}^{-1} \text{ s}^{-1}$
7	$\text{O}_3^{\bullet-} + \text{HO}^\bullet \rightarrow \text{O}_3 + \text{OH}^-$	$k_7 = 2.5 \times 10^9 \text{ M}^{-1} \text{ s}^{-1}$
8	$\text{O}_3 + \text{HO}^\bullet \rightarrow \text{HO}_2 + \text{O}_2$	$k_8 = 3 \times 10^9 \text{ M}^{-1} \text{ s}^{-1}$
In acidic medium		
9	$\text{O}_3 \leftrightarrow \text{O} + \text{O}_2$	
10	$\text{O} + \text{H}_2\text{O} \rightarrow 2\text{HO}^\bullet$	
11	$\text{HO}^\bullet + \text{O}_3 \rightarrow \text{HO}_2^\bullet + \text{O}_2$	$k_{11} = 1.1 \times 10^8 \text{ M}^{-1} \text{ s}^{-1}$
12	$\text{HO}_2^\bullet + \text{O}_3 \rightarrow \text{HO}^\bullet + 2\text{O}_2$	$k_{12} < 10^4 \text{ M}^{-1} \text{ s}^{-1}$

An important reaction is the first one in Table 2, where ozone reacts with OH^- and hence, it is greatly dependent on pH. At alkaline pH, Eq. (5) describes the generation of HO^\bullet . Higher concentration of hydroxyl ions leads to the increased generation of HO_2^- , O_2^- , O_3^- and HO^\bullet . At $7 < \text{pH} < 9$, the generation of hydroxyl radicals is slow corresponding to the rate constant of the reaction No.5 ($20\text{--}30 \text{ s}^{-1}$). The propagation and termination reactions [i.e., those given by Eqs. (6)–(8)] are very fast, leading to a lower concentration of HO^\bullet (115).

However, in acidic medium, a different mechanism is involved, as the reaction with OH^- cannot be the initiation step. According to Sehested *et al.*, it is proposed the thermal dissociation of ozone to form an oxygen atom, which is followed by the reaction of this atom with water to form the hydroxyl radical [i.e., those given by Eqs. (9)-(10) (114)]. Then, the hydroxyl radical reacts with ozone to form the perhydroxyl radical (HO_2^\bullet).

3.1.1.3. Ozone interaction with microorganisms

Ozone even in low concentrations (0.01 ppm) is effective against bacteria due to its high oxidation potential. There is limited information in the literature concerning the inactivation mechanisms of microorganisms by ozone. The bactericidal efficiency lies on the fact that there are many ozone reactions with chemicals of high biological importance. First of all, it is suggested that ozone attacks the glycoproteins and glycolipids in the cell membrane resulting in rupture of the cell. In addition, another bactericidal activity is the oxidation of the sulfhydryl groups of certain enzymes which results in disruption of cellular enzymatic activity and loss of function. Moreover, ozone attacks the purine and pyrimidine bases of nucleic acids leading to DNA damage (116).

The proposed mechanism for the inactivation of *E. coli* proceeds in the following order of viability indicators: (14)

- I. Direct oxidation/destruction of the cell wall with leakage of cellular constituents outside of the cell.
- II. Reactions with radical by-products of ozone decomposition entering the cell.
- III. Damage to constituents of the nucleic acids (purines and pyrimidines).
- IV. Breakage of carbon-nitrogen bonds leading to depolymerization and to cell wall disintegration causing cell lysis.

The antimicrobial capacity of ozone includes not only bacteria, but also molds, viruses, and protozoa. Ozone can react with numerous organic compounds and generate radical species such as hydroxyl radical that have more oxidative potential. Both HO_2^\bullet and the HO^\bullet radicals are highly reactive and play a fundamental role in the disinfection process. After the direct protoplasmic oxidation of bacteria, the free radicals produced react with the nucleic acids and provoke a sufficient damage, and incontrovertibly achieve inactivation (117).

3.1.2. Properties of ozone micro- and nanobubbles

One factor credited for the stability of MNBs in aqueous solutions is their zeta potential. High zeta potential values prevent the bubbles from coalescence by increasing the repulsive electrostatic forces (10). In the case of OzMNBs, the long term stability has a strong effect on dissolved ozone concentration and consequently on enhanced disinfection efficiency. It should be noted that small diameter with high specific area and low rising velocity increases the mass transfer rate and the ozone reactivity to target contaminants (118). The main factors that have a great impact on OzMNBs are the following:

Temperature

The temperature is considered a crucial factor that can influence the stability of OzMNBs. A recent study by Hewage *et al.* investigated the effect of temperature on the size of ozone nanobubbles and the zeta potential. They reported elevated temperatures resulted in an increase of diameter and a decrease of the zeta potential. The size was in the range of 100–300 nm, and the negative zeta potential values were within the range of -25 to -14 mV. To elucidate the fact that temperature is inversely proportion to zeta potential, the adsorbed ions at the gas-liquid interface should be taken into account since in high temperature they decrease owing to higher mobility (119).

pH

The aforementioned studies have emphasized the strong impact of solution pH on zeta potential and specifically suggested that NBs produced in water at a high pH value exhibit small diameter and high zeta potential (46). In the case of OzMNBs, the same trend was confirmed by another study where they investigated the values of zeta potential over a range of pH conditions (120). It was reported that the zeta potential value increased in absolute values as the pH values increased. Specifically, at pH=2, 4.5, 7.5 and 8, zeta potential values were found to be 9.92, 2.35, -32.34, -37.55, respectively (120). Another research study produced similar results. The zeta potential of OzMNBs in deionized water was approximately -33 mV at pH=8 and above -20 at pH=7 (121). Hence, it is clear from these results that at high pH the stability of OzMNBs is greater, mainly due to increased adsorbed OH⁻ ions at the interface. However, since

ozone decomposes more quickly at high pH (15), in order to achieve the same levels of ORP, a greater amount of bubbles is required at higher pH (122).

Salt concentration

The generation of ozone nanobubbles under various salt concentrations (0.01, 0.1 and 1M) showed that increasing sodium chloride (NaCl) concentration resulted in a decrease in the magnitude of zeta potential with a slight increase in diameter (46). It is noted that the values of the zeta potential were negative in all cases. Another experiment focused on the effect of salinity on the stability of OzMNBs in terms of zeta potential and size distribution showed that OzMNBs are stable under various salinity levels, since they remained negatively charged. Specifically, the salinity caused a reduction in negative zeta potential when no obvious effect on the diameter of OzMNBs was observed (123).

Hydroxyl radicals

Hydroxyl radicals exhibit microbicidal activity, and as such, their generation should be taken into consideration in order to provide some insight into the observed disinfection efficiency. Takahashi *et al.* reported that the generation of free radicals occurs by the micro- and nanobubbles collapse thanks to the high density of ions in the gas-liquid interface and they concluded that ozone microbubbles generate hydroxyl radicals under strong acidic conditions (124). Several studies have proven that hydroxyl radicals existed in water containing ozone microbubbles using fluorescence intensity (120,121,125). It is noted that the capacity for generating free radicals is of high importance as hydroxyl radicals are strong oxidants and not selective, and thus the oxidation processes can be accelerated (120).

3.1.3. Ozone dissolution with micro- and nanobubbles

Even though conventional ozonation is widely used for ozone dissolution in aqueous phase, the main drawback is the high amount of escaping ozone gas resulting in a high level of gas consumption. When microbubbles is used for ozonation, the degradation of trace organic compounds were found to be efficiently enhanced since the solubility of ozone in water is increased (126). Several research studies suggest an association between bubble size diameter and the enhancement of ozone solubilization rate in the aqueous phase. Table 3 lists a number of existing studies, which have

examined the comparison of ozone dissolution between macro and MNBs. All the available information about the experimental conditions is provided. A notable increase in peak value of dissolved ozone concentration was reported more recently by Hu and Xia as the ozone level for OzMNBs was 10.09 mg/L compared to macrobubbles which provided a very low ozone value (0.64 mg/L) within a generation time 30 min (123). Kobayashi *et al.* noted that aqueous dissolved ozone concentration is higher when the water is treated with microbubbles compared to macrobubbles. In 5 min ozonation with microbubbles, the concentration of ozone reached 1.58, 1.24 and 0.82 ppm at 15°C, 25°C and 30°C, respectively. On the other hand, when macrobubble ozonation was applied, the concentration was found 3-fold and 4-fold lower at 15°C and 25°C, respectively and no ozone was detected at the highest temperature (127). Another comparison of ozone microbubbles and normal bubbles demonstrated that the dissolved ozone concentration was approximately 2.5 times higher than that obtained by ordinary bubbling (128). More recent evidence showed that ozone dissolution using micro- and nanobubbles was approximately 50% higher after 5 min-aeration compared to a classical mixing pump with larger bubbles (129). The findings of another study confirm the observation that bubbles with smaller diameter can enhance the dissolution of gaseous ozone into the aqueous phase (130). In fact, the concentration of dissolved ozone by the regular method of ozone delivery was found to be 0.5 mg/L at 20°C, when microbubble ozonation could reach the value of 1.67 mg/L in the presence of para-chlorobenzoic acid (pCBA) (130). An increase in ozone concentration with nanobubbles was also reported in the study conducted by Batagoda *et al.*, where the initial dissolved ozone concentration was 52.79 mg/L, higher than 48.28 mg/L found with ozone macrobubbles (118). Fan *et al.* illustrated that the concentration of dissolved ozone after MNBs aeration was 3.54 mg/L in 25 min while after the millibubbles ozonation the ozone reached only 1.74 mg/L in 30 min. The most striking result to emerge from this study is that the ozone solubility was calculated about 4 times higher in 5% acetic acid solutions after OzMNBs aeration reaching the ozone value of 15.26 mg/L. It is well documented that acetic acid is considered an ozone stabilizer due to non-reactivity with it and thus, it can be beneficial to the ozonation process (131). Further confirmation is given by another research study, where the saturated ozone concentration with microbubble ozonation reached the value of 9.6 mg/L within 7 min and was found to be enhanced since the macrobubble ozonation achieved a lower dissolved ozone concentration at longer time period. This can be elucidated by the fact

that ozone mass-transfer coefficient was 2.2 times higher than that of the conventional ozonation process (132). Research findings from two other studies corroborate with the previous result as the augmentation of total mass transfer in microbubbles ozonation was also proved for simulated dyestuff wastewater treatment (1.8 times higher) and for landfill leachate pre-treatment (1.5 times higher) (125,133). Similar results were reported by a team which recently explored experimentally the raise in ozone dissolved concentration, when ultrafine bubbles are used. Within 10 min, the maximum dissolved ozone concentration reached the value of 8.3 and 3.5 mg/L, during ozonation with MNBs and MaBs, respectively (134). The most recent evidence confirms once more the higher dissolved ozone concentration of 4 mg/L in microbubbles ozonation instead of 2.49 mg/L (135). In three test fluids, pure water, tap water and phosphate buffered saline, the ozone dissolution velocity (mg/L/min) was found higher by 1.5, 1.6 and 2.7 times when ozone injected by microbubble generator instead of porous diffuser (136). In the course of the ozonation of synthetic semi-conductor wastewater containing tetramethyl ammonium hydroxide within 7 min, the gas transfer to water by nanobubbles (1.67 mg/L/min) was 9.8 times faster than that of macro-ozone (0.17 mg/L/min) (137). Consistently, the ozone dissolution was found once again 1.5 times higher by ozone microbubbles injection in tap water (138). Finally, a group of researchers in 2021 has investigated the ozone mass transfer coefficient with nanobubble aeration and compared it with macrobubble aeration. Their findings are in line with all the previous results. In fact the volumetric mass transfer coefficient (K_{La}) was estimated 0.179 min^{-1} , reaching the peak value of ozone concentration of 13.4 mg/L, while in macrobubble aeration the volumetric mass transfer coefficient was 4.7 times lower (0.038 min^{-1}) with a dissolved ozone concentration up to 7.9 mg/L (139). These findings demonstrate the strong effect of MNBs to ozone solubilization. In general, it can be concluded that the use of MNBs in ozonation leads to a more efficient process as the ozone utilization efficiency is higher.

3.1.4. Ozone decomposition rate

The half-life time of ozone in gas phase is much higher than in aqueous phase. In more detail, at 20°C the gaseous ozone will be degraded in 3 days, in contrast the degradation of dissolved ozone in water will take place within only 20 minutes (140,141). Due to its low utilization efficiency, nanobubbles technology is gradually used for ozone application in a more efficient way. However, there are very limited

research studies that investigated the comparison of the half-life times between OzMNBs and macrobubbles owing to the fact that the academic interest is focused on the study of ozone solubility and mass-transfer. Hu and Xia have also investigated the half-life time of dissolved ozone with and without the use of MNBs and their results demonstrated that the average lifespan for the MNB system was 10.51 min, whereas that for macrobubbles system was only 0.70 min for 30 minutes generation time (123). A 2007 research study observed that a longer half-life was found when a microbubble generator injected ozone in tap water instead of a porous diffuser (1.6 times longer at 19.2°C) (136). The lifespan when ozone delivered through nanobubbles in water was greater than conventional ozone bubbles. In fact, ozone is retained in water approximately four time longer than using a sandstone diffuser (118). In another research study, ozone decomposition was investigated when OzMNBs were present in various concentrations of acetic acid and in water alone. In this case, the results showed that the average half-lives of ozone were longer by 1.39, 2.04 and 3.52 times in 0.5, 3 and 5% acetic acid solutions, respectively. The evidence from this study points towards the idea that acetic acid can further enhance the longevity of ozone in water apart from MNBs (131). Remarkably in a very recent study, it was shown that half-life of ozone generated by nanobubbles was found to be 23 times higher than that of macro-ozone (137). The ozone lifespan was investigated in nanobubble and macrobubble aeration groups and was found to be 3.50 h and 1.75 h in the latter. In the presence of hydroxypropyl- β -cyclodextrin (HP β CD), which is used as an ozone stabilizer, the ozone half-life time were 2.8, 4.3, 9.3 and 2.2 times higher than those estimated from the macrobubbles aeration under different HP β CD:O₃ molar ratios (1:1, 3:1, 5:1 and 10:1, respectively) (139). The results so far confirmed that the utilization of MNBs can extend the ozone half-life. Moreover, it can be concluded that the addition of an ozone stabilizer can further intensify the ozone lifespan and can be utilized to strengthen the ozonation process.

Table 3. Comparison of ozone dissolution between ozone macrobubbles (OzMaBs) and ozone micro- and nanobubbles (OzMNBs)

Ref.	Size	Flow Rate (L/min)	Ozone conc. (mg/L) or rate (g/h)	Time (min)	Volume (L)	Temp.(oC) /pH	Type of water	Peak Concentration (mg/L) OzMaBs vs OzMNBs
(123)	Micro/Nano (32-460 nm, 4.55 x 10 ⁷ bubbles/mL)	4 L/min	50 mg/L	30	20	20	Deionized	0.64 vs 10.09
(127)	Micro (<50 μm)	2.5 L/min		5	10	15 25 30	De-chlorinated	3 fold lower-1.58 ppm 4-fold lower-1.24 ppm No ozone detected in OzMaBs vs. 0.82 ppm in OzMBs.
(128)	Micro (Peak at 15 μm)	1 L/min	50 mg/L	30	5	Ambient	Distilled	2.5 fold higher than OzMaBs
(129)	Micro/Nano		25 g/h	5	20	20 ± 1 /6	Distilled	5.5 vs 8.3
(130)	Micro (5-25 μM=50%)		0.61-0.72 g/h	5	20	10 / 7 20 / 7 30 / 7	Ultrapure	0.65 vs 2.16 0.50 vs 1.67 0.40 vs 1.32
(118)	Nano			3	20	20 / 7		48.28 vs 52.79
(142)	Micro/Nano (3.38 μm 2.41 × 10 ⁵ bubbles/mL)	0.5 L/min	11 mg/L	30	20	17.4 ± 1.2	Distilled	1.74 vs 3.91

(132)	Micro ($<45 \mu\text{m}$ 3.9×10^5 counts/mL)	0.5 L/min	5 g/h	14	3	20 / 8	Wastewater from acrylic fiber manufacturing industry	8.4 vs 9.6
(125)	Micro ($<58 \mu\text{m}$, 2.9×10^4 counts/ ml)	0.5 L/min		10	20	18 ± 2	Deionized	~ 8 vs 13
(133)	Micro	0.2 L/min	36 mg/L	40	8	20	Tap	~ 4 vs 11
(134)(134)	Ultra-fine ($0.5\text{-}3 \mu\text{m}$)	30 mL/min		10	1	25	Distilled	3.5 vs 8.3
(135)	Micro		3-4 mg/L	12	80		Secondary treated sewage water	2.49 vs 4.00
(137)	Nano (133.7 nm 5.25×10^9 particles/mL)			7		25 / 7	synthetic semi- conductor wastewater containing TMAH	~ 1 vs 12
(138)	Micro			5	20		Tap	3.5 vs 5.3 (reached in 2 min)
(139)	Nano (580 nm 2.16×10^5 particles/ mL)	0.5 L/min	38 mg /L	30				7.9 vs 13.4

3.1.5. Application of ozone-based Macro- and Nanobubble Technology in Disinfection

3.1.5.1. Antimicrobial and disinfection process

Bacterial contamination and subsequent infections are recognized as being a major threat to human health and there is an urgent need to inactivate pathogenic organisms and prevent the waterborne diseases spread to users and the environment. In this regard, the development of novel technologies based on the application of OzMNBs is of paramount importance.

Furuichi *et al.* reported that OzNBs water deactivates both gram-positive and gram-negative bacteria while this approach does not show any cytotoxicity against human gingival fibroblasts, unlike conventional mouth wash. Dissolved ozone concentration of 1.5 mg/L provided a sufficient bactericidal activity for periodontal pathogens. Specifically, the inactivation of the bacterial cells (*S. aureus*- 2.4×10^8 CFU/mL, *S. sanguinis*- 1.5×10^8 , *K. pneumoniae*- 7.6×10^8 CFU/mL and *E. coli*- 1.6×10^9 CFU/mL) was >99.99% since the viable bacteria were below detection limit (< 10 CFU/mL). For *P. gingivalis* cells with initial bacterial concentration 7.0×10^7 CFU/mL, the percentage of killed bacteria was higher than 99.99%, while the disinfection activity was deteriorated in case of *S. mutans* with initial bacterial concentration 1.7×10^6 CFU/mL, since it reached a maximum disinfection of 94.69% within three minutes (143). Another study for the evaluation of the bactericidal activity against periodontal pathogenic bacteria (*P. gingivalis* and *A. actinomycetemcomitans*) reported that OzNBs water with concentration 1.5 mg/L was capable to reduce the numbers of colony forming units (CFUs)/mL below the limit of detection (<10 CFUs/ mL) after only 0.5 min of exposure, providing evidence that it is not cytotoxic to cells of human oral tissues (144).

As it is mentioned before, ozone is highly unstable and this is a problem posed in terms of stocking ozone aqueous solutions. This issue was explored by Seki *et al.* implementing OzNBs technology for the storage of ozone. It was found that such an approach produces good efficiency in storage as the microbicidal activity was adequate for different set time periods. OzNBs stored at 4°C retained more than 90% of ozone after a week and more than 65% after a month. Moreover, the residual concentration of ozone

stored at 4°C for 1 year was adequate to kill one of the most resistant bacteria, *M. smegmatis*, within 15 min; even though *E. coli* was not entirely killed even after a 60-min exposure (145).

3.1.5.2. Disinfection of wastewater treatment plant effluents

Apart from the importance of disinfection, attention must also be paid on the occurrence and fate of trace organic compounds that are considered of emerging concern. It is of major importance to eliminate these pollutants as they can be discharged to water bodies and induce adverse and undesirable effects onto humans, living organisms and environment even at low concentrations (146). As demonstrated in literature, the ozone amounts required for PPCPs oxidation may lead to a partial disinfection, hence it is crucial to highlight the influence of emerging contaminants existence on the ozone disinfection capacity (147,148).

In aspect of wastewater treatment, an analysis on deactivation of faecal and total coliforms in domestic waste water in Peru indicated that through applying air- ozone micro-nanobubbles, it was obtained 99.58% for faecal coliforms and 99.01% for total coliforms (149). Lee *et al.* investigated the degradation of pharmaceuticals compounds by a microbubble ozonation process and showed that it was markedly enhanced by the decrease in diameter of the ozone bubbles. It was found that the residual concentrations (C/C_0) of the selected pharmaceuticals compounds, including 17 α -ethinylestradiol (EE2), ibuprofen (IBU) and atenolol (ATE) was estimated (at 20°C) 0.61, 0.75 and 0.77, respectively, when treated with microbubbles and differ significantly from ozone millibubbles treatment, where the residual concentrations were found to be 0.79, 0.88 and 0.87 (130). Another investigation on the degradation of 39 pharmaceuticals in water showed that the introduction of microbubble ozonation improved significantly the removal rate by 8-34% (150). Concerning the degradation of tetracycline, the removal was found 50% and 95% with millibubble and ultrafine bubbles ozonation, respectively, within 20 min, indicating the enhanced degradation of the antibiotic when lowering the bubble size. The same study concluded that the most-favourable degradation and mineralization of the target persistent pollutant was achieved when ultrafine bubbles ozonation was performed at lower pH levels and higher reaction temperature (134). In another research study, the degradation of 26

PPCPs was examined and the average elimination was found to be 53% and 63.9% in macrobubbles and microbubble ozonation at low concentration, respectively (135).

Bisphenol A is a toxic endocrine disrupting chemical which is widely used in some industries such as synthetic polymer and thermal paper industry and is extensively released into the environment (151). A recent study suggest that the removal efficiency of BPA by OzMBs was improved from 41 to 98% within 600 s of ozonation. In addition, the utilization of OzNBs led to a considerably high range of ozone utilization efficiency (i.e., 52%–86%) for the complete removal of BPA (152).

In this section, the degradation behaviour of target organic compounds by OzMNBs was explored in tertiary treatment of wastewater and it was found that their application provides a better performance compared to conventional ozonation and as a result OzMNBs can minimize the discharge of emerging contaminants into water bodies.

3.1.5.3. Aquaculture

Fisheries and aquaculture are a growing industry and seafood consumption has reached 20.3 kg per capita in 2017. Additionally, seafood remains at the top level of the global market as in 2018, 88% of total fishery and aquaculture production was used for direct human production (153). Seafood contamination is associated with a number of pathogenic microorganisms and has become a key challenge regarding the food safety. In this regard, effective pathogen intervention strategies have been applied (154).

Several studies have been recently conducted in order to explore the effect of ozone nanobubbles (OzNBs) in aquaculture against aquatic pathogens (Table 4). Specifically, *Jhunkeaw et al.* have investigated the disinfection efficiency against *Streptococcus agalactiae* and *Aeromonas veronii* in fresh water which are considered pathogenic fish bacteria. Three consecutives ozone treatments (10-min exposure at OzNBs at 15 min intervals) were tested. The first 10- min treatment reduced the bacterial load of *S. agalactiae* and *A. veronii* 26 and 48 fold or 96.11% and 97.92%, respectively. The next two 10-min ONBs treatment reduced further the bacteria load in water reaching higher than 99.9% reduction for both pathogenic bacteria. In water taken from a Nile tilapia-cultured tank (initial bacterial concentration: 8.18×10^5 CFU/mL) with the presence of organic

matter the disinfection property of ozone nanobubbles was reduced and reached the 59.63% after the first treatment and the other two treatments were required to reach the 99.29%. The loss in the disinfection capacity can be illustrated by the fact that the presence of the organic matter led to the rapid ozone oxidation and degradation (155). In another research study, the disinfection of *Vibrio parahaemolyticus* at a concentration 10^6 CFU/mL in 15‰ saline water was studied. At the end of the experiment, the bacterial concentration (CFU/mL) was estimated 2.3×10^1 , 2.2×10^0 and 0 CFU/mL for 2-, 4- and 6- minute OzNBs exposure, respectively. The results of the oxidation–reduction potential (ORP) showed that the initial ORP value, which was 240 mV rose to 830 ± 70 mV after six minutes operation and remained stable at over 900 mV as the nanobubbles generator continued working for ten more minutes (156).

Table 4. Applications of ozone micro- and nanobubbles (OzMNBs) in Aquaculture

Target Microorganism	Bacterial Conc. (CFU/mL)	Type of Water	ORP	Time (min)	Disinfection Efficiency with NBs	Reference
<i>S. agalactiae</i>	3.45×10^6	Dechlorinated Tap Water	834 ± 22 mV	10	96.11%	(155)
<i>A. Veronii</i>	1.65×10^6				97.92%	
<i>V. parahaemolyticus</i>	10^6	15‰ Saline	830 ± 70 mV	6	100%	(156)
<i>V. parahaemolyticus</i>	1.8×10^5	Artificial Sea water	960 mV (~ 3.5 mg-O ₃ /L)	5	100%	(157)

Thanh Dien *et al.* reported that even though, the bacterial concentration was high ($\sim 2 \times 10^7$ CFU/mL), multiple OzNBs treatments in the first two days reduced the bacteria between 15.9% and 35.6% of total bacterial load in water, while bacterial concentration increased from 13.1% to 27.9% in the untreated control (158). OzNBs sea water at 960 mV ORP was used to carry out disinfection experiments against *V. parahaemolyticus* EMS/AHPND strain. From these results it is clear that OzNBs treatment provide a high disinfection efficiency, since after 1-min incubation over 99.99% of tested bacteria were killed and after 5 min or longer incubation the sterilization efficiency was 100% (157). Apart from the ozone disinfection efficiency, Kurita in 2017 demonstrated the killing effect of cavitation treatment on small planktonic crustaceans that can cause detrimental problems in invertebrate aquaculture tanks through predatory damage or competition for food

resources with the aquaculture species (159). The results showed that micro and nanobubbles reduced the planktonic crustaceans in the aquaculture tanks by 63.3% compared with the control by killing crustaceans of all sizes equally.

Effect of ozone nanobubbles on fish health

Ozone has found its greatest use as disinfectant in closed recirculating aquaculture systems in order to reduce the pathogenic bacteria and prevent any fish disease (160). The residual ozone concentration is of high importance since it has been found that concentrations within the range 0.01-0.1 mg/L can be highly toxic to fish in fresh- and seawater. There is significant difference between the ozone reaction with saline and freshwater in terms of disinfection. The presence of bromide ion (Br^-) in seawater results in the formation of brominated compounds like bromate (BrO_3^-) by ozone oxidation, which is toxic to aquatic organisms (161). On the other hand, in fresh water ozone decomposes to oxygen elevating the levels of dissolved oxygen in the system, which may also have detrimental effects on fish if it is very high (161). In terms of ORP, several studies suggest that the levels in the range from 300 to 425 mV can ensure the safety of fish, crustaceans and molluscs (158). Summarizing, in order to apply a safe ozone disinfection system, the lethal limits, which depend on the cultured species and the type of water, have to be determined and not exceeded during operation.

A study from Jhunkeaw *et al.* suggested that a single 10 min exposure to OzNBs with an ozone level 860 ± 42 mV is safe for Nile tilapia in fresh water. Even though no mortality was observed after receiving the second and the third consecutive OzNBs treatments, the increased exposure caused damage in the gill filaments (155). However in another study, they set up a modified recirculation system to reduce direct exposure to the fish, in order to avoid any alterations in exposed fish. In this case, juvenile Nile tilapia did not exhibit any abnormalities in behaviour or mortality by the application of multiple OzNBs treatments (158). OzNBs in seawater containing ozone dose at 3.5 mg/L and 960 mV ORP was proven to be toxic to shrimp, therefore a twofold dilution of ozonated seawater was suggested as shrimp survival and excellent inactivation activity was observed (157). An additional study in the literature regarding the exposure of Nile tilapia (*Oreochromis niloticus*) to ozone nanobubbles noted that innate immunity genes involved

in the systematic frontline defence system were stimulated. In all examined organs, these genes expressed an upregulation very fast within 15 min- post ozone nanobubbles treatment and lasted from 12 to 24 h in the gills, the head kidney and the spleen. It was thus concluded that based on the efficient stimulation of the genes by OzNBs treatment, a protection to cultivated animals from potential pathogenic infections can be provided (162). In addition, any possible negative effect of the ultrafine bubbles in cavitation treatment on two juvenile sea cucumbers (*Apostichopus japonicus*) and sea urchins (*Strongylocentrotus intermedius*) was evaluated and it was found that all individuals were intact and uninjured four days after exposure to ozone nanobubbles (159).

Experimental results provide a basis for the application of ozone nanobubbles in aquaculture since it is efficient for reducing pathogenic bacteria. Future studies should aim to replicate results in a larger scale and further explore the efficiency to prevent disease outbreaks. The safety of using OzNBs is a core issue and should be investigated in more detail in order to gain a better understanding of the toxicity to fish, which depends upon species and the life stage.

3.1.5.4. Agriculture

The effect of ozone ultra-fine bubbles on washing fresh vegetables was tested and when acidic electrolyzed water containing ozone ultra-fine bubbles and strong mechanical action combined, the lowest viable bacterial count was recorded among other treatments including sodium hypochlorite (163). The disinfection efficiency of *F. oxysporum f. sp. melonis* spores was tested and the results confirmed that ozone microbubbles exhibited higher disinfection efficiency than macrobubbles. In addition, spores treated with OzMBs showed surface injury after 30 s and wavy deformation of cell membrane was observed after 180 s, which may be caused by the generation of hydroxyl radicals penetrating into the spores (164). Two phytopathogens, *Fusarium oxysporum f. sp. melonis* and *Pectobacterium. carotovotum subsp. carotovorum* have been investigated and the results suggest that ozone-rich microbubbles showed higher disinfection activity than the millibubbles over the same period of application. It is reported that the number of these two phytopathogens decreased rapidly thanks to elevated initial ozone concentration (3 logs at 0.33 min). At the same ozone level, they concluded that OzMBs provided higher

disinfecting activity against both pathogens (127). Micro and nanobubbles technology was also implemented to tackle tomato airborne disease. The results highlighted that the inactivation activity against *Alternaria solani* Sorauer conidia was reduced by 2 logs when ozone concentration of 1.6 mg/L was applied. In the case of *Cladosporium fulvum* conidia, it was found that one log reduction was achieved when 1.8 mg/L of ozone was used. This level of ozone application did not affect tomato growth (129). The study by Kwack *et al.*, have verified that using ozone microbubbles for seed sterilization is the most feasible treatment since the germination and growth of alfalfa sprouts have not been negatively affected (138). Another study provides additional support into the superiority of OzMBs over other sanitizers such as sodium hypochlorite (165). After washing with OzMBs at 1 mg/L for 7 minutes, the bacterial reduction of *S. Typhimurium* was the highest reaching the value of 2.6 log CFU/g or 99.8%, converting into percentage. Increasing attention has been given to the removal of persistent, highly toxic and accumulative pesticides which are extensively used in agriculture. The degradation of fluopyram is more efficient with OzMBs, among different treatment methods. More specifically, when OzMBs are utilized, the half-life of fluopyram was found to be 6.1 times higher than that in ozonated water and 1.3 times that in OzMBs treatment (166). The removal of fenitrothion in three kinds of vegetables (lettuce, cherry tomatoes and strawberries) was investigated and was found to be higher when OzMBs generated by decompression compared to OzMBs generated by gas-water circulation were used. This can be explained by the creation of a larger number of smaller OzMBs by the former, yielding a higher efficiency of fenitrothion degradation as the infiltration of smaller OzMBs into vegetables is easier (167).

Table 5. Applications of ozone micro- and nanobubbles (OzMNBs) in Agriculture

Target Microorganism	Bacterial Conc. (CFU/mL)	Ozone Conc. (mg/L)	Disinfection Efficiency with OzMBs	Reference
<i>F. oxysporium f. sp. melonis</i>	1×10 ³ -1×10 ⁴	1.5 ppm (15°C)	The number of surviving spores reached the detection limit in 45 s with OzMBs instead of 60 s with OzMaBs.	(164)
<i>F. oxysporium f. sp. melonis</i> <i>P. carotovorum subsp. carotovorum</i>	~ 1×10 ³	0.1 ppm (20°C)	2.6 logs of surviving cells with OzMBs instead of 2.9 logs with OzMaBs after 180 s. 2.5 logs of surviving cells with OzMBs instead of 2.9 logs with OzMaBs after 180 s.	(127)
<i>Alternaria Solani Sorauer conidia</i>	1×10 ⁵	1.6 ppm	2 logs reduction	(129)
<i>Cladosporium fulvum conidia</i>		1.8 ppm	1 log reduction	
<i>S. Typhimurium</i>	1×10 ⁶ - 1×10 ⁷ (CFU/g)	1 ppm (30°C)	2.6 logs reduction	(165)

3.1.6. Drinking water disinfection

A common strategy used to ensure safety in drinking water is ozonation. The rapid decomposition of ozone in water and the low residual concentration are the main drawbacks of this process. Utilizing NBs serve as a more efficient alternative to drinking water disinfection as the decomposition of ozone in water is decelerated and the ozone dosage required against contaminants or pathogens is reduced thanks to a greater dissolution. Sumikura *et al.* found that the ozone dose was lower when OzMBs were used instead of the conventional ozonation with macrobubbles providing the same inactivation rate of target pathogen *E. coli* (136). One of the most crucial parameters of conventional ozonation is the cost effectiveness of installation. A recently conducted cost-benefit analysis indicated that the installation of a OzNBs generator is beneficial for existing water treatment plants as the total cost would be four times less and could save 375 k\$ per year (118).

Another important parameter is the effect of inlet ozone gas concentration on the removal rate. This issue has been investigated on the log reduction of *B. subtilis* by microbubble ozonation and the results showed that higher gaseous ozone concentration led to higher disinfection efficiency after 2 min of operation (reduction by 5 log for 140 mg/L

O₃ in gas phase, compared to 1.6 log and 0.3 log for 110 mg/L and 40 mg/L, respectively). This can be justified by the fact that the size of bubbles in higher ozone inlet was found to be smaller inducing higher volumetric mass transfer coefficient (K_{La}) and consequently an increased utilization efficiency. It was also found that the K_{La} had almost been doubled from inlet gas concentration 40 mg/L to 140 mg/L, while the Sauter mean diameter was decreased from 75.7 μm to 49.7 μm , respectively (168). Combination of ozonation and hydrodynamic cavitation showed the best performance in disinfection of *E. coli* with an initial bacterial concentration of approximately 10^5 CFU/mL was decreased to zero within 45 min whereas for the same ozone concentration using only ozonation without cavitation, the bacterial concentration reached zero after 60 minutes (169).

Summarizing, the higher mass transfer leading to lower ozone dosage renders the use of OzMNBs a promising and an efficient technology in terms of cost and disinfecting capacity.

3.1.7. Ballast water treatment

The vast majority of world cargo handling takes place by sea with suitable ships. For decades, shipping has been the leading choice for the movement of goods around the world (170). However, this inevitably leads to a large environmental footprint on the planet that has attracted increasing attention because international shipping is considered a significant source of pollution derived from the emissions of toxic pollutants from internal combustion engines (171) and the largely uncontrolled disposal of seawater that is used as ballast (172). Ballast water is a large amount of seawater that is stored in ballast tanks and is essential to maintain ship buoyance and maneuverability. Ballast tanks on a ship fill and drain seawater to offset the weight reduction that occurs when loading and unloading goods. Therefore, from just one ship, thousands of cubic meters of seawater loaded from a potentially polluted marine area can be disposed of in another area with completely different quality characteristics (173). In fact, the ballast water discharged into a new marine environment may include nonindigenous species (NIS) that can result in extensive ecological and economic damage due to the changes they cause to the structure and functioning of marine ecosystems (174,175). To reduce the global spread of these invasive aquatic species, international regulations have set environmental limits for the number of

organisms present in the ballast water discharged by ships. Since 2018, the International Maritime Organization (IMO) has defined the D2 standard to determine the maximum amount of viable organisms that are allowed to be discharged, a limit that all ships must meet by 2024 (Table 5) (176).

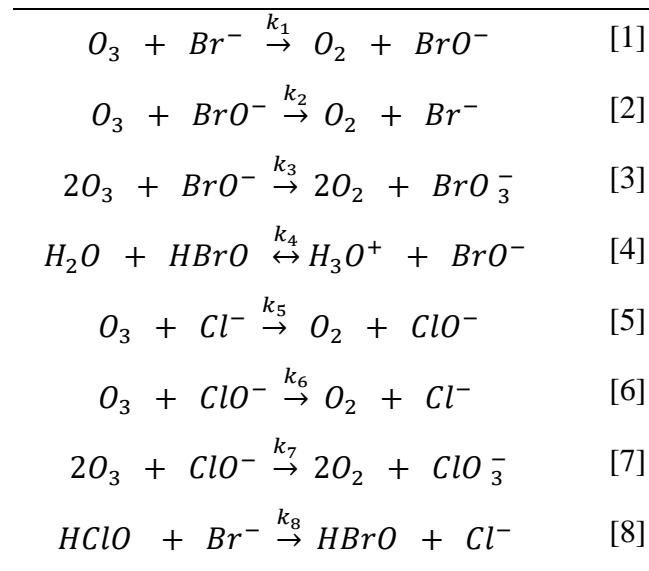
Table 5. Acceptable limit of indicator microbes according to the D2 standard (176).

Indicator microbes	Acceptable Limit
<i>Escherichia coli (E. coli)</i>	<250 CFU per 100 mL
<i>Intestinal Enterococci</i>	<100 CFU per 100 mL
<i>Toxicogenic Vibrio cholerae</i>	<1 CFU per 100 mL
Size of microbes	
≥50 μm	<10 viable organisms per m ³
≥10 μm and <50 μm	<10 viable organisms per mL

In general, within the context of minimizing environmental risks, the implementation of ballast water treatment systems is addressed, with a view to providing discharged water quality according to the regulations. There are many systems that, through natural, chemical, and biological processes, eliminate microorganisms and suspend their growth. The most commonly employed methods for disinfection/sterilization are chlorination, ozonation, and ultraviolet (UV) irradiation (177). Ozonation has been used in ballast water treatment. Several studies have been conducted on seawater ozonation and their findings confirmed that, when ozone is applied to seawater, secondary oxidants with disinfection capacity are formed that are expressed as total residual oxidants (TRO) (178–185). In conventional ozonation, ozone is directly bubbled into the aqueous solution and, since it has a low half-life, it decomposes rapidly, resulting in a low residual activity. An increasing number of studies that employ ozone delivery by nanobubbles (NBs) has been found to improve the disinfection capacity and residual concentration (16). Although most studies have focused on water treatment and, particularly, on the inactivation of various microorganisms in the effluents by OzNBs (38,155,158,186,187) research on their disinfection capacity in seawater remains limited. As mentioned by Meegoda *et al.* (46), the generation of OzNBs under increasing salt concentrations by adding sodium chloride

(NaCl) leads to a decrease in the magnitude of the zeta potential and a slight increase of the bubble size. Another experiment showed that the diameters of OzNBs under various salinity levels are stable, while a reduction of zeta potential in absolute value was reported (123). The ozone demand in seawater ozonation is considerably influenced compared to freshwater ozonation, since the bromide Br^- and the chloride Cl^- (both of which are present in seawater) react with ozone very quickly, leading to the formation of oxidants that also have a disinfecting efficiency of their own, as shown in Table 6. Specifically, bromide is oxidized by ozone to secondary oxidants, such as hypobromous acid (HBrO) and the more stable forms, hypobromite ion (BrO^-) and bromate (BrO_3^-). The half-life of ozone in water is estimated to be only 5 s in the presence of high concentrations of bromide, while there is no hydroxyl radical formation observed in seawater (188). In most oceanic waters, the pH is about 8 and, since the acid dissociation constant (pKa) of HBrO/ BrO^- is approximately 9, the dominant bromine form will be HBrO (189).

Table 6. Reaction of bromide and chloride with ozone (185).



Despite the fact that the application of OzNBs technology has been widely investigated on wastewater, water disinfection, and degradation of organic contaminants, no studies have focused their application on ballast water treatment. The main objective of this research is to evaluate whether the use of OzNBs has any significant impact on microorganism inactivation and residual activity of ozone.

3.2. Materials and Methods

3.2.1. Ozonation experiments

In this study, tap water and seawater collected from a small harbor located in Agios Onoufrios (Chania, Crete, Greece) was used to run the batch disinfection tests. The main water quality parameters are given in Table 7. The water quality parameters were measured using a calibrated HQ4300 Portable Multi-Meter (Hach).

Table 7. Fresh water and Seawater Content Description: Physicochemical Parameters

	Fresh Water	Seawater	Unit
pH	8	8.28	-
T	17.5	17.5	°C
Conductivity	0.297	59.8	mS/cm
TDS		38.2	g/L
Salinity		39.9	PSU
ORP		221.8	mV
Chloride (Cl⁻)		32769.84	mg/L
Bromide (Br⁻)		94.01	mg/L

The ozonation disinfection experiments were conducted in batch mode. The experimental process used in this study is shown schematically in Image 2. For OzNBs generation, the commercially available MK1 Nanobubbler™ (Fine Bubble Technologies (Pty) Ltd, Porterville, South Africa) was employed which is a submersible device with the capability to generate nanobubbles at a concentration of approximately 10^8 bubbles/mL. The experimental set up consisted of a 350 L tank, filled with tap water, in which the nanobubble generator was submerged. Ozone supplied by an ozone generator (Azure 2G, Wassertec) was injected into the water through the gas intake of the MK1 Nanobubbler™. To increase the ozone concentration in the output of the ozone generator, high-purity oxygen from a compressed gas cylinder with a suitable pressure regulator was used as the feed gas. Ozone exhaust gas from the tank was carefully captured by ozone traps filled with 2% potassium iodide (KI) solution in order to ensure that no ozone gas escapes to the

environment. The concentration of dissolved ozone was monitored directly from the tank during the generation of the ozone nanobubbles by an ozone amperometric sensor (Hach, Germany) with a working range of 0.005 - 2 mg-O₃/ L and an accuracy of 3% or ± 10 ppb O₃.

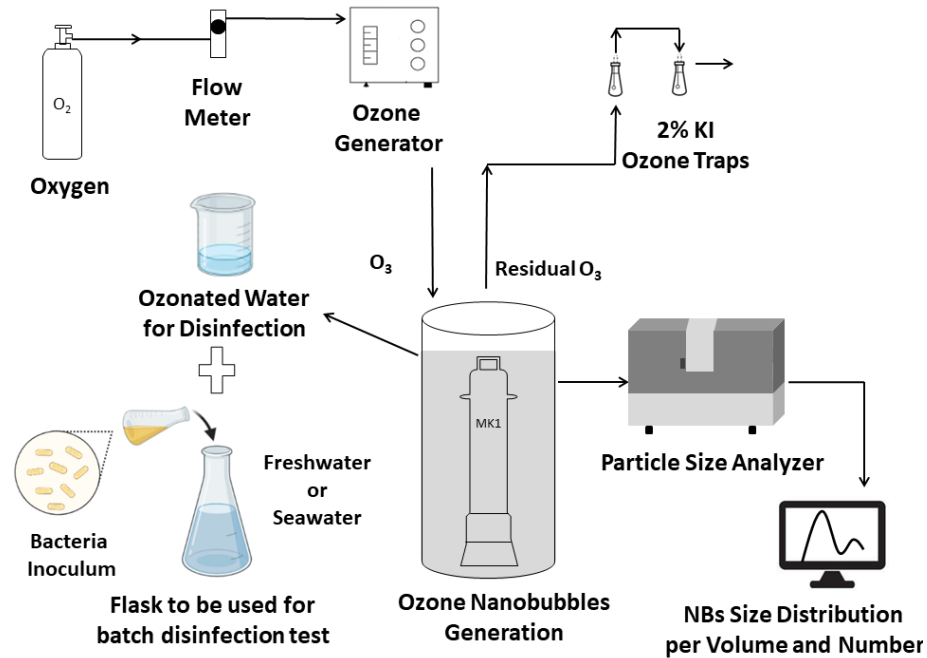


Image 2. Experimental set-up for generation of fresh water with dissolved ozone and with the presence of ozone nanobubbles for treatment of tap water and seawater.

Tap water with dissolved O₃ and with nanobubbles containing ozone in different concentrations was used to conduct the disinfection experiments. After achieving a desired bacterial concentration level (CFU/mL) by spiking the pathogens from a stock culture, OzNBs tap water was added bringing the microbial count to the desired initial conditions and samples were collected at predetermined time intervals (1, 5, 10 and 20 min) into sterile tubes for further analysis. Duplicate samples were taken for each time interval to estimate the microbial count and for the measurement of the residual dissolved ozone. In order to stop the disinfection in the samples taken, the residual ozone in the sample was immediately neutralized with excess sodium thiosulfate and thus the ozone disinfection was completely stopped. In order to determine the difference in the efficacy between the treatments with dissolved ozone and dissolved ozone supplemented with OzNBs, a conventional ozonation system was also set up. The dissolved ozone was obtained by

bubbling ozone gas into 1 L of tap water using a ceramic diffuser and the aforementioned experimental procedure was followed here too.

In the case of seawater ozonation experiments, tap water containing ozone at the desired ozone level with and without the presence of OzNBs was added in unsterilized seawater in different ratios to obtain different salinities. The salinity in seawater samples was between 1.5 and 15 practical salinity units (PSU). The ozone disinfection of *E. coli* in three different bacterial concentrations (10^7 , 10^6 and 10^5 CFU/ mL) was added to ozonated solution and samples were collected at predetermined time intervals (1, 5 and 10 min) into sterile tubes for further analysis. The measurement of the ozone concentration (and the possible residual oxidants formed) in the aqueous solution used for disinfection was also tested by the Indigo Colorimetric Method (190). The reaction of indigo trisulfonate with the bromine formed in seawater is slow and is further inhibited by the addition of malonic acid (Figure A. 1& Table A. 1). Hence, it is considered that the indigo decolorization is exclusively due to the ozone concentration, which will be expressed in the results as TRO (Total Residual Oxidants) (mg-O₃/ L).

For drinking water treatment with dissolved ozone, the transferred ozone dose (TOD) was calculated according to the following equation:

$$TOD_{TW} = \frac{C V_{OW}}{V_{TW} + V_{OW}}$$

For seawater treatment with dissolved ozone, the transferred ozone dose (TOD) was calculated according to the following equation:

$$TOD_{SW} = \frac{C V_{OW}}{V_{SW} + V_{OW}}$$

where C is the ozone concentration in the ozonated water (mg/L); V_{OW} is the volume of ozonated water added in the flask (mL); V_{TW} is the volume of tap water added in the flask (mL), and V_{SW} is the volume of seawater added in the flask (mL).

3.2.2 Microorganisms, growth condition and cell viability test

Four typical bacterial pathogens of drinking water, *Escherichia coli*, *Enterococcus faecalis*, *Staphylococcus cereus* and *Bacillus aureus* were examined in order to estimate the inactivation rate with ozone as disinfectant. The four strains of bacteria was cultured in nutrient broth for 16 h and then the solution was centrifuged. The pellet of bacteria cells was washed by sterilized water 0.8% NaCl. Each sample was centrifuged at 3500 rpm for 15 min and resuspended in solution. The bacterial suspension reached an optical density equal to absorbance of 0.1 at 600 nm as this corresponds to approximately 10^8 CFU/mL according to McFarland standard. The initial bacterial concentration was confirmed in every disinfection experiment. In each sample the residual ozone was immediately neutralized with excess sodium thiosulfate. After the ozone treatment, 0.1 mL of each sample in different dilutions was spread evenly over the nutrient agar-plate in triplicate. Following incubation at 37°C for 24 h, the total viable count (CFU/mL) of the isolate was determined by the spread plate technique. The measurement is considered valid when 10 to 100 colonies are spotted. The calculation of CFU/mL is done by the following equation:

$$\frac{CFU}{mL} = \frac{10^v CFU}{100 \mu L}$$

where v is the dilution of the bacterial concentration.

In the case of seawater ozonation experiments, all the disinfection experiments were investigated in terms of bacterial regrowth after 5 days as suggested in the D2 standard.

3.2.3. Measurement of dissolved ozone- Indigo Colorimetric Method

The concentration of dissolved ozone was monitored directly from the tank during the ozone nanobubbles generation by an ozone amperometric sensor (Hach, Germany) with a working range of 0.005 - 2 mg/L O₃ and an accuracy of 3% or ± 10 ppb O₃. The dissolved ozone concentration in the process of the experiment was determined by the Indigo Colorimetric Method (191). The Indigo Method is a colorimetric procedure that is selective, quantitative and simple. Moreover, this method is applicable to lake water, extremely hard groundwaters and biologically treated domestic wastewaters. The high

purity indigo trisulfonate corresponds to a molar absorptivity of $20000 \text{ M}^{-1}\text{cm}^{-1}$ at 600 nm and this exactly why the purity and the age of the reagent are extremely important since they affect the stoichiometry of the reaction with ozone (191). The specific method is based on the fact that the Indigo Reagent reacts instantly with ozone in acid solutions, bleaching the blue indigo colour leading in the decrease in absorption proportionally to present ozone amount.

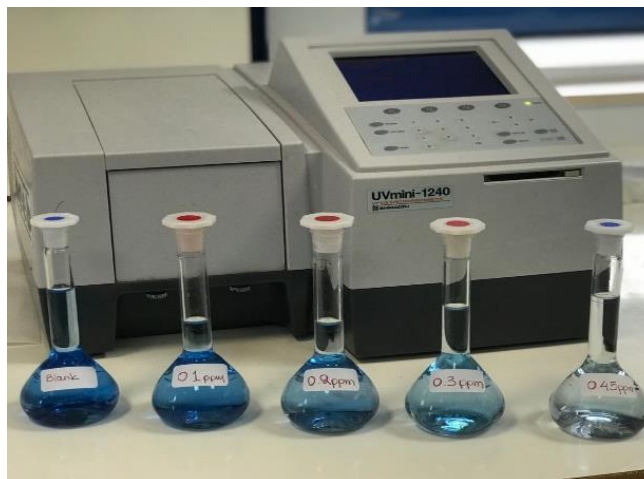


Image 3. Indigo decolorization with regards to ozone concentration.

The detection limit for the Indigo Reagent I and II is $2 \mu\text{g/L}$ and $6 \mu\text{g/L}$, respectively. In our case, some preliminary results were performed in order to compare the results derived from the indigo method with those from the ozone test kit, Accuvac (Hach). Different ozone concentrations were tested and it was concluded that indigo method was absolutely in line with the ozone kit according to the graph set out in Appendix B.

Reagents

•Potassium Indigo Trisulfonate

The reagent Potassium Indigo trisulfonate, $\text{C}_{16}\text{H}_7\text{N}_2\text{O}_{11}\text{S}_3\text{K}_3$ is used for the quantification of the ozone concentration in the aqueous phase. The ozone decolorizes stoichiometrically (1:1) the intense blue dye at low pH and the decrease in absorbance at 600 nm is directly proportional with increasing ozone concentration. The purity of this reagent is above 60% and normally the commercially available reagents reach the value of 50-85%

•Indigo Stock Solution

An indigo stock solution is prepared by adding 1 mL of concentrated, analytical grade phosphoric acid and 770 mg of potassium indigo trisulfonate, $C_{16}H_7N_2O_{11}S_3K_3$ (Sigma-Aldrich) to 1 L volumetric flask filled to the mark with distilled water with stirring. It is noteworthy that when the absorbance of a 100-fold dilution is below 0.16/cm, the indigo solution should be discarded and a fresh indigo solution must be prepared.

•Indigo Reagent II

Since the anticipated range of ozone concentration is 0.05 to 0.5 ppm we proceed with the preparation of Indigo Reagent II. To 1 L volumetric flask, 100 mL of Indigo Stock Solution, 11.5 gr of analytical grade sodium dihydrogen phosphate, $NaH_2PO_4 \cdot H_2O$ (Merck) and 7 mL of concentrated, analytical grade phosphoric acid, H_3O_4P (Fisher) were added and were diluted with distilled water to the mark.

•Malonic Acid Reagent

Since in the tap water that is used for the experimental procedure, residual concentration of chlorine is present, it is necessary to add malonic acid, $CH_2(COOH)_2$ (Sigma-Aldrich) in order to mask the interference of the chlorine, since it decolorized indigo at a moderate rate. The procedure is that 5 gr of analytical grade malonic acid in water are diluted to 100 mL.

Spectrometric determination

Regarding the quantification of ozone, depending on the range of the ozone concentrations in the experiments, the Indigo I or II reagent is used. The estimation of the absorbance is performed in the spectrophotometer UV-Vis (Shimadzu). For anticipated range 0.01 to 0.1 mg/L ozone the addition of 10 mL of Indigo Reagent I to two 100 mL volumetric flasks was executed. The first one was filled the tap water as blank and the second with the ozone-containing sample and the measurement of absorbance at 600 nm was carried out as soon as possible with glass cuvette since the wavelength was in visible range. The dissolved ozone concentration was estimated by the Equation 1. For anticipated range 0.05 to 0.5 mg/L ozone, the Reagent II was used and in case of higher ozone

concentration, bigger volume of Indigo Reagent II is added and the Equation below was adjusted in terms of added sample volume.

$$C_{O_3} = \frac{100 \times \Delta A}{f \times b \times V}$$

where:

ΔA	the difference in absorbance between blank and sample
f	0.42
b	path-length of the cuvette (cm)
V	volume of the sample added (mL)

3.2.5. Dynamic Light Scattering (DLS) method

The nanobubble size distribution was measured by a SALD 7500nano nanoparticle size analyzer (Shimadzu, Japan) which uses the dynamic light scattering (DLS) method and is applicable to particle diameters between 7 nm and 800 μm . The refractive index of the material was chosen to be 1, since the refractive index of the air is less than that of water. After the generation of the nanobubbles and before the onset of the experiment, OzNB tap water samples were collected in triplicate from the upper and lower part of the tank and were analyzed immediately. In order to investigate the stability of the formed OzNBs with respect to time, samples after generation were sealed in glass vials, stored at ambient temperature and were measured every 24 h over the next three days.

Data were plotted as mean \pm SD from at least three independent experiments. In every experiment, duplicate samples were taken at each time interval to estimate the microbial count and to measure the residual dissolved ozone. The temperature and salinity did not change in all experiments.

In order to meet the requirements for sterilized conditions, all glassware used for the experiment was washed with deionized distilled water and autoclaved at 121°C for 15 minutes and the OzNBs tap water was also tested for any bacterial contamination. The disinfection experiments were conducted at ambient temperature, which was approximately 18°C throughout the experiments.

3.3. Results

3.3.1. The size distribution of Ozone Nanobubbles (OzNBs) over time

Before starting the batch ozonation experiments, an experiment with air nanobubbles was performed in order to evaluate the performance of MK1 nanobubbler in terms of size distribution and zeta potential in different operation times (10, 20 and 30 min). In addition, the effect of time was investigated as the zeta potential and size distribution of the samples were measured anew three days after the generation of NBs. Figure 2 displays the size distribution and zeta potential of NBs generated within 10, 20 and 30 times of nanobubbler operation on the first and third day. It can be seen that the first day of generation the zeta potential is similar in different time periods of operation. Nanobubbles are negatively charged, therefore it is reasonable the obtained zeta potential to be negative. Zeta potential was reported -19.30, -19.57, -20 mV in 10, 20 and 30 minutes, respectively. After three days, these values were -13.73, -17.37 and -17.53 mV, respectively. The diameter after the generation was 177, 135 and 124 nm, whereas after 3 days of storage these values were found to be 681, 471, 429 nm within 10, 20 and 30 minutes of operation, respectively. The change in size may be dominated by the Ostwald ripening effect, in which smaller bubbles are deposited on a larger bubbler leading to the growth of size.

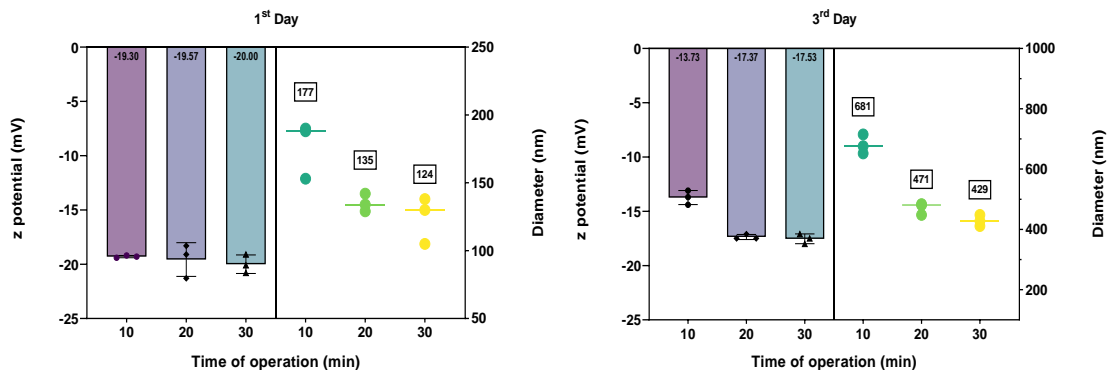


Figure 2. Effect of time on air NBs diameter distribution and zeta potential.

As shown in Figure 3, the effect of time after the preparation of the OzNBs water on the median diameter was examined. It is demonstrated that the OzNBs grow over time and become larger in size. Also in this case, the growth mechanism of OzNBs can be

elucidated by Ostwald ripening process, in which smaller bubbles tend to dissolve and redeposit to larger bubbles (192). Before any ozonation experiment, samples were collected to evaluate the median diameter of the nanobubbles. On the first day, the median diameter was found to be 136 nm as shown in Table 8. After one day, the ozone median diameter was increased to 328 nm. The size of the ozone nanobubbles was further increased with time to 388 in 3 days and to 484 nm after 4 days.

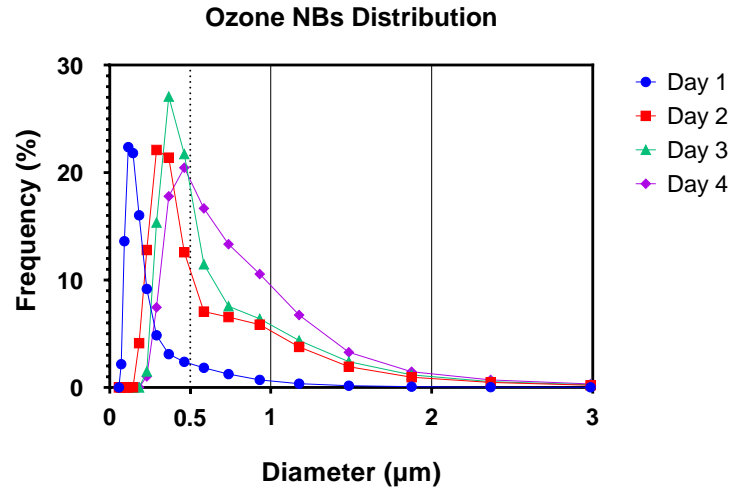


Figure 3. Effect of time on OzNBs diameter distribution.

Table 8. Effect of time on OzNBs median diameter.

Days	1	2	3	4
Median bubble diameter (µm)	0.136 ± 0.036	0.328 ± 0.059	0.388 ± 0.011	0.484 ± 0.087

3.3.2. Drinking water disinfection

3.3.2.1. Ozone decay

The ozone decay was studied when ozone was produced with and without the presence of the nanobubbles and is displayed in Figure 4. It is a well-known fact that the mineral content in water affects the retention time of ozone and more precisely, it is expected the ozone half-life time to be shorter in tap than distilled water, since the concentration of minerals accelerates the decay of ozone. Previous research showed that the ozone has a shortest retention time in water with high mineral content, which was estimated 20 minutes at 5°C (193). The main focus of the experiment was to investigate the

effect of nanobubbles in the ozone retention time in test fluid (tap water) at different pH and temperature. Another factor that can influence the ozone residual concentration is the total organic carbon (TOC) (107), which in tap water tested in these ozone experiments was estimated 7.62 ppm. After the ozone generation, a sample of ozonated water with and without the presence of NBs was selected and the ozone was measured in predetermined time intervals by Indigo Method. At the lowest temperature (13.5°C), the influence of pH was evaluated. As it was aforementioned, high pH leads to a high zeta potential and small diameter, resulting in a greater stability of OzNBs. As it can be seen from Figure 4, at the lowest temperature the ozone decay with the presence of NBs is greatly enhanced when OzNBs are employed. Indeed, when pH increases the ozone decay rate is higher since within 30 min the residual ozone concentration in case of dissolved ozone with MaBs reached at 86% and 34%, in pH 5 and 7.5, respectively, In the case of OzNBs the ozone decay rate is smaller. In fact, the residual ozone concentration within 30 min at the highest pH the residual ozone concentration was estimated to be 66%. These results confirmed that although the high pH leads to more rapid decomposition of ozone, NBs exhibited a higher stability. As it can be seen the difference in ozone decay with and without the presence of OzNBs is more evident at the highest pH. At the highest temperature, there is a slight difference between treatments and the ozone decay rate is higher compared to the lowest temperature since the residual ozone concentration dropped to 85% and 90% within first minute for MaBs and NBs, respectively.

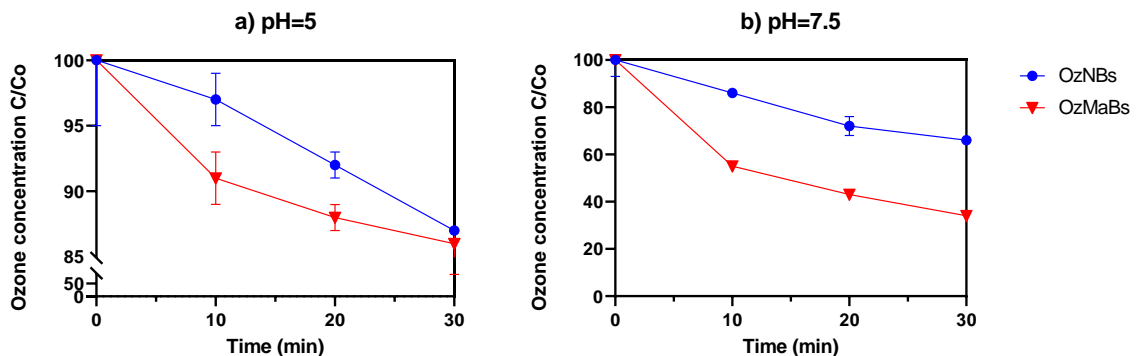


Figure 4. Ozone decay rate with and without the presence of OzNBs in pH a) 5, and b) 7.5 at 13.5°C.

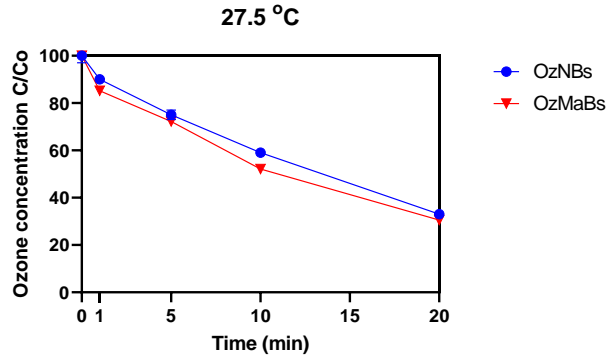


Figure 5. Ozone decay rate with and without the presence of OzNBs at 27.5°C.

3.3.2.2. Inactivation of bacteria

Escherichia coli

In Figure 6, the disinfection efficiency of *E. coli* in three different ozone concentrations is displayed. When the applied dissolved ozone concentration was 1.16 ppm, there is a total disinfection of *E. coli* in case of OzNBs, while there is a significant decrease in bacterial counts; 5 log removal was highlighted just after contact time of 1 min in tap water, with a steady state in the subsequent time intervals. Regarding the ozone concentration, in the first minute of reaction it was found to be greater with NBs, while it was close to zero after 5 min of reaction. As it can be seen by the graph, the same trend is followed by the other two concentrations. The disinfection efficiency with the presence of NBs and the ozone concentration within the first minute of reaction were found to be greater. At the highest bacterial of *E. coli* and in three ozone concentrations, results show that the disinfection efficiency of ozone is found to be greater in the case of presence of NBs.

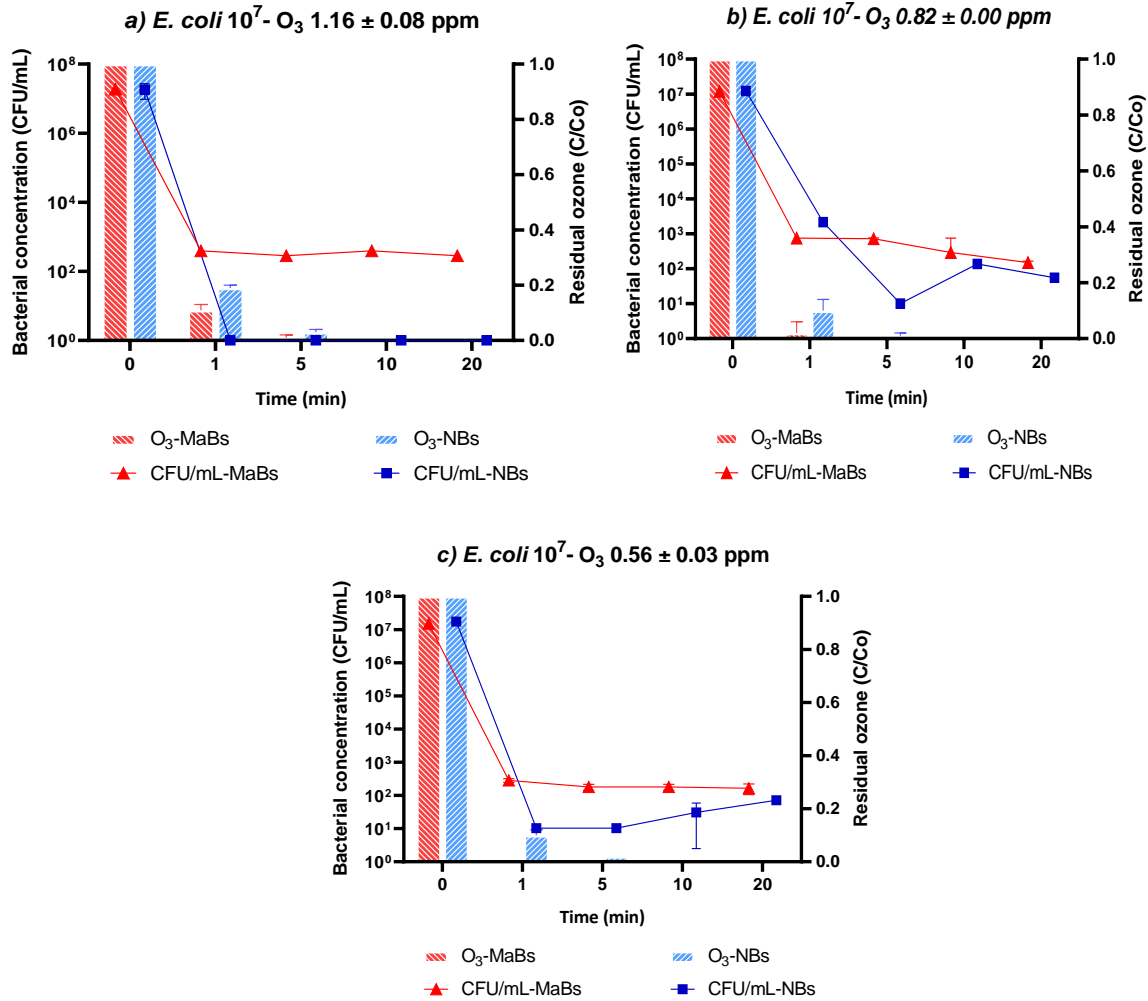


Figure 6. Inactivation of *E. coli* at bacterial concentration 10^7 CFU/mL and ozone concentration a) 1.16, b) 0.82 and c) 0.56 ppm with and without the presence of NBs.

Based on the previous results, the ozone half-life time were estimated. In Table 9, it can be seen that in all cases the half-life of ozone was estimated low, since it was 0.42 and 0.31 min for NBs and MaBs, respectively. The presence of NBs increased the half-life of ozone in all ozone concentrations.

Table 9. Ozone half-life time at ozone concentration 1.16, 0.82 and 0.56 ppm with and without the presence of NBs.

Ozone concentration (ppm)	t1/2 (min)	
	NBs	MaBs
1.16	0.42	0.31
0.82	0.30	0.16
0.56	0.30	0.17

At lower bacterial concentration and two different ozone concentrations (1.11 and 0.74 ppm), there is a total disinfection in both treatments, while there is no essential difference in residual ozone concentration (Figure 7). Also, the ozone half-life time in two concentrations did not differ in both treatments as it can be seen in Table 10.

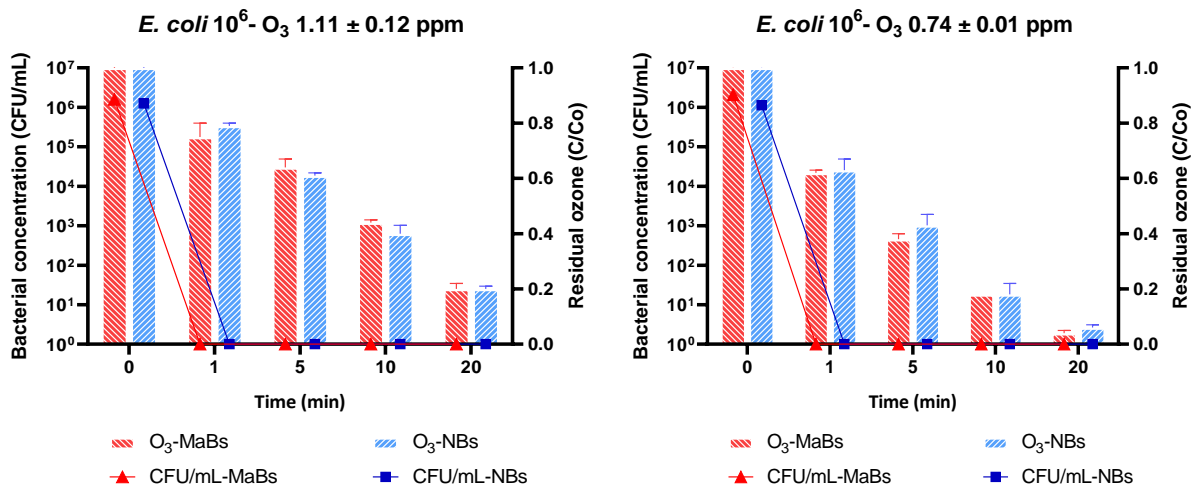


Figure 7. Inactivation of *E. coli* at bacterial concentration 10^6 CFU/mL and ozone concentration a) 1.11 and b) 0.74 with and without the presence of NBs.

Table 10. Ozone half-life time at ozone concentration 1.11 and 0.74 ppm with and without the presence of NBs.

Ozone concentration (ppm)	t1/2 (min)	
	NBs	MaBs
1.11	8.3	8.6
0.74	4.0	3.8

Staphylococcus aureus

As regards the *S. aureus*, different initial bacterial concentration was tested in batch ozonation experiments at initial ozone concentration of 1.20 ppm. In all experiments, a total microbial inactivation was achieved with and without the supplementation of OzNBs. However, a significant difference can be observed in residual ozone concentration from the highest to the lowest bacterial concentration. At initial bacterial concentration 10^7 , 10^6 , 10^5 and 10^4 CFU/mL, the half-life time with the presence of OzNBs was 3.7, 2.3, 2.3 and 1.8 times higher that those with only dissolved ozone, respectively.

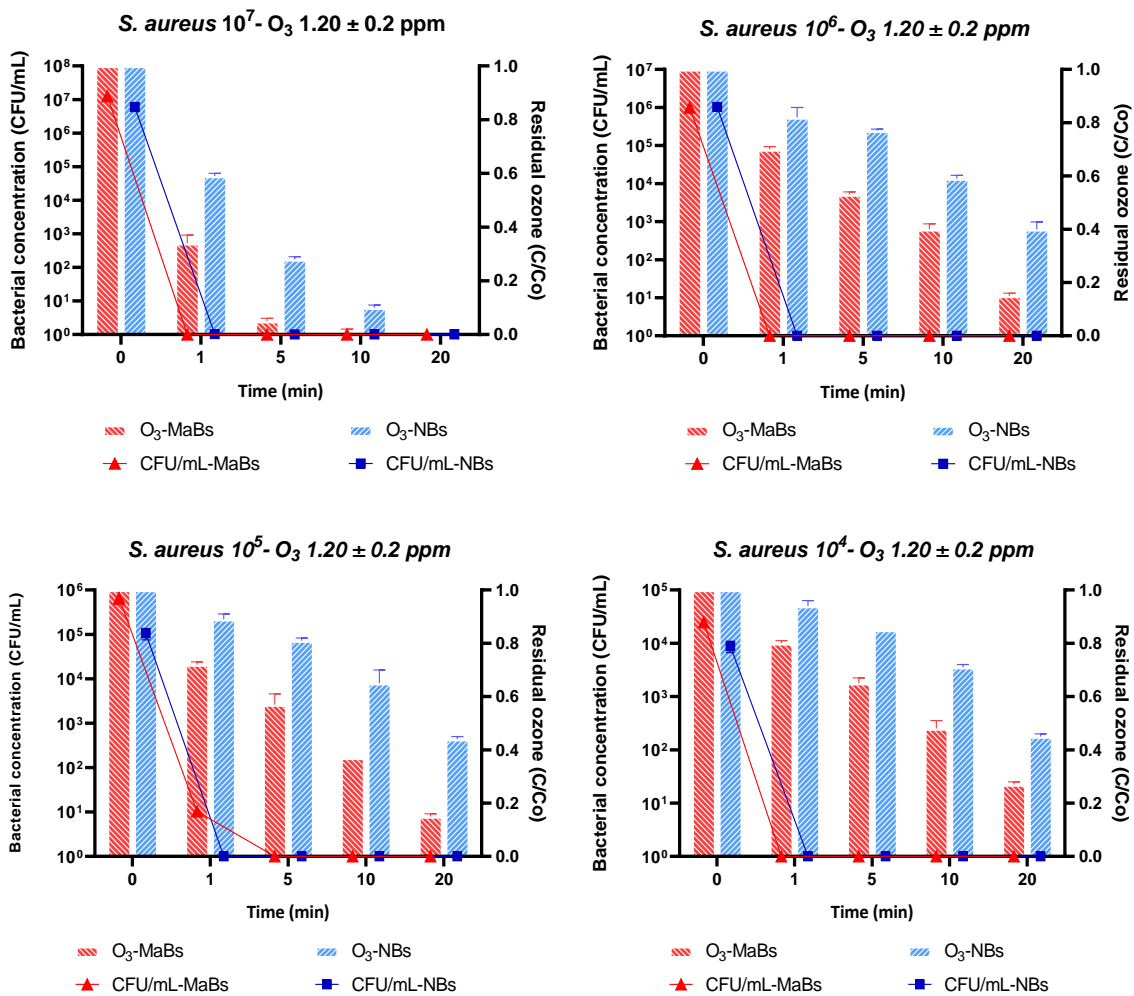


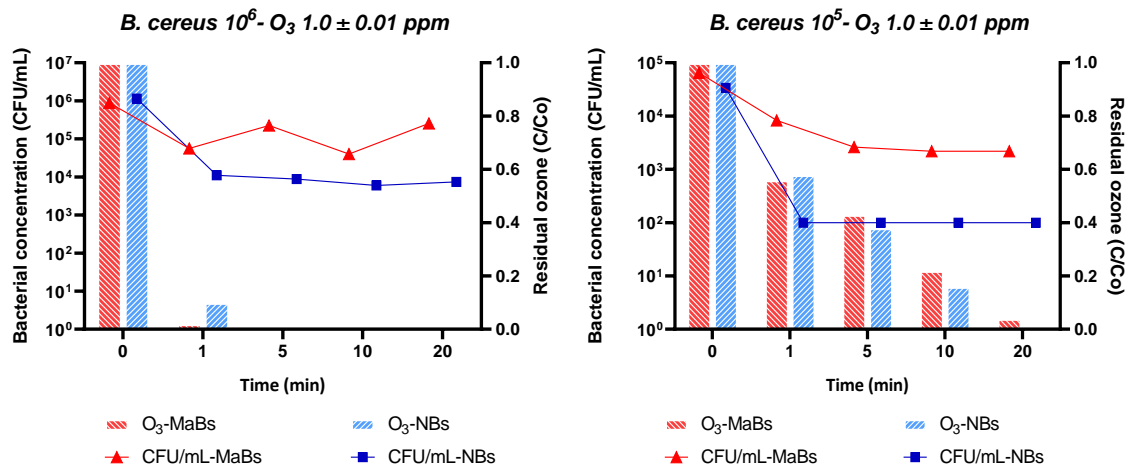
Figure 8. Inactivation of *S. aureus* at ozone concentration 1.20 ppm a) 10^7 , b) 10^6 , c) 10^5 and b) 10^4 CFU/mL with and without the presence of NBs.

Table 11. Ozone half-life time at ozone concentration 1.20 ppm and bacterial concentration of *S. aureus* 10^7 , 10^6 , 10^5 and 10^4 CFU/mL with and without the presence of NBs.

Bacterial concentration (CFU/mL)	t1/2 (min)	
	NBs	MaBs
10^7	2.52	0.68
10^6	14.84	6.57
10^5	17.50	7.68
10^4	18.60	10.44

Bacillus cereus

As far as *B. cereus* is concerned, ozone concentration of 1 ppm did not affect significantly the disinfection at initial bacterial concentration 10^6 CFU/mL in both treatments. The presence of OzNBs reduced the concentration from 10^6 to 10^4 , while only dissolved ozone led to one order of decrease. At lower initial bacterial concentration, the sterilization was higher when NBs are present, whilst in residual ozone concentration there is no substantial difference. The disinfection efficiency in the lower bacterial concentrations (10^4 and 10^3 CFU/mL) is high, as solution is eventually sterilized in both treatments. Investigating residual ozone concentration, there is no appreciable difference between the nanobubble- and conventional ozonation, which was also shown in half-life times as seen in Table 12.



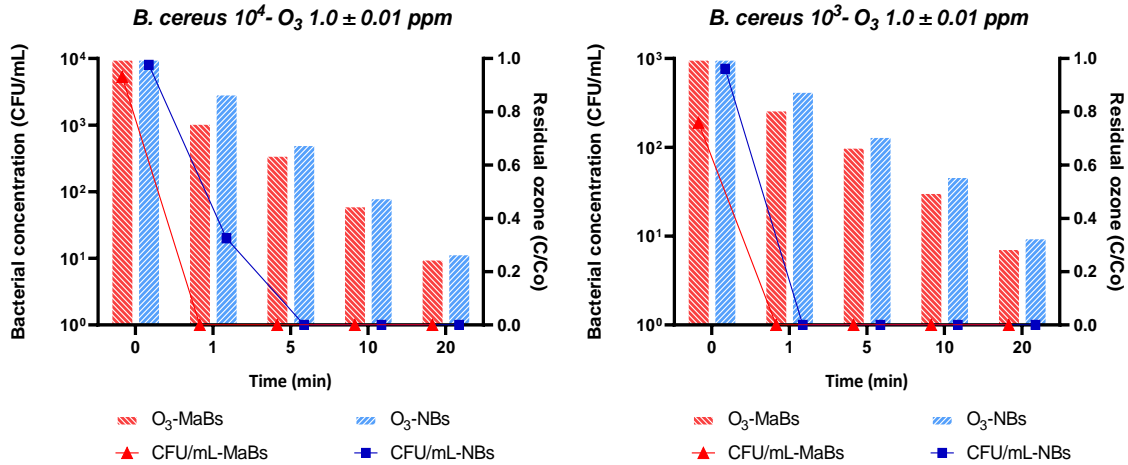


Figure 9. Inactivation of *B. cereus* at ozone concentration 1.0 ppm a) 10⁶, b) 10⁵, c) 10⁴ and b) 10³ CFU/mL with and without the presence of NBs.

Table 12. Ozone half-life time at ozone concentration 1.0 ppm and bacterial concentration of *B. cereus* 10⁶, 10⁵, 10⁴ and 10³ CFU/mL with and without the presence of NBs.

Bacterial concentration (CFU/mL)	t1/2 (min)	
	NBs	MaBs
10 ⁶	0.29	0.18
10 ⁵	3.6	4.2
10 ⁴	10.2	9.8
10 ³	12.7	12.4

Enterococcus faecalis

Figure 10 presents the effect ozonation with and without OzNBs has on bacterial survival on untreated sample inoculated by *E. faecalis* at four different bacterial concentration. In the case of ozone concentration 1 ppm with NBs, the initial microbial concentration ~ 10⁷ was totally disinfected in 20 minutes of reaction. The same trend was followed in the lower bacterial concentrations. The NBs enhanced again the ozone residual concentration. The ozone half-life time in 10⁷, 10⁶, 10⁵ and 10⁴ with the supplementation of NBs was found to be 1.7, 4.2, 2 and 2 times higher than those with the absence of NBs

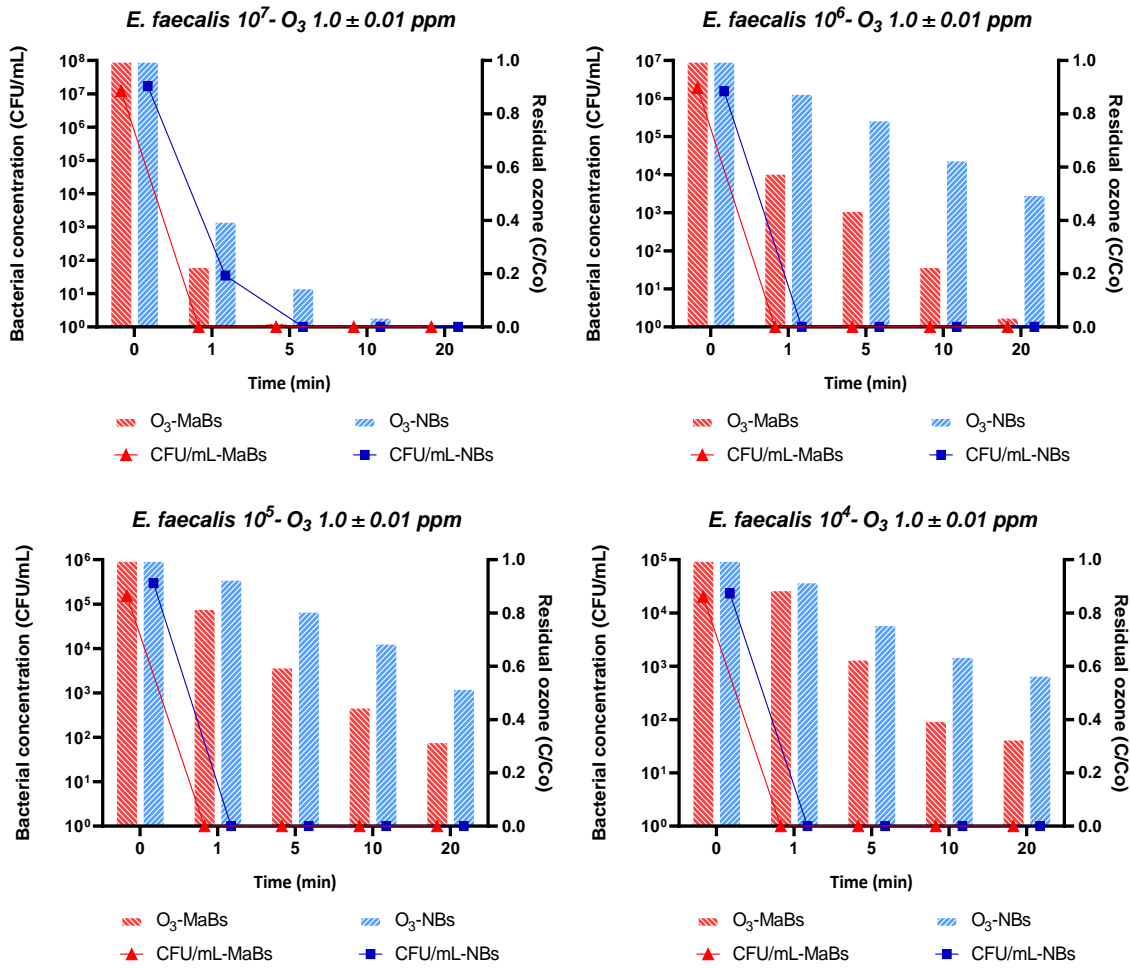


Figure 10. Inactivation of *E. faecalis* at ozone concentration 1.0 ppm a) 10^7 , b) 10^6 , c) 10^5 and b) 10^4 CFU/mL with and without the presence of NBs.

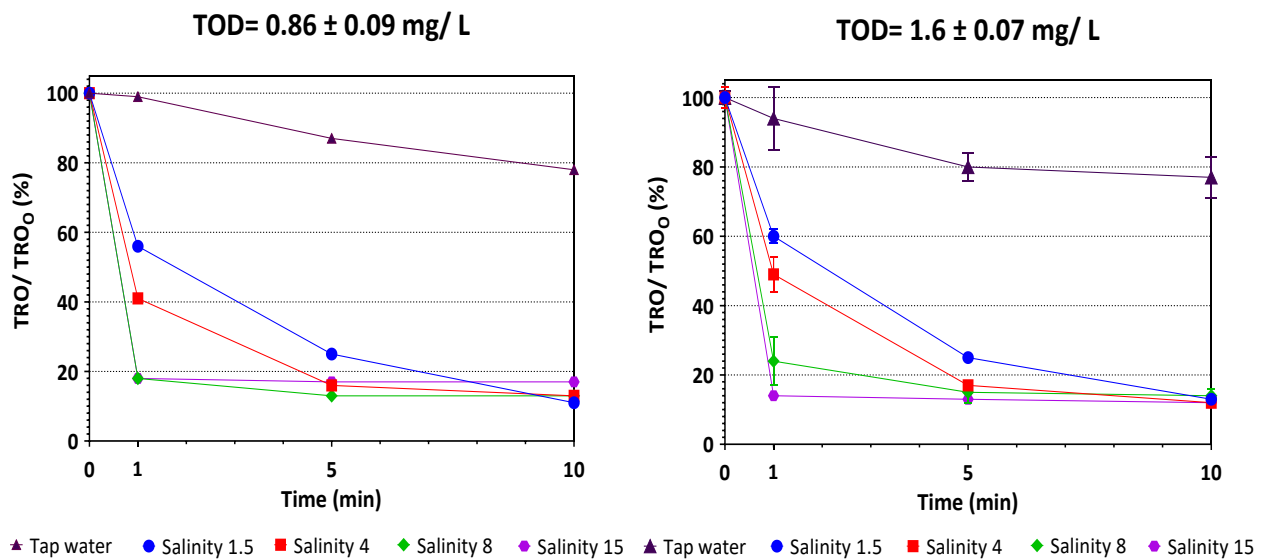
Table 13. Ozone half-life time at ozone concentration 1.0 ppm and bacterial concentration of *E. faecalis* 10^7 , 10^6 , 10^5 and 10^4 CFU/mL with and without the presence of NBs.

Bacterial concentration (CFU/mL)	t1/2 (min)	
	NBs	MaBs
10^7	1.45	0.86
10^6	19.7	4.7
10^5	20.6	10.4
10^4	23.1	11.0

3.3.3. Seawater disinfection

3.3.3.1. The effect of ozone concentration and salinity on ozone reaction

The fate of dissolved ozone in seawater is complicated compared to fresh water. In order to have a direct comparison, a series of batch experiments was performed identical to the ones for disinfection without the presence of microbes. In Figure 11, the ozone reduction with respect to time is shown for four salinities (1.5, 4.0, 8.0 and 15 PSU) and at different initial ozone concentrations 0.86, 1.6 and 2.6 ppm. In the same figure, the ozone decay in tap water is also shown. As seen, the residual TRO was attenuated in both tap and saline water. In tap water, the residual TRO declined steadily reaching to a remaining percentage of approximately 77 % in all initial ozone concentrations at a reaction time of 10 min. This is consistent with first order decomposition kinetics suggesting a half time of about 26 min (at 18°C). The estimated half life time ($t_{1/2}$) of tap water is in agreement with the degradation of dissolved ozone in distilled water, where the ozone $t_{1/2}$ is only 20 minutes (at 20°C) (140,141). On the other hand, in water with the highest salinity (15 PSU), the residual ozone was lower than 20% of the initial ozone concentration within 10 min of reaction. At the highest ozone concentration (2.6 ppm), the $t_{1/2}$ of TRO levels at salinities 1.5, 4, 8 and 15 PSU were found to be 3.4, 0.98, 0.52 and 0.40 min, respectively. It is obvious that the half-life time of TRO is substantially influenced when salt concentration is increased.



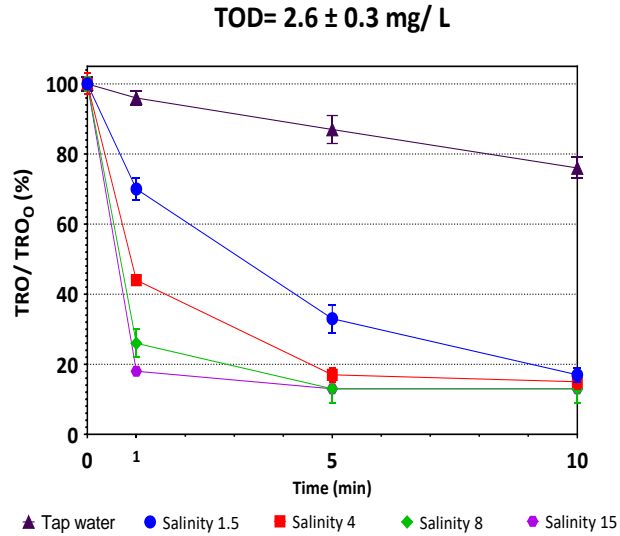


Figure 11. Effect of salinity on TRO remaining expressed as a percentage of different initial ozone concentrations (0.86 ppm, 1.6 ppm and 2.6 ppm).

Table 14. TRO half-life time in different salinities

Salinity	Half-life time of TRO (min)
No salinity	26
1.5	3.4
4	0.98
8	0.52
15	0.40

As shown in Figure 12, the ozone dose did not have any strong effect on the ozone consumption at any salinity level, since the reduction is essentially the same among all the ozonation experiments. On the other hand, salinity displayed a significant impact on ozone depletion. The highest ozone consumption was observed at the highest salinity, as shown in Figure 11.

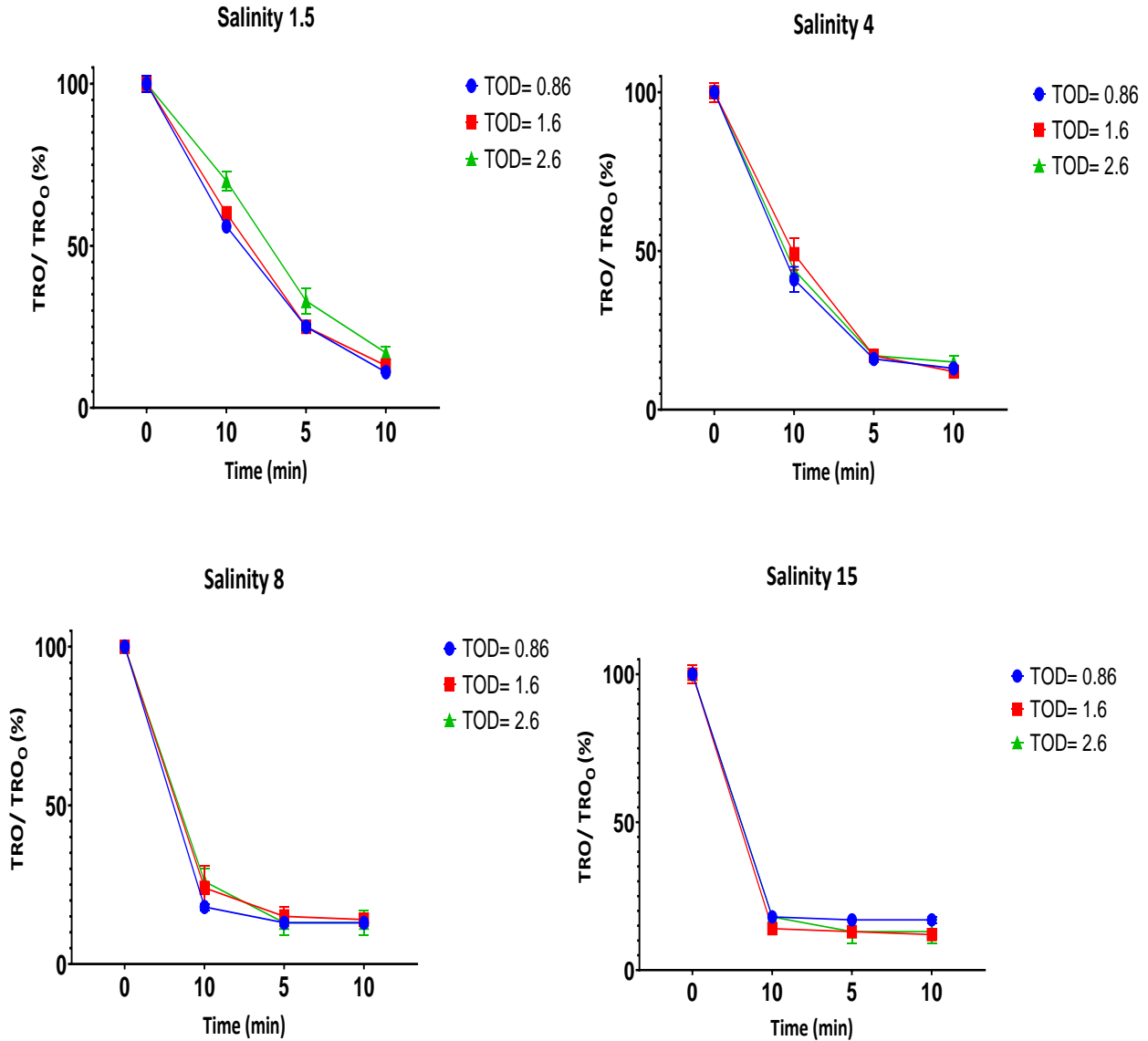


Figure 12. Effect of ozone dose on TRO remaining expressed as a percentage of different initial ozone concentrations resulting from transferred ozone doses of 0.86, 1.6 and 2.6 ppm at different salinities (1.5, 4, 8 and 15 PSU).

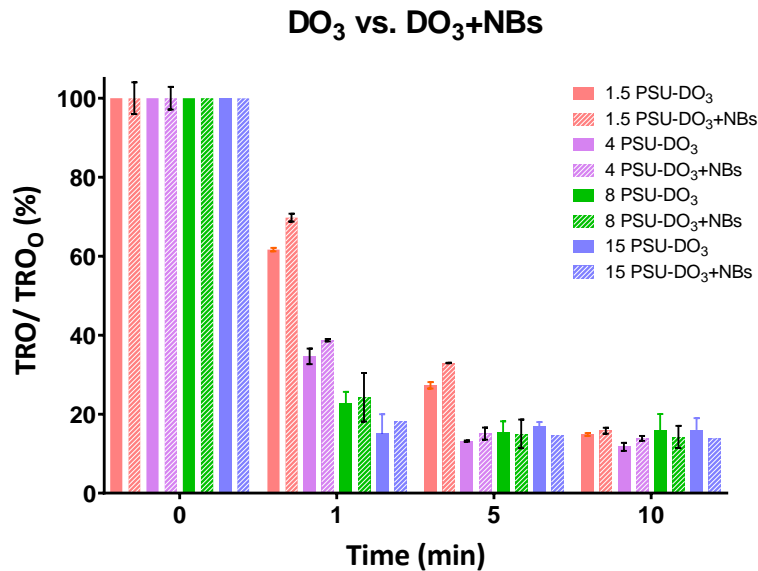
Upon ozone addition, the ORP values rapidly increased from 221.8 to 883.7, 806.0, 795.0 and 779.8 mV at salinity 1.5, 4.0, 8.0 and 15 PSU, respectively. During seawater treatment experiments, various oxidant residuals are formed exhibiting lower disinfection capacity compared to ozone. Thus, the highest ORP value was observed at salinity 1.5 PSU, where the concentration of oxidants formed in the ozonated saline water are lower due to reduced quantity of chlorides and bromides.

Table 15. ORP values in different salinities at ozone concentration 2.5 ppm

	1.5 PSU	4.0 PSU	8.0 PSU	15 PSU
ORP (mV)	883.7	806.0	795.0	779.8

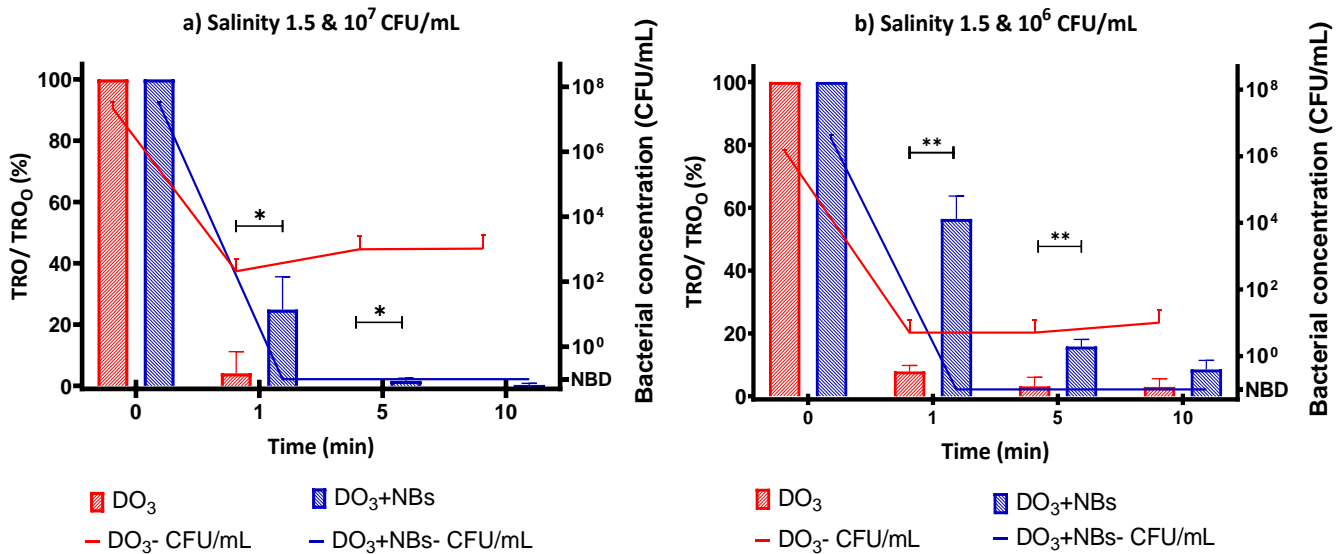
3.3.3.2 Comparison of effect on ozone reaction with and without the presence of OzNBs

In order to investigate if the addition of OzNBs has an effect on TRO concentration, an experiment was conducted with the same transferred ozone dose with and without the presence of OzNBs, where the concentration of residual oxidants was recorded at time intervals (1, 5 and 10 min) in each case. Figure 13 displays the remaining percentage of TRO concentration when the nanobubbles are present or not for every salinity level investigated in this study. The difference of treatments is evident during the early minutes of reaction where the presence of OzNBs enhanced the remaining concentration of TRO. In the fifth minute of reaction, only at salinity 1.5 PSU, a difference can be observed, while at the higher salinities no significant variations are shown. In the last ten minutes of the ozone reaction, no significant difference was observed in all tests.

**Figure 13.** TRO remaining in different salinities (1.5, 4, 8 and 15 PSU) with and without the presence of OzNBs.

3.3.3.3 Comparison of disinfection capacity of ozone with and without OzNBs at different salinities

Batch ozonation experiments with the addition of *E. coli* inoculum in three different concentrations in ozonated water containing OzNBs or DO₃ were conducted with a TOD of 0.89±0.1 mg/L. Firstly, as shown in Figure 14 at salinity 1.5 PSU it is clear that the residual concentration of TRO is higher when the OzNBs are present for every bacterial concentration, therefore it can be concluded that the residual activity is enhanced. On the other hand, it can be seen that the *E. coli* was totally disinfected in all initial bacterial concentrations. This is not the case for ozonated water containing OzMaBs for the initial concentration of 10⁷ CFU/mL, where the log reduction of bacterial concentration was approximately 4. It is worth mentioning, that a t-test analysis was performed in order to investigate if the differences are statistically significant (Stars indicate significance levels : * for p< 0.05 and ** for p< 0.01). It is clear from the results, that the concentration of residual oxidants was observed to be significant within the time of ozone reaction.



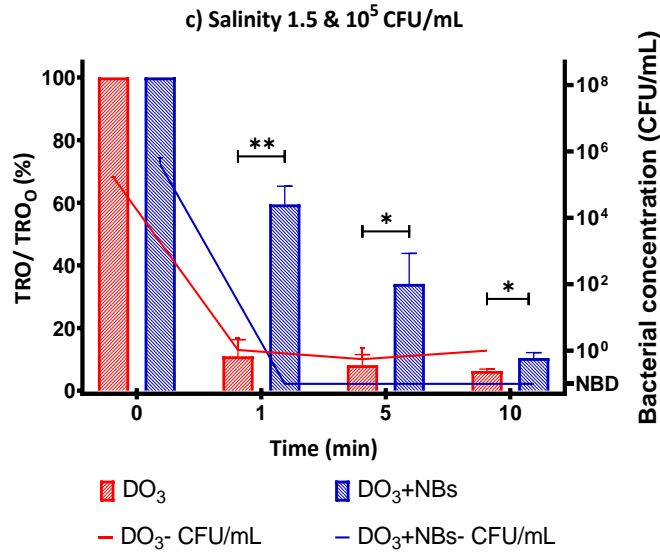


Figure 14. TRO remaining and bacterial concentration after disinfection experiment with and without the presence of ONBs in salinity 1.5 PSU and at bacterial concentration a) 10^7 , b) 10^6 and c) 10^5 CFU/mL (NBD=No bacteria detected).

The investigation of saline water at 4 PSU with dissolved ozone supplemented with OzNBs showed that in the highest bacterial concentration no significant difference was observed in comparison to the treatment with dissolved ozone without any OzNBs. The *E. coli* bacteria were successfully disinfected in both treatments. When the bacterial concentration was reduced to 10^6 CFU/L, a higher residual concentration of oxidants was observed however it was not statistically significant. It should also be highlighted that after the first minute of ozone treatment, the concentration of TRO was stable confirming the formation of by-products derived from the saline water ozonation, which are more stable than ozone. The formation of stable oxidants can be also confirmed in Figure 15c and it should be noted that in this experiment the remaining concentration of TRO is significantly higher when OzNBs are present at the first minute of reaction.

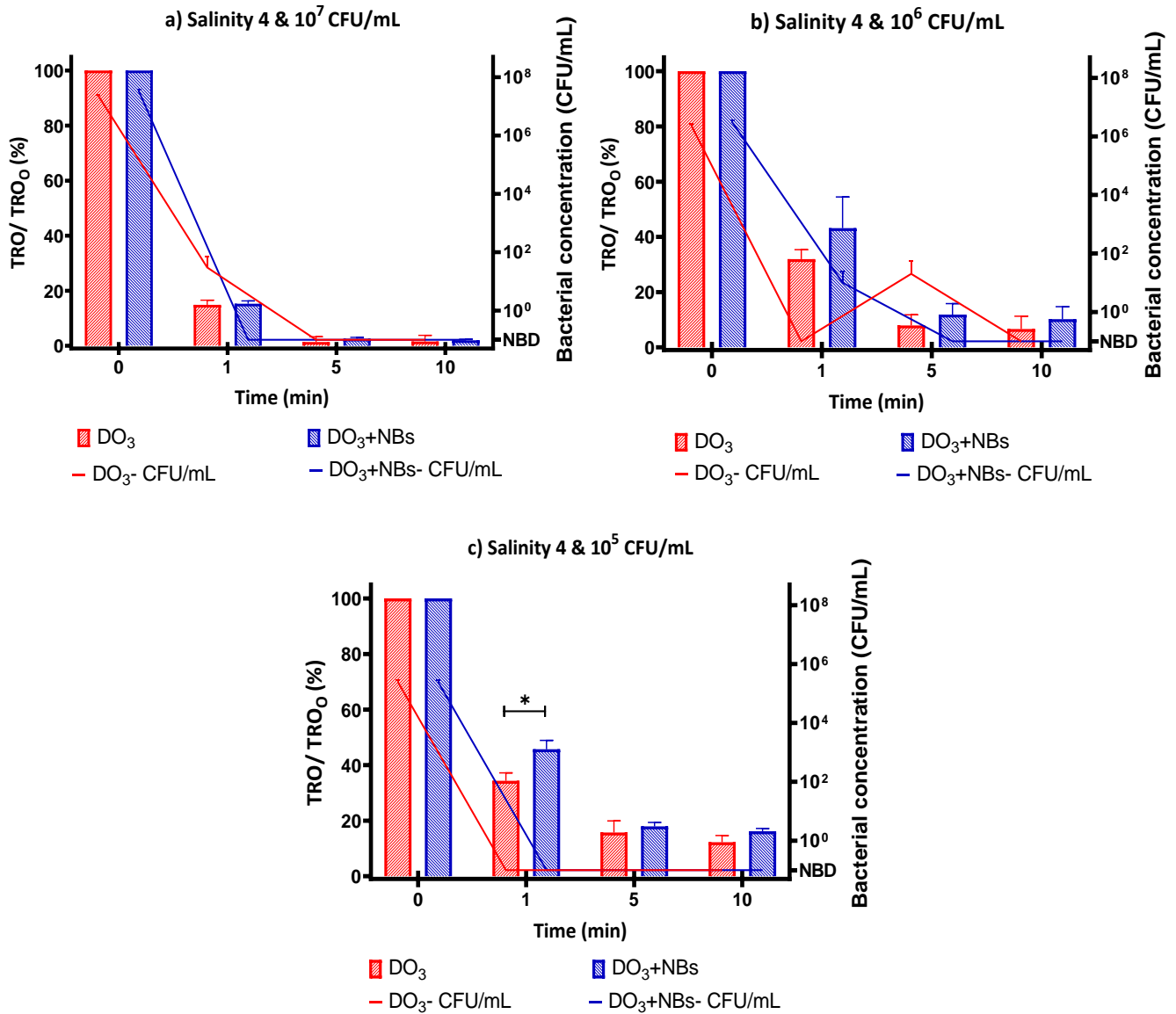


Figure 15. TRO remaining and bacterial concentration after disinfection experiment with and without the presence of OzNBs in salinity 4 PSU and at bacterial concentration a) 10⁷, b) 10⁶ and c) 10⁵ CFU/mL (NBD=No bacteria detected).

At salinity 8 PSU, the ozonation experiments with the highest bacterial concentration did not exhibit any difference in residual concentration of oxidants while a 10-min exposure led to total disinfection in both treatments. For the other two bacterial concentrations, the TRO oxidants concentration was greater when OzNBs were present, however no statistically significant difference was observed between the two treatments. Moreover, at the end of the experiment, a total inactivation of *E. coli* was achieved.

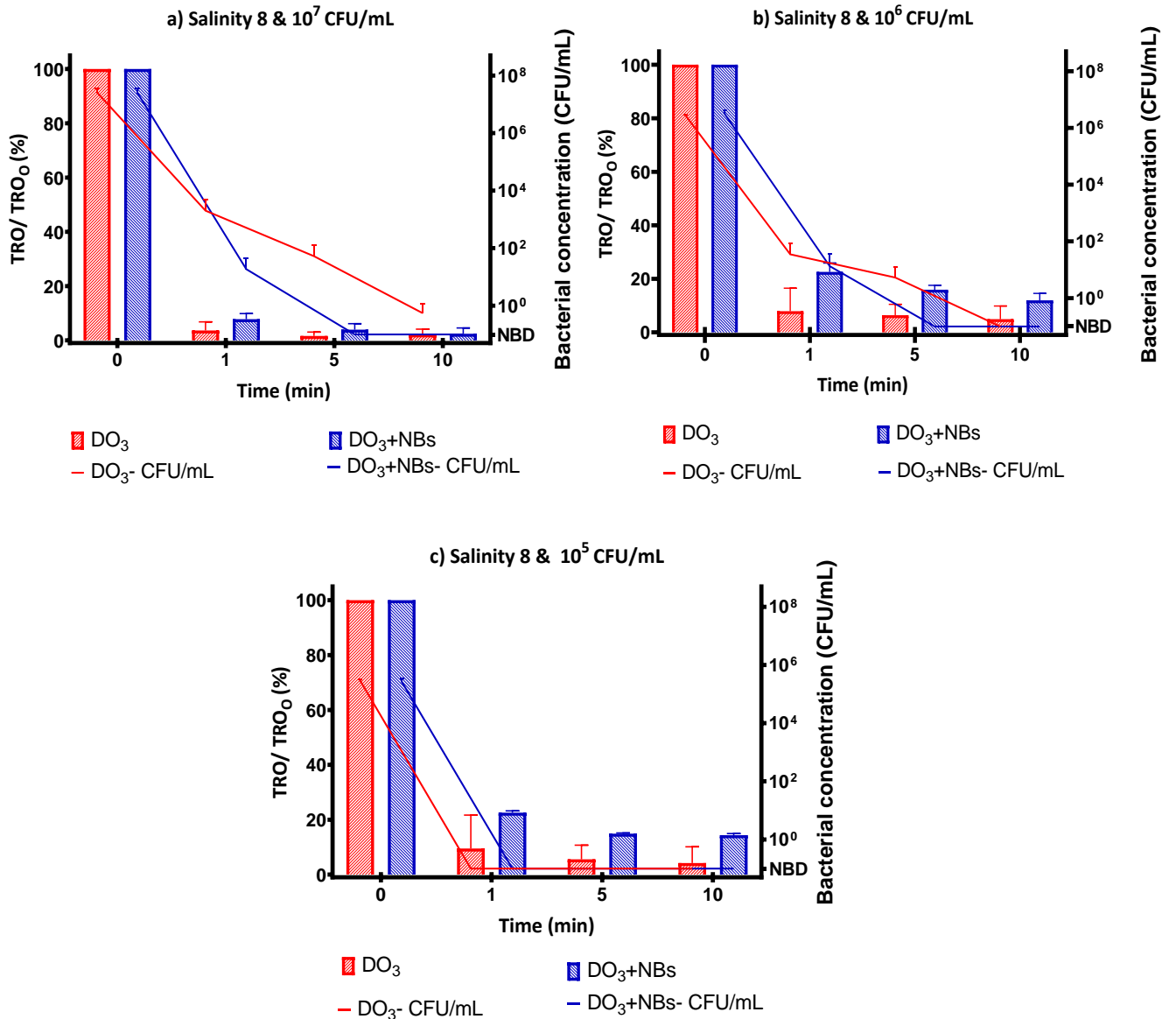


Figure 16. TRO remaining and bacterial concentration after disinfection experiment with and without the presence of OzNBs in saline water (8 PSU) and at an initial bacterial concentration a) 10⁷, b) 10⁶ and c) 10⁵ CFU/mL (NBD implies No Bacteria Detected).

When the salinity was increased to 15 PSU, there is no variation between the treatments as seen in Figure 16. As seen, there is no significant effect on the residual concentration of TRO in all bacterial concentrations with and without the presence of OzNBs.

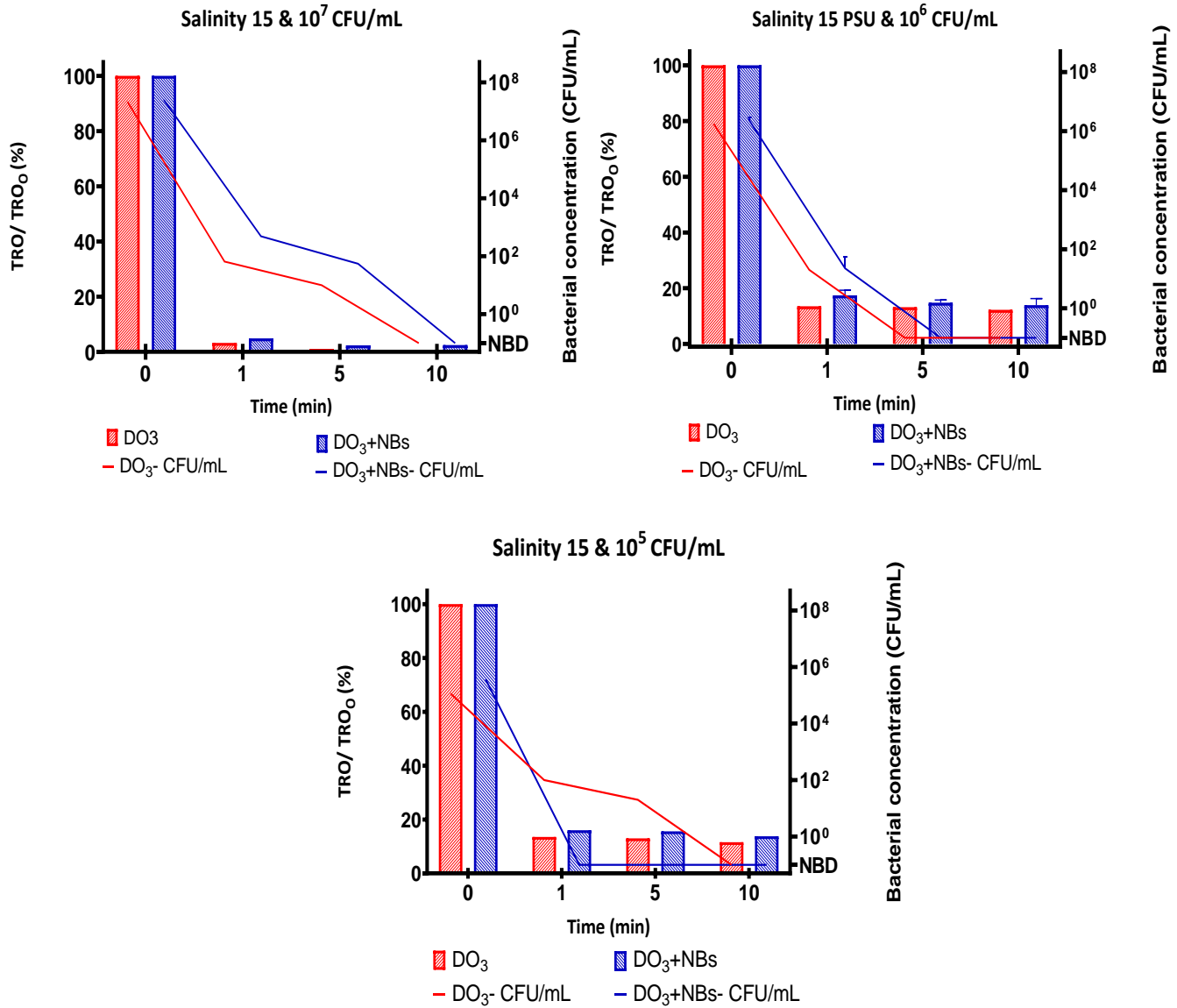


Figure 17. Total residual oxidants (TRO) remaining and bacterial concentrations after disinfection experiments with and without the presence of OzNBs in salinity 15 PSU and at bacterial concentrations: a) 10⁷, b) 10⁶ and c) 10⁵ CFU/mL (NBD, No Bacteria Detected).

In all disinfection experiments, the microbial regrowth after 5 days was investigated, and in all cases no regrowth was observed. More specifically, the bacterial concentration was maintained to the level that recorded or decreased. It is notable that a control experiment without any ozone dose was performed to test any bacterial loss due to salinity or any other factor. During the experimental process, there was no decrease in bacterial concentration since it was stable for 10 minutes. In 5 days, the bacteria

concentration in some cases was reduced only by one order of magnitude, therefore the reduction was due to the disinfection capacity of ozone (Figure C. 1). Treatment with ozone at all salinities formed bromate levels well below that of the maximum contaminant level of 10 µg/ L.

3.3.3.4 Reduction of chloride (Cl⁻) and bromide (Br⁻) at salinity 15 PSU

Since the results from ozonation experiments did not exhibit any difference between the treatments with and without the OzNBs in the highest salinity (15 PSU) (Figure S.4), samples were collected in order to determine the chloride and bromide content at the end of the disinfection experiments. Figure 18 demonstrates that utilization of ozonated water with OzNBs leads to an elevated reduction of chloride and bromide. This reduction cannot be captured by the indigo method since only ozone-based by-products were evaluated as malonic acid was used in order to avoid any interference from brominated and chlorinated disinfection byproducts. Thus, it can be concluded that when saline water with dissolved ozone contains OzNBs, it exhibits a higher residual activity.

This result is not surprising, although the total amount of ozone within the NBs is rather small, it remains for a longer period of time since the half-life of ozone at 20°C in the gas phase is about 3 days compared to only 20 min if it is dissolved in water. Hence, the ozone within the nanobubbles decomposes at a much slower rate compared to dissolved ozone. Notably, among the different bacterial concentrations with the presence of OzNBs as well as with only DO₃ no substantial increase was detected. This can be elucidated by the fact that the transferred ozone reacts immediately with chloride and the bromide ions which are in high concentration and not with the bacteria leading to the total ozone depletion. Therefore, the reduction is the same in all treatments and the formed oxidants exhibit the observed disinfection capacity.

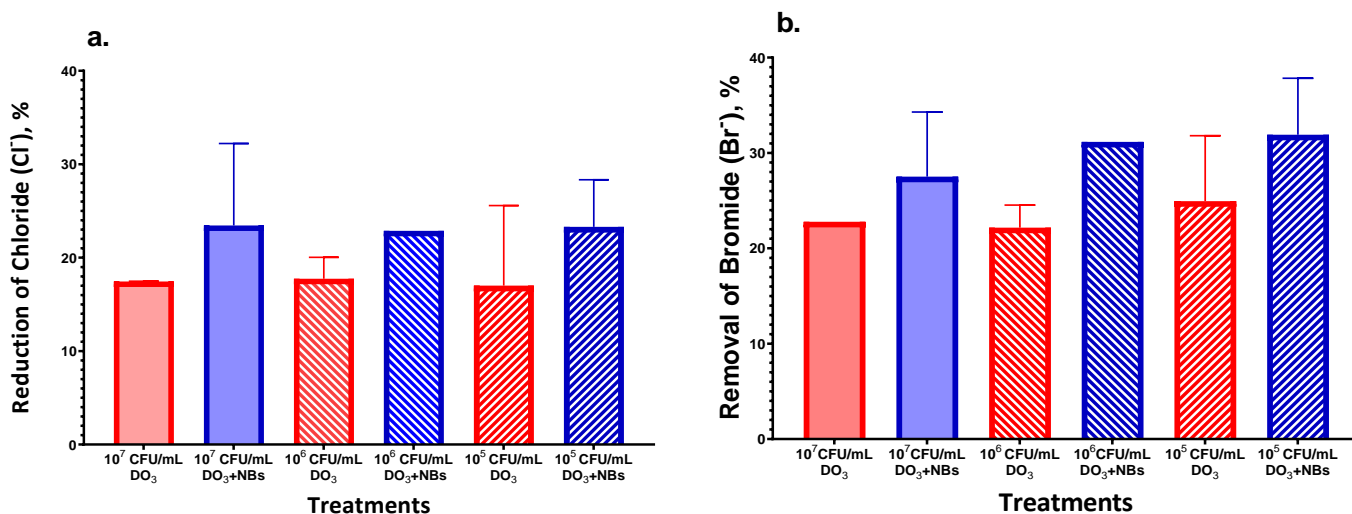


Figure 18. Reduction of Chloride (Cl⁻) and Bromide (Br⁻) at salinity 15 PSU after 10 min of exposure to dissolved ozone with and without OzNBs and for three different initial microbial concentrations.

3.3.4. BPA degradation

It is proved that OzNBs are effective for the oxidation of various organic pollutants. Batch ozonation experiments with and without the presence of OzNBs were conducted in order to compare the oxidation efficiency of BPA, which belongs to the category of endocrine disruptors. Figure 19 showed that both dissolved ozone with and without OzNBs could oxidize BPA within 1 min, which can be deemed as an instant reaction. When the initial BPA concentration was 0.85 mg/L, remaining BPA concentration was 21.95% and 32.95% of initial with and without OzNBs, respectively. The residual ozone concentration was slightly higher when NBs were supplemented.

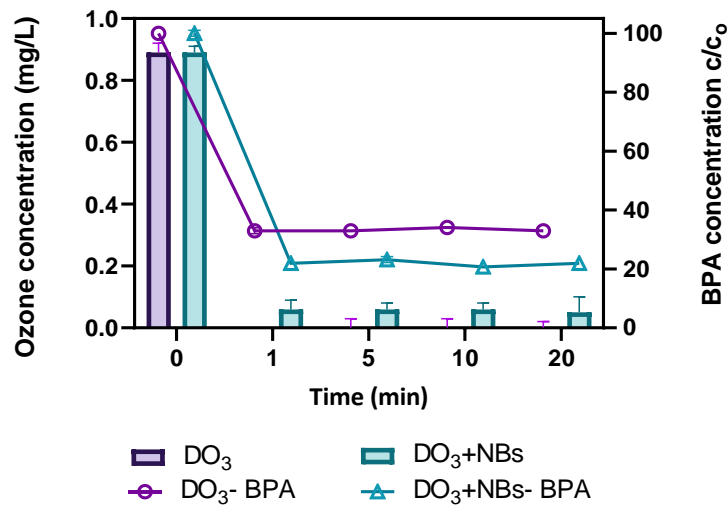


Figure 19. Degradation of BPA by dissolved ozone with and without OzNBs at initial BPA concentration 0.85 ± 0.04 ppm.

When the initial BPA concentration was 2.1 mg/L, the degradation rate of BPA by OzNBs reached 47.17% in 1 min, which was approximately 8% higher than that by dissolved ozone. In 20 minutes of reaction, the degradation efficiency reached 52.83%. As regards, the ozone residual concentration was higher with the supplementation of NBs than those of dissolved ozone.

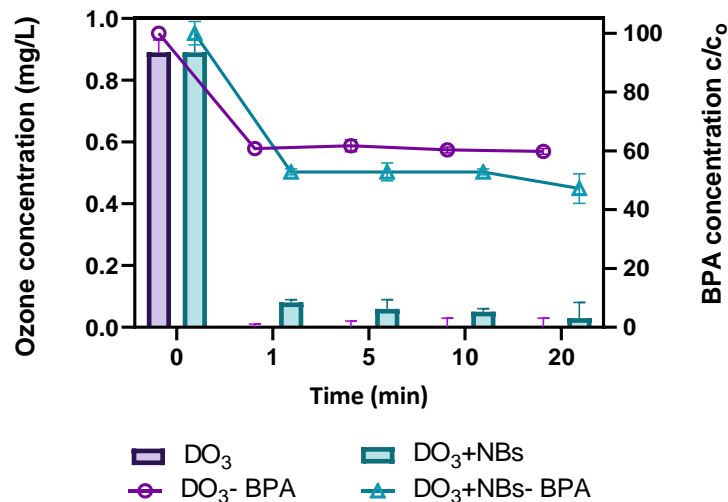


Figure 20. Degradation of BPA by dissolved ozone with and without OzNBs at initial BPA concentration 2.1 ± 0.06 ppm.

When the concentration almost tripled, there was no difference in BPA elimination between treatments with and without OzNBs. The removal efficiency was reported approximately at 38% during the reaction in both treatments. The ozone concentration reached rapidly to zero within 1 minute.

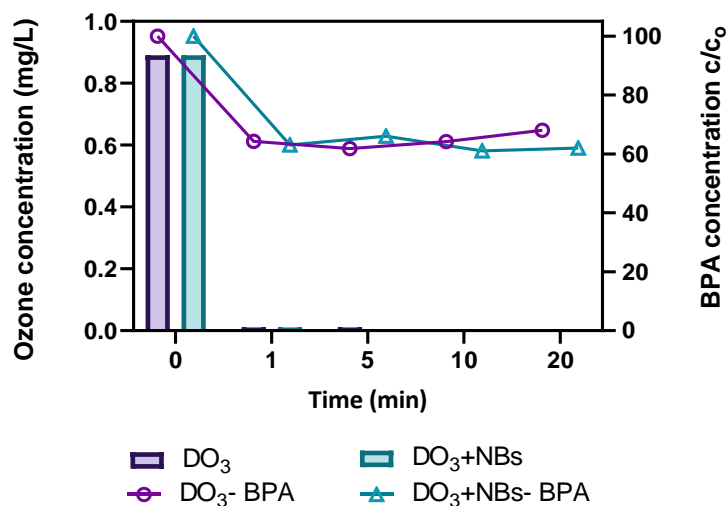


Figure 21. Degradation of BPA by dissolved ozone with and without OzNBs at initial BPA concentration 5.7 ± 0.04 ppm.

3.4. Conclusions

The main conclusion is that the study of OzNBs characteristics illustrates that NBs detected after 4 days in aqueous phase demonstrating a marked stability in a period of four days. The mean value of size distribution were found to be increase from day 1 to day 4, according to Ostwald ripening rules. The decomposition rate of dissolved ozone concentration was greatly enhanced by the presence of NBs in tap water. Specifically, the significant difference in ozone decomposition between the both treatments was reported at the lowest temperature and the highest pH confirming that the increased pH results in a higher stability of NBs since according to literature it can lead to higher zeta potential values and lower diameter. OzNBs had a substantial effect on four harmful pathogens (*E. coli*, *E. faecalis*, *B. cereus*, *S. aureus*). In particular, the supplementation of OzNBs technology had a significant impact on the inactivation of the microorganisms and in most cases the residual ozone concentration was substantially elevated.

Moreover, this study set out to compare the disinfection capacity and the concentration of total residual oxidants (TRO) in saline water containing OzNBs compared to conventional ozone disinfection, since research on their use in ballast water treatment is limited. The results of the present study showed the efficacy of ozone (as TRO concentration) at different salinities. The implementation of OzNBs in the lowest salinity exhibited significantly higher TRO in comparison to dissolved ozone produced by bubbling ozone gas using a porous diffuser for all bacterial concentrations. At the highest bacterial content (10^7 CFU/mL) and at salinity 1.5 PSU, the utilization of NBs led to a 6 times higher residual concentration of oxidants within the first minute of reaction and 1.6 times at the fifth minute, while at lower bacterial concentration (10^6 CFU/mL) the enhancement of TRO concentration was 7-fold and 5-fold at 1st and 5th minute, respectively. Dissolved ozone supplemented with OzNBs had a significant effect on the whole period of reaction at the lowest bacterial concentration. The utilization of nanobubbles in ozonation led to a 5-fold, 4-fold and 2-fold increase in residual TRO concentration at 1st, 5th and 10th minute of reaction, respectively. On the other hand, at the highest salinity, no difference was observed in TRO concentration, however the results obtained from ion chromatography indicated that a greater reduction of bromide and chloride was achieved when OzNBs were used. Among the treatments at different bacterial concentrations, there was no statistically significant variation indicating that the reaction with the halide anions was substantially rapid, leading to formed secondary oxidants that also exhibit disinfection capacity. The findings have practical implications for ozone nanobubbles to be used for drinking and ballast water treatment to inactivate microorganisms present in seawater as shown that OzNBs application leads to a more efficient ozonation as ozone utilization efficiency is higher.

“This page intentionally left blank”

Chapter 4.

Air Nanobubbles in constructed wetlands

This chapter is based on the following publication:

Seridou P, Vamvakia M, Syranidou E, Vlysidis A, Kalogerakis K. Hydrocarbon removal in an air nanobubble- and an electrolysis-integrated horizontal subsurface-flow constructed wetland.

In preparation

4.1. Hydrocarbon removal performance of CWs supplied by oxygen

4.1.1. Constructed wetlands (CWs)

Constructed wetlands has been proved to be an efficient technology for removal of not only conventional pollutants (COD, phosphorus and nitrogen) but also emerging contaminants and is preferred compared to traditional treatment technologies owing to their simple equipment, low investment and operating costs, and easy and simple operation (194). This ecotechnological wastewater treatment is developed to mimic the natural processes found in natural wetland ecosystems for the removal/degradation of contaminants in wastewater (195). The processes that take place in CW are physical, chemical and biological processes including evaporation, substrate adsorption, plant uptake, microbial degradation, filtration, and sedimentation (196). Different types of wastewater, including municipal, urban, industrial, agricultural etc. have been treated by CW systems displaying a high treatment efficiency (18). In general, a CW is shallow basin, filled with filter material, usually sand or gravel and planted with vegetation preferably tolerant to saturated conditions (23). According to the type of flow, CWs are classified in

CWs with surface flow (SF) and with subsurface flow (SSF). In the latter type, there are two categories: horizontal flow (HSSF) and vertical flow (VFSS). In this study, three horizontal subsurface flow (HSSF) CWs were designed.

4.1.2. Artificial aeration

One of the most vital factors in the operation of CWs is the dissolved oxygen (DO) since it can influence the microbial activity and pollutants removal efficiency. Due to the low concentration of dissolved oxygen in the effluent of CWs, an aeration system is highly beneficial, since it has been found that aerated wetlands are capable of increased pollutant removal rate. Aeration in CWs attributed a positive effect in the performance compared to non-aerated systems therefore a variety of oxygen supplementation technologies have been designed in order to elevate the oxygen content in wetland beds. It has been found that artificially aerated CWs can increase oxygen transfer rate by compressing air from the atmosphere into the wetland bed with the use of a blower (23,197). In addition, the oxygen transfer rate can be influenced by the size of the bubble and the air flow rate. An increase in oxygen transfer can be achieved by smaller air bubbles owing to the high specific area (9). Moreover, the high zeta potential in absolute value can create repulsion forces and prevent the coalescence among the bubbles, which could lead smaller bubbles to attach each other or to larger bubbles and decrease the OTR (198).

4.1.3 Electrochemical technology

Electrochemical technology widely used in wastewater has been employed to enhance the removal efficiency of CWs for nitrogen, phosphorus and organic pollutants by anode oxidation, cathode deoxidation, electro-coagulation processes (199–201). An increasing number of studies have applied the electrochemical technology using iron electrodes in the operation of CWs for the enhancement of decontamination efficiency for conventional as well as emerging pollutants (such as antibiotics) (199,200,202,203). This treatment has been widely used as iron element is economical and moreover, the root iron plaque can promote the plant health and reduce environmental stress (199). A principal advantage of an electrolysis-integrated CW is the oxygen production that takes place in the anode. An electrolytic air-water dispersion is generated by a direct current between two

immersed electrodes. Water electrolysis is able to generate bulk micro-nanobubbles in the solution as oxygen and hydrogen gas bubbles are released at the anode (oxidation) and cathode (reduction), respectively (204). The average size of oxygen nanobubbles in electrolyzed water was measured 30 nm the first day by DLS, 180 nm the second day, while it became 250 nm on the third day (64). Therefore, it is important to investigate the oxygen that is supplied via electrochemical production through small sized gas bodies.

4.1.4. Hydrocarbons removal in CWs

Hydrocarbon contamination is considered a serious concern for the environment and is becoming prevalent across the globe due to their extensive use. Among the various hydrocarbons, fuel hydrocarbons such as BTEX compounds (benzene, toluene, ethylbenzene and xylenes) and phenolic compounds derived from industrial, agricultural and domestic activities exist into water bodies (17). CWs have been effectively applied for the treatment of water contaminated with hydrocarbons and a number of studies have investigated the fate of MTBE and phenolic compounds, indicating that there is an efficient removal of various hydrocarbons (19).

4.1.4.1 Phenol

Phenolic compounds are among the chemicals that have raised great concern owing to their persistence in the environment and their accumulation into humans and animals inducing short- and long-term effects. Anku *et al.* (17) reported that some phenolic compounds can occur in nature associated with the colors of fruits and flowers, while others can be synthesized and derived by anthropogenic activities. The United States Environmental Protection Agency (USEPA) and the European Union (EU) have prioritized the phenolic compounds in the list of toxic pollutants due to their devastating effects on human and aquatic lives. Therefore, a number of wastewater treatment techniques have been developed in order to minimize their disposal into water bodies (17).

4.1.4.2. Toluene

Toluene (also known as methylbenzene) is a clear liquid is a natural substance of gasoline and crude oil. It is an organic compound that it is highly lipophilic. It is widely

used in industry for synthesis of chemicals, including nylon, plastics, paints, and solvents (205). The most common way of exposure to toluene is via inhalation. Occupational exposure to toluene occurs in painters and other workers, but it is debated whether low-level toluene exposure has any detrimental effects. Clinical studies have shown that regular exposure to toluene for months and years led to dementia, ataxia, and various other neurologic deficits (206). The permissible exposure limit for toluene is 200 ppm for a 8-hour shift (207).

The aim of this chapter was to investigate the hydrocarbon removal performance of constructed wetlands supplied by oxygen via two different methods; the electrochemical oxygen production and the nanobubble injection.

4.2 Materials and Methods

4.2.1 Experimental set-up

The experimental set-up consists of three horizontal subsurface flow (HSF) CWs which were constructed in the green house at the Technical University of Crete under ambient air with protection against rain (Image 4). Phenol and toluene were selected as the representative hydrocarbons. Three polyethylene tanks with dimensions 90x30x40 cm (LxWxH) and volume of ~100 L were filled with gravel (1 cm) covering the entire root system. Larger gravel (3.5 cm) was placed at the effluent tube to avoid any clogging. The CWs had a constant water level (~25 L) and they operated in a continuous mode with complete recirculation with the use of a peristaltic pump and the external 10 L-tanks containing the contaminated water. Specifically, the experimental set-up includes a control CW (CW1), consisting only of the plant and the gravel, a CW further supplied by direct oxygenation by air nanobubbles injected via a porous pipe distributor (CW2), and a CW supplemented by oxygen nanobubbles generated in situ by electrochemical production with stainless steel electrodes (CW3).

In CW2, a PE nano tube bubble diffuser (Holly technology, China) placed at the bottom of mesocosm was used constantly connected to an air compressor with an air flow rate of 14 lpm. This nanotube is of great efficiency since it needs lower gas consumption than the conventional diffusers with its aeration pore diameter ranging from 0.3 μm to 100

μm . No bubbles were detected at surface of CW. CW3 was designed following the experimental process as reported by Gao *et al.*, 2017 (208). Three iron plates were used as electrodes with dimensions 20x10x2 cm (HxLxW). The anode was set in the center of the unit close to rhizosphere and the cathodes were set on both sides of the anode providing a cathode/anode surface area ratio 2:1. Moreover, these iron plates contained many pores diameter of 1 cm along the surface to assure easy passage of water through the wetland. The electrodes were connected using copper wires to a DC regulated power supply, which was used to provide constant current for electrolysis. The experimental process was conducted under ambient temperature.

4.2.1.1. Vegetation

J. acutus plants were collected from the Souda Bay of Chania (Greece) carefully in order the roots to be maintained intact and were transferred in the greenhouse of the Technical University of Crete (Chania, Greece). Then, the roots were rinsed with tap water to remove any soil and impurities. They were transplanted in every CW and were acclimatized for one month before the beginning of the experiment.

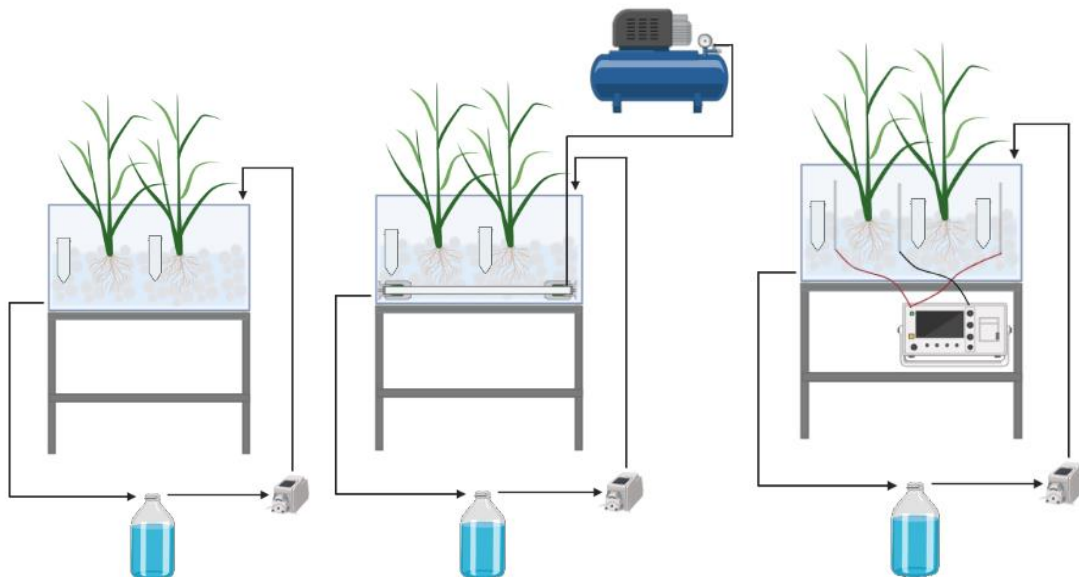


Image 4. Three constructed wetlands; left) control- CW1, middle) air nanobubble-integrated- CW2, and right) electrolysis-integrated- CW3.

Measurements were taken daily in terms of pH, oxidation-reduction potential (ORP (mV)) and dissolved oxygen (DO (mg/L)) from a point close to the rhizosphere (middle) and close to the effluent (end) in CW1 and CW2 as well as in CW3 close to the cathodes (in, end) and to the anode (middle). The electrical conductivity was measured only in CW3.

4.2.2 Experimental cycles

During the experimental period, several cycles (Table 16) were performed where the hydraulic residence time (HRT), the type of contaminant and the initial hydrocarbon concentration changed. Moreover, primary-treated wastewater from WWTP of the region Platania (Chania) were collected and used in combination with the hydrocarbons. The physicochemical and wastewater parameters as well as the concentration of the two selected hydrocarbons were monitored in the effluent of CWs and the external tanks on a daily basis in order to evaluate their performances.

Table 16. Experimental design of CWs.

Cycles	Phenol [ppm]	Toluene [ppm]	Wastewater	HRT [hours]
1	50	-	-	12
2	50	-	-	24
3	100	-	-	24
4	200	-	-	24
5	-	50	-	24
6	-	100	-	24
7	100	100	-	24
8	100	100	+	24

4.2.2.1. Physicochemical parameters

At each cycle, pH, oxidation-reduction potential (ORP), dissolved oxygen (DO), temperature (T) and the electrical conductivity (EC) only in CW3 were monitored daily by a Hach HQ40d multi parameter meter.

4.2.2.2. Wastewater quality parameters

COD, TN, TP were analyzed using standard test kits (Hach-Lange GmbH) and DR 2800 spectrophotometer (Hach-Lange GmbH). Analysis of total suspended solids (TSS), was conducted according to Apha standard methods (209). All the above were measured in Biochemical Engineering and Environmental Biotechnology Laboratory at TUC

4.2.2.3 Cell concentration and microbial analysis

At the end of every cycle, cell concentration (events/mL) close to rhizosphere was evaluated in every wetland using a flow cytometer (Beckman Coulter). The cell concentration was identified by staining with SYBRGreen, which penetrates all cells and is bound selectively to double-stranded DNA (210). Furthermore, in every experimental cycle, samples close to rhizosphere were collected for microbial analysis when the removal efficiency of CWs reached 100%. In CW3, an additional sample was collected close to the cathode in the entrance of wetland. The cycles selected were listed in Table 17 and firstly they were measured in terms of cell concentration by the cell counter. Then, DNA extraction was performed (Qiagen, CA, USA) and the extracted samples were sent for 16s rRNA gene sequencing (Novogene Company Limited, Cambridge, United Kingdom) using the bacterial primers 341F/806R (5'-CCTAYGGGRBGCASCAG-3'/5'-GGACTACNNGGGTATCTAAT-3'). Bioinformatics analysis was performed in R version 4.0.0 and in the R Studio environment version 1.3.959. The DADA2 pipeline was employed for the analysis of the resulting fastq files using the corresponding R package (211).

Table 17. Selected cycles for microbial analysis.

Cycles	1	2	3	4
Phenol	100 ppm	-	100 ppm	100 ppm
Toluene	-	100 ppm	100 ppm	100 ppm
Matrix	Tap water	Tap water	Tap water	Wastewater

4.2.2.4. Organic compounds analysis

Phenol concentration was determined by High Performance Liquid Chromatography (HPLC). Separation of phenol was performed on a Nucleosil 100-5 C-18 column (Macherey-Nagel, Duren, Germany). The mobile phase was acetonitrile (ACN): ultra pure water (50:50), the excitation and emission wavelengths of the Fluorescence Detector (FLD) were set at 277 and 300 nm respectively, the analysis time was 10 min and the oven temperature 27 °C. Samples of volume 40 µL were direct injected into the rheodyne valve. The maximum permissible phenol concentration in wastewater stream is less than 1 mg/L (212). The aforementioned method can detected phenol concentration up to 0.05 mg/L. Therefore it is considered that a total removal of phenol was achieved when the phenol concentration is below 0.05 mg/L.

A Gas Chromatography (GC) HP 5890 Series II (Hewlett Packard Co.) connected with a headspace sampler HP 7694G was used to estimate the toluene concentration. Carrier gas was He at 1 mL/min, the temperature of the vial was 80 °C, while the temperature of GC injector was 250 °C and oven temperature was increased from 60 °C to 250 °C at a rate of 20 °C/min. The maximum allowable concentration of toluene in drinking water is 70 µg/L (205), while the detection limit of concentration is 50 µg/L. Also, in this case a removal efficiency is deemed to be 100% below this concentration.

When the mixture of the two hydrocarbons was investigated, the HPLC was used for analysis. The UV detector was set at 254 nm, The column used was Nucleosil 100-5 C-18 with an isocratic elution and the flow rate was 1 mL/min in mobile phase consisting of ACN:ultra pure water (70:30).

4.3. Results

4.3.1 Cycle 1

Initially, a hydraulic retention time of 12 h was tested and the targeted pollutant was phenol at initial concentration 50 ppm (Figure 22). The CW2 exhibited the higher performance since phenol was totally removed within 3 days, while the other two systems

needed more than 5 days to remove the phenol. Specifically, a total removal of phenol was achieved in the CW3 at 6th day while in the control CW1 at 7th day.

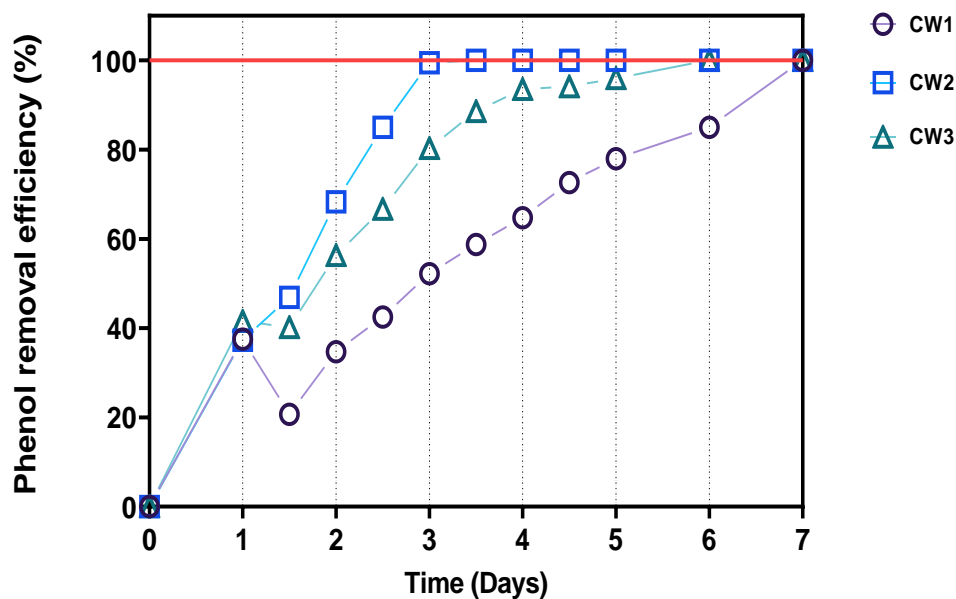


Figure 22. Phenol removal efficiency (%) versus time (Cycle 1: initial conc.=50 ppm & HRT=12 h).

Regarding the oxidation-reduction potential, it can be seen from Figure 23 that in CW1 and CW2 positive values of ORP were reported, in contrast to the CW3, where the ORP was negative throughout the experiment in the three points of sampling. In particular, the average ORP values in the middle and end point in CW1 were approximately 167 mV and 146 mV, respectively. In CW2, the ORP values were elevated as the values in the middle and the end were 205 mV and 219 mV, respectively. All the sampling points in CW3 showed negative values in values and specifically lower than -300 mV. Regarding the DO level, a rather low concentration was detected in CW1 and CW3, while in CW2 the oxygen content was above 8 mg/L indicating that the aeration was sufficient, while the rest wetlands showed a low concentration of dissolved oxygen approximately 2 mg/L. The pH values throughout the first cycle in CW1 were similar between the two sampling points as the average values were estimated 7.39 in the middle and 7.33 in the end. Elevated pH values were reported in CW2, approximately 8.15 in both sampling points. In CW3, the pH was 8.71 and 9.43 in the cathode of the entrance and the effluent, respectively while in

the anode it was 7.66. Finally, the average temperature was measured 16.3°C in the first experimental cycle.

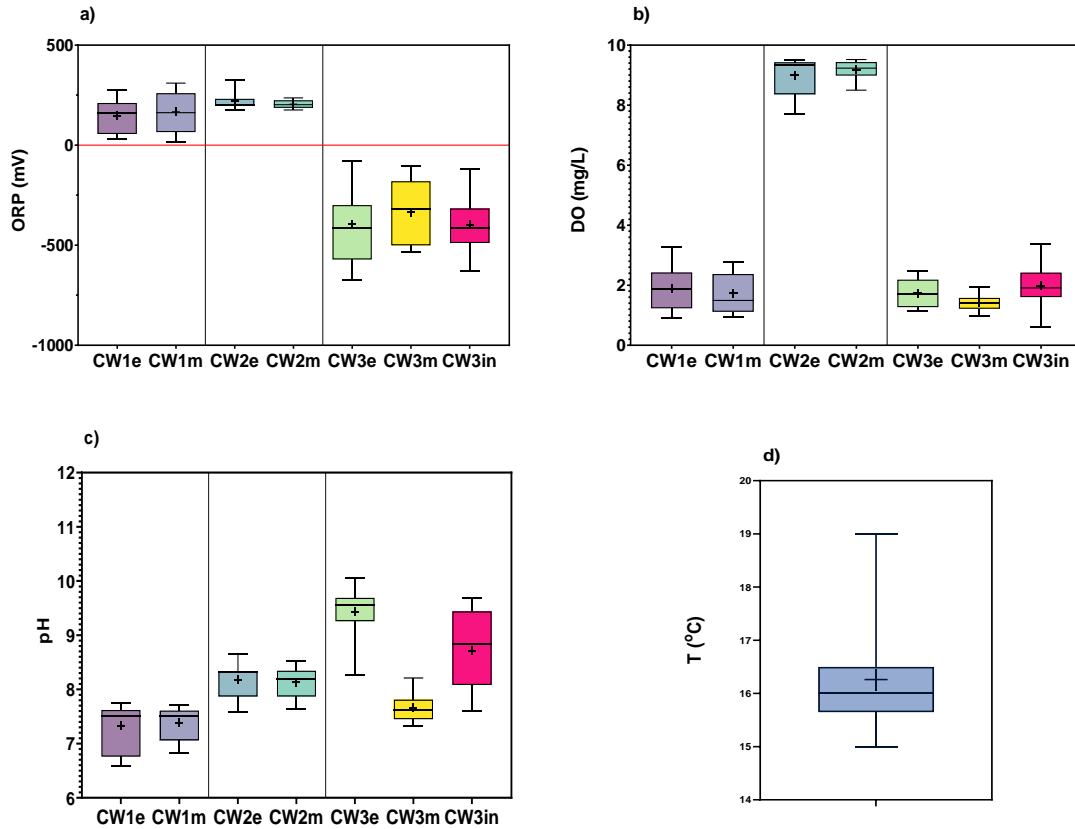


Figure 23. Oxidation- reduction potential (mV) and b) dissolved oxygen (mg/L), c) pH and d) temperature (T oC) in wetlands throughout Cycle 1.

4.3.2. Cycle 2

In higher HRT (Figure 24), the performance of three systems was greater with the constructed wetland supplied by air nanobubbles exhibiting the higher removal rate as the total removal was reported within 1.5 days. Given that the phenol removal was 100% within 2 days in all systems in HRT of 24 hour, the same HRT was chosen for the higher tested concentrations.

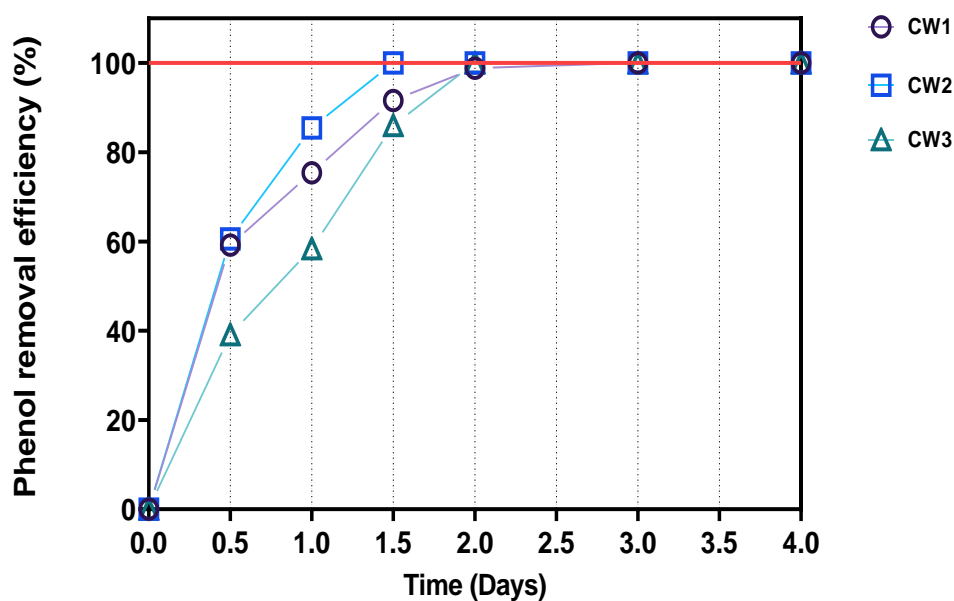


Figure 24. Phenol removal efficiency (%) versus time (Cycle 2: initial conc.=50 ppm & HRT=24 h).

When the HRT was increased from 12 h to 24 h, the average ORP values in wetland CW1 was 229 mV slightly increased in comparison to experiment cycle 1. A stable trend was demonstrated in CW2 as ORP value was estimated 213. In CW3, in the sampling points close to the cathodes, in and end, ORP ranges from -268 to 95 mV and from -217 to 186 mV were reported, respectively. In contrast to the experiment cycle 1, the ORP in the anode of CW3 was positive with an average value of 202 mV. The increased HRT appeared not to influence the dissolved oxygen content as it remained high and slightly increased (above 8.5 mg/L) in CW2. Moreover, the dissolved oxygen concentration in the control wetland (CW1) was found to be increased as dissolved oxygen was found around 6.10 ppm. In the electrolysis-integrated wetland (CW3) the level of oxygen were increased in the middle and in the end with DO values of 6.88 mg/L and 6.04 mg/L, respectively, whilst in the anode the oxygen content remained stable close to 2 mg/L. As regards. the pH values did not differ significantly compared to the previous cycle (Figure 25c). In CW1 and CW2, the pH values were found 7.82 and 8.40, approximately. pH was monitored at the entrance and the end of the CW3 and the average values were measured 8.41 and 8.92, respectively, while in the middle it was found to be lower, 7.98. The average temperature value throughout the experiment was 18.4°C.

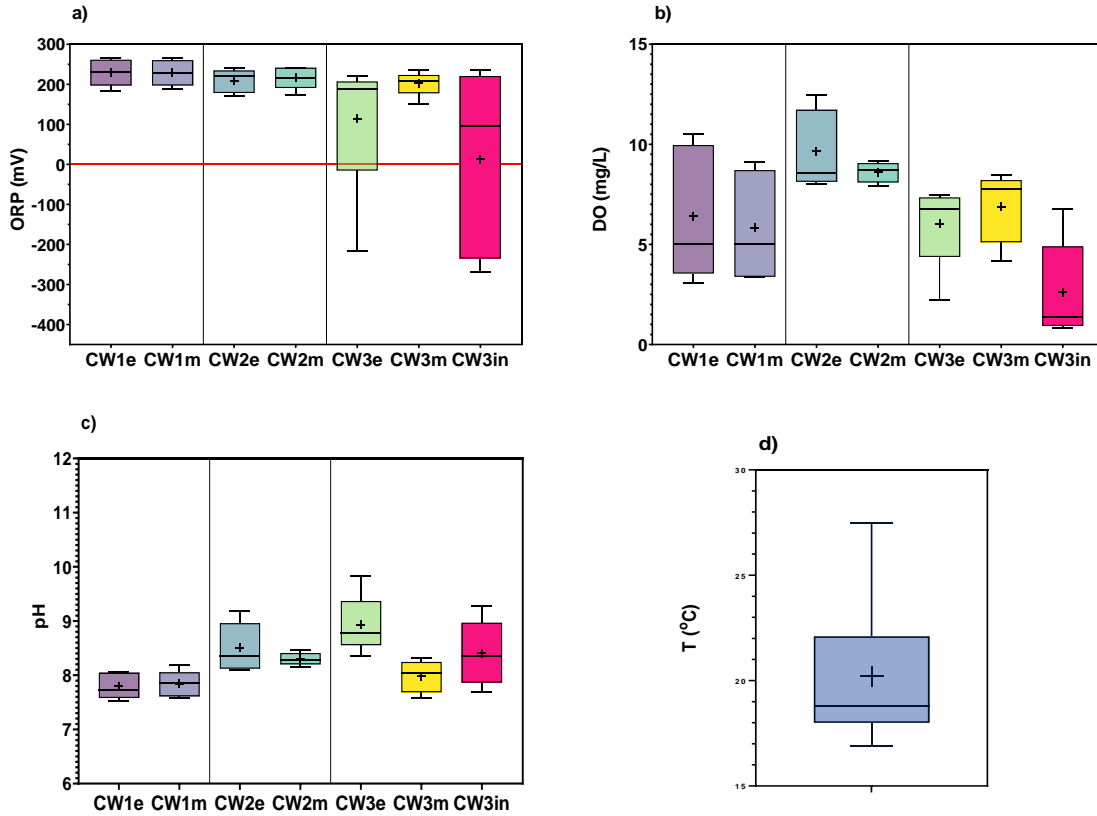


Figure 25. Oxidation- reduction potential (mV) and b) dissolved oxygen (mg/L), c) pH and d) temperature (T °C) in wetlands throughout the Cycle 2.

4.3.3. Cycle 3

According to Figure 26, results showed that CW2 and CW3 exhibited greater performance than the control, since the phenol was removed at approximately the 5th day and the 8th day, respectively, while more than 8 days needed for control. Among the treatments also in this case, the air nanobubbles injected via the porous diffuser enhanced the removal rate of phenol.

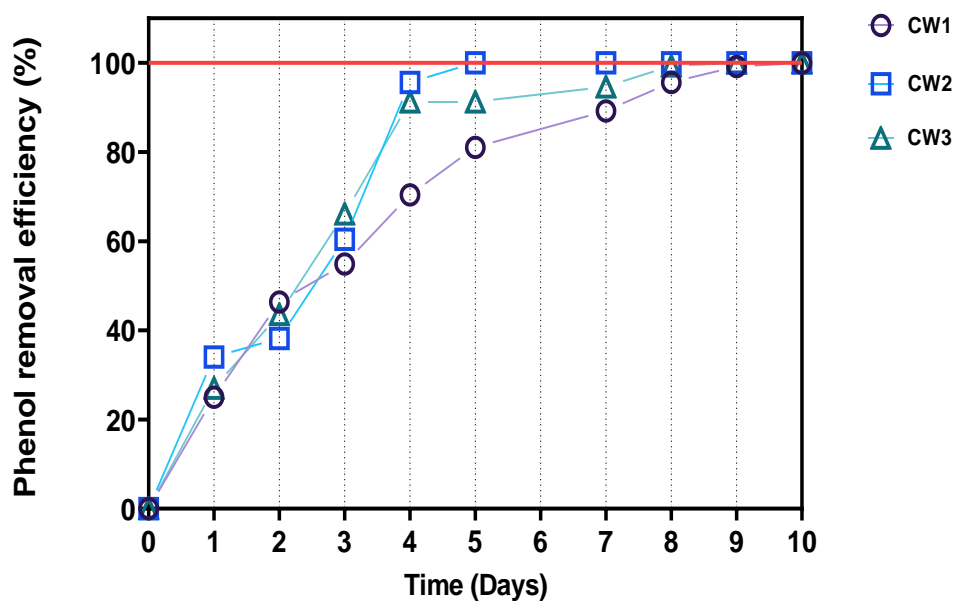


Figure 26. Phenol removal efficiency (%) versus time (Cycle 3: initial conc.=100 ppm & HRT=24 h).

The increase of phenol concentration from 50 ppm to 100 ppm at HRT of 24 h, resulted in decreased ORP in CW1 and CW2 (Figure 27a). The ORP values in the middle and the end of CW1 were estimated 156 mV and 100 mV, respectively. In the CW3, the average values of 152 mV and 77 mV were reported in the middle and end, respectively. The cathode in the entrance displayed mostly negative ORP values with an average value of -5.8 mV. In addition, the dissolved oxygen in the CW2, even if the influent concentration was doubled remained at a high level also in this experiment cycle (above than 8.5 mg/L). In the other two wetlands, the oxygen content close to rhizosphere were 2.25 and 7.25 mg/L in CW1 and CW3, respectively. No significant difference can be observed in pH values among the treatments. In CW1, the average pH was monitored 7.40 both in the middle and in the end sampling points. In CW2, the pH values were found marginally increased, 7.79 and 7.74, in the middle and in the end, respectively. In CW3, similar values were displayed at the sampling points with the pH in the middle being slightly lower. The average temperature value was 14.4°C.

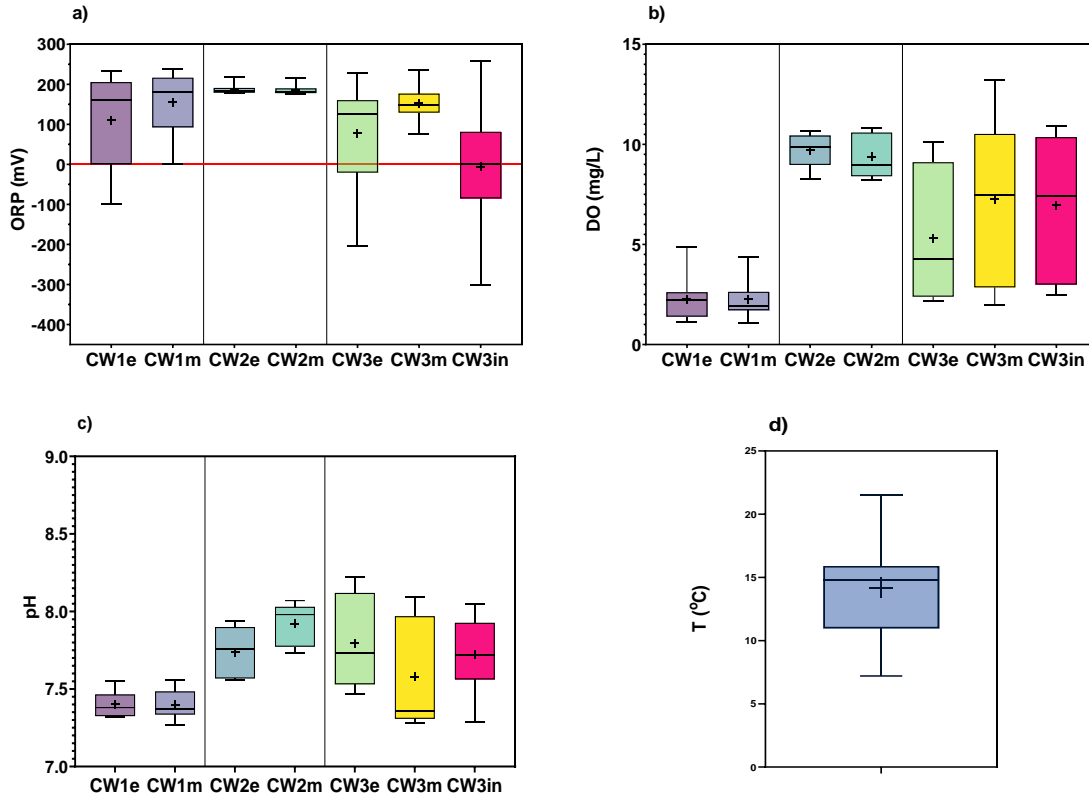


Figure 27. a Oxidation- reduction potential (mV) and b) dissolved oxygen (mg/L), c) pH and d) temperature (T °C) in wetlands throughout the Cycle 3.

4.3.4. Cycle 4

In the next experimental cycle, the phenol concentration was 200 ppm, the highest concentration during the experimental period. It can be seen in Figure 28 that phenol was totally removed within 4 days when air nanobubbles produced by the nanotube (CW2) were supplemented. In the other two systems, 10 days were required in order phenol not to be detected in wetlands bed. CW1 and CW3 exhibited similar performance.

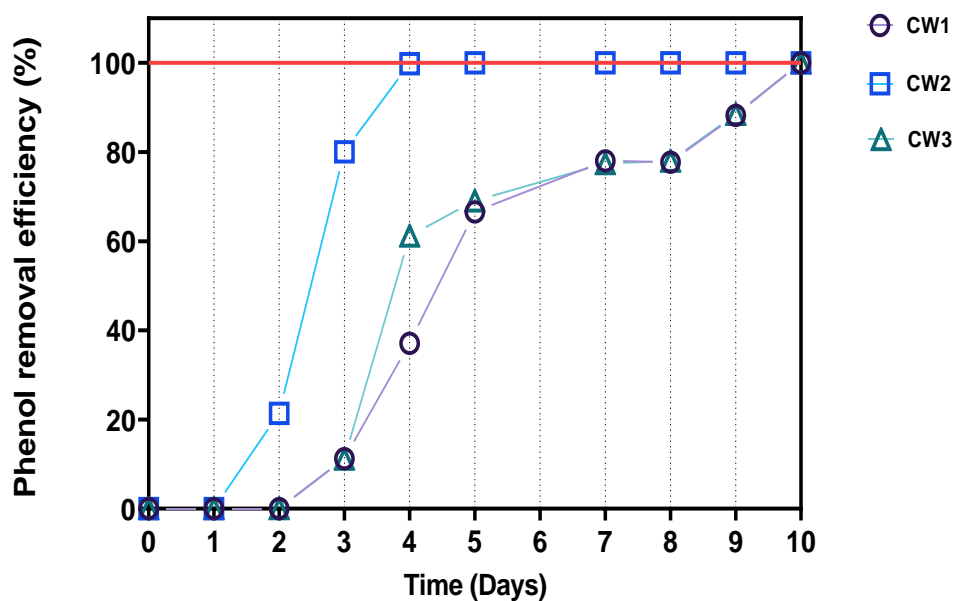


Figure 28. Phenol removal efficiency (%) versus time (Cycle 4: initial conc.=200 ppm & HRT=24 h).

When the phenol concentration was alleviated to 200 ppm (Figure 29), the ORP in CW1 was reported approximately 74 mV, both in the middle and the end sampling points. The highest ORP values were showed in the CW2 with values of 185 mV and 202 mV, in the middle and in the end, respectively. In this experimental cycle, both cathodes in CW3 displayed negative values, in particular -202 and -97, in the entrance and in the end of the wetland, respectively while in the anode positive values of ORP were observed; the average value was estimated 122 mV. As regards the oxygen content, the highest phenol concentration did not have any strong impact as remarkably it remained above 8 mg/L in CW2. In the other two wetlands low oxygen concentration was reported. In CW1, the dissolved oxygen concentration was 2.54 mg/L, while in the CW3 it was 3.60 mg/L in the cathodes and 4.23 mg/L in the anode. No significant difference was observed in the range of pH among the wetlands and compared to the previous experimental cycle. Specifically, the pH values were 7.43, 7.69 and 7.56 in CW1, CW2 and CW3, respectively. The average temperature during the experimental cycle 4 was 16.4°C.

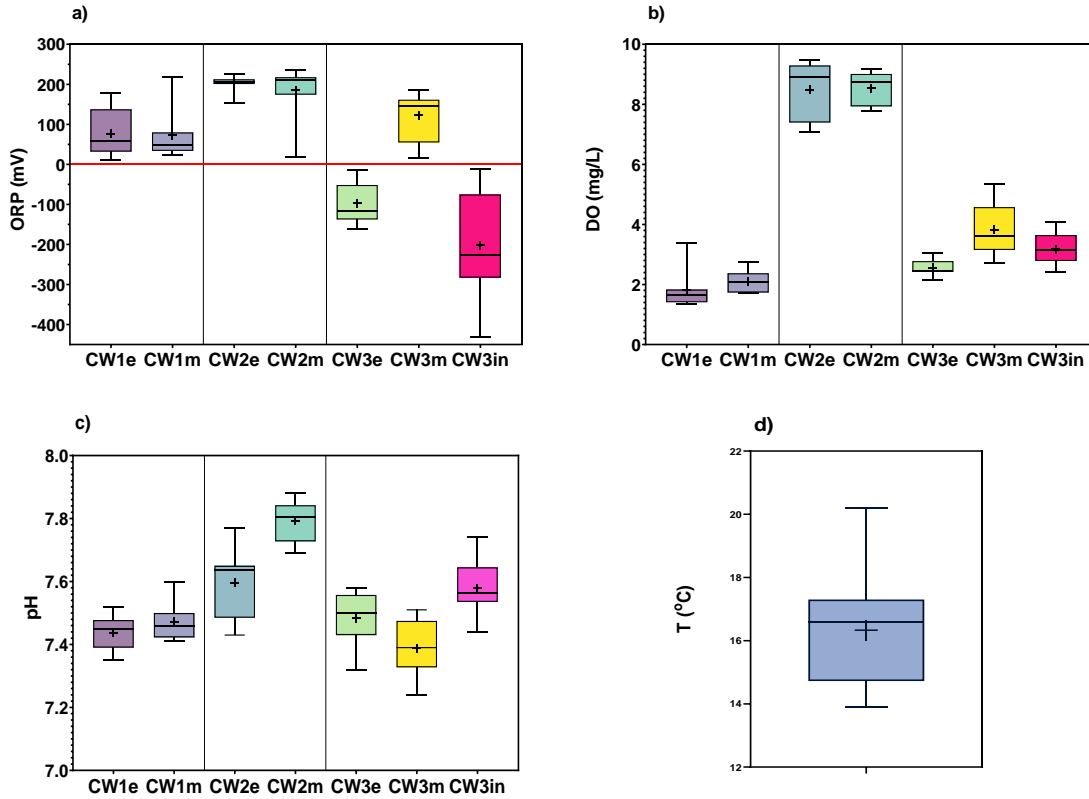


Figure 29. Oxidation- reduction potential (mV) and b) dissolved oxygen (mg/L), c) pH and d) temperature (T °C) in wetlands throughout the Cycle 4.

4.3.5. Cycle 5

In this experimental cycle, the targeted contaminant was toluene and initially it was tested at the lowest concentration of 50 ppm. As it can be shown by Figure 30, toluene was removed from the three wetland beds very quickly as on the first day of the experiment, more than 90% removal was reported. CW2 exhibited greater performance since toluene was efficiently removed on the second day of experiment. Although, CW3 exhibited higher removal efficiency compared to the control (CW1) the first two days, from the 3rd day the two systems displayed similar performance and the total removal in both treatments was detected at the 5th day.

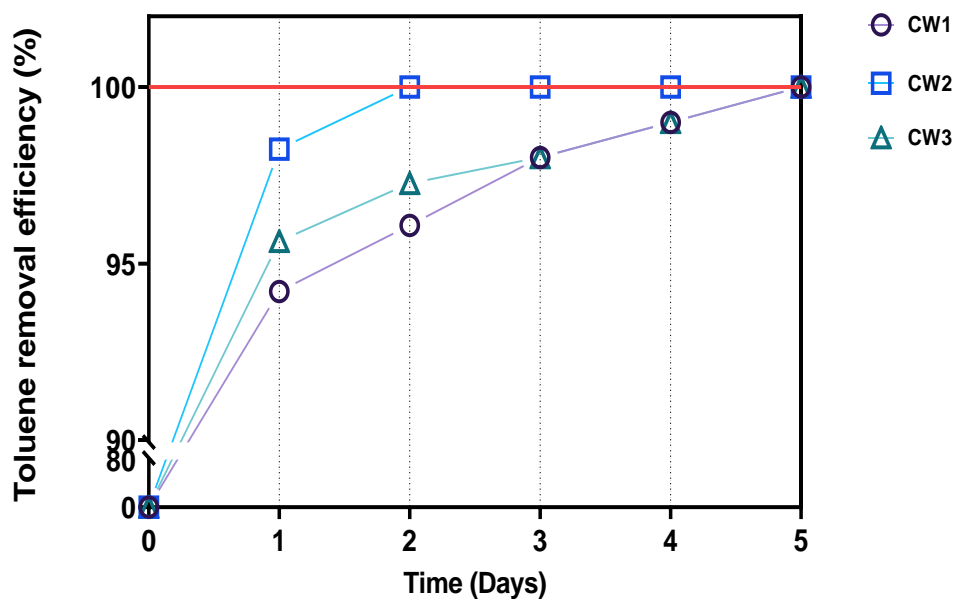


Figure 30. Toluene removal efficiency (%) versus time (Cycle 5: initial conc.=50 ppm & HRT=24 h).

As shown in Figure 31, the ORP values in CW1 exhibited for the first time negative values in both sampling points (middle: -112 mV, end: -69 mV) among the experimental cycles. Positive values were reported in CW2, with an average value of 142 mV. As regards the CW3, only in the cathode at the effluent of wetland the average ORP value was negative and equals to -90 mV. At the other two points, negative valued were also reported, however the average values were positive and equal to 66 mV and 58 mV in the anode and the cathode at the entrance, respectively. The levels of oxygen in the CW1 and CW3 remained very low close to 2 mg/L, while notably again in CW2 the oxygen content was reached approximately to 7 ppm. The pH values did not show any significant difference among the wetland, as the average values in wetland beds were close to 7. Finally, the average temperature was 28.5°C.

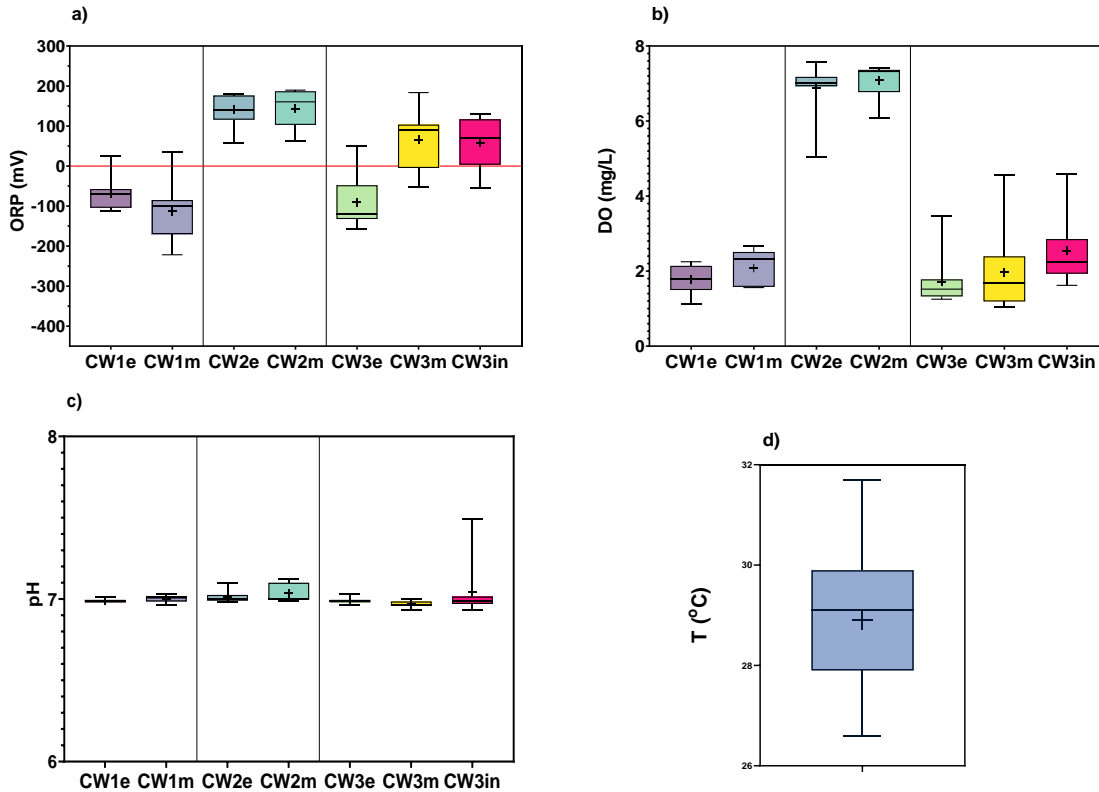


Figure 31. Oxidation- reduction potential (mV) and b) dissolved oxygen (mg/L), c) pH and d) temperature (T °C) in wetlands throughout the Cycle 5.

4.3.6. Cycle 6

In the next experiment cycle, the toluene concentration was increased to 100 ppm. The removal of toluene was anew very fast since the first days more than 85% removal was reported in all systems. On the fourth day, a 100% removal was reported in CW2, exhibiting again greater performance in comparison to the other two systems. Even though CW3 displayed lower removal rate evidently until the sixth day, on the eighth day of experiment it reached 100% removal when the CW1 the removal percentage was estimate 99.87%. The next day, also CW3 achieved total removal of toluene at 100 ppm.

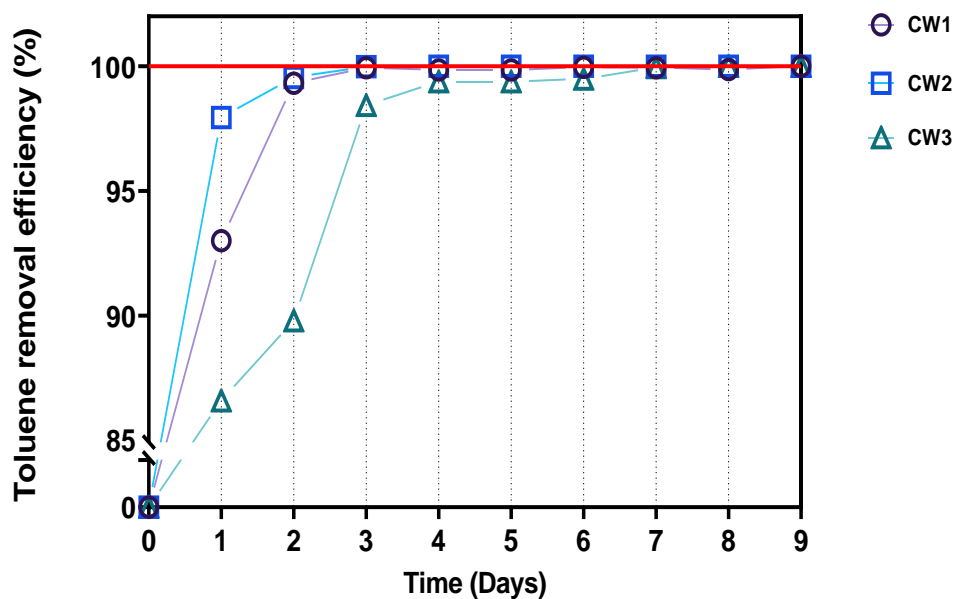


Figure 32. Toluene removal efficiency (%) versus time (Cycle 6: initial conc.=100 ppm & HRT=24 h).

The measured parameters can be observed in Figure 33, when the concentration was increased to 100 ppm. The ORP values were positive in all wetlands with an average values of 134 in all treatments. The only point that negative ORP was detected was the first day of the experiment at the cathode in the end of CW3. The same trend was observed in the measured oxygen content as in the CW1 and CW3 was low and equal to 2 mg/L and 3 mg/L, respectively. In contrast to CW2, in which the oxygen concentration remained high and close to 7 mg/L. The temperature was recorder 28.2°C.

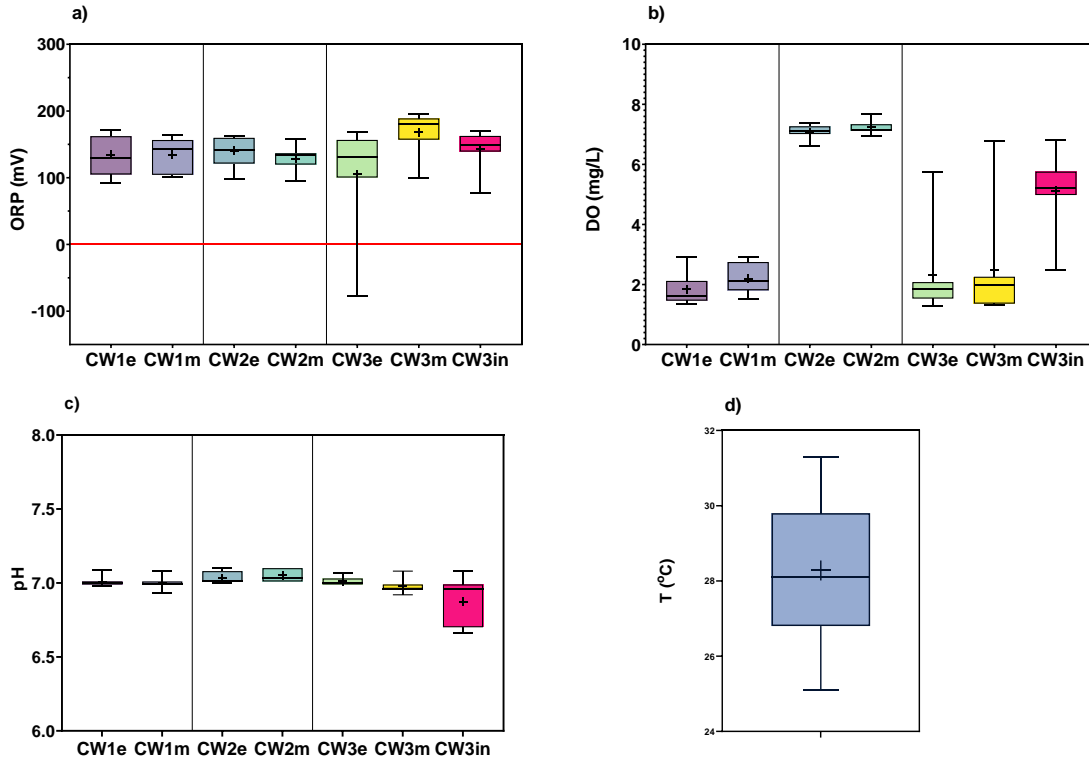


Figure 33. Oxidation- reduction potential (mV) and b) dissolved oxygen (mg/L), c) pH and d) temperature (T °C) in wetlands throughout the Cycle 6.

4.3.7. Cycle 7

In the next experimental cycle, both phenol and toluene were tested at concentration of 100 ppm. It can be observed that toluene can be degraded rapidly as previously reported even though phenol was present in wetlands. However, more time was needed in order CW2 reached 100% removal efficiency of toluene and in particular 6 days. Concomitantly, phenol was removed within 2 days in CW2. CW1 exhibited greater performance than CW3 in phenol elimination and, inversely in toluene elimination.

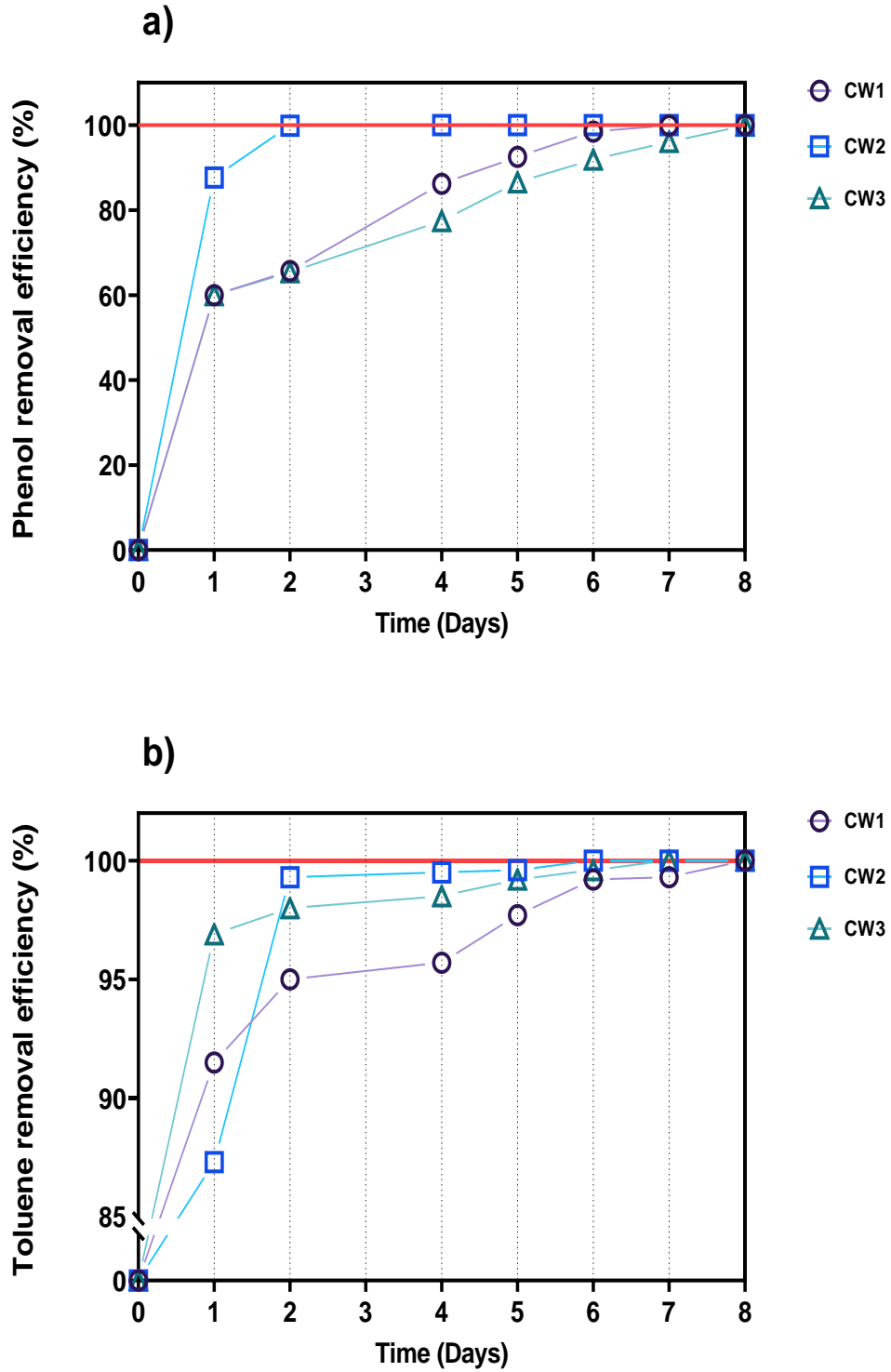


Figure 34. a) phenol and b) toluene removal efficiency (%) versus time (Cycle 7: initial conc.=100 ppm & HRT=24 h).

The same trend in the measured parameters was also detected when the mixture of hydrocarbons were tested. According to Figure 35, the ORP values were reported positive in all wetlands with the highest value monitored in CW2 and equals to 211 mV, while slight decreased values were reported in CW1 and CW3, with values of 200 mV and 173 mV. Notably, the dissolved oxygen concentration remained at high level even in this experimental cycle with the two contaminants, while the other two wetlands exhibited low oxygen content close to 2 ppm. In addition, the pH values showed similar trend among the treatments with values 7.15, 7.46 and 7.40 for CW1, CW2, CW3, respectively. The average temperature during the experimental period was 28.3°C.

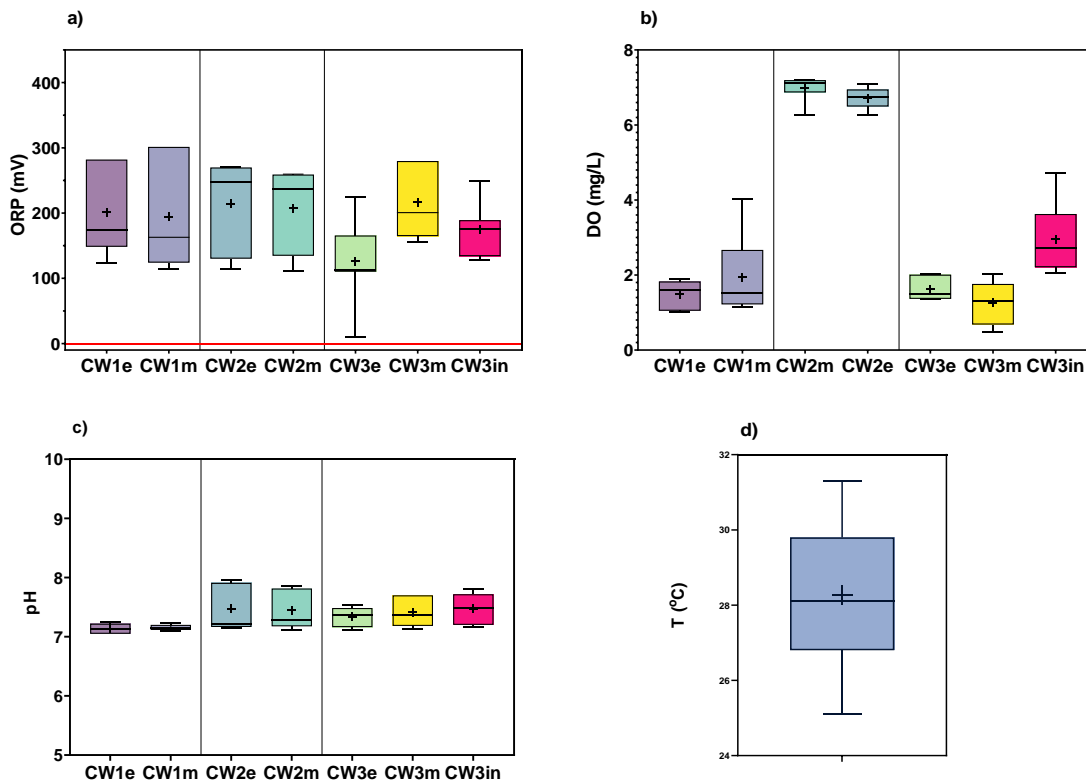


Figure 35. Oxidation- reduction potential (mV) and b) dissolved oxygen (mg/L), c) pH and d) temperature ($T^{\circ}\text{C}$) in wetlands throughout the Cycle 7.

4.3.8. Cycle 8

In the final experimental cycle both phenol and toluene were added in the systems in wastewater matrix. According to Figure 32, the systems with the artificial aeration either via nanotube diffuser or via electrochemical production exhibited greater performance than

control in both contaminants, since phenol and toluene were rapidly removed. CW3 showed a higher reduction rate compared to the previous cycle when wastewater was added.

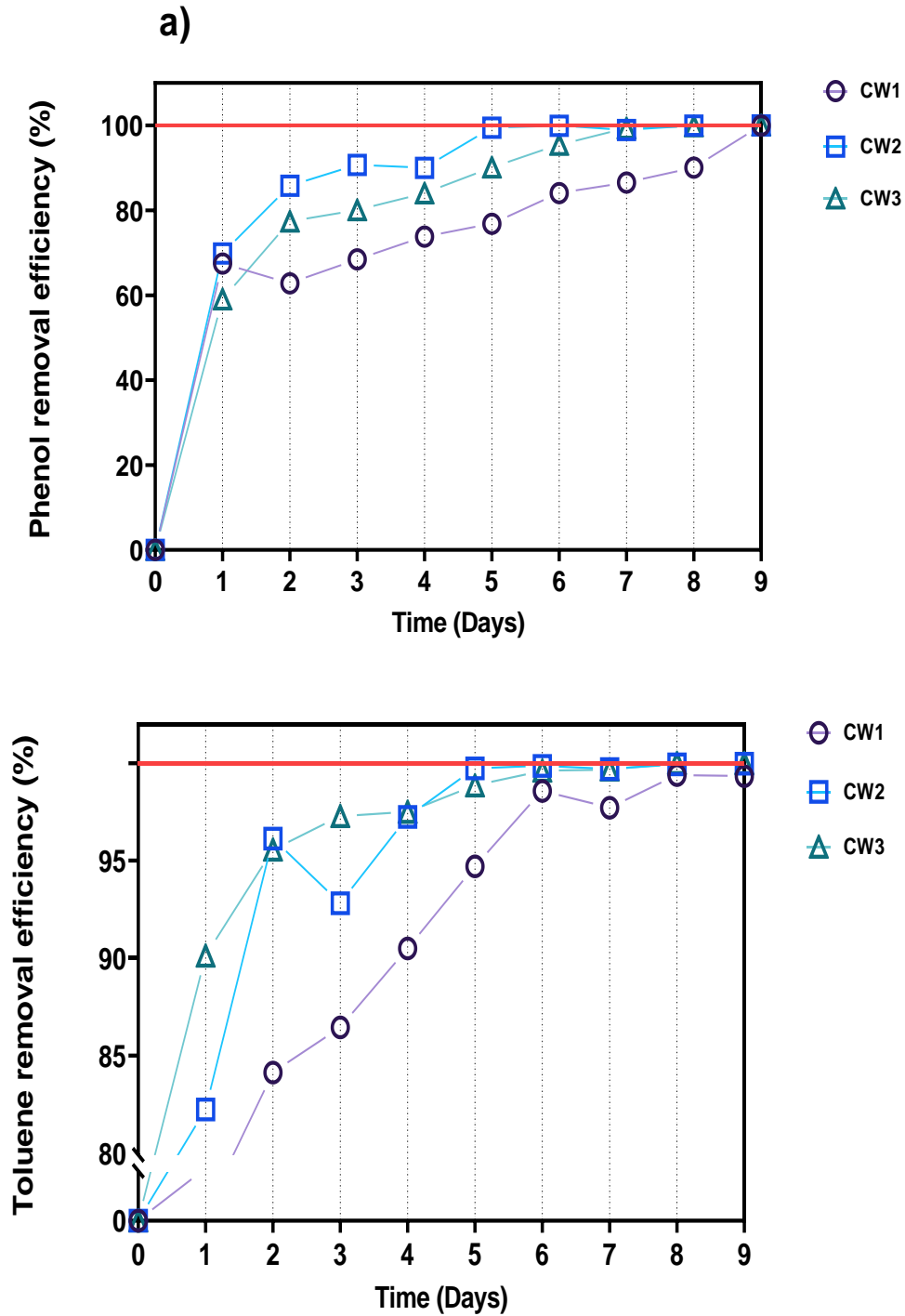


Figure 36. a) phenol and b) toluene removal efficiency (%) versus time in wastewater matrix (Cycle 8: initial conc.=100 ppm & HRT=24 h)

The addition of the primary-treated wastewater had a significant impact in the measured parameters compared to the previous experimental cycle as shown in Figure 37. In particular, even though the ORP values remained positive in CW2, the wastewater matrix led to negative values in CW1. The average values were recorded -8 mV and -22 mV. Also, the average ORP value was negative in the cathode of the CW3 in the effluent (-48 mV). Although negative values were reported also in the rest sampling points in the CW3, the average values of ORP were positive. The same trend in oxygen level was followed also in this cycle. Again, CW2 displayed higher dissolved oxygen concentration, approximately 7.35 mg/L, whilst CW1 and CW2 exhibited rather low oxygen level close to 1.5 mg/L. The pH values were not significantly affected as values in CW1, CW2 and CW3 were 7.32, 7.45 and 7.54, respectively. The average temperature was measured 28°C.

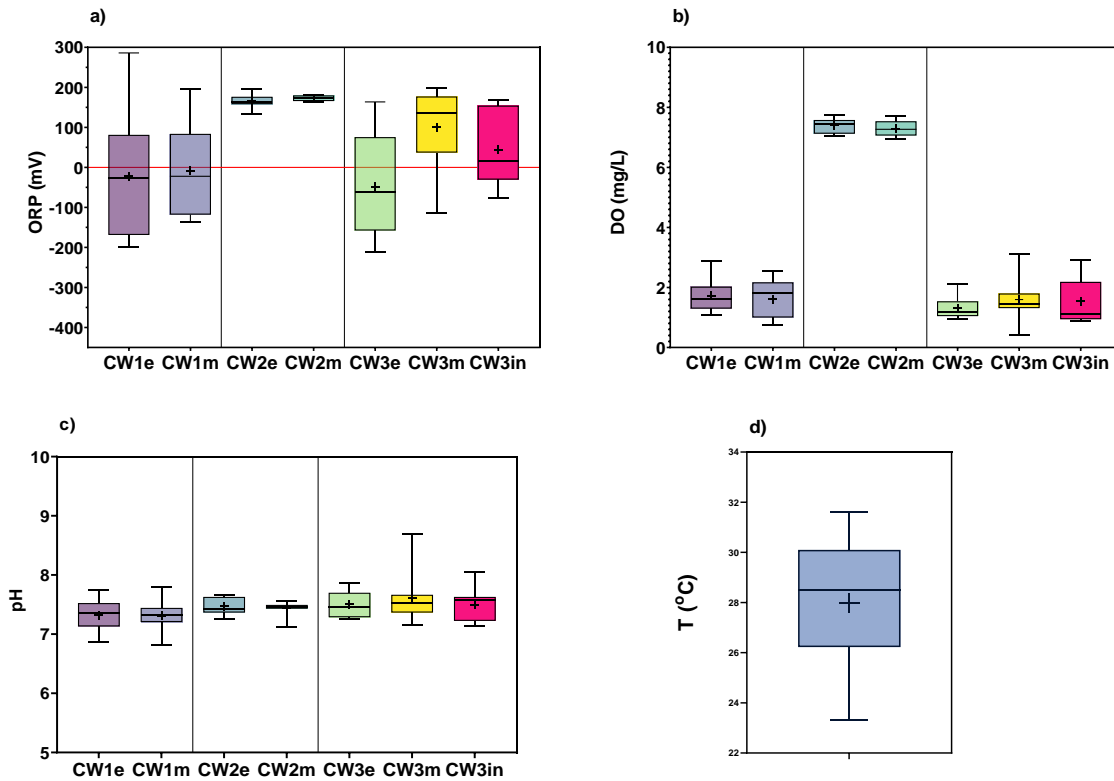


Figure 37. Oxidation- reduction potential (mV) and b) dissolved oxygen (mg/L), c) pH and d) temperature (T °C) in wetlands throughout the Cycle 7.

The wastewater quality parameters were calculated during the experiment every three days. In general, there was no significant difference among the treatments, except from the nitrate as more rapid decline was observed in CW2. A nitrate reduction of 50%,

89% and 77% were observed for CW1, CW2 and CW3, respectively. As regards the COD, a 95%, 97% and 97% removal was detected in CW1, CW2, CW3, respectively. Concerning the phosphate was declined by 93%, 95% and 89% for CW1, CW2 and CW3, respectively. Within 12 days, total nitrogen was reduced in all treatments at rate of above 80%. Finally, reduction of TSS was reported approximately 65% for all wetlands. Conclusively, all the systems showed satisfactory removal for all the conventional pollutants, except for CW1 which exhibited mediocre removal efficiency for nitrate within 12 days.

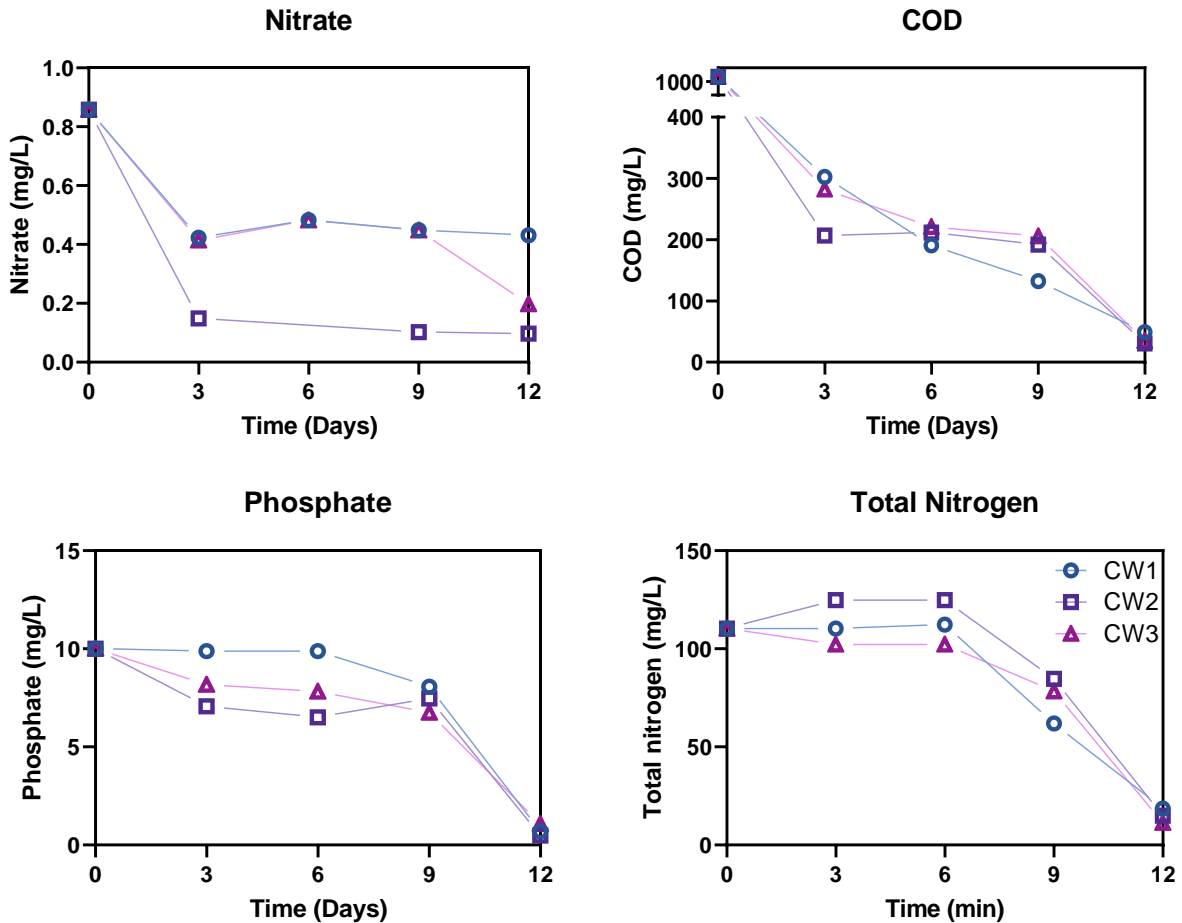


Figure 38. Wastewater quality parameters in wetlands.

4.3.9. Microbial Analysis

As it be seen by the graph below (Figure 39), the cell concentration measured by the flow cytometer in every wetland for the selected experimental cycles (Table 17) from sampling point close to rhizosphere was reported. Only for CW3, also a sample close to

the cathode in the entrance was collected. There are no significant differences among the wetlands. In particular, a gradual decrease among the cycles in CW1 was measured, while a stable cell concentration in CW2 and CW3_in was detected. Notably, the highest decline in concentration was shown in CW3 system close to the rhizosphere, since from 3.56×10^6 cells/mL in cycle 1, the concentration was decreased one order of magnitude in cycle 2.

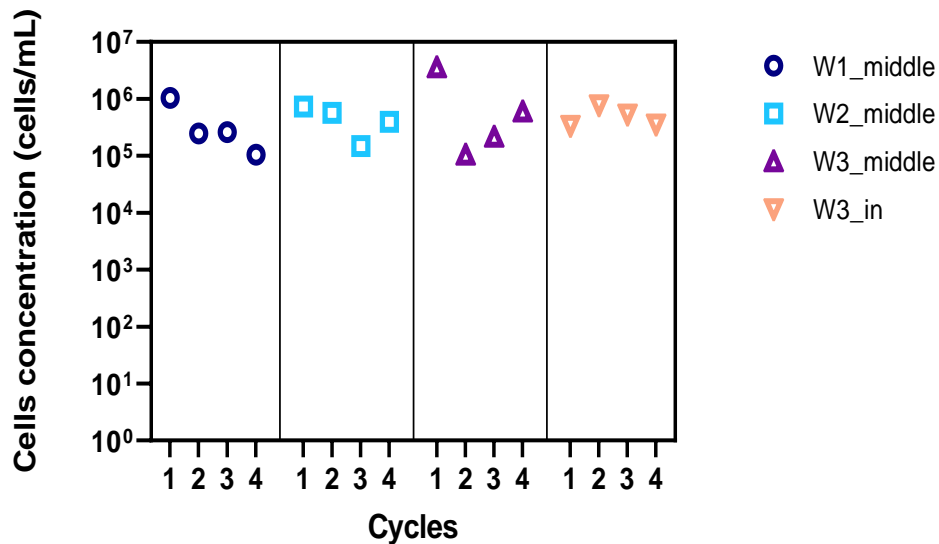


Figure 39. Cells concentrations in the three CWs in every cycle.

4.3.9.1 Diversity and composition of bacterial community based on the contaminant and the matrix

Initially, microbial analysis is based on the type of contaminant and in particular phenol, toluene and the combination of both in tap water and wastewater matrix. The taxonomic classifications of the effective bacterial sequences from samples at three different taxonomic levels (phylum, class and genus) are displayed below.

The top predominant phyla are shown in Figure 41. Proteobacteria was the most dominant phylum in all wetlands among the different contaminants, followed by *Actinobacteria*, *Bacteroideta* and *Firmicutes*. These phyla were also reported as dominant in other CWs systems (213–215). As regards phenol, the relative abundances of Proteobacteria were 85.26%, 94.80% and 57.38% close to the rhizosphere in CW1, CW2 and CW3, respectively. When the toluene was targeted pollutant, values in CW1 and CW2

were substantially declined as they reported 70.22% and 70.91%, respectively and there was a stable trend in CW3 as it was found 67.42%. In combination of both contaminants, there was an increase in values in CW1, CW2 and CW3 compared to aforementioned percentages as they reported 79.18%, 77.33% and 88.55%, respectively. In CW3 at the point close to the cathode, the relative abundance of Proteobacteria was decreased from phenol to toluene as contaminant and there was a further increase when both contaminants were investigated in wetland bed, higher than those when phenol was tested. Notably, the highest abundance of *Firmicutes* was displayed in CW3 close to rhizosphere when phenol was tested, being substantially decreased in the next experimental cycles.

As shown in Figure 40, in the bacterial community of the wastewater collected from WWTP in Platanias, the predominant phyla are *Proteobacteria* (27%), *Nitrospirota* (16%), *Actinobacteriota* (14%), *Bacteroidota* (14%) and *Chloroflexi* (10%). Lower abundancies (less than 5 %) exhibited the phyla, *Verrucomicrobiota*, *Acidobacteriota*, *Patescibacteria* and *Firmicutes*.

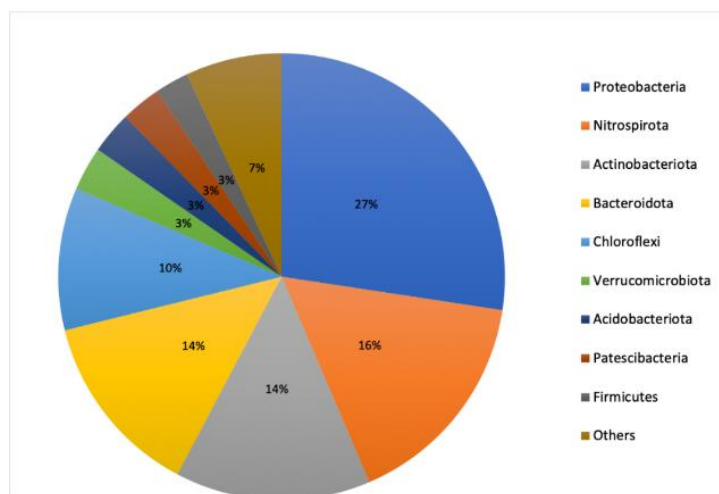


Figure 40. Bacterial community at phylum level in WW.

After treatment in CWs, the predominant phylum was *Proteobacteria* in wastewater, as the same found in tap water. In CW1, CW2, CW3 the values were found 61.43%, 67.09% and 71.47% in wastewater, respectively. *Nitrospirota* and *Patescibacteria* detected in wastewater were totally eliminated in wetland bed. The relative abundance of *Actinobacteriota* was decreased from raw wastewater to treatment in wetlands, in particular from 14% values were reached to 5.79%, 7.66% and 6.87%, in CW1, CW2 and CW3,

respectively. The same trend was followed by relative abundances of *Bacteroidota*, *Chloroflexi*, *Acidobacteria* and *Verrucomicrobiota* as they were decreased after treatment. On the contrary, *Firmicutes* was increased in wetland bed and it was found higher in wastewater matrix than tap water.

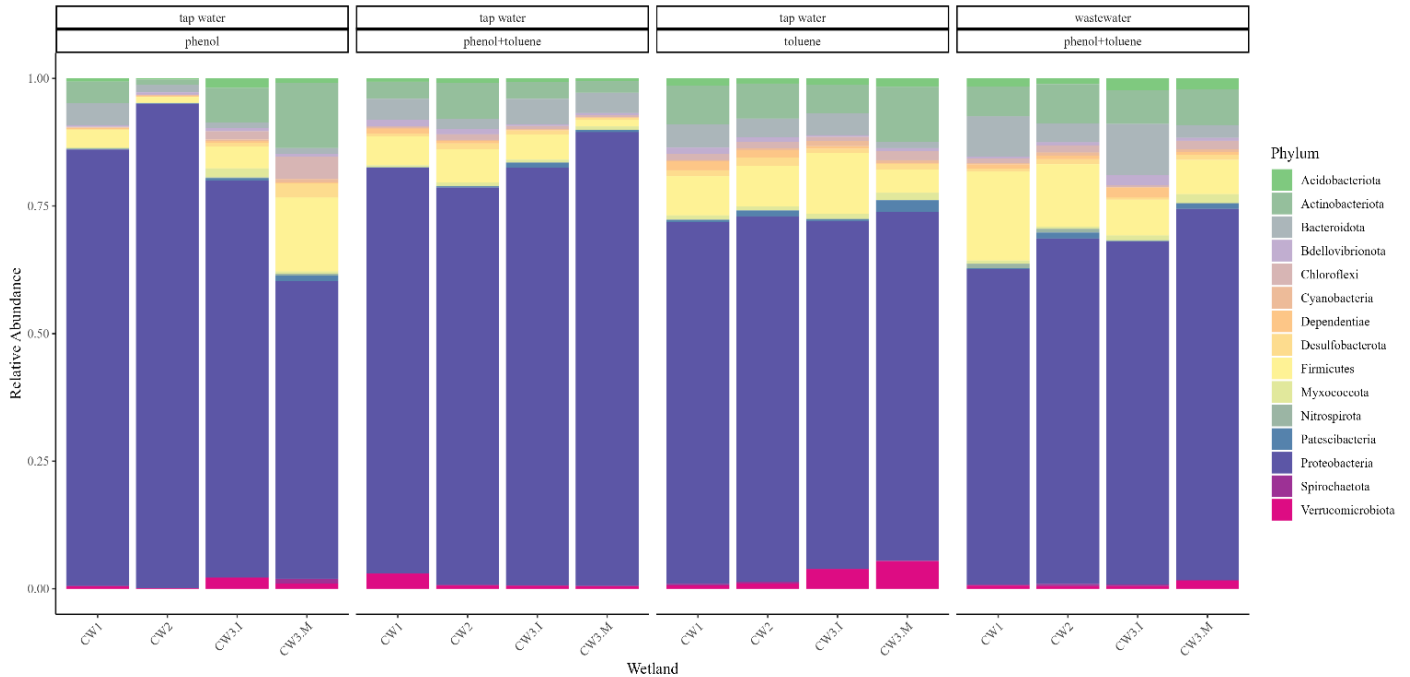


Figure 41. Bacterial community at phylum level in CWs.

At the class level, the classes *Alphaproteobacteria* and *Gammaproteobacteria* had a high distribution. In CW1 *Alphaproteobacteria* (36.15%) and *Gammaproteobacteria* (49.08%) were lower in phenol than when toluene tested (33.06% and 37.16%, respectively). However, the distribution of *Alphaproteobacteria* (16.74%) and *Gammaproteobacteria* (62.44%) was substantially decreased and increased, respectively in both contaminants. In CW2, relative abundance of *Alphaproteobacteria* (61.14%) was significantly decreased to 39.08% in toluene, while *Gammaproteobacteria* (33.66%) was slightly decreased (31.82%). When both contaminants were tested, the relative abundances of *Alphaproteobacteria* and *Gammaproteobacteria* were 35.31% and 42.01%, respectively. Finally, in CW3 the relative abundances of *Alphaproteobacteria* and *Gammaproteobacteria* were 17.37 and 40.01%, respectively in phenol, 27.71 and 39.69%, respectively in toluene and 37.75% and 50.79%, respectively in toluene and phenol. In

addition to these two classes, portions of microorganisms in the CWs were distributed in the classes *Actinobacteria*, *Bacteroidia* and *Clostridia*.

According to Figure 42, the predominant classes in WW are *Gammaproteobacteria* (23%), *Nitrospiria* (16%), *Bacteroidia* (11%). *Anaerolineae*, *Actinobacteria*, *Acidimicrobiia*, *Alphaproteobacteria* etc. displayed relative abundance lower than 10%.

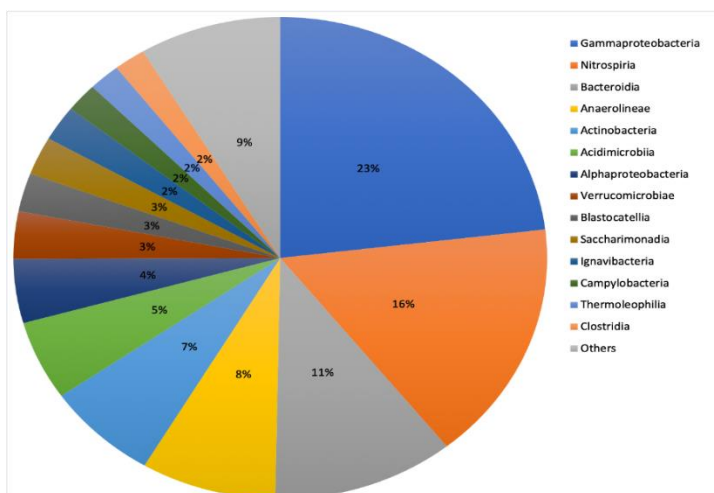


Figure 42. Bacterial community at class level in WW.

As shown in Figure 43, for *Alphaproteobacteria* and *Gammaproteobacteria* had the greatest relative abundances. The relative abundance of *Gammaproteobacteria* was the highest in all wetlands after treatment in wastewater, increased from 23% in wastewater, 50.71%, 54.71% and 45.63%, in CW1, CW2 and CW3. The next dominant class in CW1 was *Clostridia* (14.64 %), whereas *Alphaproteobacteria* accounts for 10.72%. In CW2 and CW3 the *Alphaproteobacteria*, essential increased from wastewater (4%) to 12.91% and 24.68%, in CW2 and CW3, respectively with *Clostridia* being the next dominant class. In all wetlands, some other subdominant phyla, *Actinobacteria* and *Bacteroidia* were decreased after treatment in wetlands. In CW3 close to cathode, *Gammaproteobacteria* is the dominant class (42.22%) and the next dominant class was *Alphaproteobacteria*. The relative abundancies of other classes that showed moderate proportion were *Actinobacteria*, *Bacteroidia* and *Clostridia*.

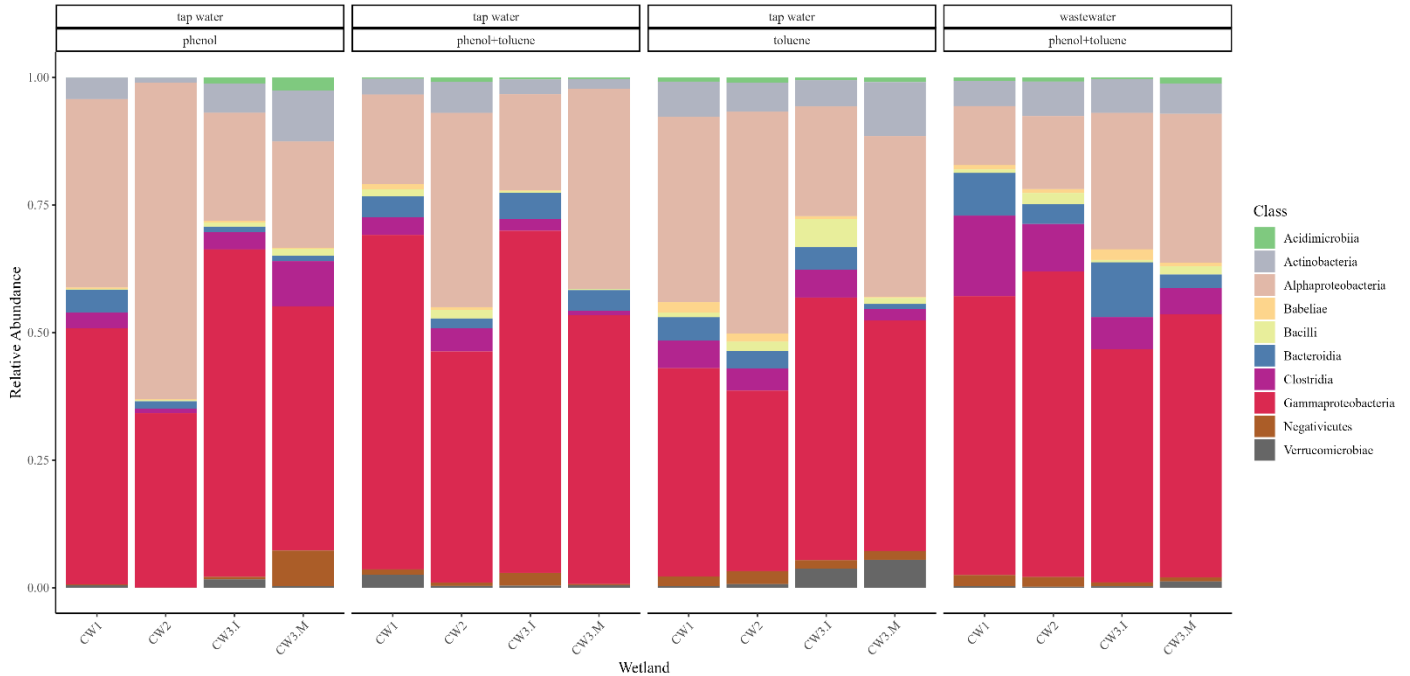


Figure 43. Bacterial community at class level in CWs.

At the 15th top dominant genera (Figure 45), the dominant genus is different between the treatments as well as the type of contaminant. In the case of phenol treatment, it was found that *Niveispirillum* was the dominant genus in CW1 (25.18%) and CW2 (53.86%), whilst also *Pseudomonas* exhibited moderate relative abundance (approximately 10%). On the contrary, CW3 close to the rhizosphere (12.14%) and the cathode (33.15%) was the *Pseudomonas*, whilst the relative abundance of *Niveispirillum* was rather low. When the type of contaminant changed from phenol to toluene, the dominant genera were also changed. In CW1 the dominant genus was found to be *Xanthobacter* (9.64%), in CW2 the *Azospirillum* (13.87%). In CW3, the dominant genus was still *Pseudomonas* as well as close to cathode, however with substantially decreased percentage (from 32.66% to 5.52%). In this wetland bed, other genera that displayed elevated relative abundances were *Azospirillum* (8.06%) close to the rhizosphere and *Azospira* (4.92%), *Azospirillum* (3.15%), *Enterobacter* (4.28%) and *Legionella* (2.64%) close to cathode. Finally, in treatment of two contaminants, a different trend in dominant genera was observed. In CW1, the dominant genera were *Azospira* (12.98%) and *Pseudomonas* (9.33%). In CW2, the top three dominant genera were *Niverispirillum* (8.33%), *Pseudomonas* (7.62%) and *Azospirillum* (6.40%). Correspondingly in CW3 they were *Pseudomonas* (15.26%),

Azospirillum (19.95%) and *Zoogloea* (16.32%). Close to cathode, *Pseudomonas* displayed the highest relative abundance (36.49%), whereas the second predominant genus was *Acinetobacter* (6.85%).

According to Figure 44, the identified genera detected in wastewater were *Nitrospira* that displayed the highest proportion in relative abundance, whereas *Dechloromonas* was the next dominant genus (10%). Other genera were *Mycobacterium*, *Phaeodactylibacter*, *Pseudomonas* and *Pseudarcobacter* (less than 5%).

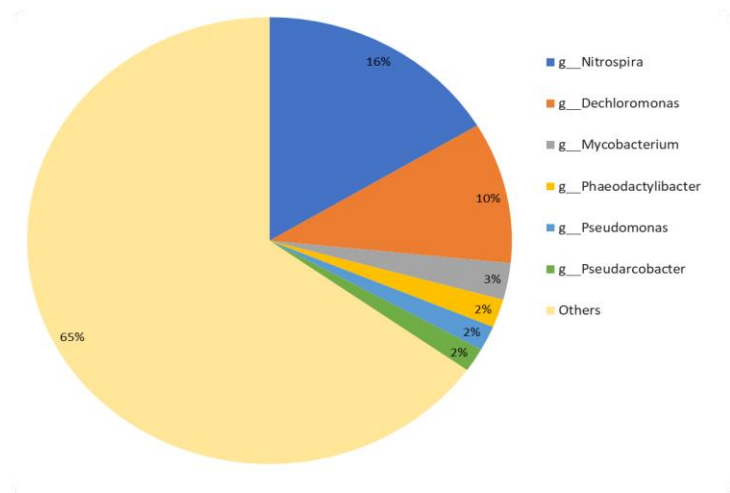


Figure 44. Bacterial community at genus level in WW.

When wastewater was used as substrate, a different trend in high relative abundancies in every wetland was shown. For instance, in CW1 and CW2 the dominant genus after the addition of wastewater was *Dechloromonas* (17.52% and 12.74%, respectively). In CW3, *Pseudomonas* exhibited the highest relative in wastewater (8.62%), decreased compared to tap water. *Azospirillum* and *Zoogloea* were decreased while *Acinetobacter*, *Azobacter*, *Dechloromonas*, *Legionella* and *Xanthobacter* were increased when wastewater used as substrate. Finally, in the cathode *Pseudomonas* was the dominant genus (36.49%) in tap water, whereas in wastewater its relative abundance was essentially low (0.99%). The top four dominant genera in this case were *Azospira* (7.59%), *Dechloromonas* (6.29%), *Legionella* (6.27%) and *Sediminibacterium* (4.46 %)

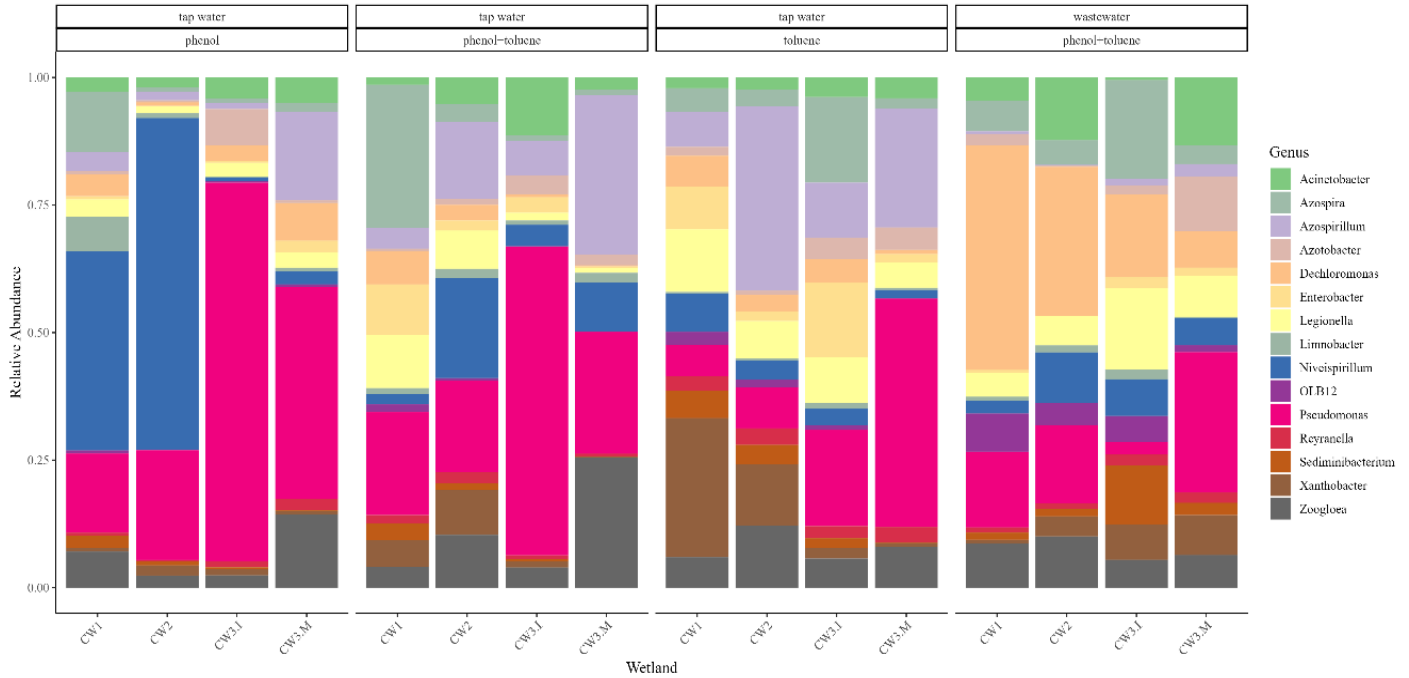


Figure 45. Bacterial community at genus level in CWs.

4.4 Conclusions

In this experiment, air nanobubble-integrated wetland can achieve better phenol and toluene removal efficiency with and without the presence of wastewater than that of the electrolysis-integrated and control wetland, which was mainly attributed to the high level of oxygen concentration during the experimental cycles. In particular, the dissolved oxygen in the constructed wetland remained above the value of 7 mg/L in every cycle indicating that a sufficient aeration was provided. This can illustrate that a high metabolic activity was maintained throughout the experimental cycles leading to a more efficient degradation of the organic compounds as well as to a satisfactory elimination of the conventional pollutants (nitrate, COD, phosphate and total nitrogen).

Compared to the control, electrolysis had an increased removal rate in cycles 1 & 3, whilst the elimination efficiency was found to be declined in cycles 2 & 6. In cycles 4 & 5, these two systems exhibited similar performance. The difference in the performance in CW3 may be connected to the shift from negative to positive ORP values. Generally, negative ORP values refer to the development of the reduction conditions, indicating the

predominance of anoxic conditions that may enhance the degradation of the hydrocarbons in this wetland. The addition of wastewater enhanced the performance of electrolysis-integrated wetland in the organic compounds' removal with the concomitant great potential for wastewater treatment. The only limitation of this method is the rapid oxidation of iron electrode and it should be further considered to keep long term operation of the wetland.

The microbial composition structure of the total bacteria in wetlands was investigated. In all wetlands, *Proteobacteria* as the main phylum level bacteria exhibited noteworthy high relative abundance. The higher abundance of *Alphaproteobacteria*, *Gammaproteobacteria* in tap water was reported in wetland beds and except from the previous ones, high relative abundance of *Clostridia* was detected in wastewater. At the level of genera, the dominant genera among the wetlands mainly belonged to *Niveispirillum*, *Pseudomonas* and *Dechloromonas*.

Conclusively, the constructed wetland with the ultra fine bubbles exhibits the best performance at all levels and types of pollution. The air nanobubble-integrated constructed wetland technology represents an innovative approach for enhancing wastewater treatment efficiency and intensifying the degradation of hydrocarbons. So far, artificial aeration have been employed in constructed wetlands. However, the energy consumption is high therefore air nanobubbles is a promising technology as the stability and the long residence time will result in reducing the energy requirements.

“This page intentionally left blank”

Chapter 5.

Oxygen Nanobubbles in bioremediation

Part of this chapter is based on the following publication:

Seridou P, Monogyiou S, Syranidou E, Kalogerakis N. Capacity of Nerium oleander to Phytoremediate Sb-Contaminated Soils Assisted by Organic Acids and Oxygen Nanobubbles. *Plants*. 2023;12(1):91.

5.1 Sb phytoremediation by *N. oleander* assisted by biostimulation and oxygen nanobubbles

5.1.1. Introduction

Heavy metal and metalloid pollution is of great concern due to the detrimental effects on the environment as well as the human health. One of the most toxic elements is antimony (Sb). This metalloid is typically encountered as the sulfide mineral stibnite (Sb_2S_3) and rarely in its native form due to its strong affinity for sulfur and other metals (216). Furthermore, it exists in the environment mainly in two oxidation states; antimonite, Sb(III) and antimonate, Sb(V) with the trivalent oxidation state being more toxic (10 times) than the pentavalent (162,163,193). Sb is recognized as a priority pollutant, which can cause acute environmental issues since it is released into soils and aquatic environments by natural processes and mainly by human activities such as mining, coal combustion, and shooting (26). The release of Sb into the environment is derived from geogenic processes and anthropogenic activities such as mining, coal combustion and Sb products (flame retardants, plastics, textiles etc.) (29,218,219). The pollution of

this metalloid is rapidly emerging worldwide due to its extensive use, especially in China, which is the leading producer of Sb (29). Apart from the environmental risk, Sb is considered hazardous to human health, as it is a suspected carcinogen due to its toxicity (27). Sb removal from environmental water bodies has received a great deal of attention in the last decades; therefore, technologies such as coagulation, adsorption, and the electrochemical method have been widely tested and found to be effective (220–222). However, the main disadvantages of these methods are the use of chemicals, the high energy consumption, and the risk of secondary pollution; hence, the efficient removal of the antimony compounds from the environment remains a challenge (223).

The maximum concentration of Sb determined by World Health Organization (WHO) that is permitted in drinking water is 20 µg/L, whereas the maximum permissible concentration in soil is 36 mg/kg (224). Specifically, in soil Sb is mostly encountered in the forms of Sb(III) and Sb(V) and the latter shows higher water solubility. Sb has been reported to exceed the value of 5000 mg/kg when background concentration in the natural environment is only 0.2 mg/kg (165,166,175,176). The predominant species are Sb(V) under oxic conditions and Sb(III) under reducing conditions (227). In active Sb mining areas, a high Sb fraction is bioavailable, comprised primarily of Sb(V) (228). At shooting ranges, the leading form of Sb is noted as Sb(V) due to the relatively fast oxidation of Sb(III) (229). Previous studies suggest that the trivalent neutral complex Sb(OH)₃ is sorbed to Fe (hydro)oxides over a wide range of pH, and hence Sb(III) is considered immobile in neutral soils (230).

Even though Sb is a trace element and not essential for plants, it can be accumulated in their edible parts according to numerous studies. A technology that can be employed to manage Sb pollution at contaminated sites is phytoremediation using plant species that can accumulate antimony at a high level (231). Previous studies have shown that plants display different abilities to uptake the various forms of Sb speciation. These findings might indeed pose a risk to human health since Sb can enter food chain and subsequently the human body (232,233). In general, Sb(III) is easily oxidized into Sb(V) in the soil environment, while plants can accumulate both Sb(III) and Sb(V). Specifically, several studies have indicated that plants display higher affinity to sorb more Sb(III) than Sb(V) (224,234,235). On the contrary, *Shtangeeva et al.* (236) recorded that rye absorbed

a higher amount of Sb(V) than Sb(III). *Pteris cretica* var. *nervosa* has been investigated for Sb phytoremediation and was found to be a Sb hyperaccumulator with no high translocation from root to shoots. When the test plant was exposed to 500 mg/kg of Sb, 672.8 mg Sb/kg were accumulated in the plant while when the initial concentration was 1000 mg/kg, the plant uptake was estimated 2054.8 mg Sb/kg (233). Seedlings of *S. bicolor* in Sb-contaminated soil were treated with different levels of TiO₂ nanoparticles and the results showed that the bioconcentration factor was above one for each treatment, indicating that this plant also has phytoremediation potential (237).

In mining areas with high Sb content in soil, a high accumulation in plants was reported (238–240). For instance, *Achillea ageratum* accumulates Sb in basal leaves (1367 mg/kg) and inflorescences (1105 mg/kg), *Plantago lanceolata* in roots (1150 mg/kg) and *Silene vulgaris* in shoots (1164 mg/kg) (241). A study by Murciego *et al.* investigated the Sb accumulation patterns for three plant species: *Cytisus striatus*, *Cistus ladanifer* and *Dittrichia viscosa*, which exhibited low, moderate to high, and elevated Sb level in leaf samples, respectively (242). Oppositely, *D. viscosa* extracted Sb from the soil to the root but does not translocate it in large quantities to the aerial parts (243). In another study, adult pines (*Pinus sylvestris*), birches (*Betula pendula*) and the bulrush (*Juncus effusus*) found in old mine areas were examined and reported that they were mostly root accumulators with low translocation from roots to shoots (244). It is clear that the uptake mechanism varied significantly between individual plant species as Sb can accumulate in roots or translocate to the aboveground part of the plant. To date, the mechanism of Sb accumulation in plants is not well understood and there is need for in-depth studies.

Among the plant species that have been widely used for phytoremediation of heavy metals, halophytes are suggested as ideal candidates since they can tolerate harsh conditions and develop tolerance mechanism not specific to salt ions and, hence other toxic elements secreted by their salt glands or trichomes (245). Precisely, halophytes can adopt different strategies upon metal stress in order to moderate the toxicity induced by heavy metals. The main mechanism is that the organic matter exuded from the roots, forms a complex with the metals and then adsorbs the metals into the carbohydrates of the cell wall. Afterwards, the metals transported into cells are intracellularly chelated by protein molecules or localized to vacuoles for storage. Finally, some metals are excreted by

specific salt glands on leaf surface (246). In addition, this tolerance mechanism of halophytes to salt stress is correlated with an oxidant defense system considerably more efficient thus exhibit a greater capability to cope with heavy metals in relation to common plants (247).

Nerium oleander is an evergreen shrub native to the Mediterranean region, which is grown as an ornamental plant of high aesthetic value. Moreover, this plant is salt tolerant and resistant to drought. Generally, it is able to tolerate high concentrations of heavy metals (HMs) in soil (248). It has been shown to have the capability to accumulate HMs, thus making it a promising candidate for phytoremediation applications. In a recent study, *Ibrahim and El Afandi* (249) concluded that Cd and Zn were concentrated in the aerial parts of the *N. oleander* plant, while Pb was accumulated in the root. *N. oleander* has shown a good capacity to bioaccumulate the following metals: Pb, Cr, Cu, Li, Ni, and Zn (250). Another study confirmed that Pb was accumulated in the plant roots with a low translocation to aerial part. No visible toxicity symptoms were observed or no chlorophyll content reduction was reported when exposed to a high Pb concentration of 2400 mg/kg, rendering *N. oleander* a plant suitable for phytostabilization (251).

Proper amendments can be applied to achieve optimal growth of plants and soil amelioration. One option is the addition of low molecular weight organic acids (OAs), which are typical root exudates for plants. The bioavailability of HMs in soils can be enhanced, since organic acids can solubilize metal oxides and assist the plant to uptake the contaminants from soil (252). Due to the limited secretion of OAs by plant roots, adding exogenous OAs is an effective method to improve phytoremediation, since they are efficient chelating agents for the cleaning up of toxic HMs from soils (253,254). In addition, oxygenation can increase the oxygen content and hence, the aerobic respiration of crop roots is improved, increasing enzyme activity in the soil. The aeration efficiency can be increased by the oxygen delivery via small sized gaseous bubbles (255,256). Nanobubble technology has attracted significant scientific interest in disinfection (257), flotation (258) and organic pollutant removal (50). There are also several studies focusing on nanobubbles application in agriculture. Irrigation water containing NBs promoted higher germination rates in seeds (259–262) and had also a beneficial effect on plant growth (11,263).

5.1.2. Materials and Methods

5.1.2.1. Pot experiment

The phytoremediation potential of *Nerium oleander* was investigated carrying out a pot experiment for a period of 6 weeks in the greenhouse at the Technical University of Crete (Chania, Greece) under ambient air with protection against rain. Six-month-old plants were picked from a nursery garden in the Kounoupidiana district, Chania, and were divided into 3 experimental groups with similar total biomass (weight and height) in order to assure homogeneity among the treatments. The detailed experimental design is shown in Table 18. Specifically, each treatment had four replicates, resulting in a total of 12 pots being used. Plants were watered every 2-3 days, depending on the soil moisture content with approximately 50-100 mL of tap water. In the case of the treatment TR.2, plants were irrigated with tap water containing ONBs. Finally, plastic trays were placed under the pots to avoid any water leakage and hence any metal loss.

Table 18. Experimental Design.

Experimental Treatment (Code Name)	Sb Concentration [ppm]	Organic Acids Concentration [mmol/kg]	ONBs
TR.0 (control)	1.17 (background level)	0	-
TR.1	50	7	-
TR.2 (with NBs)	50	7	+

The soil pH was measured in each treatment before and after the end of the experimental period and the values are listed below (Table 19). The initial pH of the soil was found to be 7.42. In the control treatment, the pH dropped to 7.17, while in the treatment with soil spiked with antimony the pH was slightly increased to 7.51. The addition of OAs led to acidification of the soil. In particular, the addition of a low concentration of OAs reduced the soil pH to 6.61 and after the end of the experiment, the pH of the soil was increased approximately to 7.65 and 7.61 without and with the supplementation of ONBs, respectively.

Table 19. Measurement of pH before and after the experiment for all treatments.

pH	Treatment		
	TR.0 Control	TR.1 Sb 50 ppm OAs 7 mmol/kg	TR.2 Sb 50ppm OAs 7 mmol/kg with ONBs
Before	7.42	6.61	6.61
After	7.17	7.65	7.61

5.1.2.2. Soil Characterization

Soil was collected from a shooting range in Kampani area (Chania, Greece). The soil was passed through a 2 mm-sieve and was analyzed in terms of metals content. Since the antimony level was found to be very low (~1.17 ppm), laboratory spiking with Sb was performed (264). In particular, potassium antimonyl tartrate trihydrate ($C_8H_4K_2O_{12}Sb_2 \cdot 3 H_2O$) was added to achieve the desired initial antimony concentration of 50 ppm. Soil pH was measured using 10 g air-dried soil adding 25 mL 1 M KCl (265). Particle size was measured by the soil hydrometer Bouyoucos (266). The physical and chemical properties of the spiked soil are listed in Table 20.

Table 20. Physical and chemical characteristics of the soil used in this study.

Soil Property	Value
Sand (%)	72.53
Clay (%)	21.87
Slit (%)	5.6
Texture	sand clay loam
Organic matter (%)	1.83
TKN (g/kg soil)	0.76
pH	7.42
Sb concentration (ppm)	48.8 ± 1.3

5.1.2.3. Soil amendments

Organic Acids

The addition of organic acids aimed to decrease the pH below the initial value of 7.42. Due to the strong buffer capacity of soil, the concentration that achieved this decrease was 7 mmol/kg. Solution of citric acid (CA), oxalic acid (OA) and ascorbic acid (AA) were added to pots four times in low concentration of 7 mmol/kg (mass of acid /mass of soil) during the period of experiment.

Oxygen Nanobubbles (ONBs) production

ONBs were prepared by the commercially available MK1 NanobubblerTM (Fine Bubble Technologies Pty Ltd, South Africa). The device was submersible in a 350- L water tank and was operated for 20 min with high-purity oxygen (99.9%) as feed gas before each irrigation event. In order to ensure that irrigation water did not contain any large bubbles, the NBs water was collected 10 min after the NB generation was completed in order to allow any larger bubbles to come up to the surface, where they burst out. Samples from the tank were used to obtain the NBs density using nanoparticle tracking analysis (NTA) (Nanosight, Malvern, UK) and the average diameter size combining dynamic light scattering (DLS) (Sald 7500 nano, Shimadzu, Japan) and NTA analysis. The average particle size and the concentration were found to be 175 ± 17 nm and $2.1 \times 10^7 \pm 6.8 \times 10^6$ particles/mL, respectively. The estimated oxygen concentration was found to be five times higher than oxygen solubility in equilibrium.

5.1.2.4. Chlorophyll measurements

At the end of the experiment, representative samples to plant condition were collected to estimate the chlorophyll content (267). Leaf samples (0.2 g) were collected and grounded in a ceramic mortar with 10 mL of 80% acetone. The absorbance of the supernatant after centrifugation was measured at 663 and 646 nm using a UV–VIS spectrometer to determine chlorophyll a, chlorophyll b and total chlorophyll concentrations.

5.1.2.5. Measurement of antioxidant enzymes activity

For extraction of enzymes, 1 g of fresh leaves and roots was grounded and homogenized in potassium phosphate buffer 100 mM (pH =7) containing 0.1 mM EDTA and 1% (w/v) PVP. The extract was filtered through multiple layers of cheesecloth and the supernatant was centrifuged at 16000g for 25 min. Protein concentration was determined using the Bradford assay (268). The activity of guaiacol-peroxidase (GPOD) was determined by monitoring the increase in absorbance due to the oxidation of guaiacol at 470 nm for 3 min using a UV–vis spectrometer (coefficient of absorbance, $\epsilon=25.5 \text{ mM}^{-1}\text{cm}^{-1}$). Briefly, a reaction mixture was prepared by phosphate buffer (50 mM, pH=5.8), guaiacol (15 mg/mL), a suitable amount of plant extract and H_2O_2 (1% v/v) (269). The activity of catalase (CAT) was determined recording the decrease in absorbance as a result of H_2O_2 degradation at 240 nm for 3 min (coefficient of absorbance, $\epsilon=43.6 \text{ mM}^{-1}\text{cm}^{-1}$). The extraction mixture contained phosphate buffer (50 mM, pH=7), H_2O_2 (36 mM) and a suitable aliquot of supernatant enzyme (270). The enzymes activity unit was expressed as the change in absorbance per minute in terms of units per milligram of extracted proteins.

5.1.2.6. Water content and biomass measurement

At the beginning of the experiment, the fresh weight of the plants was measured. After the experimental period, entire plants were carefully taken out of the soil and washed with tap water and rinsed twice with deionized water to remove any dust/dirt. Then, they were separated into roots and shoots and their fresh weights (FW) were determined. Dry weights (DW) were determined after oven drying for 48 h at 70°C and cooled down to room temperature. Water content (WC, %) were estimated according to the equation below:

$$\text{WC}(\%) = \frac{\text{FW} - \text{DW}}{\text{FW}} \times 100\%$$

The loss total weight was estimated from the weight of the plants before (FW_o) and after (FW_t) the experiment based on the following formula:

$$\text{Loss of total weight} = \frac{FW_o - FW_t}{FW_o}$$

5.1.2.7. Heavy metal analysis

Plants tissues were air dried (48 h at 70 °C) and digested for the metal content determination. 0.5 g of milled plant samples was ashed in the muffle furnace for 16 h at 480 °C and then was dissolved with 1.5 mL citric acid (5 M) and 7.5 mL HNO₃ (> 69%) on a hot plate (~ 100 °C). Solution was diluted with ultrapure water to 45 mL and agitated for 24 hours. Afterwards, the samples were filtered (0.45 µm, Whatman) and analyzed by ICP-MS. In parallel, the soil metal contents determination was performed. The total amount of soil was collected from the pots, was air- dried in plastic bags and was passed once more through 2mm mesh size sieve. Soil samples (0.2 g) was treated with citric acid (5 M) and HNO₃ (> 69%) following the aforementioned procedure.

5.1.2.8. Bioaccumulation factor (BC) and translocation factor (TF)

The evaluation of the metal accumulation efficiency in the *N. oleander* was assessed by estimating two main parameters: the bioconcentration factor and translocation factor according to the following equations.

$$BCF = \frac{C_{\text{Plant}}}{C_{\text{Soil}}}$$

where C_{Plant} is the metal concentration in plant (roots and shoots) and C_{Soil} is the metal concentration in soil after culture experiment.

$$TF = \frac{C_{\text{Shoots}}}{C_{\text{Root}}}$$

where C_{Shoots} is the metal concentration in shoots and C_{Root} is the metal concentration in roots after culture experiment. BCF is expressed as the ratio of metal in the plant to that in soil, while TF as the ratio of the metal in the aerial parts to the roots. A BCF value higher than one indicates that a plant is an accumulator and a TF value higher than one is indicative of a high translocation ability of metals from roots to shoots.

Triplicate measurements in the extracts, measurement of calibration blanks, laboratory reagent blanks, as well as analysis of standard reference material were employed in order to address data quality control. All data are presented as mean \pm standard deviation. Statistical analysis was performed using GraphPad Prism 9 software. Data variation was analyzed with one-way analysis of variance (ANOVA) at significant level of $p < 0.05$.

5.1.3. Results

5.1.3.1. Protein content

The protein content was examined in the root and leaves of *N. oleander* for each treatment. As shown in Figure 46, a significant difference was found between the root of treatment without the supplementation of ONBs, exposed to the antimony and the low concentration of OAs and those irrigated with ONBs. In particular, 17.8 mg protein per g fresh root was found in TR.1 and 4.4 mg protein per g fresh root in treatment TR.2, while in control the protein content was found to be 9.4 mg/g fresh root. The protein concentration of leaves is considerably higher than in the root. The protein content of leaves was not statistically different in treatment TR.2 from the TR.1 treatment. The protein content was found to be 23.8 mg/g in the TR.0, 40.7 mg/g in the TR.1 and 33.9 mg/g of fresh leaves in TR.2.

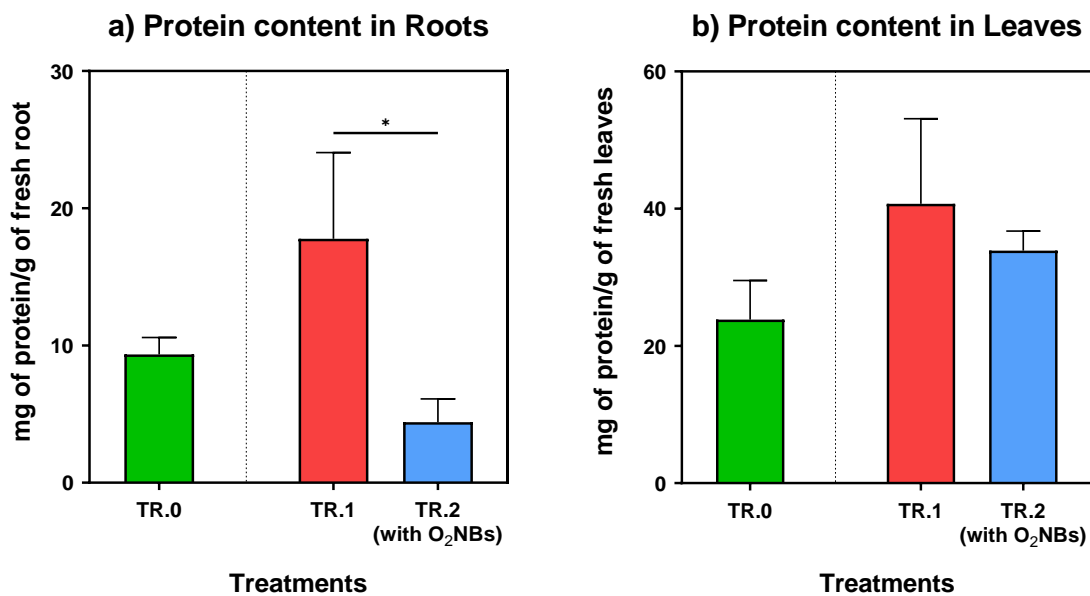


Figure 46. Protein content (mg protein/g FW) in (a) root and (b) leaves for all treatments; control (TR.0), irrigated with tap water (TR.1) and with ONBs (TR.2) (star indicates the level of significance: * for $p < 0.05$).

5.1.3.2. Loss of biomass and water content

Physiological changes in plants were also evaluated by measuring the loss of fresh weight of roots and leaves and the water content (Figure 47). By examining the weight, in both treatments, a loss was observed, with the lowest percentage observed in the TR.2, which contains ONBs, exhibited a loss of weight that is statistically lower than those in treatment without the presence of nanobubbles. Additionally, the water content was found to be higher with the use of ONBs, close to those of control treatment, however it is not significantly different.

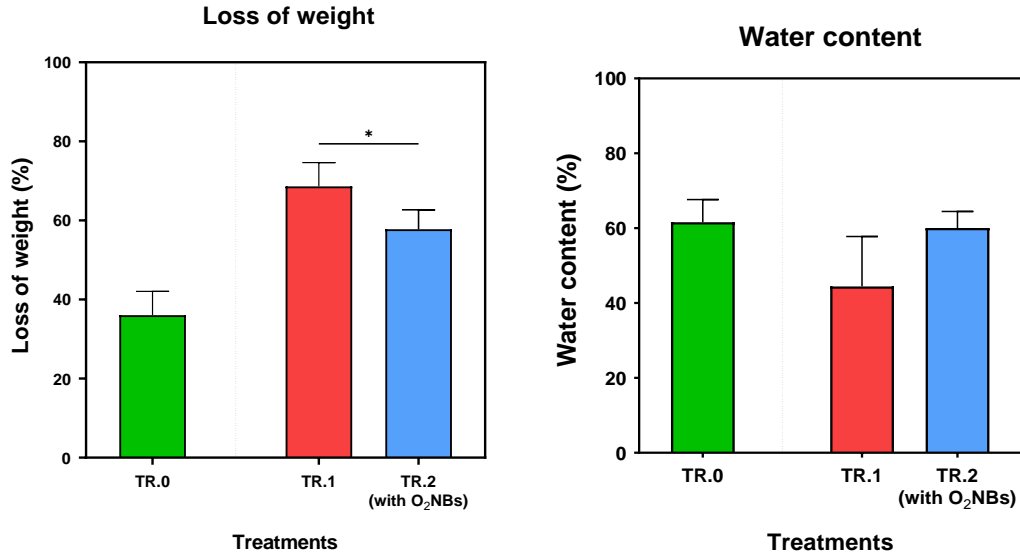


Figure 47. Loss of weight and water content at the end of the experiment for all treatments; control (TR.0), irrigated with tap water (TR.1) and with ONBs (TR.2) (star indicates the level of significance: * for $p < 0.05$).

The enzymes activity involved in antioxidant defense were determined in the root and leaves (Figure 48). Specifically, the catalase (CAT) activity in the root was not significantly affected by exposure to antimony, since no statistical difference was observed. Moreover, as shown in Figure 48, a statistically significant increase of GPOD activity in the roots was observed between treatments TR.1 and TR.2. In the presence of ONBs, the antioxidant activity was statistically significantly higher. Moreover, a statistical difference was observed between the control and treatment TR.1, in which the antioxidant activity was lower. Higher GPOD activity in treatment TR.2 was found to be significantly higher compared to the control. The enzyme production in leaves from treatments TR.1 and TR.3 were significantly elevated compared to the activity of the enzyme in leaves of non-spiked soil. In general, the level of GPOD activity was higher in roots than in leaves in all treatments. Only in treatment TR.2, a significant increase in GPOD activity was recorded both in the root and the leaves.

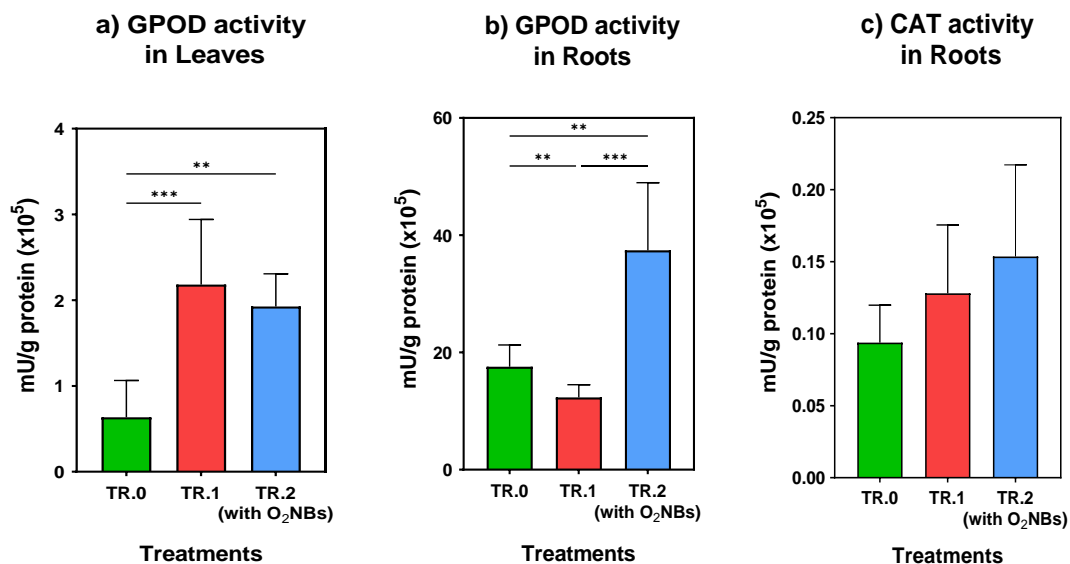


Figure 48. GPOD activity in a) leaves b) roots and c) CAT activity in roots per g protein for all treatments; control (TR.0), irrigated with tap water (TR.1) and with ONBs (TR.2) (star indicates the level of significance: *** for $p < 0.001$).

Regarding total chlorophyll, chlorophyll a, and chlorophyll b, statistically significant differences were not found for treatments control and irrigated with and without ONBs. As shown in Figure 49, the chlorophyll content (mg/g FW) of TR.2 was to close to those of control treatment and there is a slight decrease in treatment TR.2, although this difference is not statistically significant.

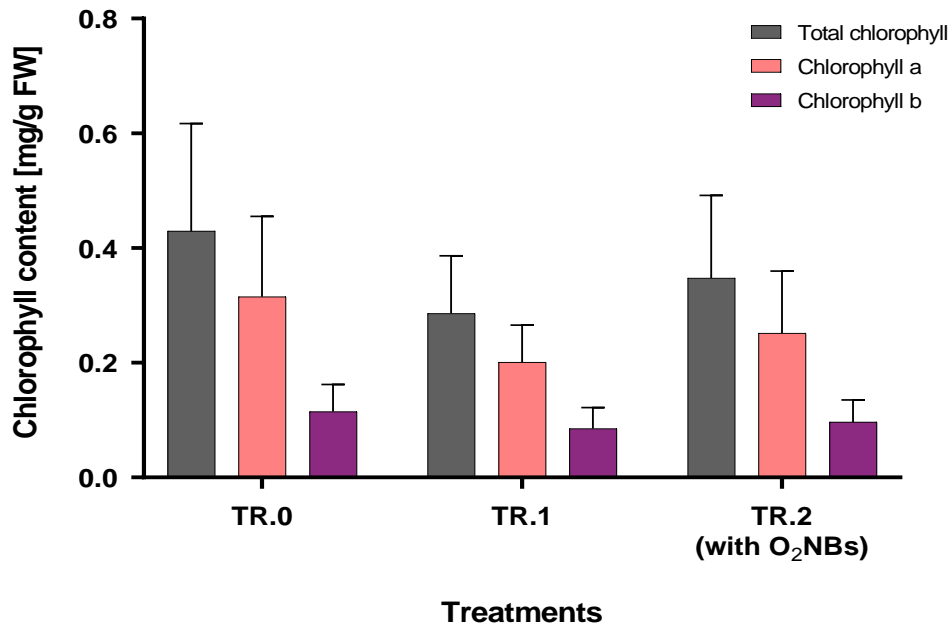


Figure 49. Chlorophyll (a, b, total) content in plant tissues (leaves) for all treatments; control (TR.0), irrigated with tap water (TR.1) and with ONBs (TR.2) at the end of the experiment.

In Figure 50, the Sb content accumulated in roots and leaves is shown. In Sb-contaminated soil irrigated with ONBs, the Sb content was detected significantly higher, with 31.64 mg/kg DW biomass in the roots and 2.89 mg/kg DW biomass in the leaves. On the contrary, lowest Sb concentration was found in treatment TR.1, where again, the majority of the Sb remained in the roots. In the control with the background concentration of Sb, the accumulation was found to be 0.61 mg/kg DW biomass in the roots and 0.66 mg/kg DW biomass in the leaves. The estimated translocation factor was close to unity, much higher compared to other treatments where Sb is present at a much higher concentration in the soil.

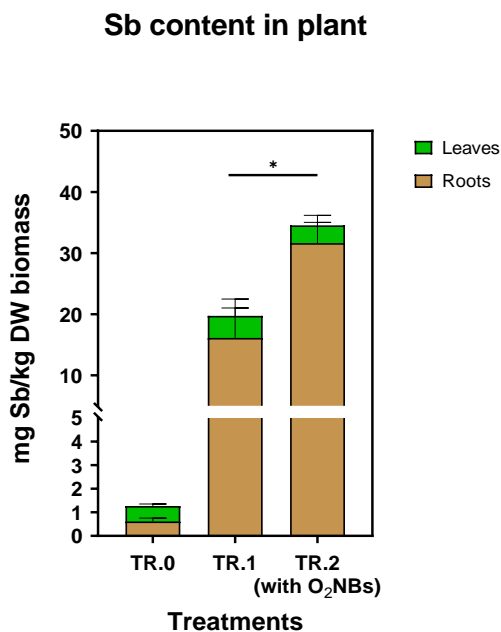


Figure 50. Sb accumulation in roots and leaves for for all treatments; control (TR.0), irrigated with tap water (TR.1) and with ONBs (TR.2) (star indicates the level of significance: * for $p < 0.05$).

In all treatments including the control, the bioconcentrations factors were found to be less than 1, indicating a low mobilization of Sb from the soil to the plant. Regarding the translocation factor, the values in all treatments have been found to be significantly lower than one, suggesting that Sb could not be readily transferred from the roots to the above-ground tissues. According to Table 21, the TF in treatment TR.1 was significantly higher (0.23) compared to TR.2, which was significantly lower (<0.1).

Table 21. Sb bioconcentration factor (BCF) and translocation factor (TF) for treatments without and with ONBs (star indicates the level of significance: **** for $p < 0.0001$).

Factors	Treatment	
	TR.1	TR.2 (with ONBs)
BCF	0.51	0.90
TF	0.23****	0.09

Besides the Sb concentration in plant tissues, Fe, Mg, and Mn uptake by *N. oleander* was also measured, since these elements are essential for plant growth. As seen in Figure 51 in treatment TR.2 containing nanobubbles, the accumulation of Fe, Mn, Mg from the soil to the plant was enhanced, as each metal concentration (mg/kg DW biomass) was found to be significantly higher in treatment TR.2, which was irrigated with nanobubbles.

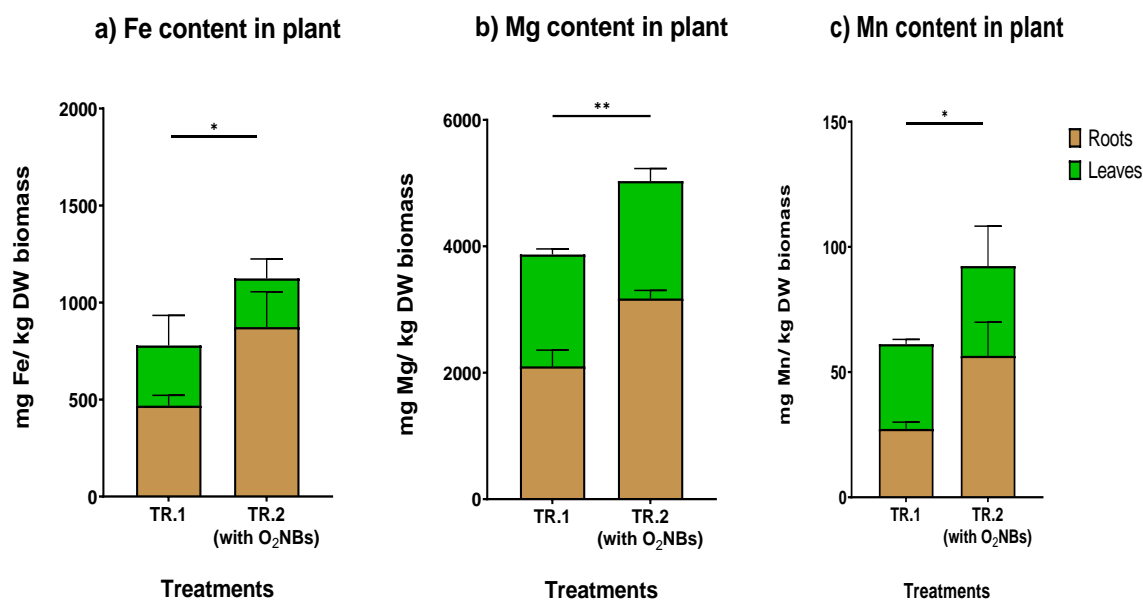


Figure 51. Accumulation of (a) Fe, (b) Mg, (c) Mn and (d) Sb in roots and leaves for treatments irrigated without and with ONBs (Star indicates the level of significance: * for $p < 0.05$, ** for $p < 0.01$).

The translocation and bioconcentration factor of the elements Fe, Mg and Mn were estimated in treatment with and without the supplementation of ONBs. According to Table 22, the bioconcentration and translocation factors of Fe were less than unity for both treatments. In respect to Mg, the bioconcentration factors were above unity indicating that in both treatments, Mg could be transferred from soil to plant tissue. In TR.2 the BCF was significantly higher. Regarding, the translocations factors, both were estimated less than one, however in TR.1 the TF was significantly greater than TR.2. Finally, BCF of Mn in both treatments was evaluated less than one. TF in TR.1 was found to be above one, whilst in TR.2 lower than unity, indicating that in treatment irrigated only with tap water plant could translocate Mn from root to aboveground part.

Table 22. Fe, Mg and Mn bioconcentration factor (BCF) and translocation factor (TF) for treatments irrigated with and without ONBs * for $p < 0.05$, **for $p < 0.01$, **** for $p < 0.0001$).

mg/kg biomass	Fe		Mg		Mn	
	BCF	TF	BCF	TF	BCF	TF
TR.1	0.03	0.65	5.4	0.85**	0.36	1.25*
TR.2 (with ONBs)	0.05	0.30	8.2****	0.59	0.53*	0.69

5.1.4. Conclusions

The results demonstrate that there was a loss in plant growth in treatments with and without the supplementation of ONBs as well as in the control treatment. However, in the treatment where nanobubbles were used, the loss in weight was significantly lower compared to treatment irrigated with tap water. In addition, the results demonstrated that the presence of OAs and ONBs assisted the plant to maintain the water content at the level close to the control. The plant was not affected with regards to chlorophyll content in all treatments, while the antioxidant enzyme activity of guaiacol peroxidase (GPOD) in the roots was found to be significantly higher in the presence of Sb.

The translocation of Sb for every treatment was very low, confirming that *N. oleander* plant cannot transfer Sb from the root to the shoots. In addition, the bioconcentration factor was less than unity, indicating that Sb could not be transferred from roots to aboveground of the plant. However, when ONBs were employed a higher amount of Sb was accumulated in the plants, which was significantly greater, although the translocation of Sb was not increased.

Regarding the other elements investigated in this study (Fe, Mg and Mn), the results are similar as the concentration is substantially higher in the roots comparing to the aboveground tissue, except from Mn content in treatment TR.1. In this instance, the TF was estimated greater than 1. With respect to the bioaccumulation of these elements

from soil to plant tissues, Fe and Mn were not be mobilized, whereas Mg was extracted as BCF was evaluated above one for the two tested treatments. The BCF of Mn and Mg were significantly higher in TR.2 than TR.1, while the opposite trend was observed regarding the translocation factor. This can lead to the conclusion that nanobubbles can enhance the stabilization of these elements in roots and not the translocation to the upper part of the plants.

5.2. Mobilization of Sb from soil by non-bioaugmented and bioaugmented processes coupled with nanobubble technology.

5.2.1. Introduction

Several studies have indicated that Sb(III) sorbs to surfaces, primarily to Fe(III) to Mn(IV) hydroxides more strongly than Sb(V), therefore it is considered more stable. In addition, the oxide of Sb(V) is more soluble and subsequently more mobile than the oxide of Sb(III) (271). Given that antimonite is generally more toxic than Sb(V), it is crucial to be oxidized to Sb(V) as it is more mobile, since soil minerals such as Fe hydroxides and natural organic matter display low adsorption capacity for Sb(V) (272). Hence, the oxidation process of Sb(III) plays an important role in the mobility of Sb in the aqueous environment owing to the greater solubility of Sb(V).

In order to understand the fate of Sb in the environment and enhance its removal from drinking water, it is crucial to shed light on the redox conditions that may affect Sb speciation and subsequently influencing the sorption and mobility of Sb in contaminated soils. In the literature, significant oxidation and immobilization of Sb(III) has been reported by soil-derived humic acid. In particular, complete Sb(III) oxidation was reached in the presence of 0.2 mM gallic acid within 4 h whereas 94.6% Sb(III) was oxidized in the presence of 0.2 mM CA after 12 h (273). Other study revealed that the presence of ferrihydrite removed Sb(III) via adsorption, as well as it also catalyzed the oxidation of Sb(III) to Sb(V) (274). In another study, Sb(III) was photo-oxidized to Sb(V) in goethite suspension as induced by simulated solar light (275).

On the other hand, bioaugmentation process is considered an effective process to remediate contaminated areas. The addition of cultured organisms resistant to toxicity of

heavy metals has been widely used to enhance the existed microbial community and to treat contaminated soils. One of the developing mechanisms that bacteria utilize in order to survive from the exposure to heavy metals is the bio-reduction/bio-oxidation to less toxic forms (276). In the case of antimony, microbes that can oxidize Sb(III) to Sb(V), which is less toxic are called Sb-oxidizing bacteria and the microbial tolerance can be improved owing to the lower toxicity in the natural environment. The microbial oxidation for the efficiency of bioaugmentation are associated with various abiotic factors; one of them is the dissolved oxygen concentration as electron acceptor. Notably, most species of Sb-oxidizing bacteria can oxidize Sb(III) faster under aerobic than under anaerobic conditions (277). Therefore, to combine the Sb-oxidizing bacteria with the oxygen nanobubble technology may enhance the Sb(III) microbial oxidation.

In this study, the oxidation of Sb(III) a more toxic form of antimony into the less toxic and more mobile Sb(V) by the bioaugmentation process coupled with nanobubbles technology was investigated. Also it was examined whether a low concentration of organic acid can also catalyze the oxidation process and thus mobilize Sb(III).

5.2.2. Materials and Methods

5.2.2.1. First experimental phase

The experimental process consists of two phases. In the first experimental phase, preliminary experiments were conducted in flasks before scaling up to the bioreactor in order to investigate the impact of ONBs on the release of Sb from the contaminated soil. Experiments were performed under batch mode with and without the presence of oxygen nanobubbles and with concentration 10% w/v (soil/water) in flasks of 2 L volume agitated gently at room temperature (~25 °C) as shown in Image 5.

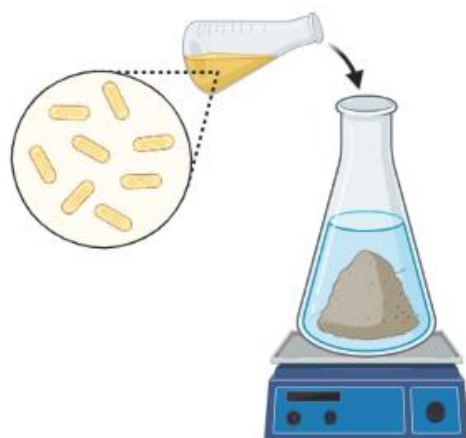


Image 5. Experimental set up of the first experimental phase.

Three concentration of Sb- contaminated soils collected from shooting ranges in Switzerland and provided by FHNW (Table 23) were tested. The generation of ONBs was described in detail in section 5.1.2.3.

Table 23. Contaminants concentrations in soils from Swiss shooting range.

Element	Unit	Soil		
		A	B	C
Mn	mg/kg	361.5	668.2	733.8
Fe	mg/kg	22,480.4	26,897.9	14,354.5
Sb	mg/kg	362.5	16.5	3.8

5.2.2.1.2. Isolation of microbial communities resistant to Sb.

Afterwards, bioaugmentation process was conducted anew with and without the presence of oxygen nanobubbles in tap water, with microbial community isolated from Sb-contaminated soil. Specifically, the effect of Sb oxidizing bacteria, which were also resistant to Sb toxicity was investigated on Sb release from soil to aqueous phase. Microbial communities and strains from three different contaminated soils (Table 23) were isolated and enrichment cultures were performed in a rich medium and then the Sb-resistant bacteria were plated on solid CDM-A medium containing 200 mg/L of Sb(III).

Then, the ability of these communities to oxidize Sb(III) was quantitatively and qualitatively assessed using the KMnO_4 method and the total Sb concentration was estimated by ICP-MS. The soil microbial community that exhibited the highest Sb(III) oxidation and reduction reached to 77% was selected for the bioaugmentation experiments. Initial bacterial concentration of 10^7 CFU/mL was inoculated in each flask and the microbial concentration was monitored during the experiment. In order to maintain a concentration close to initial, bacterial inoculum in flasks was added when it was necessary as it was observed a decrease below this level in some bioaugmentation experiments.

5.2.2.2. Second experimental phase

In the second experimental phase, a scale up from the flask to bioreactor was performed. Again, a concentration of 10% w/v (soil/water) was used. Oxygen nanobubbles were supplemented at the beginning of experiment as well as additional aeration was also supplied. Due to loss of water, the volume of bioreactor remained constant by adding nanobubble water. The same inoculum of Sb-oxidizing bacteria was added at initial bacterial concentration of 10^7 cells/mL. Samples were collected at predetermined time periods and were tested in terms of physicochemical parameters. The addition of low concentration of organic acids (citric, ascorbic and oxalic acid) was conducted in order to investigate whether the release from soil to aqueous phase is enhanced.

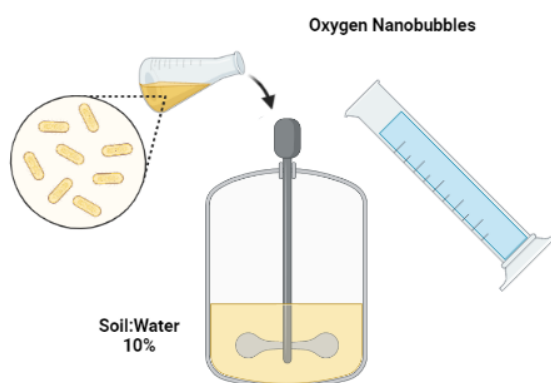


Image 6. Experimental set-up of the second experimental phase.

5.2.2.3. Heavy metals concentration

Samples were collected at predetermined time points each day in order to estimate the metals concentration in water. At the end of the experiment, soil was collected, was dried and then sieved at 2-mm mesh. 0.2 gr of soil was dissolved with 1.5 mL citric acid (5 M) and 7.5 mL HNO₃ (> 69%) on a hot plate (~ 100 °C). After 2 days, ultra pure was added to 45 mL and agitated for one more day. Then, it was filtered at 0.45 µm and analyzed by ICP-MS.

5.2.2.3. Physicochemical parameters

The physicochemical parameters such as pH, temperature and oxidation-reduction potential were measured by a Hach HQ40d multi parameter meter.

5.2.3. Results

5.2.3.1. First experimental phase

Figure 52 displays the results from the dissolved oxygen after the addition of nanobubble water in non-bioaugmented and bioaugmented. Only in soil B, the addition of the bacterial inoculum lead to a significant decrease in oxygen level. In the other soils, there is only a slight decrease in the bioaugmented experiment. The initial oxygen concentration in all flasks was estimated approximately 35 mg/L, four times higher than the saturated concentration.

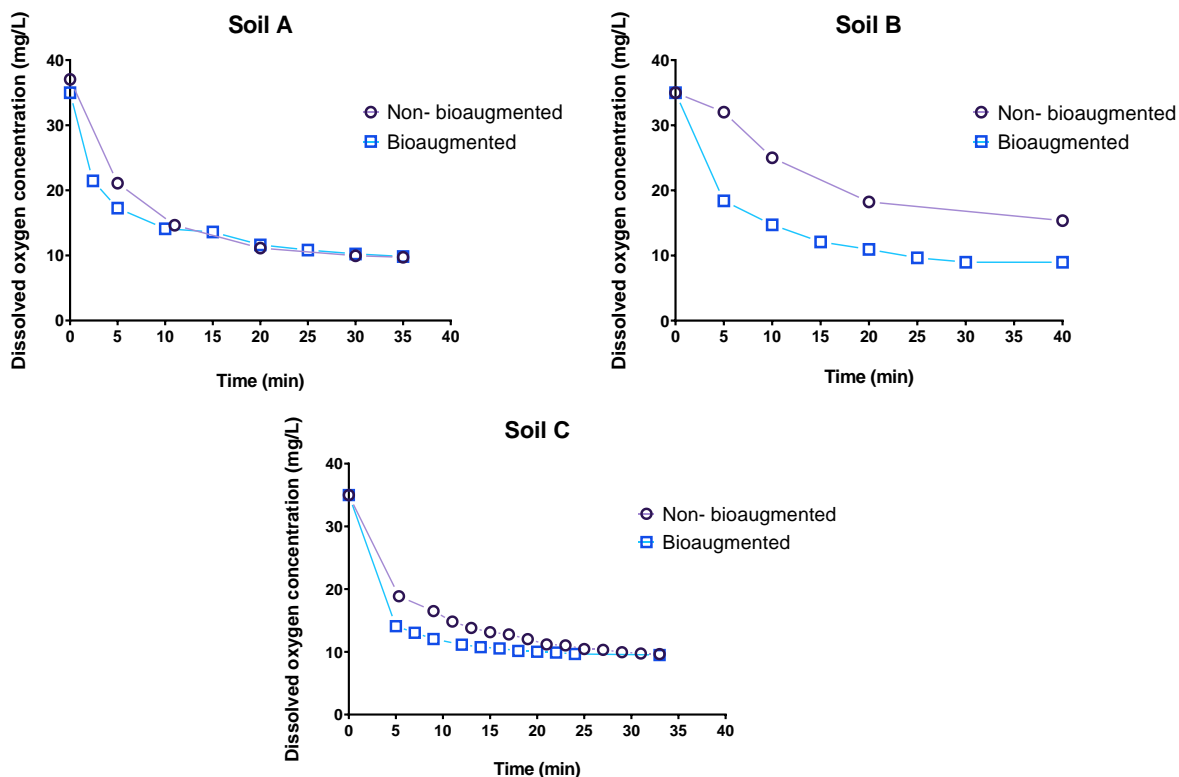


Figure 52. Dissolved oxygen concentration in flasks of non-bioaugmented and bioaugmented treatments with ONBs for the three soils (A, B & C).

Figure 53 illustrates the metals manganese (Mn), iron (Fe) and antimony (Sb) concentration in soil A with the highest concentration of antimony after the end of experiments with and without the bioaugmentation and the presence of ONBs. As it can be seen, in all experiments the concentration of metals in tested soil is lower than those of the initial soil concentration, hence it can be concluded that there is release from soil to water in all metals. As regards the antimony, the concentration in non-bioaugmented experiments was found to be lower with the supplementation of oxygen nanobubbles, while in bioaugmented experiments no difference was observed among the two treatments concerning the type of water. In bioaugmented experiments the remaining concentration in soil was found to be lower compared to non-bioaugmented experiments, indicating that the microbial community enhanced its release to water.

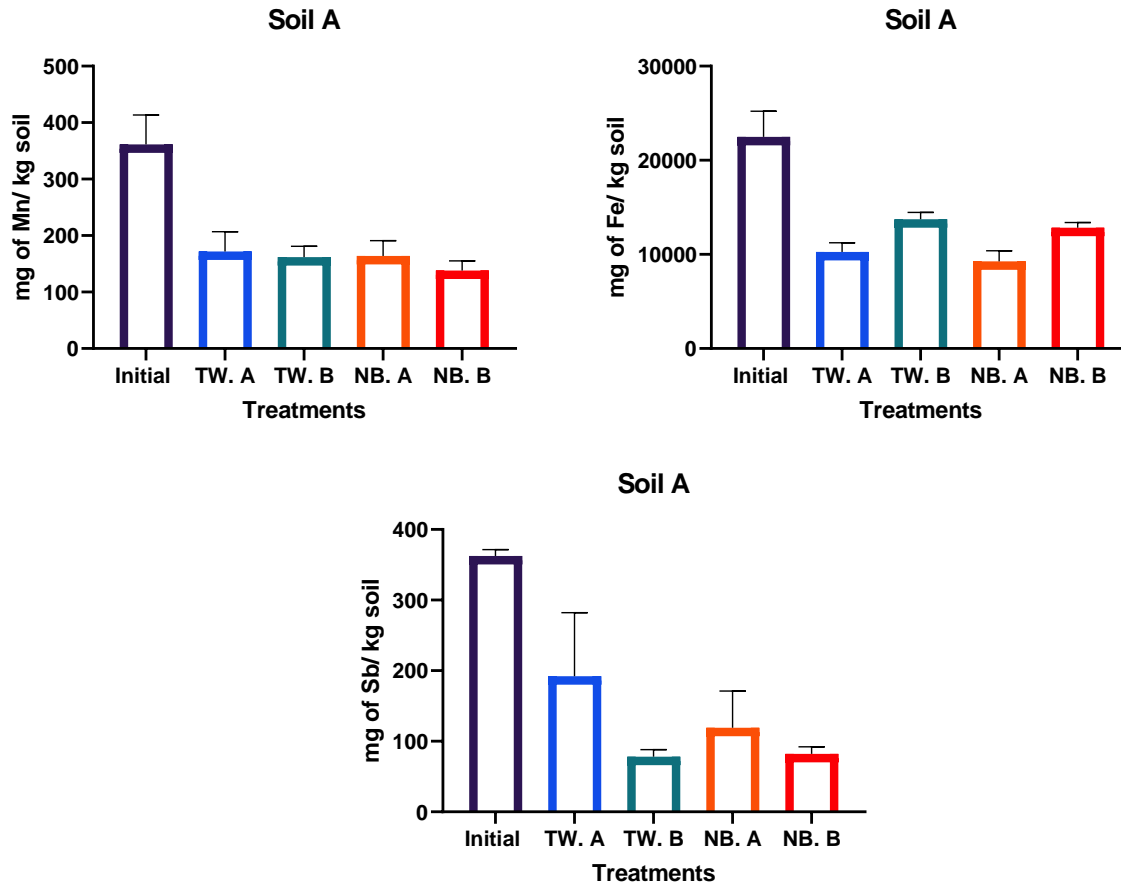


Figure 53. Initial and final concentration of Mn, Fe and Sb in soil A (mg/kg soil) [TW=tap water; NB=tap water with ONBs; A=non-bioaugmented; B=bioaugmented].

Figure 47 displays the results of the batch experiments with lower Sb concentration (soil B). It can be seen that the antimony concentration in soil was decreased to a lesser extent than for Soil A as a decrease of approximately 54 % was observed in soil B, while in soil A the maximum percentage of decrease was found to be around 78 %. There was no significant difference between bioaugmented and non-bioaugmented treatments in Sb antimony as well as between tap water and nanobubble water. The same conclusion can be drawn with regards to the other two metals. In general, the microbial inoculation and the supplementation of oxygen nanobubbles did not enhance the mobilization of Sb.

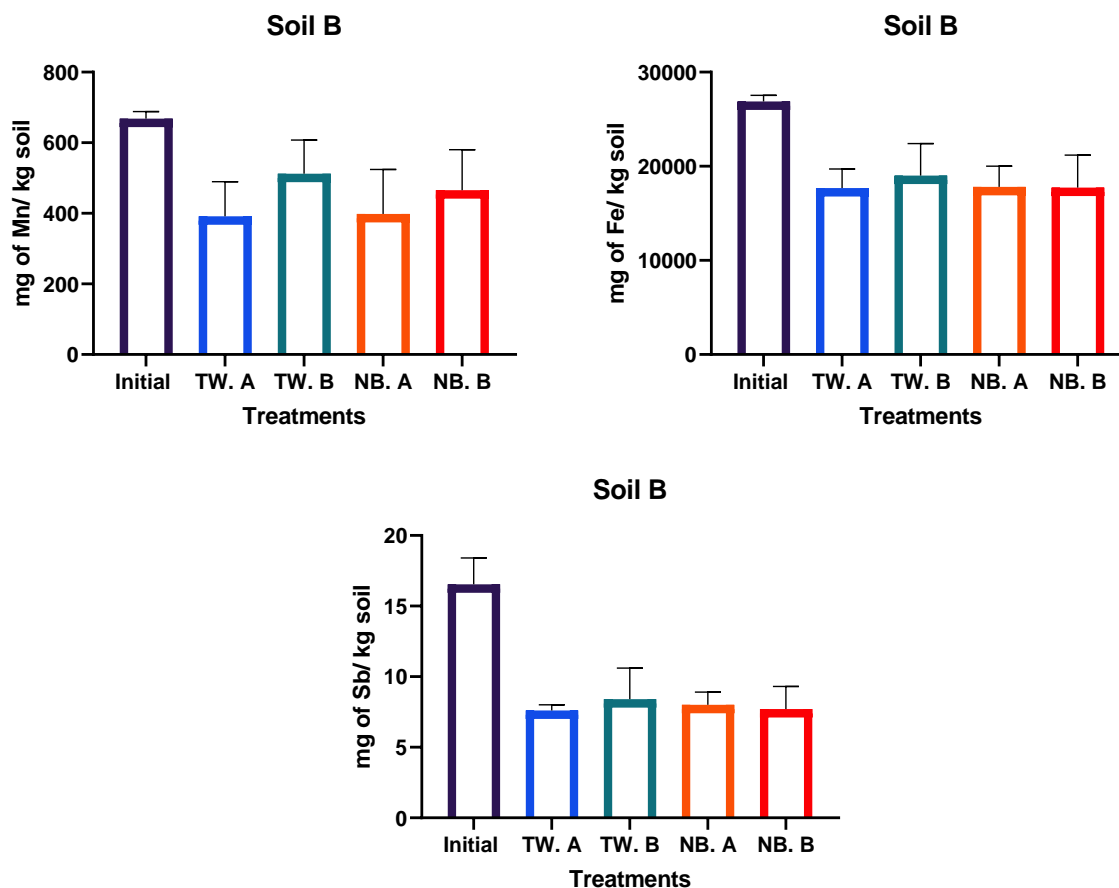


Figure 54. Initial and final concentration of Mn, Fe and Sb in soil C (mg/kg soil) [TW=tap water; NB=tap water with ONBs; A=non-bioaugmented; B=bioaugmented].

Finally, the soil C with the lowest Sb concentration was tested and the results revealed that also in this case a decrease in metals concentration was observed as shown in Figure 55. However, no significant change in Sb release was observed when different type of water is used as well as Sb-oxidizing bacteria were inoculated. Conclusively, the addition of Sb-oxidizing bacteria and ONBs did not enhance the mobility of Fe, Mn and Sb from soil to aqueous phase in soil C.

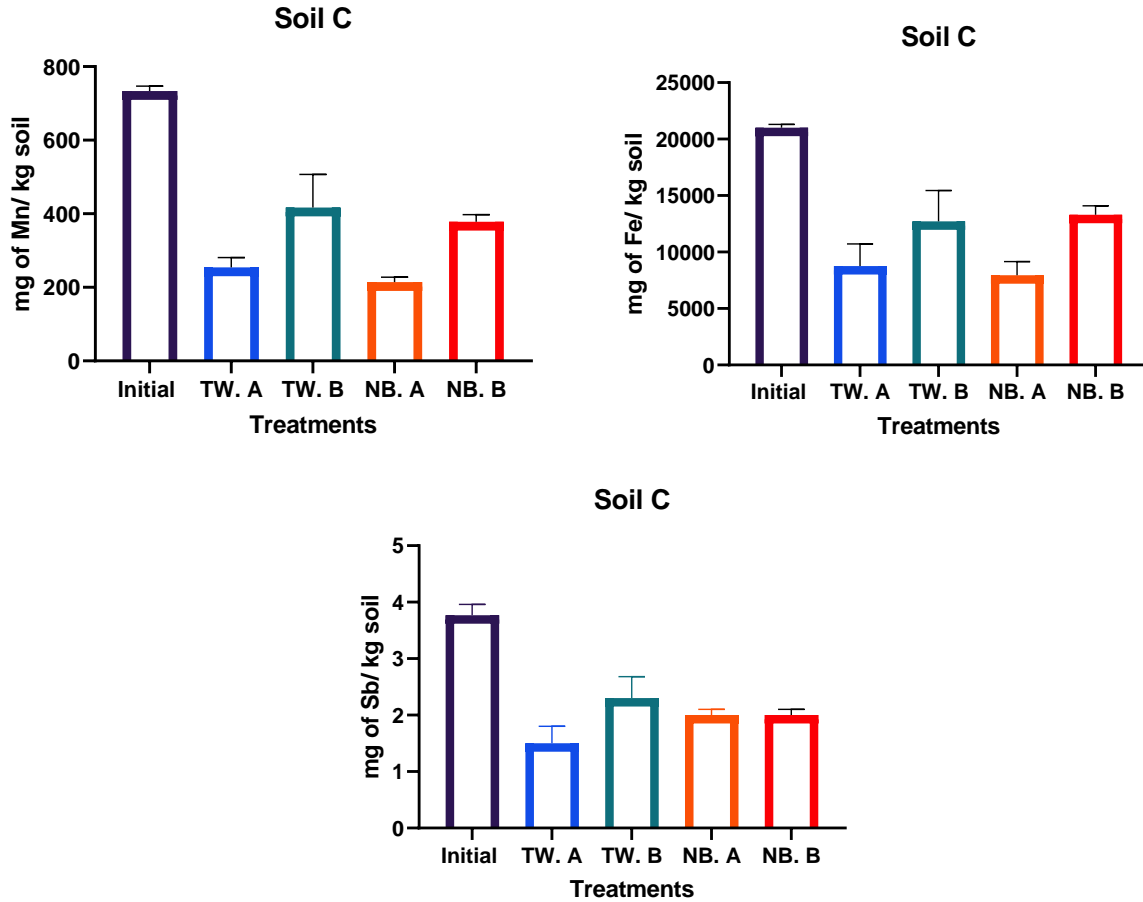


Figure 55. Initial and final concentration of Mn, Fe and Sb in soil C (mg/kg soil) [TW=tap water; NB=tap water with ONBs; A=non-bioaugmented; B=bioaugmented].

The dissolved oxygen concentration was monitored in bioaugmented and non-bioaugmented experiments, in different type of water and in soils with different concentrations (Soils A, B, C). As it can be seen in Figure 56, the oxygen level is lower in soils A and B, when the Sb-oxidizing bacteria were added whilst the type of water did not influence the dissolved oxygen concentration. In soil C, there is no difference in oxygen content among the treatments.

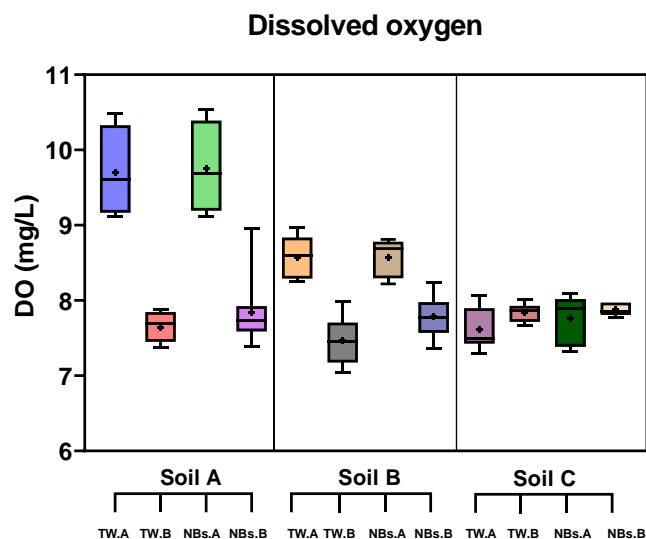


Figure 56. Dissolved oxygen concentration (mg/L) in soils A, B, C [TW=tap water; NB=tap water with ONBs; A=non-bioaugmented; B=bioaugmented].

As regards the pH, there is no difference among the different Sb soil concentrations under batch bioaugmented and non-bioaugmented experiments with and without the addition of nanobubbles. In all experiments, the mean value of pH is approximately 7.5.

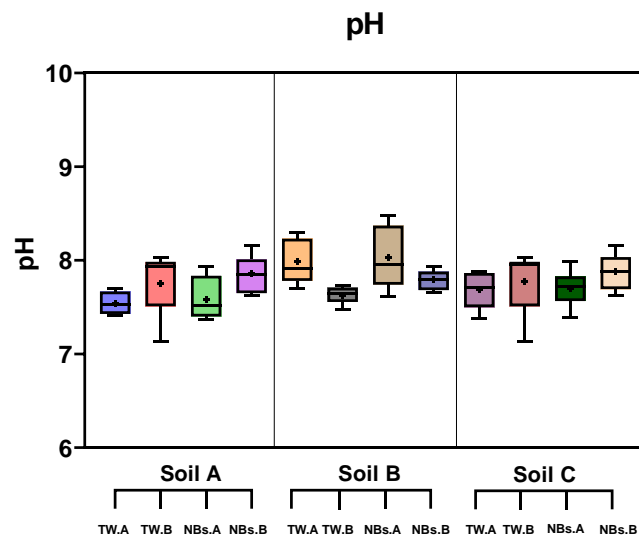


Figure 57. pH in soils A, B, C [TW=tap water; NB=tap water with ONBs; A=non-bioaugmented; B=bioaugmented].

Monitoring the oxidation- reduction potential during the experiment as shown in Figure 58, some differences can be detected. In tap water, ORP values were found to be higher than those in bioaugmented experiments. The opposite trend was observed when the type of water was changed and nanobubble water was used. The ORP values were higher with the addition of microbial community. The same trend was followed in soil C. In soil B, all the values were similar except from non-bioaugmented experiment coupled with nanobubble technology.

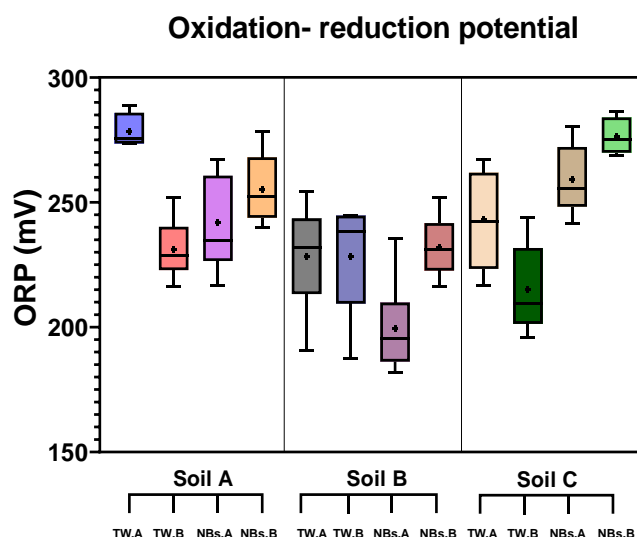


Figure 58. Oxidation- reduction potential (mV) in soils A, B, C [TW=tap water; NB=tap water with ONBs; A=non-bioaugmented; B=bioaugmented].

The Sb-oxidizing bacteria enhance the mobilization of Sb in soil A with the highest Sb concentration, indicating that bacteria can withstand the toxicity of Sb even though soil Sb is in high concentration and the bacteria were isolated from Soil B. Table 24 demonstrated the percentages of remaining Fe, Mn and Sb in soil A under bioaugmented and non-bioaugmented experiments. The final Sb concentration in soil was found to be 54.4 % of initial in tap water and 33.6 % in treatment with NBs water in non-bioaugmented experiments, indicating that the supplementation of nanobubbles enhanced the mobilization of Sb without any inoculation of Sb-oxidizing bacteria. In addition, the percentages of Fe and Mn concentrations that remained after treatments were similar

between the two types of water. It can be concluded that in soil A with the highest Sb concentration, a substantial mobilization was achieved.

Table 24. Percent of Mn, Fe and Sb remaining in soil A at the end of non-bioaugmented experiment.

Metal	Treatments	
	Tap Water (TW)	Tap Water with NBs (NB)
Mn	47.5%	45.5%
Fe	45.7%	41.3%
Sb	54.4%	33.6%

Table 25. Percent of Mn, Fe and Sb remaining in soil A at the end of bioaugmented experiment.

Metal	Treatments	
	Tap Water (TW)	Tap Water with NBs (NB)
Mn	44.8%	38.1%
Fe	61.2%	57.1%
Sb	24.4%	24.5%

Microbial concentration in the flasks was monitored by CytoFLEX Flow Cytometer (Beckman Coulter). The microbial concentration in soils A, B, C was monitored from Day 0 to the end of experiment. In all soils (Figure 59), the bacterial concentration was maintained from 10^6 to 10^7 CFU/mL.

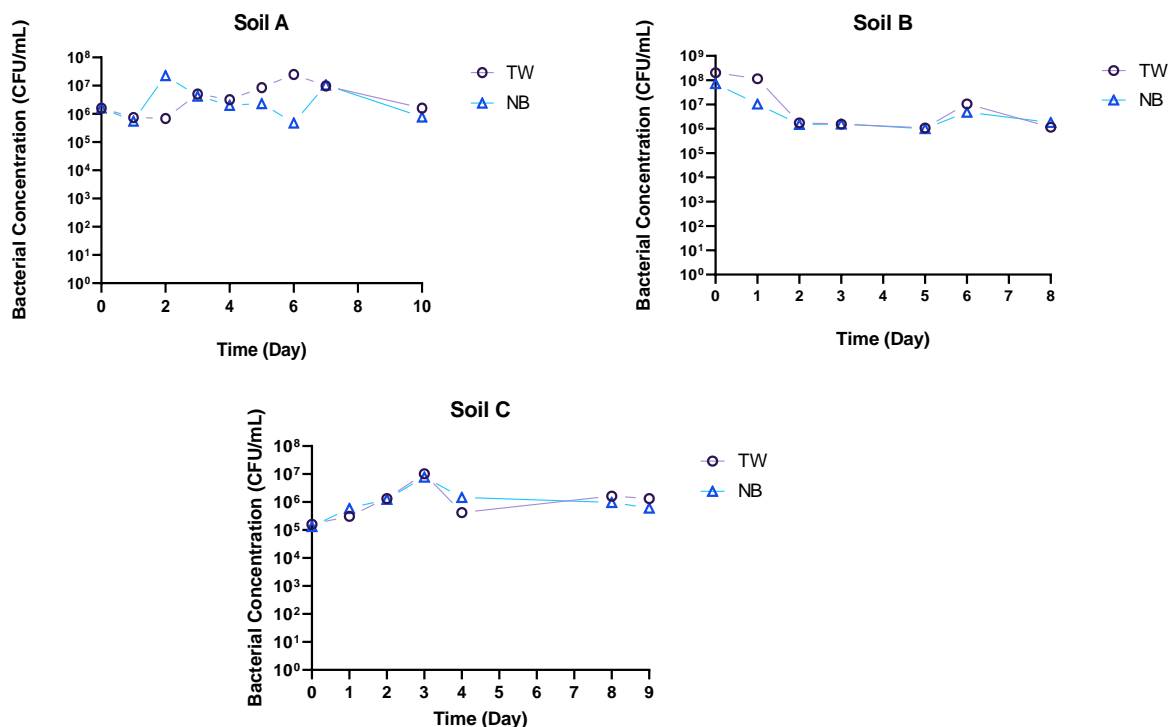


Figure 59. Bacterial concentration in soils A, B, C throughout the experiments [TW=tap water; NB=tap water with ONBs].

Samples from the aqueous solution and soil A and B were collected for DNA extraction to investigate the microbial composition since greater Sb mobilization was reported in soil A with bioaugmentation and Sb-oxidizing bacteria were isolated from soil B. According to Figure 60A, it seems that the microbial community isolated from soil B was consisted of the same phyla with the bioaugmented treatments although the relative abundances of them were different. Both soil and water communities in the same treatment displayed similarity in microbial communities. The initial microbial community consists of *Proteobacteria*, which is the most abundant phylum, as well as *Actinobacteria*, *Firmicutes*, *Bacteroidota* and *Acidobacteria*. In treatment with soil A, the five most abundant phyla were *Proteobacteria*, *Actinobacteria*, *Firmicutes*, *Bacteroidota* and *Acidobacteria*, while in treatment with soil B were *Proteobacteria*, *Actinobacteria*, *Firmicutes*, *Bacteroidota* and *Verrucomicrobiota*. *Proteobacteria* is the most abundant phylum in treatment with soil whereas it can be observed a higher decrease in relative abundance in treatment with soil B. An opposite trend was reported as regards the *Actinobacteria*, which in treatments an increase was detected with the highest abundance

reported in treatment with soil B. Higher relative abundance can be seen for *Acidobacteria* and *Chloroflexi* in treatment A and for *Firmicutes*, *Bacteroidota* and *Verrucomicrobiota* in treatment B compared to initial microbial community. The strains of Sb-oxidizing bacteria isolated from soil B are in line with the strains that have been identified in literature of which higher percentage belong to *Proteobacteria* as well as to *Actinobacteria*, *Firmicutes* and *Bacteroides*.

The 15 most abundant genera are presented in Figure 60B. Several genera exhibited similar relative abundances between the seed community and the treatments while others decreased or increased. For example, the genera *Stenotrophomonas* and *Advenella* displayed high relative abundance in the initial microbial community but decreased in the bioaugmented treatments. On the contrary, *Bacillus* presented elevated abundances in treatment B while *Sphingomonas* displayed the opposite pattern compared to initial community and treatment A. The genera *Stenotrophomanas*, *Bacillus* and *Pseudomonas* are among the most common Sb(III) oxidizing bacteria.

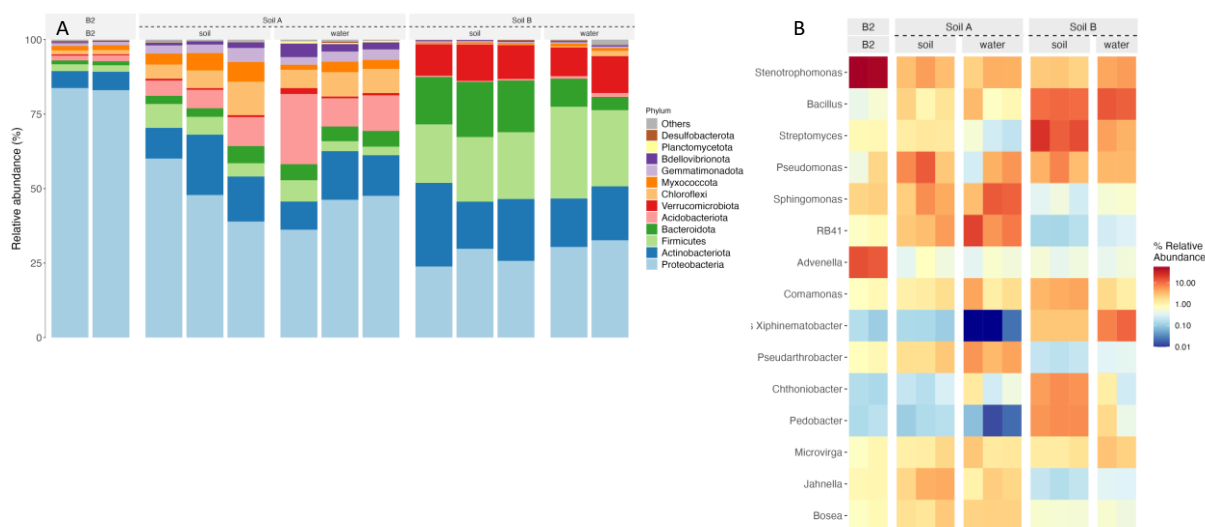


Figure 60. The microbial composition (12 most abundant phyla) of the initial community (B2), and the communities in soil and water from soil A and B (A). the heatmap of the 15 most abundant genera of the initial community (B2), and the communities in soil and water from soil A and B (B).

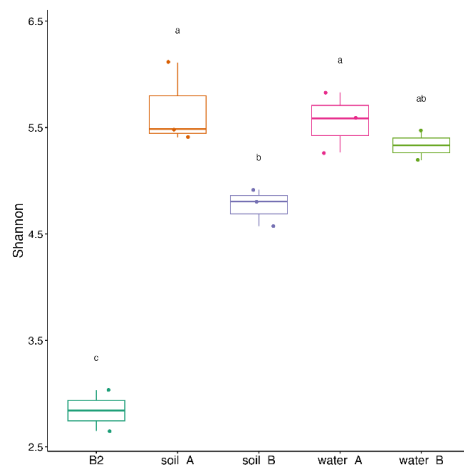


Figure 61. The diversity index Shannon within the treatments.

The significantly highest diversity indices were observed with the microbial communities in treatments A both in soil and in water phase (Figure 8). The lowest diversity was noticed in the seed community since it mostly contained the Sb(III) resistant and oxidizing strains. In treatment B, the water community presented significantly higher diversity compared to the soil.

5.2.3.2. Second experimental phase

In the second experimental phase, the bioaugmentation process in soil A coupled with ONBs technology was performed in a bioreactor. As it can be seen by Figure 62, within 14 days there was no release of the metals Fe and Mn from soil to aqueous phase since the mass of these metals detected in water is rather low. As regards the antimony, it can be observed a release from soil but still low. On the 14th day, the addition of low concentration of a combination of organic acids (OAs) was conducted and it can be observed that the same day an increase in mass of the elements Fe, Sb were detected. In manganese, after the peak in mass a sharp decrease was observed the next days. On the contrary, the mass of iron was increased after the addition of OAs displaying a stable trend within next days. The same pattern was followed by manganese where a sharp decrease was also observed. Regarding the antimony, the mass is significantly higher on the 21st day than before the addition of OAs and the next days it is slight decreased. The percentage of Sb in water phase was increased from 5% to 27 % (95 % to 73 % in soil as seen in Table 26) at the end of experiment.

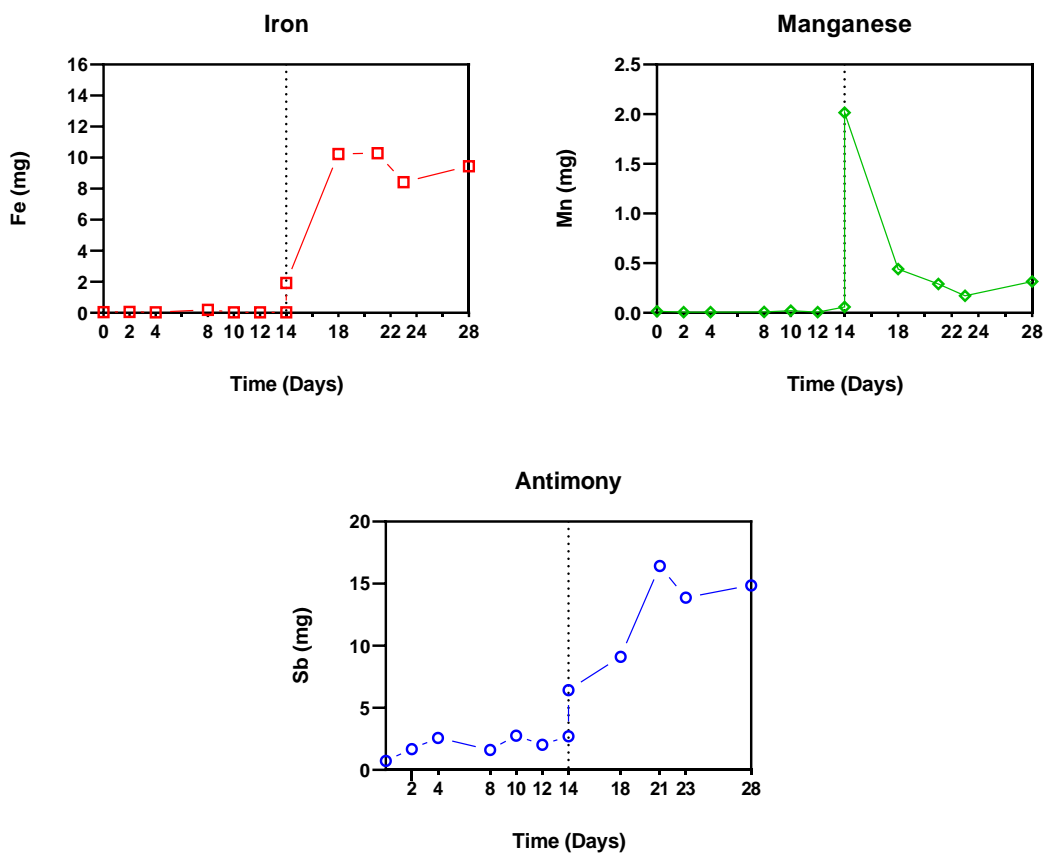


Figure 62. Final mass of Mn, Fe and Sb in aqueous phase (mg) in bioaugmented experiments with soil A coupled with ONBs technology.

Table 26. Percent of Sb remaining in soil A at the end of bioaugmented experiment.

Metal	Treatment
Before addition of OAs	95 %
After addition of OAs	73 %

The physicochemical parameters (pH, dissolved oxygen concentration and oxidation-reduction potential) were monitored during the experiment. According to Figure 63 shows a stable pattern except from Day 14, where the addition of OAs was conducted and a sharp drop was reported. As regards pH, it can be seen that the values are stable before OAs supplementation, the pH is slightly decreased when OAs were added in the bioreactor and then the values were moderately elevated until the end of experiment. The

same trend was followed in dissolved oxygen. The oxygen content was declined from 7.85 mg/L to 6.65 mg/L and then the dissolved oxygen was increased.

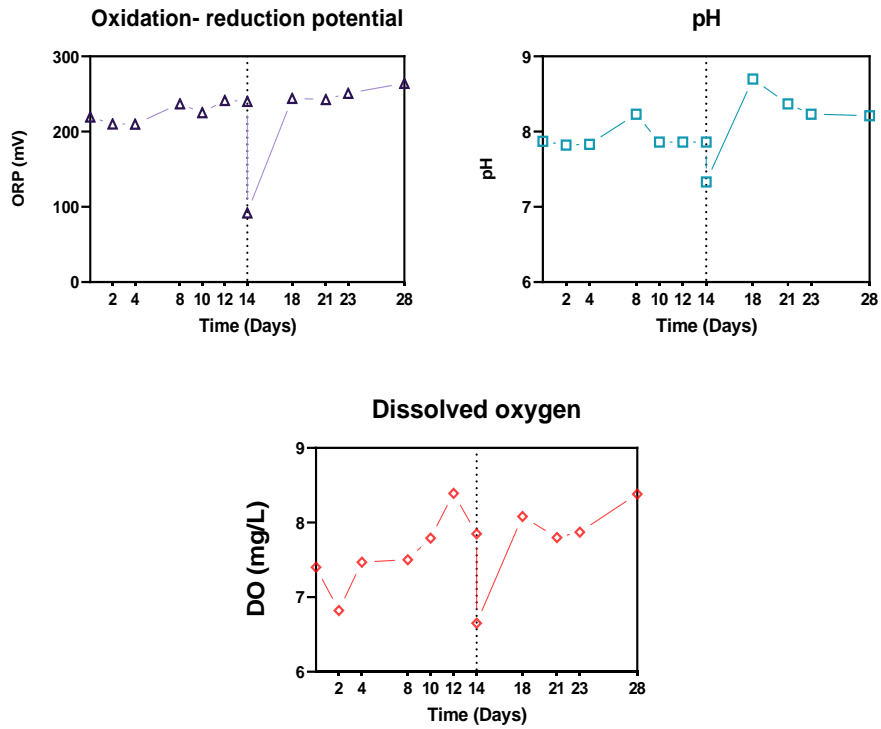


Figure 63. ORP (mV), pH, DO (mg/L) during the experiment.

Microbial concentration in the bioreactor was monitored by CytoFLEX Flow Cytometer (Beckman Coulter). The microbial concentration water phase was monitored from Day 0 to the end of experiment (Day 28). As it can be seen by Figure 64 the bacterial concentration was maintained from 10^8 to 10^9 CFU/mL, while the addition of OAs did not influence the level of microbial concentration.

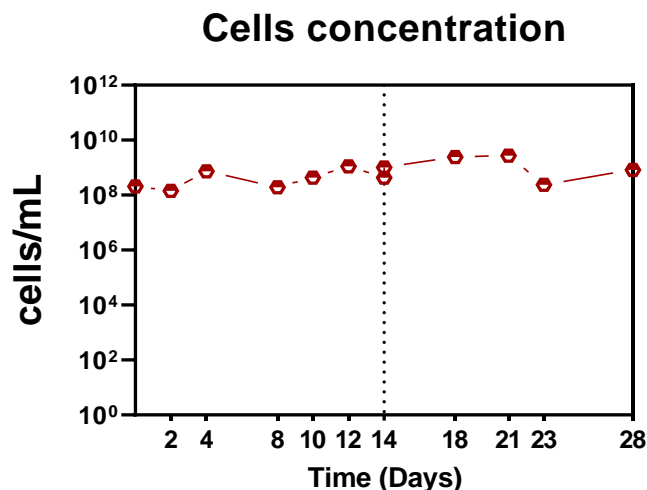


Figure 64. Bacterial concentration in bioreactor.

5.2.4. Conclusions

Soil microbial community mainly consists of *Proteobacteria*, *Actinobacteria*, *Firmicutes* and *Bacteroides*, which are considered common Sb-oxidizing bacteria according to studies found in literature. The bioaugmentation had a significant effect compared to the tap water treatment since the percentage of Sb remaining in the soil was found to be lower in the bioaugmented experiment implying the mobilization of about 75% of the original Sb in the soil. The same percentage of Sb was also found in the bioaugmented treatment with NBs water; i.e., the presence of nanobubbles had no significant effect on the mobilization of Sb in the case of bioaugmentation. When no microbial community was inoculated, ONBs had an impact on Sb mobilization from soil water phase as from 45.6% increased to 66.4% of the initial Sb in soil detected in water by the supplementation of ONBs. Regarding the metal Fe, the bioaugmentation did not enhance its mobilization in the aqueous phase in both tap water and NBs water treatments since the percentages of remaining Fe concentrations were higher in the bioaugmented experiments. The concentration of Mn was estimated to be slightly lower when bioaugmented for the tap water and NBs water treatments.

In case of scale-up to the bioreactor, lower Sb release was observed compared to experiments conducted in flasks. The addition of low concentration of OAs seems to enhance the Sb mobilization without decreasing the initial concentration of Sb-oxidizing

bacteria even though the Sb mobilization reported in flasks has not been achieved in bioreactor. In particular, the maximum percentage of Sb mobilized from soil to water phase was 27%, while a significant higher percentage was detected in flasks equals to 75%.

In conclusion, enrichment cultures isolated from Swiss shooting range soils had the ability to remove and oxidize Sb(III) to Sb(V) in soil A. The final concentration of Sb in the soil for the bioaugmented experiments was found to be less than 75% of the initial concentration, indicating that the isolated microbial community enhanced its mobilization and release to the aqueous phase. Nanobubbles were found to have an effect on Sb release from the soils in non-bioaugmented experiments in contrast to the bioaugmented experiments where no significant difference was observed.

Chapter 6.

Conclusions & Future Perspectives

This study has tried to cover most of the important research conducted in the field of nanobubble technology in order to get a better insight on the major advantages of utilizing these NBs-based processes compared to conventional aeration systems. The main conclusions derived from this research are the following:

- The OzNBs application enhanced the disinfection efficiency of ozone against bacteria used as primary indicators of contamination in fresh water quality as well as the residual activity. In case of ballast water disinfection, OzNBs utilization led to a more efficient ozonation as ozone efficacy (as TRO concentration) is higher at different salinities.
- Air nanobubble-integrated wetland achieved higher removal efficiency for phenol and toluene in both matrices; tap and waste- water. A elevated dissolved oxygen concentration (above 7 mg/L) was reported in every experimental cycle, indicating a sufficient aeration.
- In the case of phytoremediation, the application of ONBs resulted in a higher amount of Sb accumulated in the plants tissues. Nanobubbles intensified the stabilization of antimony in roots, even though the translocation to the upper part of the plants was rather low.
- When ONBs employed in bioremediation, the mobilization of Sb in the case of bioaugmentation was not substantial. When no microbial community was

inoculated, ONBs had a greater impact on Sb mobilization from soil water phase.

Although NBs technology is widely used in various applications, there are still gaps in our understanding of the behavior of NBs that need further investigation. Even though several researchers have expressed doubts about the existence and the stability of MNBs, many studies have proven that their application by different types of gas (air, oxygen, and ozone) can enhance process efficiency compared to conventional aeration since the results so far have been very encouraging. For instance, the nanobubbles technology can reduce the operation and maintenance cost of an ozonation system since it can overcome at least partially the serious weakness which is the limited residual disinfection capacity and the low solubility of ozone leading to the requirement of a high ozone dose.

The characterization of NBs with high resolution has been to some extent achieved; however, there is a chance the size measurement to be misleading as the gas cavities cannot be distinguished among nanodroplets and impurities derived from the equipment or present in the water. It is worth mentioning that most studies have investigated the use of NBs on ultrapure water and hence, typical drinking water or wastewater matrices may influence the NBs size and entangle the measurement of number concentration thanks to the existence of other colloids (51). There are several MNBs generators available commercially but without providing a detailed description concerning the size distribution and concentration of the generated bubbles (68). For that reason a standard measurement protocol should be established in order to ensure the correct characterization of MNBs.

A general limitation is that all studies have been performed in laboratory or small pilot scale (up to 50 L). It would be helpful to examine the upscaling of this process in the field and at industrial scale. Moreover, in this case it is important to mention that a cost/benefit analysis should also be conducted, since an aeration system is often portrayed by high energy requirements. Utilization of NBs is an ecological method that has a great potential to replace expensive processes currently used for wastewater treatment.

Bibliography

1. van Vliet MTH, Jones ER, Flörke M, Franssen WHP, Hanasaki N, Wada Y, et al. Global water scarcity including surface water quality and expansions of clean water technologies. *Environ Res Lett.* 2021;16(2).
2. Egbuikwem PN, Mierzwa JC, Saroj DP. Assessment of suspended growth biological process for treatment and reuse of mixed wastewater for irrigation of edible crops under hydroponic conditions. *Agric Water Manag* [Internet]. 2020;231(October 2019):106034. Available from: <https://doi.org/10.1016/j.agwat.2020.106034>
3. Dong H, Yuan X, Wang W, Qiang Z. Occurrence and removal of antibiotics in ecological and conventional wastewater treatment processes: A field study. *J Environ Manage* [Internet]. 2016 Aug 1 [cited 2018 Apr 14];178:11–9. Available from: <https://www.sciencedirect.com/science/article/pii/S0301479716302080?via%3DIhub>
4. Yan C, Nie M, Yang Y, Zhou J, Liu M, Baalousha M, et al. Effect of colloids on the occurrence, distribution and photolysis of emerging organic contaminants in wastewaters. *J Hazard Mater* [Internet]. 2015;299:241–8. Available from: <http://dx.doi.org/10.1016/j.jhazmat.2015.06.022>
5. Ahmed MB, Zhou JL, Ngo HH, Guo W, Thomaidis NS, Xu J. Progress in the biological and chemical treatment technologies for emerging contaminant removal from wastewater: A critical review. *J Hazard Mater* [Internet]. 2017;323:274–98. Available from: <http://dx.doi.org/10.1016/j.jhazmat.2016.04.045>
6. Rojviroon O, Rojviroon T. Photocatalytic process augmented with micro/nano bubble aeration for enhanced degradation of synthetic dyes in wastewater. *Water Resour Ind* [Internet]. 2022;27(October 2021):100169. Available from: <https://doi.org/10.1016/j.wri.2021.100169>
7. Agarwal A, Ng WJ, Liu Y. Principle and applications of microbubble and nanobubble technology for water treatment. *Chemosphere* [Internet]. 2011;84(9):1175–80. Available from: <http://dx.doi.org/10.1016/j.chemosphere.2011.05.054>
8. Uchida T, Oshita S, Ohmori M, Tsuno T, Soejima K, Shinozaki S, et al. Transmission electron microscopic observations of nanobubbles and their capture of impurities in wastewater. *Nanoscale Res Lett.* 2011;6(1):1–9.
9. Gurung A, Dahl O, Jansson K. The fundamental phenomena of nanobubbles and their behavior in wastewater treatment technologies. *Geosystem Eng* [Internet]. 2016;9328:1–10. Available from: <http://dx.doi.org/10.1080/12269328.2016.1153987>
10. Ushikubo FY, Furukawa T, Nakagawa R, Enari M, Makino Y, Kawagoe Y, et al. Evidence of the existence and the stability of nano-bubbles in water. *Colloids Surfaces A Physicochem Eng Asp* [Internet]. 2010;361(1–3):31–7. Available from:

<http://dx.doi.org/10.1016/j.colsurfa.2010.03.005>

11. Ebina K, Shi K, Hirao M, Hashimoto J, Kawato Y, Kaneshiro S, et al. Oxygen and Air Nanobubble Water Solution Promote the Growth of Plants, Fishes, and Mice. *PLoS One*. 2013;8(6):2–8.
12. Li H, Hu L, Xia Z. Impact of groundwater salinity on bioremediation enhanced by micro-nano bubbles. *Materials (Basel)*. 2013;6(9):3676–87.
13. Liu S, Kawagoe Y, Makino Y, Oshita S. Effects of nanobubbles on the physicochemical properties of water: The basis for peculiar properties of water containing nanobubbles. *Chem Eng Sci [Internet]*. 2013;93:250–6. Available from: <http://dx.doi.org/10.1016/j.ces.2013.02.004>
14. U.S. EPA. Wastewater Technology Fact Sheet Ozone Disinfection. Off Water Washington, DC. 1999;7.
15. Hoigné J. Chemistry of Aqueous Ozone and Transformation of Pollutants by Ozonation and Advanced Oxidation Processes. In: Hrubec J, editor. *Quality and Treatment of Drinking Water II*. Berlin, Heidelberg: Springer Berlin Heidelberg; 1998. p. 83–141.
16. Seridou P, Kalogerakis N. Disinfection applications of ozone micro- And nanobubbles. *Environ Sci Nano*. 2021;8(12):3493–510.
17. Anku WW, Mamo MA, Govender PP. Phenolic Compounds in Water: Sources, Reactivity, Toxicity and Treatment Methods. *Phenolic Compd - Nat Sources, Importance Appl*. 2017;
18. Ebrahimi A, Sivakumar M, McLauchlan C, Ansari A, Vishwanathan AS. A critical review of the symbiotic relationship between constructed wetland and microbial fuel cell for enhancing pollutant removal and energy generation. *J Environ Chem Eng [Internet]*. 2021;9(1):105011. Available from: <https://doi.org/10.1016/j.jece.2020.105011>
19. Thullner M, Stefanakis AI, Dehestani S. Constructed Wetlands Treating Water Contaminated with Organic Hydrocarbons. *Constr Wetl Ind Wastewater Treat*. 2018;43–63.
20. Zango ZU, Sambudi NS, Jumbri K, Ramli A, Bakar NHHA, Saad B, et al. An overview and evaluation of highly porous adsorbent materials for polycyclic aromatic hydrocarbons and phenols removal from wastewater. *Water (Switzerland)*. 2020;12(10):1–40.
21. Leung JYS, Cai Q, Tam NFY. Comparing subsurface flow constructed wetlands with mangrove plants and freshwater wetland plants for removing nutrients and toxic pollutants. *Ecol Eng [Internet]*. 2016;95:129–37. Available from: <http://dx.doi.org/10.1016/j.ecoleng.2016.06.016>
22. Varma M, Gupta AK, Ghosal PS, Majumder A. A review on performance of constructed wetlands in tropical and cold climate: Insights of mechanism, role of influencing factors, and system modification in low temperature. *Sci Total Environ [Internet]*. 2021;755:142540. Available from: <https://doi.org/10.1016/j.scitotenv.2020.142540>
23. Liu H, Hu Z, Zhang J, Ngo HH, Guo W, Liang S, et al. Optimizations on supply and distribution of dissolved oxygen in constructed wetlands: A review. *Bioresour Technol [Internet]*. 2016;214:797–805. Available from:

- <http://dx.doi.org/10.1016/j.biortech.2016.05.003>
24. Nivala J, Murphy C, Freeman A. Recent advances in the application, design, and operations & maintenance of aerated treatment wetlands. *Water (Switzerland)*. 2020;12(4).
 25. Kanwar VS, Sharma A, Srivastav AL, Rani L. Phytoremediation of toxic metals present in soil and water environment: a critical review. *Environ Sci Pollut Res*. 2020;27(36):44835–60.
 26. He M, Wang N, Long X, Zhang C, Ma C, Zhong Q, et al. Antimony speciation in the environment: Recent advances in understanding the biogeochemical processes and ecological effects. *J Environ Sci [Internet]*. 2019;75:14–39. Available from: <https://doi.org/10.1016/j.jes.2018.05.023>
 27. Lai Z, He M, Lin C, Ouyang W, Liu X. Interactions of antimony with biomolecules and its effects on human health. *Ecotoxicol Environ Saf [Internet]*. 2022;233:113317. Available from: <https://doi.org/10.1016/j.ecoenv.2022.113317>
 28. Winship KA. Toxicity of antimony and its compounds. *Adverse Drug React Acute Poisoning Rev [Internet]*. 1987;6(2):67–90. Available from: <http://europepmc.org/abstract/MED/3307336>
 29. He M, Wang X, Wu F, Fu Z. Antimony pollution in China. *Sci Total Environ [Internet]*. 2012;421–422(19):41–50. Available from: <http://dx.doi.org/10.1016/j.scitotenv.2011.06.009>
 30. Kang CH, Kwon YJ, So JS. Bioremediation of heavy metals by using bacterial mixtures. *Ecol Eng [Internet]*. 2016;89:64–9. Available from: <http://dx.doi.org/10.1016/j.ecoleng.2016.01.023>
 31. Park B, Yoon S, Choi Y, Jang J, Park S, Choi J. Stability of engineered micro or nanobubbles for biomedical applications. *Pharmaceutics*. 2020;12(11):1–12.
 32. Patel AK, Singhania RR, Chen C-W, Tseng Y-S, Kuo C-H, Wu C-H, et al. Advances in micro- and nano bubbles technology for application in biochemical processes. *Environ Technol Innov [Internet]*. 2021;23:101729. Available from: <https://doi.org/10.1016/j.eti.2021.101729>
 33. Li H, Hu L, Song D, Lin F. Characteristics of Micro-Nano Bubbles and Potential Application in Groundwater Bioremediation. *Water Environ Res*. 2015;86(9):844–51.
 34. Azevedo A, Etchepare R, Rubio J. Raw water clarification by flotation with microbubbles and nanobubbles generated with a multiphase pump. *Water Sci Technol*. 2017;75(10):2342–9.
 35. Temesgen T, Bui TT, Han M, Kim T il, Park H. Micro and nanobubble technologies as a new horizon for water-treatment techniques: A review. *Adv Colloid Interface Sci [Internet]*. 2017;246(June):40–51. Available from: <http://dx.doi.org/10.1016/j.cis.2017.06.011>
 36. Takahashi M, Kawamura T, Yamamoto Y, Ohnari H, Himuro S, Shakutsui H. Effect of shrinking microbubble on gas hydrate formation. *J Phys Chem B*. 2003;107(10):2171–3.

37. Li P, Tsuge H. Ozone transfer in a new gas-induced contactor with microbubbles. *J Chem Eng Japan*. 2006;39(11):1213–20.
38. Tekile A, Kim I, Lee J-Y. Applications of Ozone Micro- and Nanobubble Technologies in Water and Wastewater Treatment: Review. *J Korean Soc Water Wastewater*. 2017;31(6):481–90.
39. Khuntia S, Majumder SK, Ghosh P. Removal of ammonia from water by ozone microbubbles. *Ind Eng Chem Res*. 2013;52(1):318–26.
40. Cheng W, Jiang L, Quan X, Cheng C, Huang X, Cheng Z, et al. Ozonation process intensification of p-nitrophenol by in situ separation of hydroxyl radical scavengers and microbubbles. *Water Sci Technol*. 2019;80(1):25–36.
41. Agarwal A, Xu H, Ng WJ, Liu Y. Biofilm detachment by self-collapsing air microbubbles: A potential chemical-free cleaning technology for membrane biofouling. *J Mater Chem*. 2012;22(5):2203–7.
42. Zhang J, Huang GQ, Liu C, Zhang RN, Chen XX, Zhang L. Synergistic effect of microbubbles and activated carbon on the ozonation treatment of synthetic dyeing wastewater. *Sep Purif Technol [Internet]*. 2018;201(February):10–8. Available from: <https://doi.org/10.1016/j.seppur.2018.02.003>
43. Gao Y, Duan Y, Fan W, Guo T, Huo M, Yang W, et al. Intensifying ozonation treatment of municipal secondary effluent using a combination of microbubbles and ultraviolet irradiation. *Environ Sci Pollut Res*. 2019;26(21):21915–24.
44. Chu LB, Yan ST, Xing XH, Yu AF, Sun XL, Jurcik B. Enhanced sludge solubilization by microbubble ozonation. *Chemosphere*. 2008;72(2):205–12.
45. Ohgaki K, Khanh NQ, Joden Y, Tsuji A, Nakagawa T. Physicochemical approach to nanobubble solutions. *Chem Eng Sci*. 2010;65(3):1296–300.
46. Meegoda JN, Hewage SA, Batagoda JH. Stability of Nanobubbles. *Environ Eng Sci [Internet]*. 2018;35(11):1216–27. Available from: <http://doi.org/10.1089/ees.2018.0203>
47. Hewage SA, Kewalramani J, Meegoda JN. Stability of nanobubbles in different salts solutions. *Colloids Surfaces A Physicochem Eng Asp [Internet]*. 2021;609(October 2020):125669. Available from: <https://doi.org/10.1016/j.colsurfa.2020.125669>
48. Michailidi ED, Bomis G, Varoutoglou A, Kyzas GZ, Mitrikas G, Mitropoulos AC, et al. Bulk nanobubbles: Production and investigation of their formation/stability mechanism. *J Colloid Interface Sci [Internet]*. 2020;564:371–80. Available from: <https://doi.org/10.1016/j.jcis.2019.12.093>
49. Zhou L, Wang S, Zhang L, Hu J. Generation and stability of bulk nanobubbles: A review and perspective. *Curr Opin Colloid Interface Sci [Internet]*. 2021;53:101439. Available from: <https://doi.org/10.1016/j.cocis.2021.101439>
50. Wu J, Zhang K, Cen C, Wu X, Mao R, Zheng Y. Role of bulk nanobubbles in removing organic pollutants in wastewater treatment. *AMB Express [Internet]*. 2021;11(1). Available from: <https://doi.org/10.1186/s13568-021-01254-0>

51. Atkinson AJ, Apul OG, Schneider O, Garcia-Segura S, Westerhoff P. Nanobubble Technologies Offer Opportunities to Improve Water Treatment. *Acc Chem Res.* 2019;(Table 1).
52. Movahed SMA, Sarmah AK. Global trends and characteristics of nano- and micro-bubbles research in environmental engineering over the past two decades: A scientometric analysis. *Sci Total Environ* [Internet]. 2021;785:147362. Available from: <https://doi.org/10.1016/j.scitotenv.2021.147362>
53. Nirmalkar N, Pacek AW, Barigou M. On the Existence and Stability of Bulk Nanobubbles. *Langmuir* [Internet]. 2018;34:acs.langmuir.8b01163. Available from: <http://pubs.acs.org/doi/10.1021/acs.langmuir.8b01163>
54. Yasui K, Tuziuti T, Kanematsu W. Mysteries of bulk nanobubbles (ultrafine bubbles); stability and radical formation. *Ultrason Sonochem* [Internet]. 2018;48(May):259–66. Available from: <https://doi.org/10.1016/j.ultsonch.2018.05.038>
55. Leroy V, Norisuye T. Investigating the Existence of Bulk Nanobubbles with Ultrasound. *ChemPhysChem.* 2016;2787–90.
56. Sedláč M, Rak D. Large-scale inhomogeneities in solutions of low molar mass compounds and mixtures of liquids: Supramolecular structures or nanobubbles? *J Phys Chem B.* 2013;117(8):2495–504.
57. Jadhav AJ, Barigou M. Proving and interpreting the spontaneous formation of bulk nanobubbles in aqueous organic solvent solutions: Effects of solvent type and content. *Soft Matter.* 2020;16(18):4502–11.
58. Alheshibri M, Al Baroot A, Shui L, Zhang M. Nanobubbles and nanoparticles. *Curr Opin Colloid Interface Sci* [Internet]. 2021;55:101470. Available from: <https://doi.org/10.1016/j.cocis.2021.101470>
59. Liu H, Cao G. Effectiveness of the Young-Laplace equation at nanoscale. *Sci Rep* [Internet]. 2016;6(April). Available from: <http://dx.doi.org/10.1038/srep23936>
60. Ljunggren S, Eriksson JC. The lifetime of a colloid-sized gas bubble in water and the cause of the hydrophobic attraction. *Colloids Surfaces A Physicochem Eng Asp.* 1997;129–130:151–5.
61. Thi Phan KK, Truong T, Wang Y, Bhandari B. Nanobubbles: Fundamental characteristics and applications in food processing. *Trends Food Sci Technol* [Internet]. 2020;95(July 2019):118–30. Available from: <https://doi.org/10.1016/j.tifs.2019.11.019>
62. Padilla-Martinez JP, Berrospe-Rodriguez C, Aguilar G, Ramirez-San-Juan JC, Ramos-Garcia R. Optic cavitation with CW lasers: A review. *Phys Fluids* [Internet]. 2014;26(12). Available from: <http://dx.doi.org/10.1063/1.4904718>
63. Etchepare R, Oliveira H, Nicknig M, Azevedo A, Rubio J. Nanobubbles: Generation using a multiphase pump, properties and features in flotation. *Miner Eng* [Internet]. 2017;112(May):19–26. Available from: <http://dx.doi.org/10.1016/j.mineng.2017.06.020>
64. Kikuchi K, Ioka A, Oku T, Tanaka Y, Saihara Y, Ogumi Z. Concentration determination of oxygen nanobubbles in electrolyzed water. *J Colloid Interface Sci* [Internet].

- 2009;329(2):306–9. Available from: <http://dx.doi.org/10.1016/j.jcis.2008.10.009>
65. Ahmed AKA, Sun C, Hua L, Zhang Z, Zhang Y, Zhang W, et al. Generation of nanobubbles by ceramic membrane filters: The dependence of bubble size and zeta potential on surface coating, pore size and injected gas pressure. *Chemosphere* [Internet]. 2018;203:327–35. Available from: <https://doi.org/10.1016/j.chemosphere.2018.03.157>
66. Bu X, Alheshibri M. The effect of ultrasound on bulk and surface nanobubbles: A review of the current status. *Ultrason Sonochem* [Internet]. 2021;76:105629. Available from: <https://doi.org/10.1016/j.ultsonch.2021.105629>
67. Favvas EP, Kyzas GZ, Efthimiadou EK, Mitropoulos AC. Bulk nanobubbles, generation methods and potential applications. *Curr Opin Colloid Interface Sci* [Internet]. 2021;54:101455. Available from: <https://doi.org/10.1016/j.cocis.2021.101455>
68. Azevedo A, Oliveira H, Rubio J. Bulk nanobubbles in the mineral and environmental areas: Updating research and applications. *Adv Colloid Interface Sci* [Internet]. 2019;271:101992. Available from: <https://doi.org/10.1016/j.cis.2019.101992>
69. Jadhav AJ, Barigou M. Bulk Nanobubbles or Not Nanobubbles: That is the Question. *Langmuir*. 2020;36(7):1699–708.
70. Ulatowski K, Sobieszuk P. Gas nanobubble dispersions as the important agent in environmental processes – generation methods review. *Water Environ J*. 2020;34(S1):772–90.
71. Wang Q, Zhao H, Qi N, Qin Y, Zhang X, Li Y. Generation and Stability of Size-Adjustable Bulk Nanobubbles Based on Periodic Pressure Change. 2019;(December 2018):1–9.
72. Wu C, Nasset K, Masliyah J, Xu Z. Generation and characterization of submicron size bubbles. *Adv Colloid Interface Sci* [Internet]. 2012;179–182:123–32. Available from: <http://dx.doi.org/10.1016/j.cis.2012.06.012>
73. Kim S, Kim H, Han M, Kim T. Generation of sub-micron (Nano) bubbles and characterization of their fundamental properties. *Environ Eng Res*. 2019;24(3):382–8.
74. Oh SH, Kim JM. Generation and Stability of Bulk Nanobubbles. *Langmuir*. 2017;33(15):3818–23.
75. Gross J, Sayle S, Karow AR, Bakowsky U, Garidel P. Nanoparticle tracking analysis of particle size and concentration detection in suspensions of polymer and protein samples: Influence of experimental and data evaluation parameters. *Eur J Pharm Biopharm* [Internet]. 2016;104:30–41. Available from: <http://dx.doi.org/10.1016/j.ejpb.2016.04.013>
76. Xu R. Light scattering: A review of particle characterization applications. *Particuology* [Internet]. 2015;18:11–21. Available from: <http://dx.doi.org/10.1016/j.partic.2014.05.002>
77. Xiong R, Xu RX, Huang C, De Smedt S, Braeckmans K. Stimuli-responsive nanobubbles for biomedical applications. *Chem Soc Rev*. 2021;50(9):5746–76.
78. Gnyawali V, Wang J-Z, Wang Y, Fishbein G, So LHY, De Leon AC, et al. Individual

- nanobubbles detection using acoustic based flow cytometry. 2019;(February):84.
79. Ahmed AKA, Sun C, Hua L, Zhang Z, Zhang Y, Marhaba T, et al. Colloidal Properties of Air, Oxygen, and Nitrogen Nanobubbles in Water: Effects of Ionic Strength, Natural Organic Matters, and Surfactants. *Environ Eng Sci*. 2018;35(7):720–7.
 80. Takahashi M. ζ Potential of Microbubbles in Aqueous Solutions: Electrical Properties of the Gas–Water Interface. *J Phys Chem B [Internet]*. 2005;109(46):21858–64. Available from: <http://pubs.acs.org/doi/abs/10.1021/jp0445270>
 81. Li M, Ma X, Eisener J, Pfeiffer P, Ohl CD, Sun C. How bulk nanobubbles are stable over a wide range of temperatures. *J Colloid Interface Sci [Internet]*. 2021;596:184–98. Available from: <https://doi.org/10.1016/j.jcis.2021.03.064>
 82. Calgaroto S, Wilberg KQ, Rubio J. On the nanobubbles interfacial properties and future applications in flotation. *Miner Eng [Internet]*. 2014;60:33–40. Available from: <http://dx.doi.org/10.1016/j.mineng.2014.02.002>
 83. Alheshibri M, Craig VSJ. Generation of nanoparticles upon mixing ethanol and water; Nanobubbles or Not? *J Colloid Interface Sci [Internet]*. 2019;542:136–43. Available from: <https://doi.org/10.1016/j.jcis.2019.01.134>
 84. Batchelor DVB, Armistead FJ, Ingram N, Peyman SA, Mclaughlan JR, Coletta PL, et al. Nanobubbles for therapeutic delivery: Production, stability and current prospects. *Curr Opin Colloid Interface Sci [Internet]*. 2021;54:101456. Available from: <https://doi.org/10.1016/j.cocis.2021.101456>
 85. Kobayashi H, Maeda S, Kashiwa M, Fujita T. Measurements of ultrafine bubbles using different types of particle size measuring instruments. *Int Conf Opt Part Charact (OPC 2014)*. 2014;9232(Opc):92320U.
 86. Helmecke M, Fries E, Schulte C. Regulating water reuse for agricultural irrigation: risks related to organic micro-contaminants. *Environ Sci Eur [Internet]*. 2020;32(1). Available from: <https://doi.org/10.1186/s12302-019-0283-0>
 87. Reinhaller FF, Posch J, Feierl G, Wüst G, Haas D, Ruckebauer G, et al. Antibiotic resistance of *E. Coli* in sewage and sludge. *Water Res*. 2003;37(8):1685–90.
 88. Huang JJ, Hu HY, Tang F, Li Y, Lu SQ, Lu Y. Inactivation and reactivation of antibiotic-resistant bacteria by chlorination in secondary effluents of a municipal wastewater treatment plant. *Water Res*. 2011;45(9):2775–81.
 89. Zieliński W, Korzeniewska E, Harnisz M, Hubeny J, Buta M, Rolbiecki D. The prevalence of drug-resistant and virulent *Staphylococcus* spp. in a municipal wastewater treatment plant and their spread in the environment. *Environ Int [Internet]*. 2020;143:105914. Available from: <https://www.sciencedirect.com/science/article/pii/S0160412020318699>
 90. Monteiro S, Santos R. Incidence of enterococci resistant to clinically relevant antibiotics in environmental waters and in reclaimed waters used for irrigation. *J Water Health*. 2020;18(6):911–24.
 91. Rosenberg Goldstein RE, Micallef SA, Gibbs SG, Davis JA, He X, George A, Kleinfelter LM, Schreiber NA, Mukherjee S, Sapkota A, Joseph SW SA, Sapkota A, Joseph SW. Methicillin-

- Resistant *Staphylococcus aureus* (MRSA) Detected at Four U.S. Wastewater Treatment Plants. *Env Heal Perspect*. 2012;120(11):1551–8.
92. McKinney CW, Pruden A. Ultraviolet disinfection of antibiotic resistant bacteria and their antibiotic resistance genes in water and wastewater. *Environ Sci Technol*. 2012;46(24):13393–400.
93. Venieri D, Tournas F, Gounaki I, Binas V, Zachopoulos A, Kiriakidis G, et al. Inactivation of *Staphylococcus aureus* in water by means of solar photocatalysis using metal doped TiO₂ semiconductors. *J Chem Technol Biotechnol*. 2017;92(1):43–51.
94. Ding W, Jin W, Cao S, Zhou X, Wang C, Jiang Q, et al. Ozone disinfection of chlorine-resistant bacteria in drinking water. *Water Res [Internet]*. 2019;160:339–49. Available from: <https://doi.org/10.1016/j.watres.2019.05.014>
95. Sharma VK, Johnson N, Cizmas L, McDonald TJ, Kim H. A review of the influence of treatment strategies on antibiotic resistant bacteria and antibiotic resistance genes. *Chemosphere [Internet]*. 2016;150:702–14. Available from: <http://dx.doi.org/10.1016/j.chemosphere.2015.12.084>
96. Silva BF da, Jelic A, López-Serna R, Mozeto AA, Petrovic M, Barceló D. Occurrence and distribution of pharmaceuticals in surface water, suspended solids and sediments of the Ebro river basin, Spain. *Chemosphere [Internet]*. 2011;85(8):1331–9. Available from: <http://dx.doi.org/10.1016/j.chemosphere.2011.07.051>
97. Campbell CG, Borglin SE, Green FB, Grayson A, Wozel E, Stringfellow WT. Biologically directed environmental monitoring, fate, and transport of estrogenic endocrine disrupting compounds in water: A review. *Chemosphere*. 2006;65(8):1265–80.
98. Hopkins ZR, Blaney L. An aggregate analysis of personal care products in the environment: Identifying the distribution of environmentally-relevant concentrations. *Environ Int [Internet]*. 2016;92–93:301–16. Available from: <http://dx.doi.org/10.1016/j.envint.2016.04.026>
99. Benotti MJ, Brownawell BJ. Microbial degradation of pharmaceuticals in estuarine and coastal seawater. *Environ Pollut [Internet]*. 2009;157(3):994–1002. Available from: <http://dx.doi.org/10.1016/j.envpol.2008.10.009>
100. Sharma BM, Bečanová J, Scheringer M, Sharma A, Bharat GK, Whitehead PG, et al. Health and ecological risk assessment of emerging contaminants (pharmaceuticals, personal care products, and artificial sweeteners) in surface and groundwater (drinking water) in the Ganges River Basin, India. *Sci Total Environ*. 2019;646:1459–67.
101. Fernández-Rubio J, Rodríguez-Gil JL, Postigo C, Mastroianni N, López de Alda M, Barceló D, et al. Psychoactive pharmaceuticals and illicit drugs in coastal waters of North-Western Spain: Environmental exposure and risk assessment. *Chemosphere*. 2019;224:379–89.
102. Kuster M, López de Alda MJ, Hernando MD, Petrovic M, Martín-Alonso J, Barceló D. Analysis and occurrence of pharmaceuticals, estrogens, progestogens and polar pesticides in sewage treatment plant effluents, river water and drinking water in the Llobregat river basin (Barcelona, Spain). *J Hydrol*. 2008;358(1–2):112–23.

103. Bartelt-Hunt SL, Snow DD, Damon T, Shockley J, Hoagland K. The occurrence of illicit and therapeutic pharmaceuticals in wastewater effluent and surface waters in Nebraska. *Environ Pollut* [Internet]. 2009;157(3):786–91. Available from: <http://dx.doi.org/10.1016/j.envpol.2008.11.025>
104. Rivera-Utrilla J, Sánchez-Polo M, Ferro-García MÁ, Prados-Joya G, Ocampo-Pérez R. Pharmaceuticals as emerging contaminants and their removal from water. A review. *Chemosphere* [Internet]. 2013;93(7):1268–87. Available from: <http://dx.doi.org/10.1016/j.chemosphere.2013.07.059>
105. Matzek LW, Carter KE. Activated persulfate for organic chemical degradation: A review. *Chemosphere* [Internet]. 2016;151:178–88. Available from: <http://dx.doi.org/10.1016/j.chemosphere.2016.02.055>
106. Rodriguez-Narvaez OM, Peralta-Hernandez JM, Goonetilleke A, Bandala ER. Treatment technologies for emerging contaminants in water: A review. *Chem Eng J* [Internet]. 2017;323:361–80. Available from: <http://dx.doi.org/10.1016/j.cej.2017.04.106>
107. Crittenden JC, Trussel RR, Hand DW, Howe KJ, Tchobanoglous G. 13 Historical Perspective Methods of Disinfection Commonly Used in Water Treatment Disinfection Kinetics. *MWH's Water Treat Princ Des*. 2012;
108. WHO. Bromate in Water. 2005;
109. von Sonntag C, von Gunten U. Chemistry of Ozone in Water and Wastewater Treatment: From Basic Principles to Applications. *Chemistry of Ozone in Water and Wastewater Treatment: From Basic Principles to Applications*. 2015.
110. Rice RG, Robson CM, Miller GW, Hill AG. Uses of ozone in drinking water treatment. *J / Am Water Work Assoc*. 1981;73(1):44–57.
111. Gottschalk C, Libra JA, Saupe A. Ozonation of Water and Waste Water: A Practical Guide to Understanding Ozone and its Applications: Second Edition. *Ozonation of Water and Waste Water: A Practical Guide to Understanding Ozone and its Applications: Second Edition*. 2010.
112. Gardoni D, Vailati A, Canziani R. Decay of Ozone in Water: A Review. *Ozone Sci Eng*. 2012;34(4):233–42.
113. Tomiyasu H, Fukutomi H, Gordon G. Kinetics and Mechanism of Ozone Decomposition in Basic Aqueous Solution. *Inorg Chem*. 1985;24(19):2962–6.
114. Sehested K, Corftzen H, Holcman J, Fischer CH, Hart EJ. The Primary Reaction in the Decomposition of Ozone in Acidic Aqueous Solutions. *Environ Sci Technol*. 1991;25(9):1589–96.
115. Khuntia S, Majumder SK, Ghosh P. Quantitative prediction of generation of hydroxyl radicals from ozone microbubbles. *Chem Eng Res Des* [Internet]. 2015;98:231–9. Available from: <http://dx.doi.org/10.1016/j.cherd.2015.04.003>
116. Megahed A, Aldridge B, Lowe J. The microbial killing capacity of aqueous and gaseous ozone on different surfaces contaminated with dairy cattle manure. *PLoS One*. 2018;13(5):1–22.

117. Gray NF. Ozone Disinfection [Internet]. Second Edi. Microbiology of Waterborne Diseases: Microbiological Aspects and Risks: Second Edition. Elsevier; 2013. 599–615 p. Available from: <http://dx.doi.org/10.1016/B978-0-12-415846-7.00033-0>
118. Batagoda JH, Hewage SDA, Meegoda JN. Nano-ozone bubbles for drinking water treatment. J Environ Eng Sci [Internet]. 2018 Nov 21;14(2):57–66. Available from: <https://doi.org/10.1680/jenes.18.00015>
119. Aluthgun Hewage S, Batagoda JH, Meegoda JN. In situ remediation of sediments contaminated with organic pollutants using ultrasound and ozone nanobubbles. Environ Eng Sci. 2020;37(8):521–34.
120. Liu S, Wang Q, Sun T, Wu C, Shi Y. The effect of different types of micro-bubbles on the performance of the coagulation flotation process for coke waste-water. J Chem Technol Biotechnol. 2012;87(2):206–15.
121. Zheng T, Wang Q, Zhang T, Shi Z, Tian Y, Shi S, et al. Microbubble enhanced ozonation process for advanced treatment of wastewater produced in acrylic fiber manufacturing industry. J Hazard Mater [Internet]. 2015;287:412–20. Available from: <http://dx.doi.org/10.1016/j.jhazmat.2015.01.069>
122. Suslow T V. Oxidation-Reduction Potential (ORP) for Water Disinfection Monitoring, Control, and Documentation. Oxidation-Reduction Potential Water Disinfect Monit Control Doc. 2004;
123. Hu L, Xia Z. Application of ozone micro-nano-bubbles to groundwater remediation. J Hazard Mater [Internet]. 2018;342:446–53. Available from: <http://dx.doi.org/10.1016/j.jhazmat.2017.08.030>
124. Takahashi M, Chiba K, Li P. Formation of hydroxyl radicals by collapsing ozone microbubbles under strongly acidic conditions. J Phys Chem B. 2007;111(39):11443–6.
125. Chu LB, Xing XH, Yu AF, Zhou YN, Sun XL, Jurcik B. Enhanced ozonation of simulated dyestuff wastewater by microbubbles. Chemosphere. 2007;68(10):1854–60.
126. Jabesa A, Ghosh P. Removal of diethyl phthalate from water by ozone microbubbles in a pilot plant. J Environ Manage [Internet]. 2016;180:476–84. Available from: <http://dx.doi.org/10.1016/j.jenvman.2016.05.072>
127. Kobayashi F, Ikeura H, Ohsato S, Goto T, Tamaki M. Disinfection using ozone microbubbles to inactivate *Fusarium oxysporum* f. sp. *melonis* and *Pectobacterium carotovorum* subsp. *carotovorum*. Crop Prot [Internet]. 2011;30(11):1514–8. Available from: <http://dx.doi.org/10.1016/j.cropro.2011.07.018>
128. Takahashi M, Horibe H, Matsuura K, Tatera K. Effect of microbubbles on ozonized water for photoresist removal. J Photopolym Sci Technol. 2015;28(2):293–8.
129. He H, Zheng L, Li Y, Song W. Research on the Feasibility of Spraying Micro/Nano Bubble Ozonated Water for Airborne Disease Prevention. Ozone Sci Eng [Internet]. 2015;37(1):78–84. Available from: <http://dx.doi.org/10.1080/01919512.2014.913473>
130. Lee YG, Park Y, Lee G, Kim Y, Chon K. Enhanced degradation of pharmaceutical compounds by a microbubble ozonation process: Effects of temperature, pH, and humic

- acids. *Energies*. 2019;12(22).
131. Fan W, An W gang, Huo M xin, Yang W, Zhu S yi, Lin S shan. Solubilization and stabilization for prolonged reactivity of ozone using micro-nano bubbles and ozone-saturated solvent: A promising enhancement for ozonation. *Sep Purif Technol* [Internet]. 2020;238(November 2019):116484. Available from: <https://doi.org/10.1016/j.seppur.2019.116484>
 132. Zheng T, Wang Q, Zhang T, Shi Z, Tian Y, Shi S, et al. Microbubble enhanced ozonation process for advanced treatment of wastewater produced in acrylic fiber manufacturing industry. *J Hazard Mater* [Internet]. 2015;287:412–20. Available from: <http://dx.doi.org/10.1016/j.jhazmat.2015.01.069>
 133. Liu S, Wang Q, Zhai X, Huang Q, Huang P. Improved Pretreatment (Coagulation-Floatation and Ozonation) of Younger Landfill Leachate by Microbubbles. *Water Environ Res*. 2010;82(7):657–65.
 134. Wang C, Lin CY, Liao GY. Degradation of antibiotic tetracycline by ultrafine-bubble ozonation process. *J Water Process Eng* [Internet]. 2020;37(December 2019):101463. Available from: <https://doi.org/10.1016/j.jwpe.2020.101463>
 135. Kim I, Lee J. Comparison of ozonation removal for PPCPs in secondary treated sewage by microbubble generator and ejector. *Environ Eng Res*. 2021;27(2):200163–0.
 136. Sumikura M, Hidaka M, Murakami H, Nobutomo Y, Murakami T. Ozone micro-bubble disinfection method for wastewater reuse system. *Water Sci Technol*. 2007;56(5):53–61.
 137. Kim TK, Kim T, Lee I, Choi K, Zoh KD. Removal of tetramethylammonium hydroxide (TMAH) in semiconductor wastewater using the nano-ozone H₂O₂ process. *J Hazard Mater*. 2021;409(March 2020).
 138. Kwack Y, Kim KK, Hwang H, Chun C. An ozone micro-bubble technique for seed sterilization in alfalfa sprouts. *Korean J Hortic Sci Technol*. 2014;32(6):901–5.
 139. Fan W, An W, Huo M, Xiao D, Lyu T, Cui J. An integrated approach using ozone nanobubble and cyclodextrin inclusion complexation to enhance the removal of micropollutants. *Water Res* [Internet]. 2021;196:117039. Available from: <https://doi.org/10.1016/j.watres.2021.117039>
 140. Bataklijev T, Georgiev V, Anachkov M, Rakovsky S, Zaikov GE. Ozone decomposition. *Interdiscip Toxicol*. 2014;7(2):47–59.
 141. Cullen PJ, Tiwari BK, O'Donnell CP, Muthukumarappan K. Modelling approaches to ozone processing of liquid foods. *Trends Food Sci Technol* [Internet]. 2009;20(3–4):125–36. Available from: <http://dx.doi.org/10.1016/j.tifs.2009.01.049>
 142. Fan W, An W gang, Huo M xin, Yang W, Zhu S yi, Lin S shan. Solubilization and stabilization for prolonged reactivity of ozone using micro-nano bubbles and ozone-saturated solvent: A promising enhancement for ozonation. *Sep Purif Technol* [Internet]. 2020;238(December 2019):116484. Available from: <https://doi.org/10.1016/j.seppur.2019.116484>
 143. Furuichi A, Arakawa S, Mano Y, Morita I, Tachikawa N, Yamada Y, et al. Comparative

- Analysis of Efficacy of Ozone Nano Bubble Water (NBW3) with Established Antimicrobials. Bactericidal Efficacy and Cellular Response. An in Vitro Study. *J Oral Tissue Eng.* 2013;10(3):131–41.
144. Hayakumo S, Arakawa S, Takahashi M, Kondo K, Mano Y, Izumi Y. Effects of ozone nano-bubble water on periodontopathic bacteria and oral cells - In vitro studies. *Sci Technol Adv Mater.* 2014;15(5).
 145. Seki M, Ishikawa T, Terada H, Nashimoto M. Microbicidal effects of stored aqueous ozone solution generated by nano-bubble technology. *In Vivo (Brooklyn).* 2017;31(4):579–83.
 146. Noguera-Oviedo K, Aga DS. Lessons learned from more than two decades of research on emerging contaminants in the environment. *J Hazard Mater [Internet].* 2016;316:242–51. Available from: <http://dx.doi.org/10.1016/j.jhazmat.2016.04.058>
 147. Huber MM, Göbel A, Joss A, Hermann N, Löffler D, McArdell CS, et al. Oxidation of pharmaceuticals during ozonation of municipal wastewater effluents: A pilot study. *Environ Sci Technol.* 2005;39(11):4290–9.
 148. Ternes TA, Stüber J, Herrmann N, McDowell D, Ried A, Kampmann M, et al. Ozonation: A tool for removal of pharmaceuticals, contrast media and musk fragrances from wastewater? *Water Res.* 2003;37(8):1976–82.
 149. Cruz R, Valverde Flores J. Reduction of Coliforms presents in domestic residual waters by Air-Ozone Micro-Nanobubbles In Carhuaz city, Peru. *J Nanotechnol.* 2017;1(1):9.
 150. Azuma T, Otomo K, Kunitou M, Shimizu M, Hosomaru K, Mikata S, et al. Removal of pharmaceuticals in water by introduction of ozonated microbubbles. *Sep Purif Technol [Internet].* 2019;212(September 2018):483–9. Available from: <https://doi.org/10.1016/j.seppur.2018.11.059>
 151. Tarafdar A, Sirohi R, Athiyaman P, Reshmy R, Madhavan A, Sindhu R, et al. The hazardous threat of Bisphenol A : Toxicity , detection and remediation. *J Hazard Mater [Internet].* 2022;423(PA):127097. Available from: <https://doi.org/10.1016/j.jhazmat.2021.127097>
 152. Jabesa A, Ghosh P. Oxidation of bisphenol-A by ozone microbubbles : Effects of operational parameters and kinetics study *Environmental Technology & Innovation* Oxidation of bisphenol-A by ozone microbubbles : Effects of operational parameters and kinetics study. *Environ Technol Innov [Internet].* 2022;26(January):102271. Available from: <https://doi.org/10.1016/j.eti.2022.102271>
 153. FAO. FAO yearbook of fishery and aquaculture statistics. *Fish Aquac Dep [Internet].* 2017;0:26–8. Available from: <ftp://ftp.fao.org/FI/STAT/summary/a-0a.pdf>
 154. Kumar S, Lekshmi M, Parvathi A, Nayak BB, Varela MF. Antibiotic resistance in seafood-borne pathogens. *Foodborne Pathog Antibiot Resist.* 2017;(January 2018):397–415.
 155. Jhunkeaw C, Khongcharoen N, Rungrueng N, Sangpo P, Panphut W, Thapinta A, et al. Ozone nanobubble treatment in freshwater effectively reduced pathogenic fish bacteria and is safe for Nile tilapia (*Oreochromis niloticus*). *Aquaculture [Internet].* 2021;534(December):736286. Available from: <https://doi.org/10.1016/j.aquaculture.2020.736286>

156. Nghia NH, Van PT, Giang PT, Hanh NT, St-Hilaire S, Domingos JA. Control of *Vibrio parahaemolyticus* (AHPND strain) and improvement of water quality using nanobubble technology. *Aquac Res.* 2021;(December 2020):1–13.
157. Imaizumi K, Tinwongger S, Kondo H, Hirono I. Disinfection of an EMS/AHPND strain of *Vibrio parahaemolyticus* using ozone nanobubbles. *J Fish Dis.* 2018;41(4):725–7.
158. Thanh Dien L, Linh NV, Sangpo P, Senapin S, St-Hilaire S, Rodkhum C, et al. Ozone nanobubble treatments improve survivability of Nile tilapia (*Oreochromis niloticus*) challenged with a pathogenic multi-drug-resistant *Aeromonas hydrophila*. *J Fish Dis.* 2021;(May):1–13.
159. Kurita Y, Chiba I, Kijima A. Physical eradication of small planktonic crustaceans from aquaculture tanks with cavitation treatment. *Aquac Int.* 2017;25(6):2127–33.
160. Summerfelt ST, Hochheimer JN. Review of Ozone Processes and Applications as an Oxidizing Agent in Aquaculture. *Progress Fish-Culturist* [Internet]. 1997 Apr 1;59(2):94–105. Available from: [https://doi.org/10.1577/1548-8640\(1997\)059%3C0094:ROOPAA%3E2.3.CO](https://doi.org/10.1577/1548-8640(1997)059%3C0094:ROOPAA%3E2.3.CO)
161. Gonçalves AA, Gagnon GA. Ozone application in recirculating aquaculture system: An overview. *Ozone Sci Eng.* 2011;33(5):345–67.
162. Linh NV, Dien LT, Panphut W, Thapinta A, Senapin S, St-Hilaire S, et al. Ozone nanobubble modulates the innate defense system of Nile tilapia (*Oreochromis niloticus*) against *Streptococcus agalactiae*. *Fish Shellfish Immunol* [Internet]. 2021;112(December 2020):64–73. Available from: <https://doi.org/10.1016/j.fsi.2021.02.015>
163. Ushida A, Koyama T, Nakamoto Y, Narumi T, Sato T, Hasegawa T. Antimicrobial effectiveness of ultra-fine ozone-rich bubble mixtures for fresh vegetables using an alternating flow. *J Food Eng* [Internet]. 2017;206:48–56. Available from: <http://dx.doi.org/10.1016/j.jfoodeng.2017.03.003>
164. Tamaki M, Kobayashi F, Ikeura H, Sato M. Disinfection by ozone microbubbles can cause morphological change of *Fusarium oxysporum* f. sp. *melonis* spores. *Plant Pathol J.* 2018;34(4):335–40.
165. Phaephiphat A, Mahakarnchanakul W, Yildiz F. Surface decontamination of *Salmonella Typhimurium* and *Escherichia coli* on sweet basil by ozone microbubbles. *Cogent Food Agric* [Internet]. 2018;4(1):1558496. Available from: <https://doi.org/10.1080/23311932.2018.1558496>
166. Li C, Yuan S, Jiang F, Xie Y, Guo Y, Yu H, et al. Degradation of fluopyram in water under ozone enhanced microbubbles: Kinetics, degradation products, reaction mechanism, and toxicity evaluation. *Chemosphere* [Internet]. 2020;258:127216. Available from: <https://doi.org/10.1016/j.chemosphere.2020.127216>
167. Ikeura H, Kobayashi F, Tamaki M. Removal of residual pesticide, fenitrothion, in vegetables by using ozone microbubbles generated by different methods. *J Food Eng* [Internet]. 2011;103(3):345–9. Available from: <http://dx.doi.org/10.1016/j.jfoodeng.2010.11.002>
168. Zhang F, Xi J, Huang JJ, Hu HY. Effect of inlet ozone concentration on the performance of

- a micro-bubble ozonation system for inactivation of *Bacillus subtilis* spores. *Sep Purif Technol* [Internet]. 2013;114:126–33. Available from: <http://dx.doi.org/10.1016/j.seppur.2013.04.034>
169. Karamah EF, Amalia F, Ghaudenson R, Bismo S. Disinfection of *Escherichia coli* bacteria using combination of ozonation and hydrodynamic cavitation method with venturi injector. *Int J Adv Sci Eng Inf Technol*. 2018;8(3):811–7.
170. Li Z, Xu M, Shi Y. Centrality in global shipping network basing on worldwide shipping areas. *GeoJournal*. 2015;80(1):47–60.
171. Huang C, Hu Q, Li Y, Tian J, Ma Y, Zhao Y, et al. Intermediate Volatility Organic Compound Emissions from a Large Cargo Vessel Operated under Real-World Conditions. *Environ Sci Technol*. 2018;52(21):12934–42.
172. Wan Z, Shi Z, Nie A, Chen J, Wang Z. Risk assessment of marine invasive species in Chinese ports introduced by the global shipping network. *Mar Pollut Bull* [Internet]. 2021;173(PA):112950. Available from: <https://doi.org/10.1016/j.marpolbul.2021.112950>
173. Kim AR, Lee SW, Seo YJ. How to control and manage vessels' ballast water: The perspective of Korean shipping companies. *Mar Policy* [Internet]. 2022;138(December 2021):105007. Available from: <https://doi.org/10.1016/j.marpol.2022.105007>
174. McCarthy SA, Khambaty FM. International dissemination of epidemic *Vibrio cholerae* by cargo ship ballast and other nonpotable waters. *Appl Environ Microbiol*. 1994;60(7):2597–601.
175. Sayinli B, Dong Y, Park Y, Bhatnagar A, Sillanpää M. Recent progress and challenges facing ballast water treatment – A review. *Chemosphere*. 2021;(July).
176. IMO Marine Environment Protection Committee (MEPC). Resolution MEPC.174(58), Guidelines for approval of ballast water management systems (G8). *Mepc174 (58)*. 2008;174(October).
177. Werschkun B, Sommer Y, Banerji S. Disinfection by-products in ballast water treatment: An evaluation of regulatory data. *Water Res* [Internet]. 2012;46(16):4884–901. Available from: <http://dx.doi.org/10.1016/j.watres.2012.05.034>
178. Oemcke D, Van Leeuwen J. Seawater ozonation of *Bacillus subtilis* spores: Implications for the use of ozone in ballast water treatment. *Ozone Sci Eng*. 2004;26(4):389–401.
179. Perrins JC, Cooper WJ, van Leeuwen J (Hans), Herwig RP. Ozonation of seawater from different locations: Formation and decay of total residual oxidant-implications for ballast water treatment. *Mar Pollut Bull*. 2006;52(9):1023–33.
180. Wietz M, Hall MR, Høj L. Effects of seawater ozonation on biofilm development in aquaculture tanks. *Syst Appl Microbiol*. 2009;32(4):266–77.
181. Gonçalves AA, Gagnon GA. Seawater ozonation: effects of seawater parameters on oxidant loading rates, residual toxicity, and total residual oxidants/by-products reduction during storage time. *Ozone Sci Eng* [Internet]. 2018;40(5):399–414. Available from: <https://doi.org/10.1080/01919512.2018.1448705>

182. Scolding JWS, Powell A, Boothroyd DP, Shields RJ. The effect of ozonation on the survival, growth and microbiology of the European lobster (*Homarus gammarus*). *Aquaculture* [Internet]. 2012;364–365:217–23. Available from: <http://dx.doi.org/10.1016/j.aquaculture.2012.08.017>
183. Jung Y, Hong E, Kwon M, Kang JW. A kinetic study of ozone decay and bromine formation in saltwater ozonation: Effect of O₃dose, salinity, pH, and temperature. *Chem Eng J*. 2017;312:30–8.
184. Brookman RM, Lamsal R, Gagnon GA. Comparing the formation of bromate and bromoform due to ozonation and UV-TiO₂ oxidation in seawater. *J Adv Oxid Technol*. 2011;14(1):23–30.
185. Penru Y, Guastalli AR, Esplugas S, Baig S. Disinfection of Seawater: Application of UV and Ozone. *Ozone Sci Eng*. 2013;35(1):63–70.
186. Yu W, Chen J, Ateia M, Cates EL, Johnson MS. Do gas nanobubbles enhance aqueous photocatalysis? Experiment and analysis of mechanism. *Catalysts*. 2021;11(4).
187. Atkinson AJ, Apul OG, Schneider O, Garcia-Segura S, Westerhoff P. Nanobubble Technologies Offer Opportunities To Improve Water Treatment. *Acc Chem Res* [Internet]. 2019 May 21;52(5):1196–205. Available from: <https://doi.org/10.1021/acs.accounts.8b00606>
188. Von Gunten U. Ozonation of drinking water: Part II. Disinfection and by-product formation in presence of bromide, iodide or chlorine. *Water Res*. 2003;37(7):1469–87.
189. Gounden AN, Jonnalagadda SB. Advances in treatment of brominated hydrocarbons by heterogeneous catalytic ozonation and bromate minimization. *Molecules*. 2019;24(19).
190. Bader H, Hoigné J. Determination of ozone in water by the indigo method. *Water Res* [Internet]. 1981 Jan 1 [cited 2020 Apr 13];15(4):449–56. Available from: <https://www.sciencedirect.com/science/article/abs/pii/0043135481900543>
191. Bader H, Hoigné J. Determination of ozone in water by the indigo method. *Water Res* [Internet]. 1981 Jan 1 [cited 2019 Nov 11];15(4):449–56. Available from: <https://www.sciencedirect.com/science/article/pii/0043135481900543>
192. Shin D, Park JB, Kim YJ, Kim SJ, Kang JH, Lee B, et al. Growth dynamics and gas transport mechanism of nanobubbles in graphene liquid cells. *Nat Commun*. 2015;6:1–6.
193. Andoyo R, Prawitasari IAP, Mardawati E, Cahyana Y, Sukarminah E, Rialita T, et al. Retention time of ozone at various water condition. *J Phys Conf Ser*. 2018;1080(1).
194. Luo S, Zhao ZY, Liu Y, Liu R, Liu WZ, Feng XC, et al. Recent advancements in antibiotics containing wastewater treatment by integrated bio-electrochemical-constructed wetland systems (BES-CWs). *Chem Eng J* [Internet]. 2023;457(December 2022):141133. Available from: <https://doi.org/10.1016/j.cej.2022.141133>
195. Kalogerakis N, Christofilopoulos S. Rhizodegradation in constructed wetlands. *Immobil Biocatal bioremediation Groundw wastewater*. 2015;(London: IWA Publishing):97–105.
196. Zheng F, Fang J, Guo F, Yang X, Liu T, Chen M, et al. Biochar based constructed wetland

- for secondary effluent treatment: Waste resource utilization. Chem Eng J [Internet]. 2022;432(November 2021):134377. Available from: <https://doi.org/10.1016/j.cej.2021.134377>
197. Ilyas H, Masih I. The effects of different aeration strategies on the performance of constructed wetlands for phosphorus removal. Environ Sci Pollut Res. 2018;25(6):5318–35.
 198. Oshita S, Liu S. Nanobubble Characteristics and Its Application to Agriculture and Foods. Int Symp Agri-Foods Heal Wealth. 2013;(2011):23–32.
 199. Liu X, Xu J, Liu Y, Zhang X, Lu S, Zhao B, et al. Stable and efficient sulfamethoxazole and phosphorus removal by an electrolysis-integrated bio-rack constructed wetland system. Chem Eng J [Internet]. 2021;425(June):130582. Available from: <https://doi.org/10.1016/j.cej.2021.130582>
 200. Gao Y, Zhang W, Gao B, Jia W, Miao A, Xiao L, et al. Highly efficient removal of nitrogen and phosphorus in an electrolysis-integrated horizontal subsurface-flow constructed wetland amended with biochar. Water Res [Internet]. 2018;139:301–10. Available from: <https://doi.org/10.1016/j.watres.2018.04.007>
 201. Ju X, Wu S, Zhang Y, Dong R. Intensified nitrogen and phosphorus removal in a novel electrolysis-integrated tidal flow constructed wetland system. Water Res [Internet]. 2014;59:37–45. Available from: <http://dx.doi.org/10.1016/j.watres.2014.04.004>
 202. Liu X, Wang Y, Lu S, Liu Y, Zhao B, Xi B, et al. Intensified sulfamethoxazole removal in an electrolysis-integrated tidal flow constructed wetland system. Chem Eng J [Internet]. 2020;390(January):124545. Available from: <https://doi.org/10.1016/j.cej.2020.124545>
 203. Liu Y, Liu X, Wang H, Fang Y, Li Z, Lu S, et al. Performance and mechanism of SMX removal in an electrolysis-integrated tidal flow constructed wetland at low temperature. Chem Eng J [Internet]. 2022;434(November 2021):134494. Available from: <https://doi.org/10.1016/j.cej.2022.134494>
 204. Selihin NM, Tay MG. A review on future wastewater treatment technologies: micro-nanobubbles, hybrid electro-Fenton processes, photocatalytic fuel cells, and microbial fuel cells. Water Sci Technol. 2022;85(1):319–41.
 205. MDH. Toluene and Groundwater. Minnesota Dep Heal. 2019;1–2.
 206. Filley CM. Cerebral White Matter Disorders. Encycl Hum Brain. 2002;1:715–31.
 207. OSHA. Toluene [Internet]. United States Department of Labor. Available from: <https://www.osha.gov/toluene/standards>
 208. Gao Y, Xie YW, Zhang Q, Wang AL, Yu YX, Yang LY. Intensified nitrate and phosphorus removal in an electrolysis -integrated horizontal subsurface-flow constructed wetland. Water Res. 2017;108:39–45.
 209. APHA. Standard methods for the examination of water and wastewater. Am Public Heal Assoc. 1985;16th Editi(Washington DC).
 210. R ger M, Ackermann M, Reichl U. Species-specific viability analysis of Pseudomonas

- aeruginosa, Burkholderia cepacia and Staphylococcus aureus in mixed culture by flow cytometry. *BMC Microbiol.* 2014;14(1).
211. Callahan BJ, McMurdie PJ, Rosen MJ, Han AW, Johnson AJA, Holmes SP. DADA2: High-resolution sample inference from Illumina amplicon data. *Nat Methods* [Internet]. 2016;13(7):581–3. Available from: <https://doi.org/10.1038/nmeth.3869>
212. Saputera WH, Putrie AS, Esmailpour AA, Sasongko D, Suendo V, Mukti RR. Technology advances in phenol removals: Current progress and future perspectives. *Catalysts.* 2021;11(8).
213. Li J, Han X, Brandt BW, Zhou Q, Ciric L, Campos LC. Physico-chemical and biological aspects of a serially connected lab-scale constructed wetland-stabilization tank-GAC slow sand filtration system during removal of selected PPCPs. *Chem Eng J* [Internet]. 2019;369(January):1109–18. Available from: <https://doi.org/10.1016/j.cej.2019.03.105>
214. Wang Q, Xie H, Ngo HH, Guo W, Zhang J, Liu C, et al. Microbial abundance and community in subsurface flow constructed wetland microcosms: role of plant presence. *Environ Sci Pollut Res.* 2016;23(5):4036–45.
215. Guan W, Yin M, He T, Xie S. Influence of substrate type on microbial community structure in vertical-flow constructed wetland treating polluted river water. *Environ Sci Pollut Res.* 2015;22(20):16202–9.
216. Dembele S, Akcil A, Panda S. Technological trends, emerging applications and metallurgical strategies in antimony recovery from stibnite. *Miner Eng* [Internet]. 2022;175(October 2021):107304. Available from: <https://doi.org/10.1016/j.mineng.2021.107304>
217. Xiang L, Liu C, Liu D, Ma L, Qiu X, Wang H, et al. Antimony transformation and mobilization from stibnite by an antimonite oxidizing bacterium *Bosea* sp. AS-1. *J Environ Sci (China)* [Internet]. 2022;111:273–81. Available from: <https://doi.org/10.1016/j.jes.2021.03.042>
218. Herath I, Vithanage M, Bundschuh J. Antimony as a global dilemma: Geochemistry, mobility, fate and transport. *Environ Pollut* [Internet]. 2017;223:545–59. Available from: <http://dx.doi.org/10.1016/j.envpol.2017.01.057>
219. Nishad PA, Bhaskarapillai A. Antimony, a pollutant of emerging concern: A review on industrial sources and remediation technologies. *Chemosphere* [Internet]. 2021;277:130252. Available from: <https://doi.org/10.1016/j.chemosphere.2021.130252>
220. Zhang X, Xie N, Guo Y, Niu D, Sun H bin, Yang Y. Insights into adsorptive removal of antimony contaminants: Functional materials, evaluation and prospective. *J Hazard Mater* [Internet]. 2021;418:126345. Available from: <https://doi.org/10.1016/j.jhazmat.2021.126345>
221. Li M, Liu Y, Shen C, Li F, Wang CC, Huang M, et al. One-step Sb(III) decontamination using a bifunctional photoelectrochemical filter. *J Hazard Mater* [Internet]. 2020;389:121840. Available from: <https://doi.org/10.1016/j.jhazmat.2019.121840>
222. Liu Y, Lou Z, Yang K, Wang Z, Zhou C, Li Y, et al. Coagulation removal of Sb(V) from textile wastewater matrix with enhanced strategy: Comparison study and mechanism analysis.

- Chemosphere [Internet]. 2019;237:124494. Available from: <https://doi.org/10.1016/j.chemosphere.2019.124494>
223. Long X, Wang X, Guo X, He M. A review of removal technology for antimony in aqueous solution. *J Environ Sci* [Internet]. 2020;90:189–204. Available from: <https://doi.org/10.1016/j.jes.2019.12.008>
224. Ren JH, Ma LQ, Sun HJ, Cai F, Luo J. Antimony uptake, translocation and speciation in rice plants exposed to antimonite and antimonate. *Sci Total Environ* [Internet]. 2014;475:83–9. Available from: <http://dx.doi.org/10.1016/j.scitotenv.2013.12.103>
225. Filella M, Belzile N, Chen YW. Antimony in the environment: A review focused on natural waters I. Occurrence. *Earth-Science Rev.* 2002;57(1–2):125–76.
226. Natasha, Shahid M, Khalid S, Dumat C, Pierart A, Niazi NK. Biogeochemistry of antimony in soil-plant system: Ecotoxicology and human health. *Appl Geochemistry* [Internet]. 2019;106:45–59. Available from: <https://doi.org/10.1016/j.apgeochem.2019.04.006>
227. Grob M, Wilcke W, Mestrot A. Release and biomethylation of antimony in shooting range soils upon flooding. *Soil Syst.* 2018;2(2):1–17.
228. Okkenhaug G, Zhu YG, Luo L, Lei M, Li X, Mulder J. Distribution, speciation and availability of antimony (Sb) in soils and terrestrial plants from an active Sb mining area. *Environ Pollut.* 2011;159(10):2427–34.
229. Barker AJ, Mayhew LE, Douglas TA, Ilgen AG, Trainor TP. Lead and antimony speciation associated with the weathering of bullets in a historic shooting range in Alaska. *Chem Geol* [Internet]. 2020;553:119797. Available from: <https://doi.org/10.1016/j.chemgeo.2020.119797>
230. Hockmann K, Tandy S, Lenz M, Reiser R, Conesa HM, Keller M, et al. Antimony retention and release from drained and waterlogged shooting range soil under field conditions. *Chemosphere* [Internet]. 2015;134:536–43. Available from: <http://dx.doi.org/10.1016/j.chemosphere.2014.12.020>
231. Wang L, Ji B, Hu Y, Liu R, Sun W. A review on in situ phytoremediation of mine tailings. *Chemosphere* [Internet]. 2017;184:594–600. Available from: <http://dx.doi.org/10.1016/j.chemosphere.2017.06.025>
232. Feng R, Wei C, Tu S, Ding Y, Wang R, Guo J. The uptake and detoxification of antimony by plants: A review. *Environ Exp Bot* [Internet]. 2013;96:28–34. Available from: <http://dx.doi.org/10.1016/j.envexpbot.2013.08.006>
233. Xi L, Shen YQ, Zhao X, Zhou M, Mi YD, Li XR, et al. Effects of arbuscular mycorrhizal fungi on frond antimony enrichment, morphology, and proteomics in *Pteris cretica* var. *nervosa* during antimony phytoremediation. *Sci Total Environ* [Internet]. 2022;804:149904. Available from: <https://doi.org/10.1016/j.scitotenv.2021.149904>
234. Huang Y, Chen Z, Liu W. Influence of iron plaque and cultivars on antimony uptake by and translocation in rice (*Oryza sativa* L.) seedlings exposed to Sb(III) or Sb(V). *Plant Soil.* 2012;352(1–2):41–9.
235. Ji Y, Sarret G, Schulin R, Tandy S. Fate and chemical speciation of antimony (Sb) during

- uptake, translocation and storage by rye grass using XANES spectroscopy. *Environ Pollut.* 2017;231:1322–9.
236. Shtangeeva I, Steinnes E, Lierhagen S. Uptake of different forms of antimony by wheat and rye seedlings. *Environ Sci Pollut Res.* 2012;19(2):502–9.
237. Zand AD, Heir AV. Phytoremediation: Data on effects of titanium dioxide nanoparticles on phytoremediation of antimony polluted soil. *Data Br.* 2020;31.
238. Levresse G, Lopez G, Tritlla J, López EC, Chavez AC, Salvador EM, et al. Phytoavailability of antimony and heavy metals in arid regions: The case of the Wadley Sb district (San Luis, Potosí, Mexico). *Sci Total Environ* [Internet]. 2012;427–428:115–25. Available from: <http://dx.doi.org/10.1016/j.scitotenv.2012.04.020>
239. Vaculík M, Jurkovič L, Matejkovič P, Molnárová M, Lux A. Potential risk of arsenic and antimony accumulation by medicinal plants naturally growing on old mining sites. *Water Air Soil Pollut.* 2013;224(5).
240. Cidu R, Biddau R, Dore E, Vacca A, Marini L. Antimony in the soil-water-plant system at the Su Suergiu abandoned mine (Sardinia, Italy): Strategies to mitigate contamination. *Sci Total Environ* [Internet]. 2014;497–498:319–31. Available from: <http://dx.doi.org/10.1016/j.scitotenv.2014.07.117>
241. Baroni F, Boscagli A, Protano G, Riccobono F. Antimony accumulation in *Achillea ageratum*, *Plantago lanceolata* and *Silene vulgaris* growing in an old Sb-mining area. *Environ Pollut.* 2000;109(2):347–52.
242. Murciego AM, Sánchez AG, González MAR, Gil EP, Gordillo CT, Fernández JC, et al. Antimony distribution and mobility in topsoils and plants (*Cytisus striatus*, *Cistus ladanifer* and *Dittrichia viscosa*) from polluted Sb-mining areas in Extremadura (Spain). *Environ Pollut.* 2007;145(1):15–21.
243. Pérez-Sirvent C, Martínez-Sánchez MJ, Martínez-López S, Bech J, Bolan N. Distribution and bioaccumulation of arsenic and antimony in *Dittrichia viscosa* growing in mining-affected semiarid soils in southeast Spain. *J Geochemical Explor* [Internet]. 2012;123:128–35. Available from: <http://dx.doi.org/10.1016/j.gexplo.2012.08.002>
244. Jana U, Chassany V, Bertrand G, Castrec-Rouelle M, Aubry E, Boudsocq S, et al. Analysis of arsenic and antimony distribution within plants growing at an old mine site in Ouche (Cantal, France) and identification of species suitable for site revegetation. *J Environ Manage* [Internet]. 2012;110:188–93. Available from: <http://dx.doi.org/10.1016/j.jenvman.2012.06.007>
245. Sruthi P, Shackira AM, Puthur JT. Heavy metal detoxification mechanisms in halophytes: an overview. *Wetl Ecol Manag.* 2017;25(2):129–48.
246. Peng G, Lan W, Pan K. Mechanisms of Metal Tolerance in Halophytes: A Mini Review. *Bull Environ Contam Toxicol* [Internet]. 2022;109(5):671–83. Available from: <https://doi.org/10.1007/s00128-022-03487-6>
247. Zhu Z, Wei G, Li J, Qian Q, Yu J. Silicon alleviates salt stress and increases antioxidant enzymes activity in leaves of salt-stressed cucumber (*Cucumis sativus* L.). *Plant Sci.* 2004;167(3):527–33.

248. Kumar D, Al Hassan M, Naranjo MA, Agrawal V, Boscaiu M, Vicente O. Effects of salinity and drought on growth, ionic relations, compatible solutes and activation of antioxidant systems in oleander (*Nerium oleander* L.). *PLoS One*. 2017;12(9):1–22.
249. Ibrahim N, El Afandi G. Phytoremediation uptake model of heavy metals (Pb, Cd and Zn) in soil using *Nerium oleander*. *Heliyon* [Internet]. 2020;6(7):e04445. Available from: <https://doi.org/10.1016/j.heliyon.2020.e04445>
250. Al-Shayeb S. Comparison study of *Phoenix dactylifera* L. and *Nerium oleander* L. as biomonitors for lead and other elements. *Asian J Chem*. 2002;597–601.
251. Manousaki E, Kalogerakis N. Halophytes present new opportunities in phytoremediation of heavy metals and saline soils. *Ind Eng Chem Res*. 2011;50(2):656–60.
252. Qiao D, Han Y, Zhao Y. Organic acids in conjunction with various oilseed sunflower cultivars promote Cd phytoextraction through regulating micro-environment in root zone. *Ind Crops Prod* [Internet]. 2022;183(April):114932. Available from: <https://doi.org/10.1016/j.indcrop.2022.114932>
253. Wang ST, Dong Q, Wang ZL. Differential effects of citric acid on cadmium uptake and accumulation between tall fescue and Kentucky bluegrass. *Ecotoxicol Environ Saf* [Internet]. 2017;145(March):200–6. Available from: <http://dx.doi.org/10.1016/j.ecoenv.2017.07.034>
254. Qiao D, Lu H, Zhang X. Change in phytoextraction of Cd by rapeseed (*Brassica napus* L.) with application rate of organic acids and the impact of Cd migration from bulk soil to the rhizosphere. *Environ Pollut* [Internet]. 2020;267:115452. Available from: <https://doi.org/10.1016/j.envpol.2020.115452>
255. Liu Y, Zhou Y, Wang T, Pan J, Zhou B, Muhammad T, et al. Micro-nano bubble water oxygation: Synergistically improving irrigation water use efficiency, crop yield and quality. *J Clean Prod* [Internet]. 2019;222:835–43. Available from: <https://doi.org/10.1016/j.jclepro.2019.02.208>
256. Wu Y, Lyu T, Yue B, Tonoli E, Verderio EAM, Ma Y, et al. Enhancement of Tomato Plant Growth and Productivity in Organic Farming by Agri-Nanotechnology Using Nanobubble Oxygation. *J Agric Food Chem*. 2019;67:10823–31.
257. Seridou P, Kalogerakis N. Disinfection applications of ozone micro- and nanobubbles. *Environ Sci Nano* [Internet]. 2021;8(12):3493–510. Available from: <http://dx.doi.org/10.1039/D1EN00700A>
258. Zhang F, Sun L, Yang H, Gui X, Schönherr H, Kappl M, et al. Recent advances for understanding the role of nanobubbles in particles flotation. *Adv Colloid Interface Sci*. 2021;291.
259. Ahmed AKA, Shi X, Hua L, Manzueta L, Qing W, Marhaba T, et al. Influences of Air, Oxygen, Nitrogen, and Carbon Dioxide Nanobubbles on Seed Germination and Plant Growth. *J Agric Food Chem*. 2018;66(20):5117–24.
260. Liu S, Oshita S, Kawabata S, Thuyet DQ. Nanobubble Water’s Promotion Effect of Barley (*Hordeum vulgare* L.) Sprouts Supported by RNA-Seq Analysis. *Langmuir*. 2017;33(43):12478–86.

261. Liu S, Oshita S, Kawabata S, Makino Y, Yoshimoto T. Identification of ROS Produced by Nanobubbles and Their Positive and Negative Effects on Vegetable Seed Germination. *Langmuir*. 2016;32(43):11295–302.
262. Liu S, Oshita S, Makino Y, Wang Q, Kawagoe Y, Uchida T. Oxidative Capacity of Nanobubbles and Its Effect on Seed Germination. *ACS Sustain Chem Eng*. 2016;4(3):1347–53.
263. Wu Y, Lyu T, Yue B, Tonoli E, Verderio EAM, Ma Y, et al. Enhancement of Tomato Plant Growth and Productivity in Organic Farming by Agri-Nanotechnology Using Nanobubble Oxygenation. *J Agric Food Chem*. 2019;67(39):10823–31.
264. Chen L, Larson SL, Ballard JH, Ma Y, Zhang Q, Li J, et al. Laboratory spiking process of soil with various uranium and other heavy metals. *MethodsX* [Internet]. 2019;6(April):734–9. Available from: <https://doi.org/10.1016/j.mex.2019.03.026>
265. Reeuwijk van L. Procedures for Soil Analysis, International Soil Reference and Information Centre (ISRIC) Technical Paper. 2002. p. 119.
266. Gangwar DP, Baskar M. Texture Determination of Soil by Hydrometer Method for Forensic Purpose. *Cent Forensic Sci Lab*. 2019;(May).
267. Harborne J. Chlorophylls in Phytochemical methods. Chapman Hall. 1984;214–221.
268. Bradford MM. A rapid and sensitive method for the quantitation of microgram quantities of protein utilizing the principle of protein-dye binding. *Anal Biochem*. 1976;72(1–2):248–54.
269. Erdelsky K, Fric E. Practical and Analytical Methods in Plant Physiology. SPN Bratislava. 1979;
270. Aebi H. Catalase in vitro. *Method Enzyme* 105. 1984;121–130.
271. Leuz AK, Johnson CA. Oxidation of Sb(III) to Sb(V) by O₂ and H₂O₂ in aqueous solutions. *Geochim Cosmochim Acta*. 2005;69(5):1165–72.
272. Leuz AK, Mönch H, Johnson CA. Sorption of Sb(III) and Sb(V) to goethite: Influence on Sb(III) oxidation and mobilization. *Environ Sci Technol*. 2006;40(23):7277–82.
273. Wu T liang, Qin W xiu, Alves ME, Fang G dong, Sun Q, Cui P xin, et al. Mechanisms of Sb(III) oxidation mediated by low molecular weight phenolic acids. *Chem Eng J* [Internet]. 2019;356(August 2018):190–8. Available from: <https://doi.org/10.1016/j.cej.2018.09.008>
274. Qi P, Pichler T. Sequential and simultaneous adsorption of Sb(III) and Sb(V) on ferrihydrite: Implications for oxidation and competition. *Chemosphere* [Internet]. 2016;145:55–60. Available from: <http://dx.doi.org/10.1016/j.chemosphere.2015.11.057>
275. Fan JX, Wang YJ, Fan TT, Cui XD, Zhou DM. Photo-induced oxidation of Sb(III) on goethite. *Chemosphere* [Internet]. 2014;95:295–300. Available from: <http://dx.doi.org/10.1016/j.chemosphere.2013.08.094>
276. Kurniawan SB, Ramli NN, Said NSM, Alias J, Imron MF, Abdullah SRS, et al. Practical limitations of bioaugmentation in treating heavy metal contaminated soil and role of plant growth promoting bacteria in phytoremediation as a promising alternative

approach. Heliyon [Internet]. 2022;8(4):e08995. Available from:
<https://doi.org/10.1016/j.heliyon.2022.e08995>

277. Deng R, Chen Y, Deng X, Huang Z, Zhou S, Ren B, et al. A Critical Review of Resistance and Oxidation Mechanisms of Sb-Oxidizing Bacteria for the Bioremediation of Sb(III) Pollution. *Front Microbiol.* 2021;12(September):1–22.

Appendix A. The reaction of indigo trisulfonate with the bromine inhibited by the addition of malonic acid

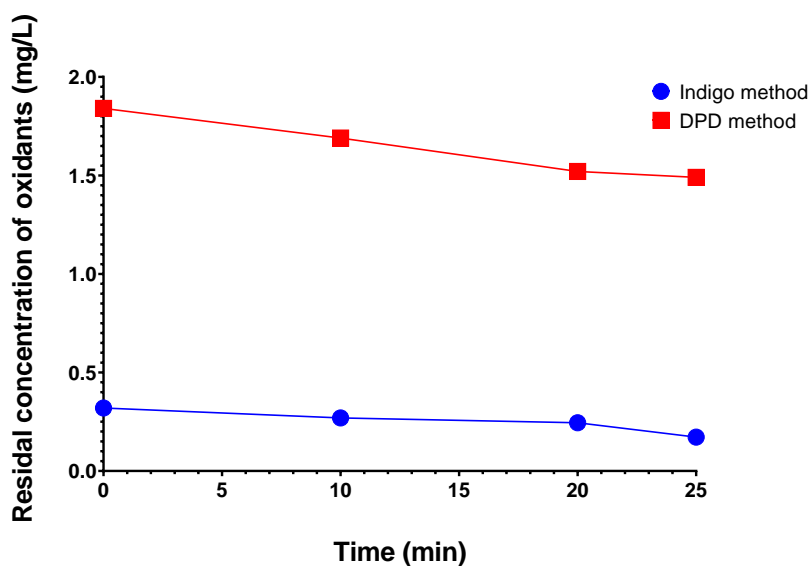


Figure A. 1. Comparison of DPD method with Indigo method for residual concentration of oxidants (mg/ L)

Table A. 1. Comparison of DPD method with Indigo method with and without malonic acid for residual concentration of oxidants (mg/ L) after 25 min.

DPD Method	Indigo Method without malonic acid	Indigo Method with malonic acid
1.49	0.634	0.172

Appendix B. Comparison Indigotrisulfonate (ITS) Method to Ozone Test Kit (Hach)

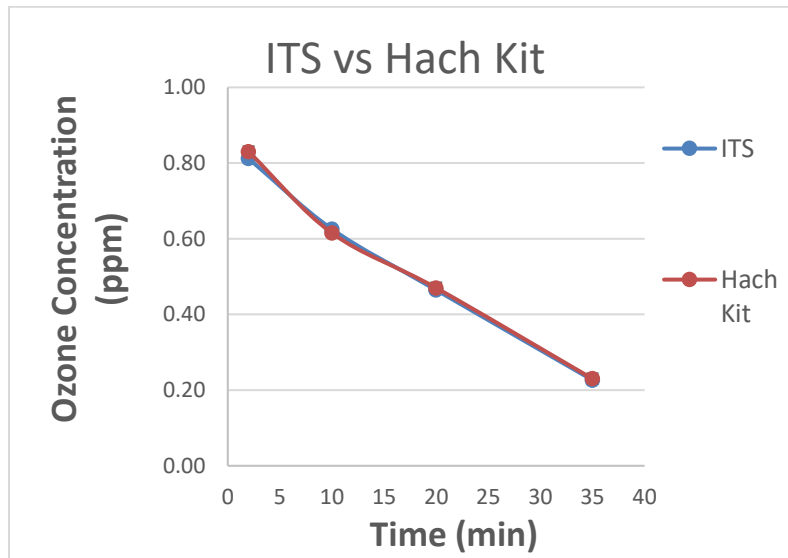


Figure B. 1. Comparison of the ozone concentrations with Indigotrisulfonate Method and the Ozone Test Kit (Hach)

Appendix C. Control bacterial concentration at different salinities without ozone addition

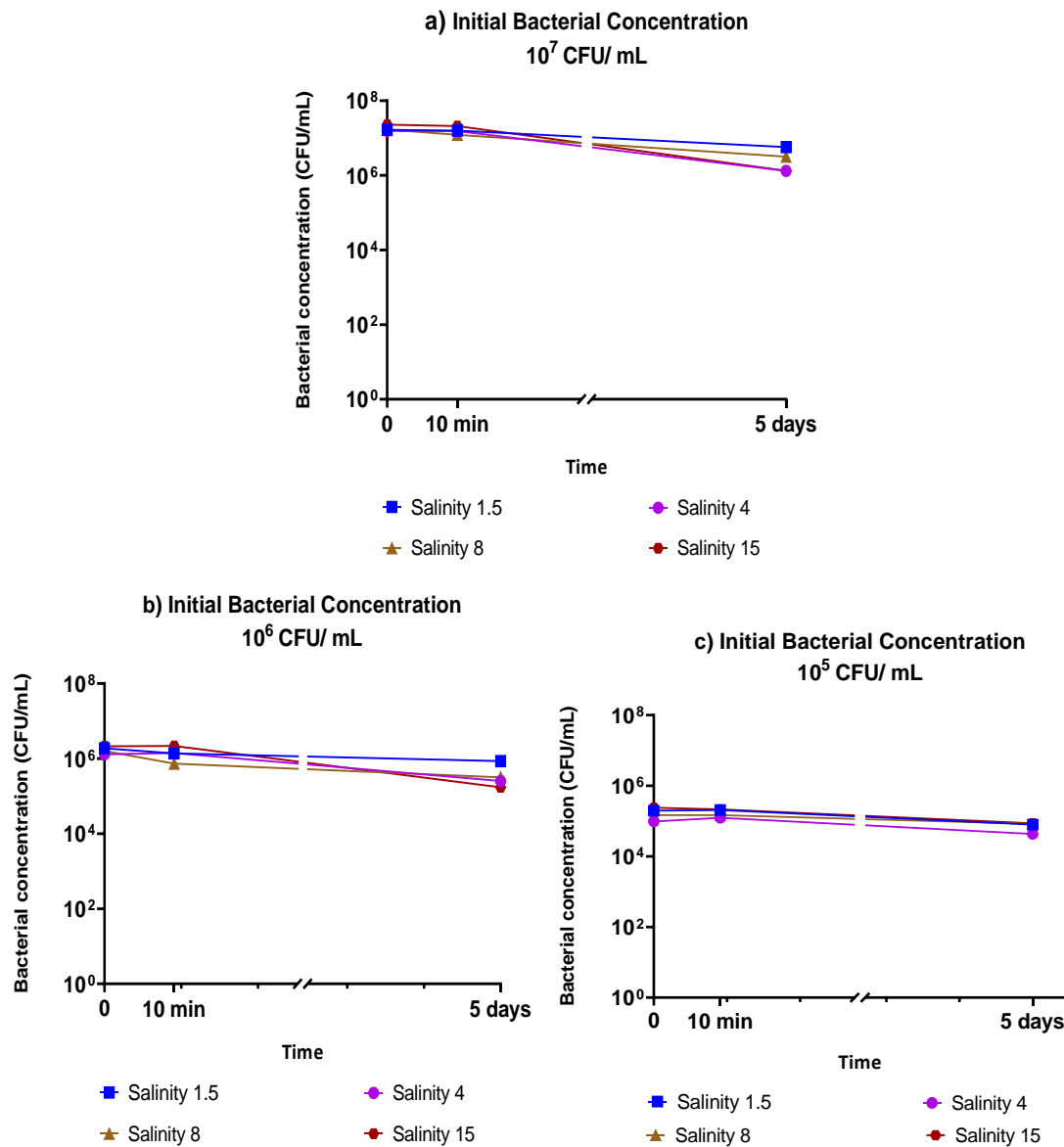


Figure C. 1. Control bacterial concentration at different salinities without ozone addition at initial bacterial concentration a) 10^7 CFU/mL, b) 10^6 CFU/mL and c) 10^5 CFU/mL.

About the Author

Petroula Seridou is a Chemical Engineer, graduated from Aristotle University of Thessaloniki (G.P.A. 8/10). The main objective of diploma thesis was to investigate the influence of metals concentration of Cu-Zn alloy on Cr(VI) removal from water. She also holds a M.Sc. degree in the field of Urban Water Engineering from the Department of Environmental Engineering at the Technical University of Denmark. Her M.Sc. thesis focused mainly on modelling of biological processes in a denitrifying moving bed biofilm reactor, using the data obtained from the targeted batch experiments. She has participated in internship programs; in the mineral water company ONE S.A., the Public Power Corporation (PPC), the Porto Carras Grand Resort and Danish company Orbicon, dealing with water analysis and further environmental studies. Finally, she has worked as research assistant in horizon EU projects INMARE and ELECTRA, and in ERA MIN 2 project nanoBT.

Refereed Journal Publications

Related to Ph.D.

1. Seridou P, Kalogerakis N. Disinfection applications of ozone micro- and nanobubbles. *Environ Sci Nano*. 2021;8(12):3493–510.
2. Seridou P, Monogiyiou S, Syranidou E., Kalogerakis N. Capacity of *Nerium oleander* to Phytoremediate Sb-Contaminated Soils Assisted by Organic Acids and Oxygen Nanobubbles. *Plants*. 2023;(12):91.
3. Seridou P, Kotzia E, Katris K, Kalogerakis N. Ballast water treatment by ozone nanobubbles. *J Chem Technol Biotechnol*. 2023; Available from: <https://doi.org/10.1002/jctb.7385>

Non- related to Ph.D.

1. Kaprara E, Seridou P, Tsiamili V, Mitrakas M, Vourlias G, Tsiaoussis I, et al. Cu-Zn powders as potential Cr(VI) adsorbents for drinking water. *J Hazard Mater*. 2013;262:606–13. Available from: <http://dx.doi.org/10.1016/j.jhazmat.2013.09.039>
2. Kampouris T.E, Syranidou E, Seridou P, Gagoulis K, Batjakas I.E, Kalogerakis N. MPs and NPs intake and heavy metals accumulation in tissues of *Palinurus elephas* (J.C. Fabricius, 1787), from NW Aegean sea, Greece. *Environ Pollut* 2023; 316(P1):120725. Available from: <https://doi.org/10.1016/j.envpol.2022.120725>
3. Seridou P, Fyntrilakis K., Syranidou E., Kalogerakis N. Hydroponic phytoremediation of antimony by *Tamarix smyrnensis* and *Nerium oleander*. *J Chem Technol Biotechnol*. 2023; Accepted.

Presentations at Conferences

Related to Ph.D.

1. Seridou P. and Kalogerakis N. Application of ozone nanobubbles in the disinfection of drinking water. 12th Panhellenic Scientific Conference in Chemical Engineering, May 29-31, 2019, Athens, Greece.
2. Seridou P. and Kalogerakis N. Application of air/ozone nanobubbles in the field of disinfection. 11th International Conference on Environmental Engineering and Management, September 8-10, 2021, Muttenz, Switzerland.
3. Seridou P., Vamvakia M., Syranidou E., Vlysidis A., Kalogerakis N. Phenol Removal in Constructed Wetlands with oxygenation systems. 13rd Panhellenic Scientific Conference in Chemical Engineering, June 02-04, 2022, Patra, Greece.
4. Seridou P., Kotzia E., Katris K., Kalogerakis N. Application of ozone nanobubbles in ballast water disinfection. 13rd Panhellenic Scientific Conference in Chemical Engineering, June 02-04, 2022, Patra, Greece. "Best poster award"
5. Seridou P. and Kalogerakis N. Application of ozonation in disinfection of saline water: Enhanced potential for ballast water treatment by Ozone Nanobubbles technology. 8th European Bioremediation Conference, June 12 - 17, 2022, Chania, Greece.
6. Seridou P., Kotzia E., Katris K. and Kalogerakis N. Ballast water disinfection by ozone micro and nanobubbles. 1st International Conference on Sustainable Chemical and Environmental Engineering, September 31 Aug – 04 2022, Rethymno, Crete, Greece.

Non- related to Ph.D.

1. Kaprara E., Seridou P., Simeonidis K., Mitrakas. Determination of chromium by GFAAS. 8th International Conference on Instrumental Methods of Analysis Modern Trends and Applications, IMA 2013, September 15-19, 2013, Thessaloniki, Greece.
2. Simeonidis K., Seridou P., Tsamili V., Tziomaki M., Kaprara E., Mitrakas M., Vourlias G., Tsiaoussis I., Kaimakamis G., Pavlidou E., Andritsos N. The efficiency of nanostructured Cu-Zn alloys on Cr(VI) removal. Clean water through Bio- and Nano-technology conference, May 7- 9, 2012, Lund, Sweden.
3. Charalampous G., Seridou P., Kalogerakis N. Characterization of a marine laccase enzyme produced by the marine fungus *Acremonium tubakii*. 7th Mikrobiokosmos Conference, April 7-9, 2017, Athens, Greece.
4. Seridou P., Charalampous G., and Kalogerakis. Enhancement of laccase enzyme activity produced by the marine fungus *Acremonium tubakii*. 7th European Bioremediation Conference & 11th ISEB Conference, June 25 – 28, 2018, Chania, Greece
5. Charalampous G., Seridou P., and Kalogerakis N. Laccase enzyme purification based on the innovative method of three-phase partitioning (TPP). 7th European Bioremediation Conference & 11th ISEB Conference, June 25 – 28, 2018, Chania, Greece